



# Presynaptic mechanisms of short-term plasticity at hippocampal mossy fibersynapses

Bernat Gonzalez I Llinares

## ► To cite this version:

Bernat Gonzalez I Llinares. Presynaptic mechanisms of short-term plasticity at hippocampal mossy fibersynapses. *Neurons and Cognition [q-bio.NC]*. Université de Bordeaux; Universiteit van Amsterdam, 2014. English. NNT : 2014BORD0424 . tel-01421839

**HAL Id: tel-01421839**

**<https://theses.hal.science/tel-01421839>**

Submitted on 23 Dec 2016

**HAL** is a multi-disciplinary open access archive for the deposit and dissemination of scientific research documents, whether they are published or not. The documents may come from teaching and research institutions in France or abroad, or from public or private research centers.

L'archive ouverte pluridisciplinaire **HAL**, est destinée au dépôt et à la diffusion de documents scientifiques de niveau recherche, publiés ou non, émanant des établissements d'enseignement et de recherche français ou étrangers, des laboratoires publics ou privés.

CO-SUPERVISED THESIS SUBMITTED

TO OBTAIN THE DEGREE OF

**DOCTOR OF PHILOSOPHY BY  
THE UNIVERSITY OF BORDEAUX**

DOCTORAL SCHOOL OF LIFE SCIENCES AND HEALTH

SPECIALITY NEUROSCIENCES

By Bernat GONZÁLEZ i LLINARES

**Presynaptic Mechanisms of Short-Term Plasticity at  
Hippocampal Mossy Fiber Synapses**

Under the supervision of: Christophe MULLE  
(co-supervisor: Matthijs VERHAGE)

Defended on 17<sup>th</sup> December 2014

Members of the jury:

Olivier THOUMINE  
Rafael FERNÁNDEZ CHACÓN  
Richard MILES  
Lydia DANGLLOT  
Matthijs VERHAGE  
Christophe MULLE

Principal Investigator at CNRS  
Professor at Universidad de Sevilla  
Principal Investigator at INSERM  
Researcher at INSERM  
Professor at VU Amsterdam  
Principal Investigator at CNRS

President  
Reporter  
Reporter  
Examiner  
Co-supervisor  
Supervisor

THÈSE EN COTUTELLE PRÉSENTÉE

POUR OBTENIR LE GRADE DE

**DOCTEUR DE  
L'UNIVERSITÉ DE BORDEAUX**

ÉCOLE DOCTORALE SCIENCES DE LA VIE ET DE LA SANTÉ

SPÉCIALITÉ NEUROSCIENCES

Par Bernat GONZÁLEZ I LLINARES

**Mécanismes présynaptiques de la plasticité à court terme  
des synapses fibres moussues de l'hippocampe**

Sous la direction de: Christophe MULLE  
(co-directeur: Matthijs VERHAGE)

Soutenue le 17 décembre 2014

Membres du jury:

Olivier THOUMINE  
Rafael FERNÁNDEZ CHACÓN  
Richard MILES  
Lydia DANGLLOT  
Matthijs VERHAGE  
Christophe MULLE

Directeur de recherche CNRS  
Professeur Universidad de Sevilla  
Directeur de recherche INSERM  
Chargée de recherche INSERM  
Professeur VU Amsterdam  
Directeur de recherche CNRS

Président  
Rapporteur  
Rapporteur  
Examinatrice  
Co-directeur de thèse  
Directeur de thèse

MEDE-BEGELEID PROEFSCHRIFT  
TER VERKRIJGING VAN DE GRAAD VAN

**DOCTOR AAN**  
**DE UNIVERSITEIT VAN BORDEAUX**

ONDERZOEKSCHOOL LEVENS- EN GEZONDHEIDSWETENSCHAPPEN  
SPECIALITEIT NEUROWETENSCHAPPEN

Door Bernat GONZÁLEZ i LLINARES

**Presynaptische mechanismen van korte-termijn plasticiteit  
in mosvezel synapsen van de hippocampus**

Promotor: Christophe MULLE  
(copromotor: Matthijs VERHAGE)

Verdedigd op 17 december 2014

Promotiecommissie:

Olivier THOUMINE  
Rafael FERNÁNDEZ CHACÓN  
Richard MILES  
Lydia DANGLOT  
Matthijs VERHAGE  
Christophe MULLE

Hoofdonderzoeker aan CNRS  
Professor aan Universidad de Sevilla  
Hoofdonderzoeker aan INSERM  
Onderzoeker aan INSERM  
Professor aan VU Amsterdam  
Hoofdonderzoeker aan CNRS

Voorzitter  
Reporter  
Reporter  
Examinator  
Copromotor  
Promotor



# Presynaptic Mechanisms of Short-Term Plasticity at Hippocampal Mossy Fiber Synapses

## Abstract

The hippocampal mossy fiber is characterized by its particular morphology, distinct synaptic transmission and presynaptic plasticity. Moreover, this synapse has been called “teacher” or “detonator” for its proposed functional role in episodic memory encoding. Nevertheless, the molecular mechanisms underlying its specific functional properties remain elusive. This work is composed of two main parts:

### 1) Phenotyping Hippocampal Mossy Fiber Synapses in VAMP7 KO Mice

VAMP7 is a vesicle SNARE of the longin family important in neurite growth during development. In the adult brain, VAMP7 is enriched in a subset of nerve terminals, particularly at the hippocampal mossy fiber. We analyzed VAMP7 function in neurotransmitter release by characterizing basal and evoked transmission at this synapse in KO mice and fully tested hypotheses relevant to short-term plasticity. Loss of VAMP7 has been previously reported not to cause major developmental or neurological deficits (Sato et al., 2011; Danglot et al., 2012). Presynaptic mechanisms of short-term plasticity at the hippocampal mossy fiber also seem unaffected for potential reasons that will be discussed.

### 2) CA3 Circuits Probed with RABV-Tracing and Paired Recordings

We developed a technique to establish paired recordings between connected dentate gyrus granule cells and CA3 pyramidal cells (GC-CA3) in mouse hippocampal organotypic slice cultures. To identify direct presynaptic partners to a defined target CA3 pyramidal cell, we combined single-cell electroporation (SCE) and mono-trans-synaptic tracing based on a pseudotyped, recombinant rabies virus (EnvA pseudotyped RABV ΔG). Using SCE we transfected a single CA3 pyramidal cell per slice with the plasmids encoding: the RABV envelope glycoprotein (RG), a fluorescent reporter, and TVA (the EnvA cognate surface receptor, which has no homologue in mammalian cells). The slices were subsequently infected with EnvA pseudotyped RABV ΔG. After 3-4 days, the RABV mono-trans-synaptic tracing revealed the presynaptic inputs of that single neuron. Then, we were able to establish paired recordings between connected GC-CA3 cells, as well as to quantify the presynaptic partners of the starter CA3 pyramidal cell.

## Keywords

Hippocampal Mossy Fiber, Short-Term Plasticity, TI-VAMP/VAMP7 KO mouse, Rabies Virus Tracing, Paired Recordings

---

## Physiology of Glutamatergic Synapses

Interdisciplinary Institute for Neuroscience, IINS – CNRS UMR 5297

146 rue Léo-Saignat

33077 Bordeaux Cedex

# Mécanismes présynaptiques de la plasticité à court terme des synapses fibres moussues de l'hippocampe

## Résumé

Les synapses fibres moussues de l'hippocampe entre le gyrus denté et les cellules pyramidales de CA3 sont caractérisées par leur morphologie particulière, et par leurs propriétés distinctives de transmission synaptique et de plasticité présynaptique. Ces synapses sont parfois appelées «détonatrices» pour leur rôle fonctionnel dans l'encodage de la mémoire épisodique. Cependant, les mécanismes moléculaires à la base des propriétés spécifiques de ces synapses restent peu connus. Ce travail est composé de deux parties principales:

1) Phénotypage des synapses fibres moussues de l'hippocampe chez les souris VAMP7 KO

VAMP7 est une protéine SNARE vésiculaire de la famille des longins, qui joue un rôle dans la croissance des neurites durant le développement. Dans le cerveau adulte, VAMP7 est enrichi dans un sous-ensemble de terminaisons nerveuses, en particulier dans les fibres moussues de l'hippocampe. Nous avons analysé la fonction de VAMP7 dans la libération de neurotransmetteurs par une caractérisation extensive de la transmission synaptique et des mécanismes de plasticité de cette synapse. L'absence de VAMP7 ne cause pas de graves déficits développementaux ou neuronaux (Sato et al., 2011; Danglot et al., 2012). Les mécanismes présynaptiques de la plasticité à court terme de la fibre moussue de l'hippocampe semblent également normaux, pour des raisons éventuelles qui seront discutées.

2) Circuits du CA3 examinés par traçage viral et enregistrements de paires

Nous avons développé une technique pour établir des enregistrements en paires entre cellules en grain du gyrus denté connectées et cellules pyramidales CA3 (GC-CA3), sur des cultures organotypiques de tranches d'hippocampe de souris. Pour identifier les partenaires présynaptiques directs à une cellule pyramidale CA3 ciblée, nous avons combiné l'électroporation cellulaire unitaire et le traçage mono-trans-synaptique basé sur un virus de la rage recombinant et pseudotypé. Nous avons transfecté une cellule pyramidale CA3 unique par tranche avec les plasmides codant la glycoprotéine d'enveloppe du virus de la rage (RG), un rapporteur fluorescent, et la protéine TVA (récepteur de surface apparenté au EnvA, qui n'a pas d'homologue chez les cellules de mammifères). Les tranches ont ensuite été infectées avec le virus de la rage recombinant et pseudotypé. Après 3-4 jours, le traçage mono-trans-synaptique révèle les entrées présynaptiques de ce neurone unique. Ensuite, nous avons pu établir des enregistrements de paires entre les cellules en grain-CA3 connectés, ainsi que de quantifier les partenaires présynaptiques de la cellule pyramidale CA3 de départ.

## Mots clés

Fibre moussue de l'hippocampe, plasticité à court terme, souris TI-VAMP/VAMP7 KO, traçage par le virus de la rage, enregistrements des paires

---

## Physiologie des synapses glutamatergiques

Institut Interdisciplinaire de Neurosciences, IINS – CNRS UMR 5297

146 rue Léo-Saignat

33077 Bordeaux Cedex

# **Presynaptische mechanismen van korte-termijn plasticiteit in mosvezel synapsen van de hippocampus**

## **Samenvatting**

De mosvezel van de hippocampus kenmerkt zich door een bijzondere morfologie, uitzonderlijke synaptische transmissie en presynaptische plasticiteit. De synaps wordt ook wel "leraar" of "detonator" genoemd vanwege zijn waarschijnlijke rol in de codering van het episodisch geheugen. Toch blijven de specifieke moleculaire mechanismen van dit synaps onbekend. Dit werk bestaat uit twee delen:

### **1) Fenotypering van mosvezel synapsen van de hippocampus in VAMP7 KO muizen**

VAMP7 is een vesicle-SNARE van de longin familie van belang bij de groei van neurieten tijdens de ontwikkeling. In de volwassen hersenen, wordt VAMP7 verrijkt in een subset van zenuwuiteinden, vooral in de mosvezel van de hippocampus. We analyseerden VAMP7 functie in neurotransmitter afgifte door het karakteriseren van basale en opgeroepen transmissie bij deze synaps in KO muizen. Eerder is al gesteld dat gebrek aan VAMP7 niet leidt tot grote ontwikkelings- of neurologische afwijkingen (Sato et al., 2011; Danglot et al., 2012). Presynaptische mechanismen van korte termijn plasticiteit in de mosvezel van de hippocampus lijken ook onaangetast te zijn, de mogelijke redenen hiervoor zullen worden besproken.

### **2) CA3 circuits onderzocht met behulp van RABV-tracing en gekoppelde opnames**

We ontwikkelden een techniek om gekoppelde opnames tussen korelcellen van de gyrus dentatus en aangesloten CA3 piramidale cellen (KC-CA3) op zogenaamde 'mouse hippocampal organotypic slice cultures' te meten. Om rechtstreekse presynaptische partners te identificeren van een specifieke CA3 piramidale cel, combineerden we single-cell electroporation (SCE) en mono-trans-synaptic tracing op basis van een pseudo-typed, recombinant rabiësvirus (EnvA pseudogetyped RABV ΔG). Met behulp van SCE transfecteerde we één CA3 piramidale cel per slice met plasmiden die coderen voor: het RABV glycoproteïne-envelop (RG), een fluorescerende reporter, en TVA (de aan EnvA verwante oppervlakte receptor die geen homoloog in zoogdiercellen heeft). De slices werden vervolgens geïnfecteerd met ENVA pseudogetyped RABV ΔG. Na 3-4 dagen bracht de RABV mono-trans-synaptische tracing de presynaptische ingangen van die ene neuron aan het licht. Hierna konden we gekoppelde opnames doen tussen verbonden KC-CA3 cellen. Daarnaast konden we de presynaptische partners van de starter CA3 piramidale cel kwantificeren.

## **Trefwoorden**

Mosvezel van de hippocampus, korte-termijn plasticiteit, TI-VAMP/VAMP7 KO muis, rabiësvirus tracing, gekoppelde opnames

---

## **Physiologie des synapses glutamatergiques**

Institut Interdisciplinaire de Neuroscience, IINS – CNRS UMR 5297

146 rue Léo-Saignat

33077 Bordeaux Cedex

# **Mécanismes présynaptiques de la plasticité à court terme des synapses fibres moussues de l'hippocampe**

## **Résumé substantiel en français**

Dans cette thèse nous avons ciblé les mécanismes responsables de la libération de vésicules contenant de neurotransmetteurs dans des synapses chimiques. Comme pour toute autre forme de communication, il faut deux neurones pour établir une synapse chimique: une cellule présynaptiques et une cellule postsynaptique. Le message dans cette communication est une signalé électrique, le potentiel d'action (PA), que devient chimique quand transverse la fente synaptique que sépare les deux cellules. Grace à la technique de «whole-cell patch clamp» nous pouvons enregistrer les courants générées quand le neurotransmetteur est détecté par de récepteurs postsynaptiques. Selon l'origine, ces courants sont classifiées comme: spontanées (si elles ne sont pas liées à l'arrivée d'un PA au terminal présynaptique) ou évoquées (quand la libération de vésicules est déclenchée par l'arrivée d'un PA au terminal présynaptique). En plus, les courantes évoquées peuvent être synchrones (dans quelques millisecondes suivant le PA) ou asynchrones (à partir d'une dizaine jusqu'à quelques centaines des millisecondes suivant le PA). Les réponses évoquées par PAs consécutifs ne sont pas identiques, bien au contraire, elles présent une plasticité remarquable, particulièrement dans certaines synapses. Cette plasticité dite 'à courte terme' peut faciliter ou déprimer la transmission synaptique et joue un rôle dans l'intégration d'information.

Les synapses fibres moussues (FMs) de l'hippocampe entre le gyrus denté et les cellules pyramidales de CA3 sont caractérisées par leur morphologie particulière, et par leurs propriétés distinctives de transmission synaptique et de plasticité présynaptique. Dans l'adulte, les FMs libèrent principalement du glutamate, mais elles peuvent co-libérer aussi autres substances comme le zinc. Ces synapses sont parfois appelées «détonatrices» pour leur rôle fonctionnel dans l'encodage de la mémoire épisodique. Cependant, les mécanismes moléculaires à la base des propriétés spécifiques de ces synapses restent peu connus.

La dernière théorie propose que chaque vésicule est sensible à l'entrée de calcium par plusieurs canaux calciques (couplage lâche à microdomains de canaux calciques), combiné à la saturation d'un tampon calcique rapide (qui n'a pas été encore identifié).

Ce travail est composé de deux parties principales:

1) Phénotypage des synapses fibres moussues de l'hippocampe chez les souris VAMP7 KO

Les vésicules des synapses glutamatergiques contient en moyen 70 copies de VAMP2, le SNARE vésiculaire canonique pour la libération de vésicules synaptiques, mais aussi quelques copies de SNAREs vésiculaires alternatifs tel que Vti1a, VAMP4, ou VAMP7. C'est discuté si tous les vésicules expriment plusieurs SNAREs, ou si par contre, il existe des pools exprimant SNAREs différents.

VAMP7 est une protéine SNARE vésiculaire de la famille des longins, qui joue un rôle dans la croissance des neurites durant le développement. Dans le cerveau adulte, VAMP7 est enrichi dans un sous-ensemble de terminaisons nerveuses, en particulier dans les fibres moussues de l'hippocampe. VAMP7 contient un long domaine terminal C (domaine longin) qui interagit avec la protéine adaptateur 3 (AP-3) pour être transporté aux terminales synaptiques. Le domaine longin se replie sur le propre motif SNARE de VAMP7 inhibant l'interaction avec des SNAREs dans la membrane. Ainsi, les vésicules contenant VAMP7 se trouvent dans un pool qui est réticent à l'exocytose et que devient libéré seulement après une forte stimulation.

Nous avons analysé la fonction de VAMP7 dans la libération de neurotransmetteurs par une caractérisation extensive de la transmission synaptique et des mécanismes de plasticité de cette synapse. Cette caractérisation a ciblé tous les modes de libération de neurotransmetteurs, soit la libération spontanée, évoquée (synchrone et asynchrone), ainsi comme la co-libération de zinc. L'absence de VAMP7 ne cause pas de graves déficits développementaux ou neuronaux (Sato et al., 2011; Danglot et al., 2012). Les mécanismes présynaptiques de la transmission synaptique et de la plasticité à court terme de la fibre moussue de l'hippocampe semblent également normaux dans ces souris: nous n'avons pas trouvé de différences dans la libération spontanée, ni dans la libération évoquée (synchrone et asynchrone),

ni dans la co-libération de zinc. Probablement VAMP7 ne joue pas un rôle dans la libération de vésicules *bona fide*.

Récemment, l'équipe de Silvio Rizzoli a proposé que les vésicules synaptiques subissent une maturation par cycles de endocytose et exocytose pendant lesquels elles transportent de protéines vers la membrane au même temps qu'elles incorporent protéines nécessaires pour la libération de calcium-dépendante. Ainsi, au début les vésicules jouent un rôle dans la libération constitutive et ne sont considérées comme vésicules synaptiques *bona fide* qu'après quelques cycles d'endocytose et exocytose. Alternativement Sorensen et Verhage ont proposé une maturation au long du transport depuis le Golgi vers la membrane. Des études complémentaires sont nécessaires pour déterminer si VAMP7 joue un rôle dans un tel mécanisme de maturation vésiculaire.

2) Circuits du CA3 examinés par traçage viral et enregistrements de paires

Depuis le début de ma thèse, on a constaté que malgré l'expertise en électrophysiologie du laboratoire de Christophe Mulle et la disponibilité de souris mutantes du laboratoire de Matthijs Verhage, on manqué une technique qui pourrait nous permettre l'analyse physiologique des différentes protéines présynaptiques par remplacement génétique sur de souris floxées.

Nous avons développé une technique pour établir des enregistrements en paires entre cellules en grain du gyrus denté connectées et cellules pyramidales CA3 (GC-CA3), sur des cultures organotypiques de tranches

d'hippocampe de souris. Pour identifier les partenaires présynaptiques directs à une cellule pyramidale CA3 ciblée, nous avons combiné l'électroporation cellulaire unitaire et le traçage mono-trans-synaptique basé sur un virus de la rage recombinant et pseudotypé. Nous avons transfecté une cellule pyramidale CA3 unique par tranche avec les plasmides codant la glycoprotéine d'enveloppe du virus de la rage (RG), un rapporteur fluorescent, et la protéine TVA (récepteur de surface apparenté au EnvA, qui n'a pas d'homologue chez les cellules de mammifères). Les tranches ont ensuite été infectées avec le virus de la rage recombinant et pseudotypé. Après 3-4 jours, le traçage mono-trans-synaptique révèle les entrées présynaptiques de ce neurone unique. Ensuite, nous avons pu établir des enregistrements de paires entre les cellules en grain-CA3 connectés, ainsi que de quantifier les partenaires présynaptiques de la cellule pyramidale CA3 de départ.

La technique que nous avons développée rend possible l'enregistrement de paires visuellement guidé d'une façon systématique. En outre, le traçage rétrograde peut être combiné avec la manipulation génétique de la cellule postsynaptique. Pour pouvoir manipuler la cellule présynaptique par contre, il serait nécessaire d'utiliser un traçage antérograde. La direction du traçage du virus de la rage pourrait être modifiée exprimant la glycoprotéine d'un autre virus (i.e. VSV ou LCMV). Des études supplémentaires seront nécessaires pour développer une tel traçage antérograde, avec lequel nous pourrions finalement analyser d'autres protéines présynaptiques (i.e. Munc18-1).



*Li dedique aquesta tesi doctoral a la memòria de mon tio Pedro, qui em va transmetre la curiositat per comprendre el cosmos mitjançant el mètode científic. Recorde com em va apassionar buscar fòssils i minerals quan anàvem d'excursió al riu.*

*“La morphologie de la cellule pyramidale n'est qu'une des conditions anatomiques de la pensée. Or cette morphologie spéciale ne suffira jamais à nous expliquer les énormes différences qui existent au point de vue fonctionnel entre la cellule pyramidale d'un lapin et celle d'un homme, ainsi qu'entre la cellule pyramidale de l'écorce cérébrale et le corpuscule étoilé de la moelle ou du grand sympathique. Aussi à notre avis est-il très probable qu'en outre de la complexité de leurs rapports les cellules pyramidales possèdent encore une structure intraprotoplasmique toute spéciale, et même perfectionnée dans les intelligences d'élite, structure qui n'existerait pas dans les corpuscules de la moelle ou des ganglions.”*

*The Croonian Lecture : «La fine structure des centres nerveux», 1894*

*Santiago Ramón y Cajal*

## Acknowledgements

I would like to thank all members of the Mülle Team with whom I had the pleasure to work. Particularly, I am grateful to Mario Carta for teaching and helping me develop the techniques used in this work; to Christophe Blanchet for his help with the Igor macros needed to analyze electrophysiological data; to Virginie Labrousse for her work in processing traced slices, imaging them, and quantifying tracing; to Nelson Rebola for his indications on how to record NMDA currents; to Gael Barthet for his help upgrading the setup LED system and discussion on plasticity elicited by trains; to Fred Lanore and Sandrine Pouvreau for their help using the confocal microscope; to Melanie Ginger for her help with the rabies project; in general to those already mentioned and to Jimmy George, Vincent Maingret, Sabine Fiebre, Joana Lourenço, Stefano Zucca, Adam Gorlewicz, Severine Deforges, Julien Veran, Sri Bettadapura, Noelle Grosjean, Zsolt Szabo, Silvia Viana da Silva, Thierry Amedée, Axel Athané, Audrey Lacquemant, David Perrais, Elisabeth Normand, François Coussen, Isabelle Seynat, Priscilla Kaulanjan-Checkmodine, Amalia Callado Pérez, Julie Rumi Massante, Marilena Griguoli, Pei Zhang, and Meryl Malezieux.

I thank Christophe Mülle for providing me the chance to carry out this work, as well as for taking part in the SyMBaD network he coordinated.

Matthijs Verhage deserves also my gratitude in that respect, and I appreciate his contribution of ideas and resources. Thanks to Robbert Zalm and Joke Wortel for mediating in the transfer of CAPS plasmids, and Munc18-1 plasmids and Loxed mice. Unfortunately, these projects could not be properly developed due to technical limitations (i.e. lack of anterogradely traced paired recordings, or full dentate gyrus transfection).

I would like to thank Didier Dulon and his team, including Rabia Fernandez, and Pierre Costet from the animal facility, for his collaboration within the Otoferlin KO project, which alas did not result in any significant result, and it has not been included in this manuscript.

In the same line, I am grateful to Thierry Galli and Lydia Danglot for the collaboration within the TI-VAMP KO project, and to Andreas Frick, Melanie Ginger, and Matthias Haberl, for the collaboration within the RABV-tracing project.

I would like to thank all the members of the IINS in general, and the administration, the culture and in vivo teams in particular. Thanks also to Rémi

Sterling for his help fighting mushrooms in the incubators and producing pieces for the setup, to the animal facilities of the Bordeaux University for the animal care, and to the Bordeaux Imaging Center for the training and use of confocal microscopy.

I was part of the ENC-Network as one of the “Twinning Cum Laude project” PhD student, thus I am grateful to the coordinator, Maaïke Leusden, and the director, Arjen Brussard, as well as to the PIs and colleagues for discussion and nice times during annual meetings.

As SyMBaD associated-student, I also thank both project managers: Pauline Lafenêtre and Antonella Caminiti, the director of this network, Christophe Mülle, as well as the PIs and colleagues for discussion and nice times during annual meetings.

I would like to thank Han de Jong for corrections of the Dutch summary, as well as his family for the good times in Salles, where mushrooms grow as much as in the slice culture incubators, but where I was happier to find them =)

Finally, I wish to express my gratitude to all my friends, to my family and infinitely to my wife Bouda, who supported me patiently and encouraged me endlessly throughout the whole thesis.

## Abbreviations

A/C	Associational/Commissural
ACSF	Artificial Cerebrospinal Fluid
AMPA	$\alpha$ -Amino-3-hydroxy-5-methyl-4-isoxazolepropionic Acid
AP	Action Potential
AP-3	Adaptor Protein-3
ATP	Adenosine TriPhosphate
AZ	Active Zone
CA	Cornus Ammonis
CAM	Cell-Adhesion Molecule
CaMKII	Calcium/Calmodulin-dependent protein Kinase II
cAMP	Cyclic Adenosine MonoPhosphate
CAZ	Cytomatrix at the Active Zone
CNS	Central Nervous System
DIV	Days <i>in Vitro</i>
EC	Entorhinal Cortex
EnvA	Envelope A
EPSCs	Excitatory PostSynaptic Currents
EGFP	Enhanced Green Fluorescent Protein
fEPSPs	Field Excitatory PostSynaptic Potentials
FF	Frequency Facilitation
GABA	Gamma-AmminoButyric Acid
GC	Granule Cell
GFP	Green Fluorescent Protein
gl	granular layer
LD	Longin Domain
LTD	Long-Term Depression
LTP	Long-Term Potentiation
MF	Mossy Fibers
mEPSCs	Miniature Excitatory PostSynaptic Currents
MFBs	Mossy Fiber Boutons
ml	Molecular Layer
NBQX	2,3-dihydroxy-6-nitro-7-sulfamoyl-benzo[f]quinoxaline-2,3-dione
NTD	N-Terminal Domain

## Abbreviations

P	Postnatal Day
PNS	Peripheral Nervous System
PP	Perforant Path
PPR	Paired Pulse Ratio
Pr	Probability of Release
PSD	PostSynaptic Density
RABV	Rabies Virus
RG	RABV Glycoprotein
RP	Reserve Pool
RRP	Release-Ready Pool
SCE	Single-Cell Electroporation
sl	stratum lucidum
slm	stratum lucidum moleculare
SM	Sec1/Munc18-like
SNARE	Soluble <i>N</i> -ethylmaleimide-sensitive factor Attachment protein REceptor
so	stratum oriens
sp	stratum pyramidale
sr	stratum radiatum
STP	Short-Term Plasticity
SV	Synaptic Vesicle
Syt1	Synaptotagmin1
t-	Target
tdTom	tdTomato
TI-	Tetanus neurotoxin-Insensitive
TM	TransMembrane
TVA	Tumor Virus receptor A
v-	Vesicle
VAMP	Vesicle-Associated Membrane Protein
ZnT3	Zinc Transporter-3

## Table of Contents

<b>Abstract</b>	<b>4</b>
<b>Résumé</b>	<b>5</b>
<b>Samenvatting</b>	<b>6</b>
<b>Acknowledgements</b>	<b>9</b>
<b>Abbreviations</b>	<b>11</b>
<b>Table of Contents</b>	<b>13</b>
<b>Introduction</b>	<b>16</b>
<b>1. Synapses</b>	<b>16</b>
1.1. Glutamatergic Synapses	20
1.1.1. Presynapse	21
1.1.2. Postsynapse	22
1.1.3. Synaptic Cleft	23
<b>2. Neurotransmitter Release</b>	<b>25</b>
2.1. Neuronal Exocytotic Machinery	25
2.1.1. SNARE and SM Proteins	25
2.1.2. TI-VAMP/VAMP7	29
2.1.3. Calcium Sensors	32
2.1.4. Regulatory Proteins	33
2.1.5. The Role of Lipids	33
2.2. Types of Release and Vesicle Pools	33
<b>3. Hippocampal Formation</b>	<b>36</b>
3.1. Circuitry and Functions	36
3.2. Mossy Fiber Synapses	39
<b>4. Synaptic Plasticity</b>	<b>43</b>
4.1. AP-dependent	43
4.1.1. Short-Term Plasticity	43
4.1.2. Long-Term Plasticity	45
4.2. AP-independent	46

<b>5. Neuronal Tracing .....</b>	<b>47</b>
5.1. Conventional Tracers .....	48
5.2. Trans-Synaptic Tracers .....	50
5.2.1. Non-Viral Tracers .....	50
5.2.1.1. <i>Radioactive Amino Acids</i> .....	50
5.2.1.2. <i>Plant Lectins</i> .....	51
5.2.1.3. <i>Clostridial Toxins</i> .....	52
5.2.1.4. <i>Diffusion MRI or DTI</i> .....	52
5.2.2. Viral Tracers .....	54
5.2.2.1. <i>Herpesviridae</i> .....	56
5.2.2.2. <i>Rhabdoviridae</i> .....	56
5.2.2.3. <i>Other Neurotropic Viruses</i> .....	62
<b>6. Scope of This Work .....</b>	<b>64</b>
<b>Results &amp; Discussion .....</b>	<b>66</b>
Phenotyping Hippocampal Mossy Fiber Synapses in VAMP7 KO Mice ....	66
CA3 Circuits Probed with RABV-Tracing and Paired Recordings .....	100
<b>Conclusions &amp; Perspectives .....</b>	<b>120</b>
Phenotyping Hippocampal Mossy Fiber Synapses in VAMP7 KO Mice ..	120
CA3 Circuits Probed with RABV-Tracing and Paired Recordings .....	121
<b>Bibliography .....</b>	<b>125</b>
<b>Annex: Rabies Virus Pathophysiology and Epidemics .....</b>	<b>145</b>



# Introduction

## Introduction

### 1. Synapses

The nervous system consists of a complex network of cells, called neurons, which are highly specialized for fast information transmission. The site where neurons exchange information is known as the “synapse”, and it has three components: a presynaptic compartment, a synaptic cleft, and a postsynaptic compartment. The human brain contains 10 to 100 billion neurons and a typical neuron receives 1,000 to 10,000 synapses. Thus, our brain has more than 100 trillion synapses (Mouton et al., 1997; Drachman, 2005). Besides neurons, the nervous tissue is also composed of neuroglia (see Figure 1). Synapses evolved early in animal evolution, central features of synaptic transmission possibly evolving during the transition to multicellularity (Burkhardt et al., 2011). Today, a great variety of synapses exists between and within organisms.

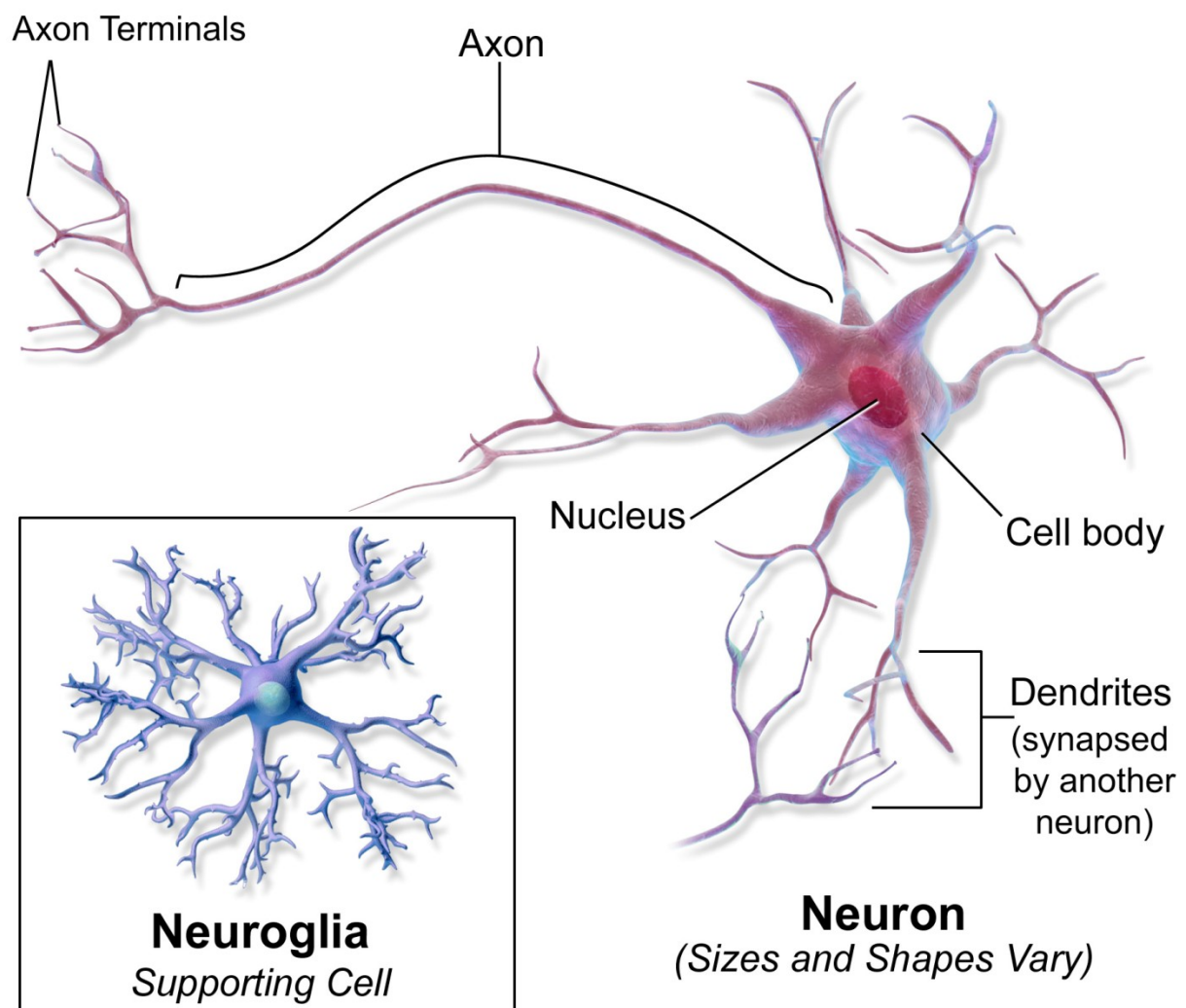
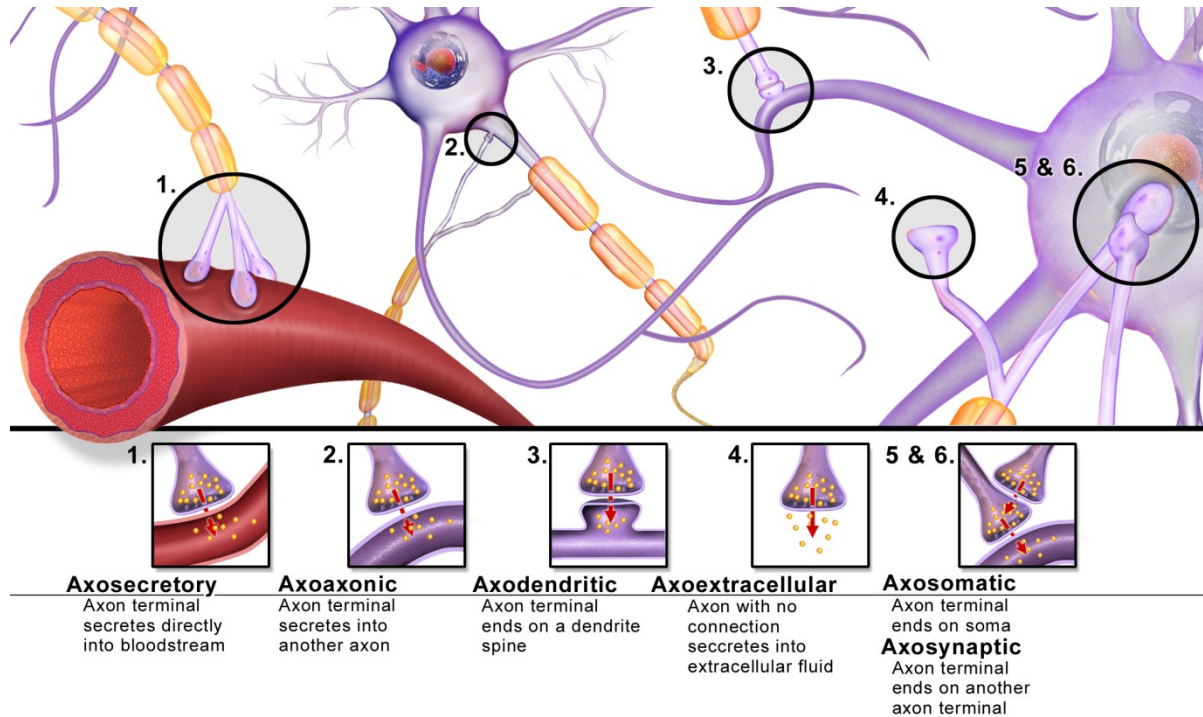


Figure 1 Nervous tissue (modified from Blausen, 2014)

The first criteria proposed to classify synapses reflected their anatomical location and type of structure targeted. The synaptic target can be a dendrite, a soma, an axon or an axon terminal, but also blood vessels or the adjacent nervous tissue (see Figure 2). In the adult brain, over 90% of glutamatergic synapses are axodendritic.



**Figure 2 Synapse types according to structure targeted (from Blaussen, 2014)**

During the last century, investigations established a classification of synapses depending on the nature of the transmission into “electrical” and “chemical” types. The former, albeit being less common in vertebrates, are present in both the Central (CNS) and Peripheral Nervous System (PNS) (Condorelli et al., 1998; Altevogt et al., 2002). In electrical synapses, the synaptic cleft is very narrow (2 to 4 nm) and ions can flow directly from one neuron to another very rapidly (in less than 0.3 ms) (Goyal and Chaudhury, 2013). Fundamentally, the electrical current can travel bidirectionally (except for rectifying synapses) through a mechanical and electrical conductive link known as “gap junction”. Vertebrate gap junctions are formed by connexins, while those of invertebrates are formed by innexins (Bennett, 2000). Gap junctions are excitatory but electrical inhibitory synapses have also been reported, first in invertebrates (i.e. septate junctions), and later in vertebrates (i.e. septate-like junctions) (Bennett, 2000; Bruzzone et al., 2003). Interestingly, the vertebrate proteins of these rare electrical inhibitory synapses are homologous with those of invertebrates (Bennett, 2000). Since electrical synapses are fast but lack gain, they are found at systems requiring fast responses such as reflexes. On the other hand,

chemical synapses have a wider synaptic cleft (20 to 40 nm) and a longer synaptic delay (typically 2 ms, ranging from 0.5 to 300 ms, at the s-EPSP ganglion) since an electrical signal is transformed into a chemical one. Moreover, mixed electrical and chemical synapses also exist (see Figure 3). Chemical transmission involves presynaptic release of neurotransmitter-containing synaptic vesicles (SVs) due to calcium influx through voltage-gated channels upon the action potential (AP) arrival in the presynapse (for AP-independent release, see section 4.2 below). Neurotransmitter detection by specialized receptors at the postsynapse can either: a) open ligand-gated ion channels –which results in rapid changes in postsynaptic membrane potential that affect the probability of the target cell to fire an AP; or b) activate slower metabotropic receptors (i.e. G protein-coupled receptors) that act through secondary messengers leading either to the opening of ion channels or to other cellular effects (i.e. protein synthesis); or c) engage both pathways simultaneously (Purves et al., 2001). Chemical synapses are mainly unidirectional, however certain retrograde trans-synaptic messengers have also been reported, including conventional neurotransmitters, gases, peptides, growth factors, and membrane-derived lipids (Regehr et al., 2009; Carta et al., 2014a).

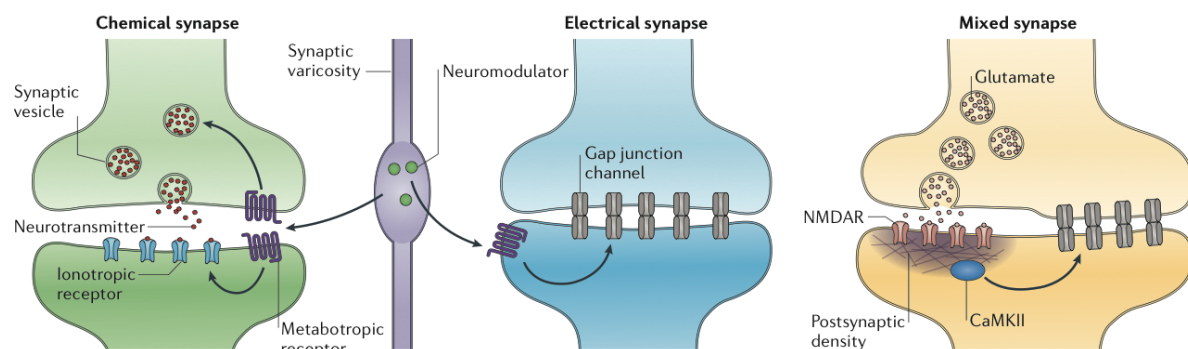


**Figure 3 Synapse types according to transmission nature (Modified from Pereda, 2014)**

Furthermore, synapses are usually classified according to their effect. The change in postsynaptic membrane potential can either depolarize (increasing the probability of AP firing) or hyperpolarize (decreasing the probability of AP firing) the postsynaptic cell, which divides chemical synapses into “excitatory” and “inhibitory”, respectively. Similarly, synapses that modulate neuronal activity via metabotropic receptors are labeled as “modulatory”. However, this classification is inaccurately used when referring to the effect caused by a particular neurotransmitter. The postsynaptic receptors and their associated channels are the ones determining the response elicited by each neurotransmitter (i.e. glutamate-gated chloride channels determine glutamate transmission as inhibitory in the invertebrate CNS).

Additionally, chemical synapses are classified on the basis of the particular neurotransmitter released. The most abundant neurotransmitters in vertebrates are two amino acids: glutamate –excitatory at over 50% of all synapses in the human brain; and  $\gamma$ -Aminobutyric acid (or GABA) –inhibitory at 30 to 40% of the synapses (Roberts, 1986; Hendry et al., 1987). Thus, in practice the terms “glutamatergic” and “GABAergic” are associated with “excitatory” and “inhibitory” transmission, respectively (for GABA excitatory role in development and co-release with glutamate see section 3.2 below). Since glutamate is a precursor for GABA synthesis (Roberts and Frankel, 1950), glutamate metabolism affects both glutamatergic and GABAergic function (Nicholls, 1989). Pure modulatory synapses represent around 10% of the synapses but are extremely diverse (see Table 1) (Nadim and Bucher, 2014). Despite the few number of pure modulatory synapses, their functional importance should not be underestimated. Furthermore, co-release of different neurotransmitters is not exceptional, but rather the rule (Trudeau and Gutierrez, 2007; Hnasko and Edwards, 2012).

However, these classifications are not sufficient. How can we differentiate among glutamatergic synapses, which make up more than half of all our synapses? Ramón y Cajal (1894) already hypothesized that the higher complexity of the functions carried out by the human brain as compared to those carried out by other animals or by the human PNS, should be reflected in a special “intraprotoplasmic structure” of brain neurons. Nowadays, there is evidence for this molecular diversity beyond the traditional neurotransmitter type classification. Differences are both qualitative and quantitative in respect to synaptic expression levels of proteins including receptor isoforms (Schwenk et al., 2014), vesicular transporters, scaffold and adhesion proteins, “guidance cue” proteins involved in neurodevelopment, “generic” signaling molecules, and “house-keeping” proteins (O'Rourke et al., 2012). Moreover, such molecular differences often correspond to differences in function (i.e. synaptic strength, kinetics or plasticity). Today, synapses are acknowledged as plastic structures, whose function depends on its own transmission history, as well as on signals from other cells. Synapses are also known to be influenced by developmental, homeostatic, pathological, and circuit remodeling events. Nevertheless, crucial aspects of synapse molecular diversity and its functional significance stand unexamined (for review of current tools in the field of molecular neuroanatomy see Pollock et al., 2014; for neurogenomics of behavioral plasticity see Harris and Hofmann, 2014).

**Table 1 Synapse types by neurotransmitter and main effect in the vertebrate CNS**

	Biomolecule	Neurotransmitter	
<b>Excitatory</b>	Amino acid	Glutamate	
<b>Inhibitory</b>	Amino acid	GABA	
		Glycine (in spinal chord)	
<b>Modulatory</b>	Amino acid	Aspartate	
		D-serine	
		Glycine	
	Ester	Acetylcholine	
	Gas*	Carbon monoxide*	
		Hydrogen sulfide*	
		Nitric oxide*	
	Ion*	Zinc* (for co-release with glutamate see 3.2 below)	
	Lipid	Endocannabinoids (i.e. anandamide)	
	Mono amine	Catecholamines	Dopamine
			Epinephrine
			Norepinephrine
		Histamine	
		Serotonin	
		Trace amines	
	Peptide	Cocaine and amphetamine regulated transcript (CART)	
		Opioid peptides (i.e. endorphins)	
		Somatostatin	
		Substance P	
		Other neuropeptides	
	Purine	Adenosine	
		ATP	

\* Consideration as neurotransmitters debated

### 1.1. Glutamatergic Synapses

Glutamatergic synapses have been extensively investigated. These studies have accumulated evidence that synaptic plasticity at this type of synapse is involved in learning and memory processes. As already mentioned, glutamatergic synapses are the most abundant in the vertebrate nervous system, where they predominantly exert an excitatory effect. Recent genomic, immunohistochemical and physiological analyses suggest a vast molecular variety and its significant implications. Nonetheless, no further molecular categorization of glutamatergic synapses has been established to date.

Despite technical limitations to precisely quantify the total number of protein types present at a canonical mammalian glutamatergic synapse, proteomic analyses of rodent brains applying large-scale mass spectrometry and subcellular fractionation have rendered vast lists. While the postsynaptic proteome contains 200 to 1,000 protein types (Peng et al., 2004; Collins et al., 2006; Dosemeci et al., 2007),



## 1. Synapses

synaptosomes consist of over 3,000 (Schimpf et al., 2005; Filiou et al., 2010), synaptic vesicle fractions comprising more than 400 protein types (Takamori et al., 2006). It seems that those types most recently added to the synaptic proteome during mammalian evolution are the ones contributing the most to synaptic diversity (Emes et al., 2008). Hence, it has been suggested an interplay between complexity and diversity (O'Rourke et al., 2012). The main components of a canonical glutamatergic synapse are described below. For clarification, the characteristics of hippocampal CA3-CA1 synapses would be considered as the canon. The use of a canon is useful for extrapolation to less studied synapses that seem comparable to CA3-CA1 synapses.

### 1.1.1. Presynapse

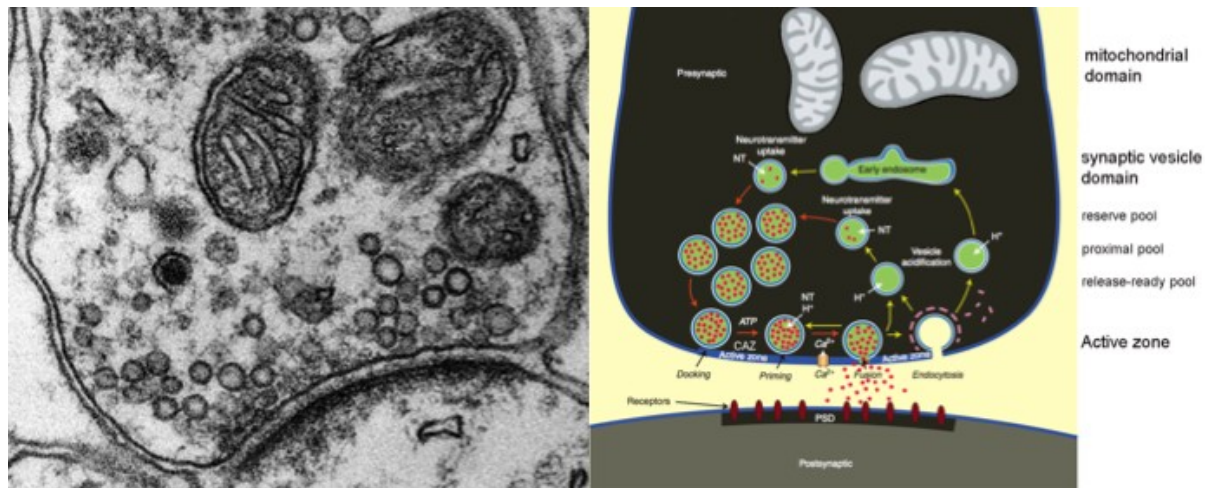


**Figure 4 Presynaptic ultrastructure (modified from Südhof and Rizo, 2011)**

The axon terminals, also called presynaptic boutons, are specialized in storing, releasing and recycling SVs. Neurotransmitters are synthesized at the axon terminal from precursor molecules transported from the soma, and subsequently packed into synaptic vesicles (Purves et al., 2001). Neurotransmitter-filled SVs are released in a regulated manner upon arrival of an AP. Following exocytosis, synaptic vesicle membranes are endocytosed to recycle SV proteins. The axon terminal is composed of three structural compartments: the active zone (AZ) (Südhof, 2012), the SV domain, and the mitochondrial domain (Garner et al., 2000; Dresbach et al., 2001).

Under the electron microscope, both sides of the synapse are seen as dark (electron dense) areas close to the membrane (see Figure 4). Thus, these ultrastructures are called presynaptic dense projection or cytomatrix at the active

zone (CAZ) (Hirokawa et al., 1989; Zhai and Bellen, 2004) and postsynaptic density (PSD) (Peters et al., 1991). The proteins composing the CAZ regulate tethering and fusion of SVs to the presynaptic membrane, which allow rapid and reliable neurotransmitter release when an action potential reaches the terminal. The active zone is the portion of the presynaptic compartment where SVs are coordinately exocytosed. The SV domain defines the region where vesicles accumulate and is further subdivided according to their distance from the plasma membrane into three functionally distinct pools (see Figure 4): the release-ready pool (RRP) –composed of fusion-competent vesicles (about 50 nm in diameter) docked or primed at plasma membrane (Jahn and Fasshauer, 2012); the proximal pool –contains 2 to 4 vesicle layers and includes SVs that seem clustered near the AZ via filamentous structures of the CAZ; and the reserve pool –those SVs stored further than 200nm from the AZ by interacting with actin filaments via synapsin proteins (Hirokawa et al., 1989; Pieribone et al., 1995; Zhai and Bellen, 2004). Finally, the furthest from the plasma membrane is the mitochondrial domain (Peters et al., 1991). Mitochondria provide ATP as energy source (Harris and Weinberg, 2012), regulate the SV cycle, and are also implicated in calcium homeostasis and neurotransmitter synthesis (Vos et al., 2010). Nonetheless, there are synapse-specific differences in presynaptic architecture; a particularly pronounced case is the ribbon structure at sensory synapses (Ramakrishnan et al., 2012).

### 1.1.2. Postsynapse

As already mentioned, the most common postsynaptic targets in the adult brain are dendritic spines. The dendritic spines of postsynaptic cells are structurally specialized to sense neurotransmitters released into the presynaptic cleft. Neurotransmitter detection is carried out by receptors abundant in the portion of postsynaptic membrane facing the presynaptic active zone. The PSD is formed by cytoskeletal and regulatory proteins, including some that interact with the cytoplasmic domain of ion channels (Ziff, 1997). The PSD is conveniently located to regulate the intracellular ionic flux and second messenger cascades initiated by neurotransmitters. A great heterogeneity exists also at the postsynaptic level including receptor regional diversity of AMPA (Schwenk et al., 2014), kainate (Carta et al., 2014b) and NMDA receptor isoforms (Monaghan et al., 1983; Bischofberger and Jonas, 2002).



## 1.1.3. Synaptic Cleft

The synaptic cleft is not a gap where neurotransmitters are released into the vacuum, but a rather complex structure where the extracellular matrix, astrocytic processes, and cell-adhesion molecules (CAMs) that bridge the pre- and the postsynaptic cells, interact. The extracellular matrix is a microenvironment around neurons and glial cells, which affects neuronal development as well as activity (Soleman et al., 2013). During the former, the extracellular matrix supports, while being developed itself, an array of processes including: neuro-, glio-, and synaptogenesis, cell migration, axon guidance, and neurite outgrowth (Bandtlow and Zimmermann, 2000; Faissner et al., 2010). During adulthood, the extracellular matrix impact ranges from cell survival and plasticity, to regeneration (Meredith et al., 1993; Grimpe and Silver, 2002; Dityatev et al., 2010; Kwok et al., 2011) (see Figure 5)). Neurons and glial cells in turn, secrete a range of molecules that become part of the extracellular matrix (Soleman et al., 2013). Secondly, among glial cells, astrocytes play a particularly important role at the synaptic cleft. Astrocytic processes are in close association with most glutamatergic synapses, the hippocampal mossy fiber cleft being one of the few reported to be astrocyte-free (Rollenhagen et al., 2007). The exact physiological impact of astrocytes on the properties, function, and plasticity of synapses is still under scrutiny (for review see Bernardinelli et al., 2014).

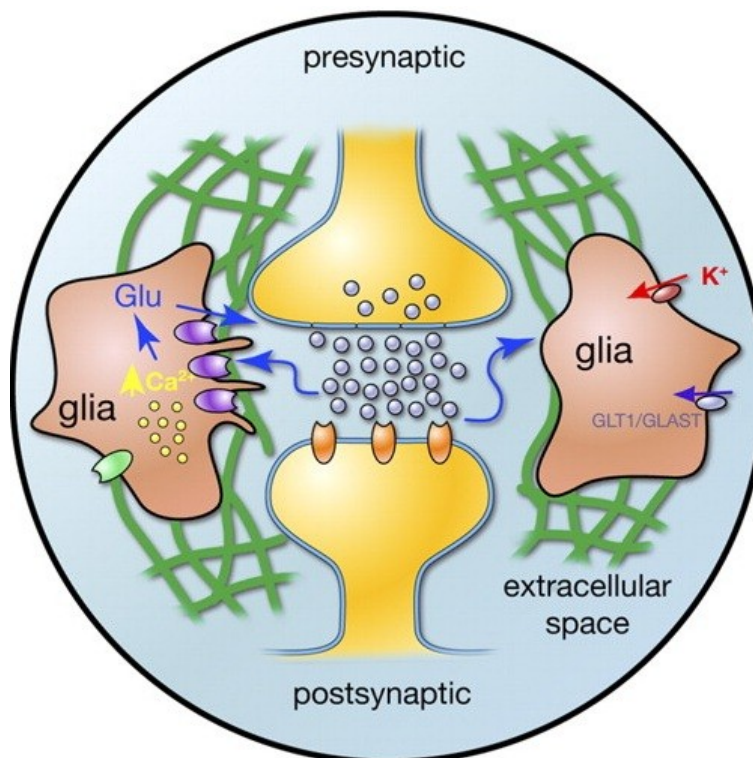


**Figure 5** Transmission at the quadripartite synapse (from Sykova and Nicholson, 2008)

The complex information processing carried out by the nervous system is achieved by the network of connections between neurons. There are two ways of neuronal communication: one relies in electrochemical transmission, and the other on membrane-bound intersynaptic proteins. CAMs are crucial not only for synapse formation, but also for an array of processes that range from cell migration and neurite outgrowth, to axonal pathfinding and target recognition. Different CAMs are particularly enriched in the vertebrate CNS and play a role in synaptic stabilization and modulation (see Figure 6) (for review see Williams et al., 2011).

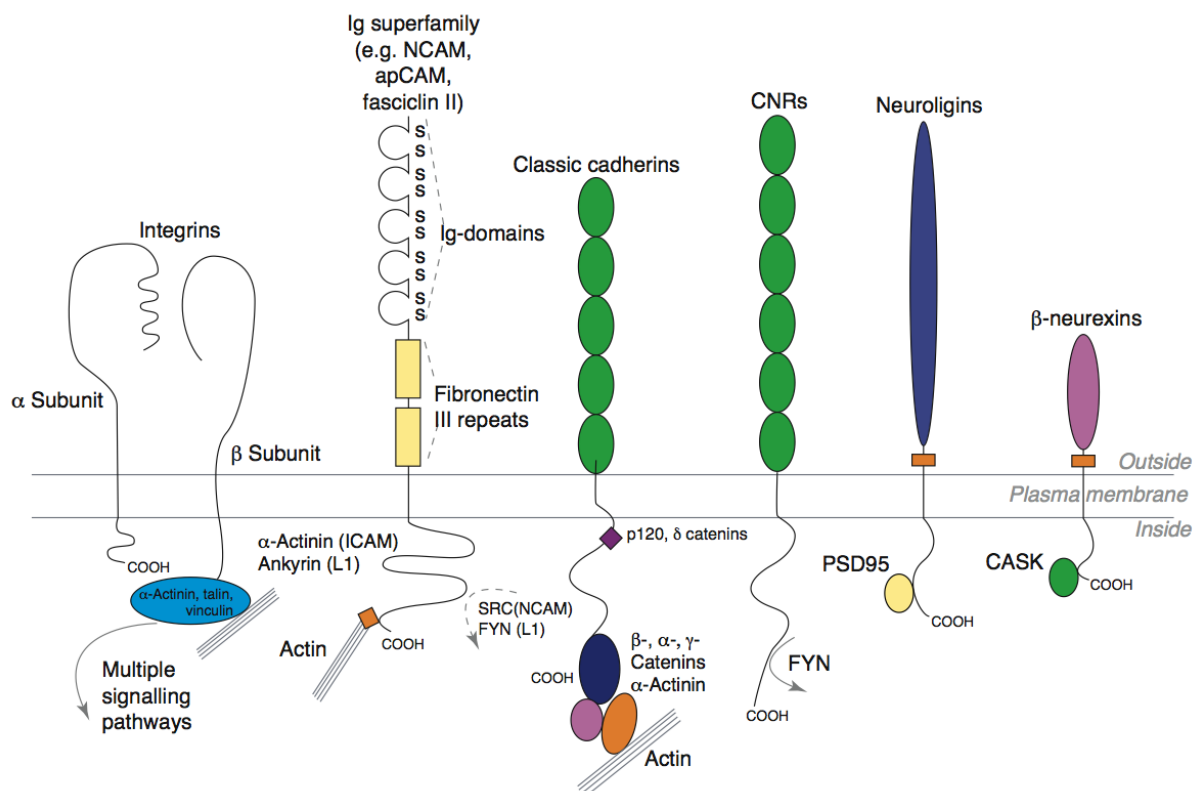


**Figure 6 Structure of neuronal CAMs (from Benson et al., 2000)**

## 2. Neurotransmitter Release

The 2013 Nobel Prize in Physiology or Medicine was awarded to three scientists –Randy Sheckman, James E. Rothman and Thomas C. Südhof- for their work on the machinery regulating vesicle traffic, including the machinery regulating synaptic vesicles exocytosis. At chemical synapses, neurotransmitter release relies on SV exocytosis. This process is mediated, like all other intracellular membrane fusion events, by SNARE (for “soluble *N*-ethylmaleimide-sensitive factor attachment protein receptor”) proteins, which are coordinated by the SM (for “Sec1/Munc18-like”) protein Munc18-1. Besides the core SNARE and SM proteins, calcium-dependent fusion is triggered by a sensor protein (i.e. synaptotagmin-1), and complex assembly is orchestrated by an array of proteins, as well as their interaction with the membrane lipids.

### 2.1. Neuronal Exocytotic Machinery

#### 2.1.1. SNARE and SM Proteins

SNAREs are small (14-40 kDa) membrane-bound proteins that contain the 60-70 amino-acid  $\alpha$ -helical coiled-coil domain called the SNARE motif (Jahn and Scheller, 2006). They are called “v-SNAREs” when they are at vesicles (v-SNAREs) and “t-SNAREs” when they are at the target membrane. A more accurate nomenclature names them as R- and Q-SNAREs according to the conserved arginine or glutamine residue, respectively (Weber et al., 1998). At the synapse, t-SNAREs are always Q-SNAREs, and v-SNAREs are mostly R-SNAREs (although vti1a, a Q-SNARE, can also be found on vesicles). The interaction between opposed v- and t-SNAREs impels the formation of a trans-SNARE complex, or SNAREpin, in which four SNARE motifs zipper into a four-helix bundle that brings the membranes together and ultimately catalyzes their fusion (Söllner et al., 1993; Weber et al., 2010) (see Figure 7).

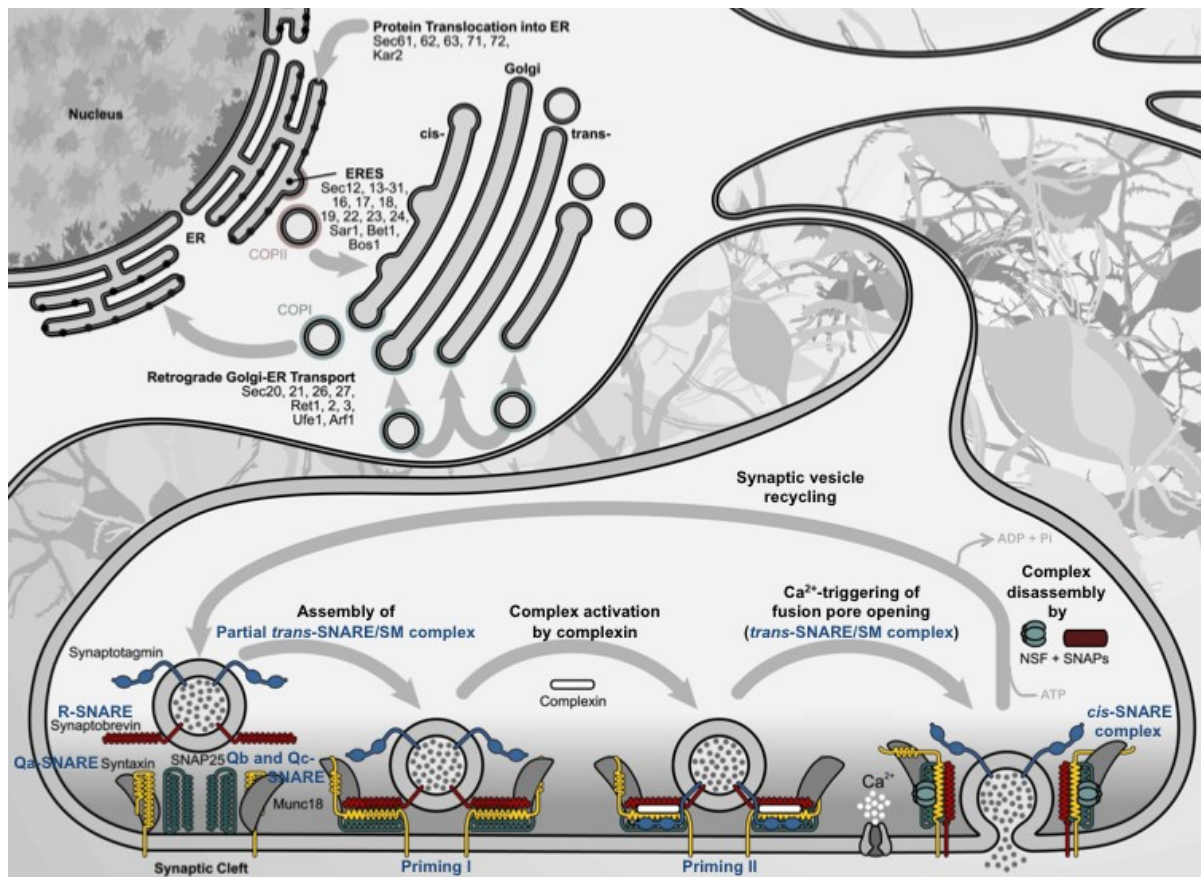


**Figure 7 SNARE/SM protein cycle (modified from Brose, 2014)**

All eukaryotes express at least one member of each of the 4 different SM protein families: Sec1/Munc18, Sly1, Vps33 and Vps45 (for review see Toonen and Verhage, 2003). The SM protein present at mammalian synapses is Munc18-1, which is soluble and expressed throughout the brain (Garcia et al., 1994). Mice lacking this protein exhibit normal embryonic development, but no regulated neurotransmitter exocytosis, which causes death at birth (Verhage et al., 2000). This suggests that Munc18-1 is a positive regulator of release, while other studies report a negative regulation, this paradox might be explained by the interaction with syntaxin (reviewed in Archbold et al., 2014). Q-SNARE syntaxins possess a Habc domain, which in combination with SM proteins inhibits the formation of SNARE complexes (Burkhardt et al., 2008; Gerber et al., 2008). The Habc domain by itself can inhibit interactions between SNARE core domains by folding onto one of them, which does not preclude formation of the SNARE complex but it alters the assembly kinetics (Fasshauer et al., 2002; Vivona et al., 2010). Moreover, other N-terminal regulatory protein domains (like the Longin domain) can also modulate SNARE complex formation (Hong, 2005; Jahn and Scheller, 2006; Schäfer et al., 2012; Di Sansebastiano, 2013).

## 2. Neurotransmitter Release

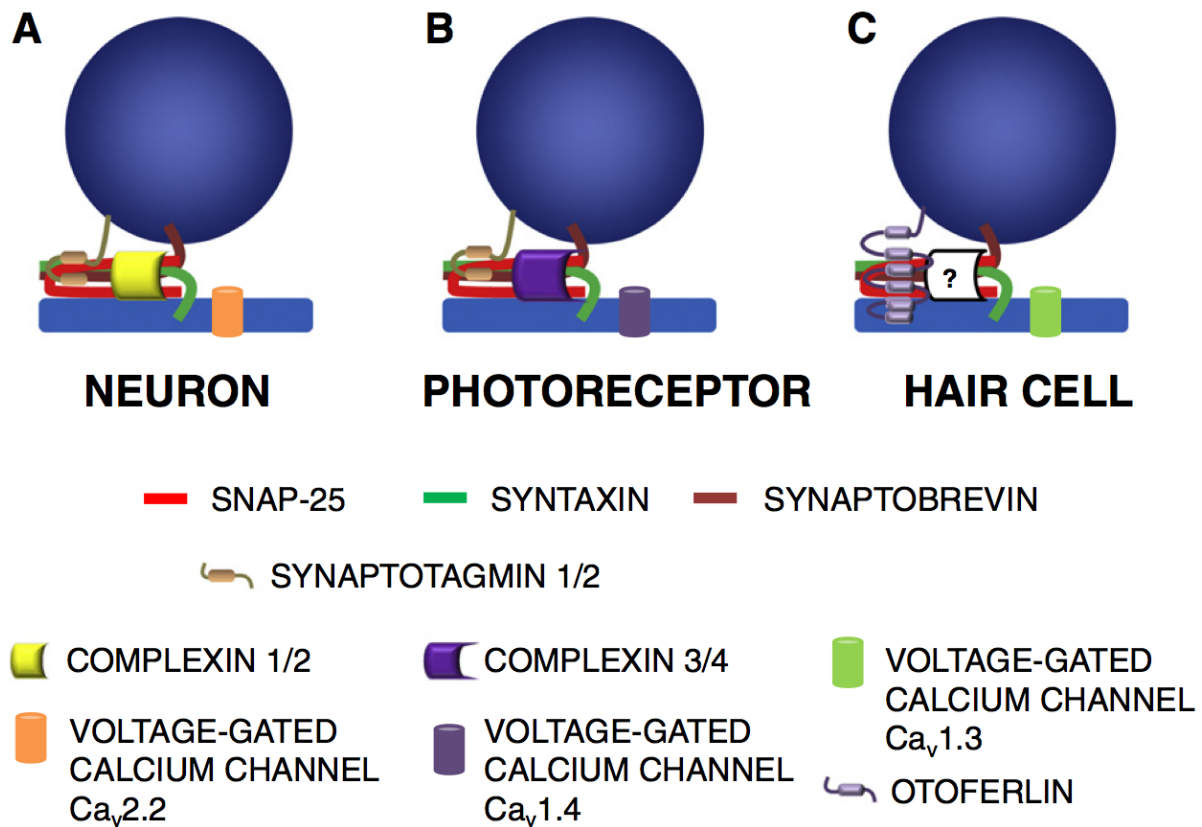


**Figure 8 SNARE complexes in neuronal and sensory cells (from Ramakrishnan et al., 2012)**

The human genome encodes 38 SNAREs, with numerous members in each subfamily, which results in a large array of possible combinations (Dacks, 2007; Gordon et al., 2010) (see Table 2). Particular SNARE collections reside predominantly in specific subcellular compartments, where they are specialized for individual intracellular fusion reactions (Jahn and Scheller, 2006; Kasai et al., 2012). Furthermore, sensory cells use different SNARE collections (Ramakrishnan et al., 2012) (Figure 8). In addition, there are redundancies in fusion pathways, such as a SNARE complex which functions at multiple compartments, or several SNARE complexes mediating the same membrane fusion (see Table 2).

**Table 2 Contribution of SNAREs, *sytl* and priming proteins to different types of exocytosis (from Kasai et al., 2012)**

	Synaptic Vesicles					Chromaffin Cells ( $Ca^{2+}$ -primed)	$\beta$ Cells	Acinar Cells	Mast Cells
	Sync	HTSS	Async	Tonic	Spont				
Time constant	1 ms		100 ms	10 s	1000 s	30 ms	1 s	10 s	10 s
VAMP2	++ <sup>a</sup>	++	++	++	+	+ <sup>k</sup>	+ <sup>r</sup>	ND <sup>z</sup>	— <sup>cc</sup>
SNAP25	++ <sup>b</sup>	++	++	++	—	++ <sup>i</sup>	++ <sup>s</sup>	— <sup>z</sup>	— <sup>dd</sup>
Munc18a	++ <sup>c</sup>	++	++	++	++	++ <sup>m</sup>	+ <sup>t</sup>	— <sup>z</sup>	ND
Munc13-1	++ <sup>d</sup>	++	++	++	++	—+ <sup>n</sup>	+ <sup>u</sup>	ND	ND
RIM	++ <sup>e</sup>	+	++	+	+	ND	+ <sup>v</sup>	ND	ND
CAPS	++ <sup>f</sup>	++	++	— <sup>j</sup>	+ <sup>f</sup>	+ <sup>o</sup>	+ <sup>w</sup>	ND	ND
Syt1	++ <sup>g</sup>	—	—	+ <sup>i</sup>	Inhibit <sup>j</sup>	+ <sup>p</sup>	— <sup>x</sup>	ND <sup>aa</sup>	— <sup>ee</sup>
Complexin	+ <sup>h</sup>	+	—	+	ND	+ <sup>q</sup>	+ <sup>y</sup>	ND <sup>bb</sup>	+ <sup>ff</sup>



v-SNAREs are classified into the following subfamilies: the “longins”, which contain the N-terminal longin domain (LD) extension of ~120 residues, and the “brevins”, which are shorter (Filippini et al., 2001) (see Figure 9, notice the similarity of the transmembrane and R-SNARE domains of tomosyn). The main SV SNARE is the brevin synaptobrevin2/VAMP2 (for “vesicle-associated membrane protein” 2). Its canonical partners at the plasma membrane are syntaxin1 and SNAP-25. In the absence of VAMP2, evoked and spontaneous neurotransmission are reduced to around 1% and 10% of control, respectively (Schoch et al., 2001).

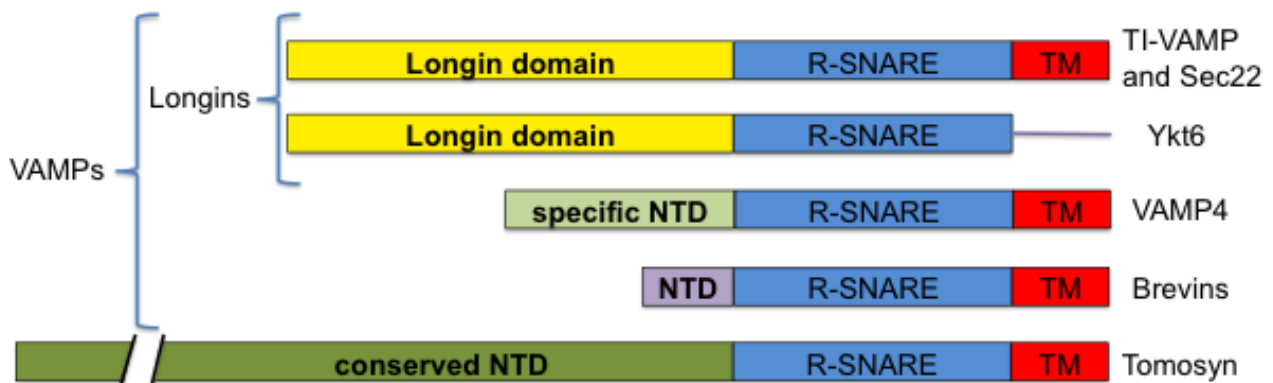


**Figure 9 Domains of VAMPs and tomosyn (modified from Rossi et al., 2004)**

In normal physiological conditions, two VAMP2 molecules are sufficient for SV exocytosis (Sinha et al., 2011). A prototypic SV contains ~70 VAMP2 copies, but also lower levels of noncanonical v-SNAREs such as VAMP1, Vti1a, VAMP4 and VAMP7 (also called “tetanus neurotoxin-insensitive” or TI-VAMP) (Takamori et al., 2006) (see **Figure 10**). The expression of these alternative v-SNAREs probably explains the residual synaptic transmission in VAMP2 KO mice. A recent report involves VAMP1 in a subpopulation of hippocampal neurons that displays release when VAMP2 is absent (Zimmermann et al., 2014). The remaining debate is whether low levels of these v-SNAREs play a role in SV exocytosis in the presence of VAMP2. The cleavage of VAMP2 by tetanus toxin (TeNT) has been reported to modify coupling between channels and release-competent vesicles at the Calyx of Held synapse (Sakaba et al., 2005). The existence of SV populations expressing different v-SNAREs, or at different ratios, has been proposed to account for distinct forms of SV exocytosis (for review see Ramirez and Kavalali, 2012). However, others claim a unique origin for SVs, independently of whether their mode of release is evoked or spontaneous (for review see Kaeser and Regehr, 2014). Given the number of different proteins expressed on a synaptic vesicle, together with the existence of isoforms and/or splice variants, the chances that all SVs are homogeneous seem

extremely low. Even if all SVs were identical in a given synapse, the great array of possible interactions with other proteins (t-SNAREs or regulatory proteins), and membrane lipids, would render them phenotypically diverse.

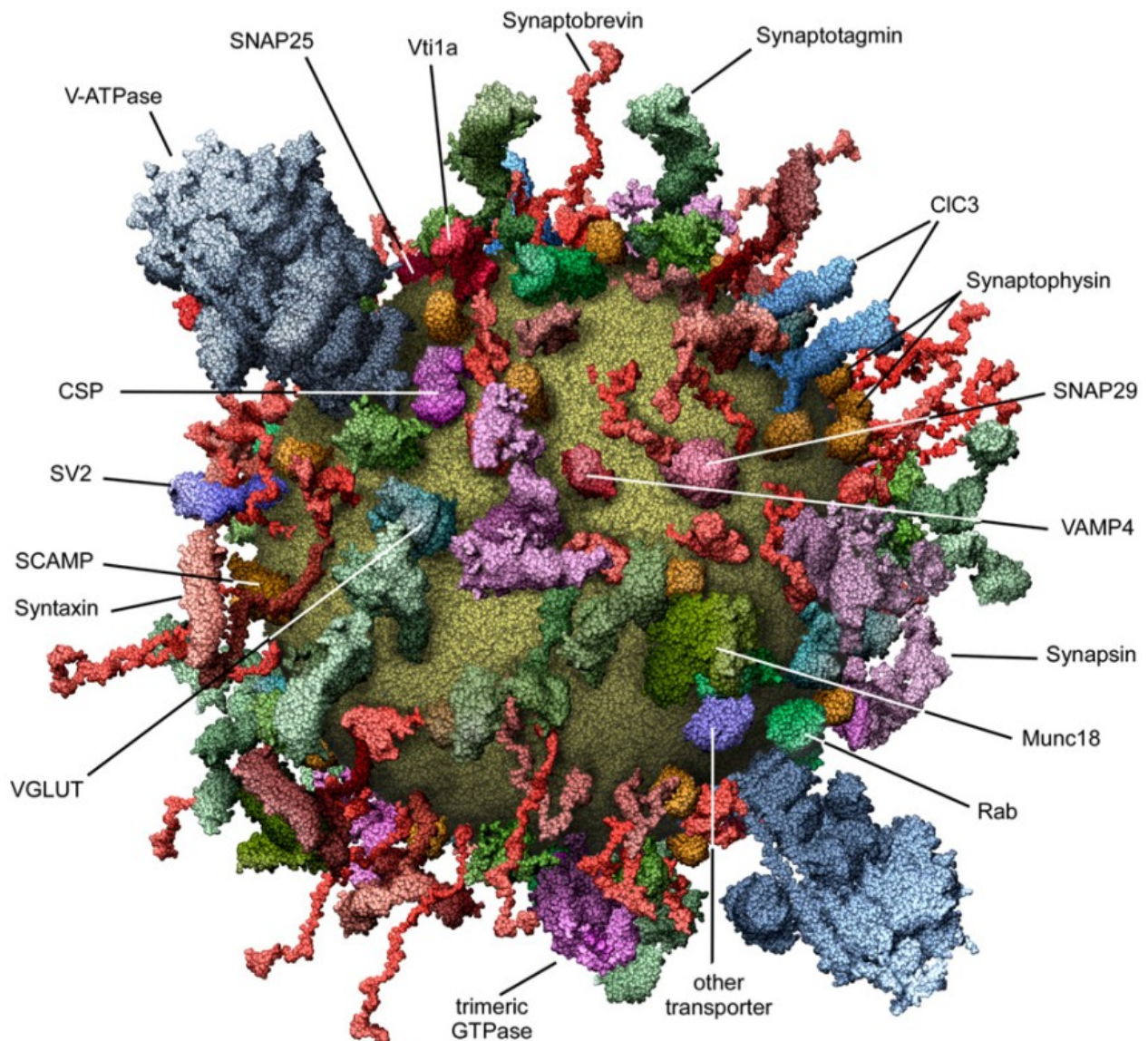


**Figure 10 Molecular model of an average SV (from Takamori et al., 2006)**

### 2.1.2. TI-VAMP/VAMP7

VAMP7 is encoded by the SYBL1 gene, the first pseudoautosomal gene ever reported to undergo X and Y inactivation, posing an exception to the already exceptional pseudoautosomal genes (D'esposito et al., 1996). VAMP7 is a longin that was first shown to associate with SNAP-23 and syntaxin3 in clostridial neurotoxin-resistant exocytotic processes at the apical plasma membrane of epithelial cells (Galli et al., 1998; for the use of clostridial neurotoxins to probe neurotransmission see Prashad and Charlton, 2014; Popoff and Poulain, 2014).

VAMP7 has been reported to mediate lysosomal and granule exocytosis in several cell types (Chaineau et al., 2009) including neurons (Burgo et al., 2012). Depending on the cell type, VAMP7 can interact with several t-SNAREs (syntaxin1, 3, 4, 6, 7, 8 and 10; SNAP-23, -25 and -29; and Vti1b), but neither with syntaxin 13, nor 16 (for review see Rossi et al., 2004). Besides t-SNAREs, VAMP7 also binds to other partners (see Figure 11).

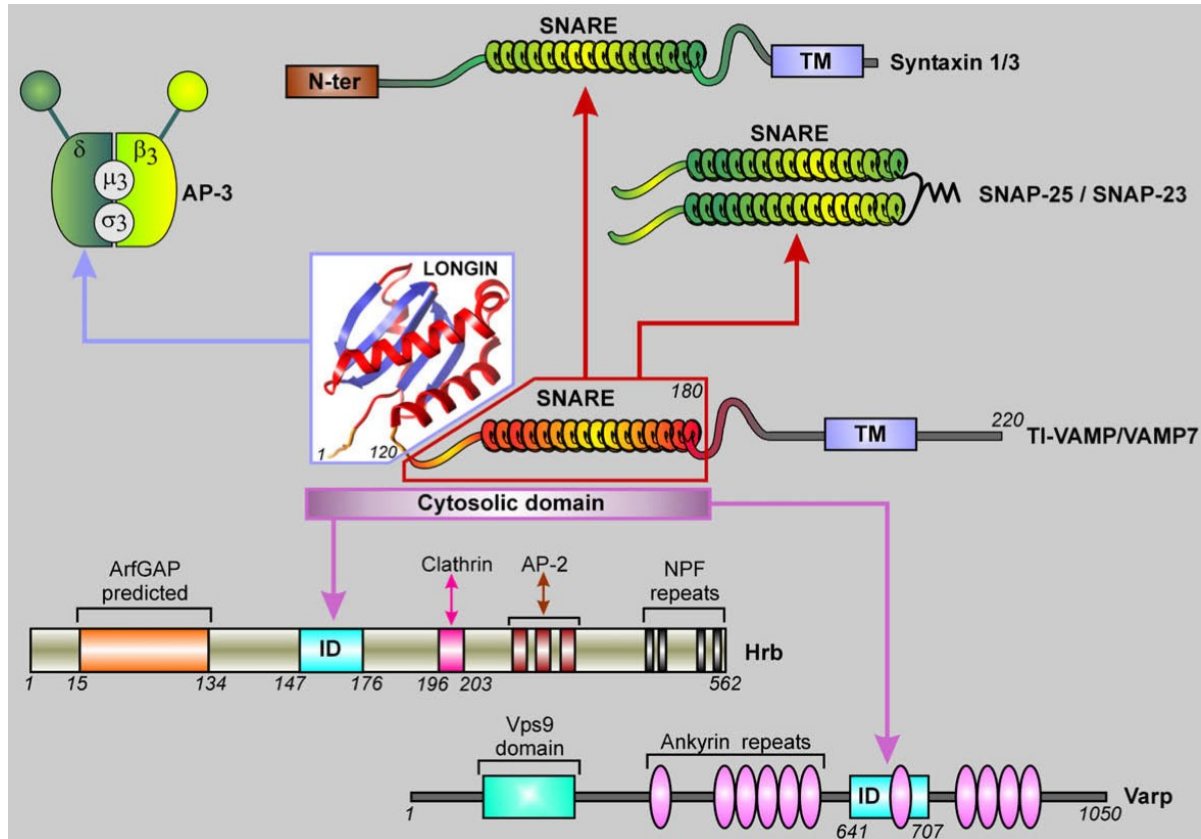


**Figure 11 Partners of TI-VAMP (from Chaineau et al., 2009)**

VAMP7 is the SNARE of secretory lysosomes contributing to ATP secretion from astrocytes (Verderio et al., 2012). Furthermore, VAMP7 localizes to axons and dendrites during development (Coco et al., 1999), where it has been shown to be important in neurite growth in cultured neurons and *in vivo* (Alberts et al., 2003; Gupton and Gertler, 2010; Heimer-McGinn et al., 2013). In the adult brain, VAMP7 is enriched in a subset of nerve terminals, particularly at the mossy fibers in the CA3 region of the hippocampus (Muzerelle et al., 2003). The LD of VAMP7 targets it to SVs by binding to the  $\delta$ -subunit of the clathrin-coat AP-3 (AP3 $\delta$ ) (Scheuber et al., 2006). In mocha mice, which lack AP3 $\delta$ , SVs do not contain VAMP7 and the zinc-transporter ZnT3 –among other cargos (see Figure 12), and the SV and RRP size have been reported to be increased (Danglot and Galli, 2007; Newell-Litwa et al., 2010). The LD also inhibits the formation of SNARE complexes (Martinez-Arca et al.,



2003). Thus, VAMP7 has a lower capacity than VAMP2 to assemble in SNARE complexes. Decreased membrane fusion efficiency due to the LD affects neurite outgrowth (Martinez-Arca et al., 2000; Martinez-Arca et al., 2001), as well as SV release (Hua et al., 2011; Burgo et al., 2013). VAMP7-mediated exocytosis relies on tyrosine 45 phosphorylation by c-Src kinase, which happens after treatment with insulin but not after depolarization or intracellular calcium rise (Burgo et al., 2013).

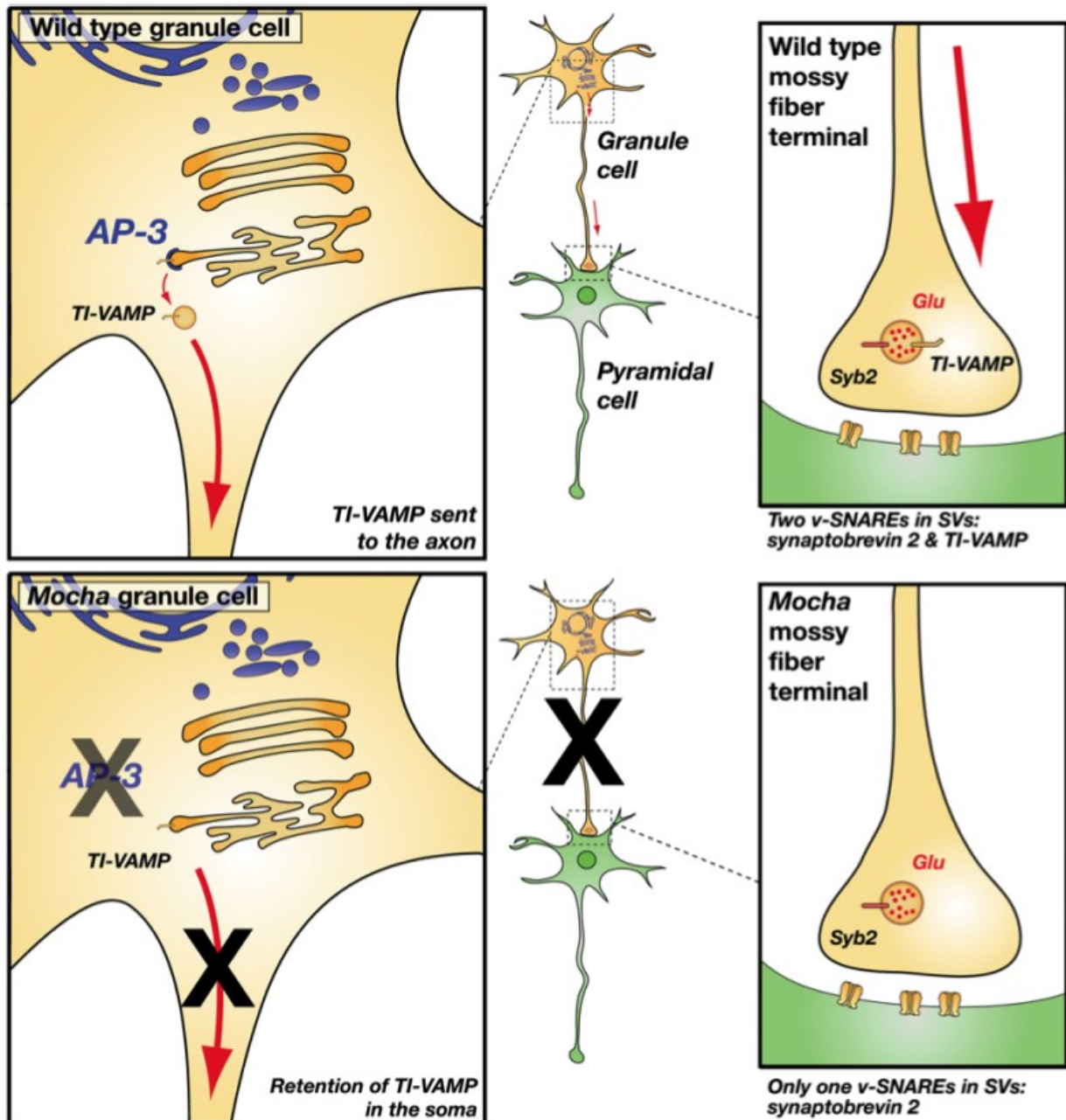


**Figure 12 Targeting of TI-VAMP in WT and mocha mice (modified from Danglot and Galli, 2007)**

VAMP7-containing SVs remain in a pool reluctant to fuse, and which seems to engage preferentially in spontaneous neurotransmitter release (Scheuber et al., 2006; Hua et al., 2011; Ramirez et al., 2012). Recently, Reelin has been reported to enhance such spontaneous release in an action potential-independent manner (Bal

et al., 2013). Here, we set out to analyze VAMP7 function in neurotransmitter release by characterizing basal and evoked transmission in a knock-out mutant mouse. Loss of VAMP7 in mice does not cause major developmental or neurological deficits (Sato et al., 2011; Danglot et al., 2012), but it has been associated with increased anxiety-related behavior (Danglot et al., 2012).

### 2.1.3. Calcium Sensors

Neurotransmitter release evoked by an incoming AP also requires a calcium sensor. In mammals, calcium is detected by one of the eight, often co-expressed, C2 domain-containing proteins identified so far (see Figure 13) (Walter et al., 2011). The two most remarkable synaptic calcium sensors are Synaptotagmin-1 (syt1) and doc2, but whether they act in parallel or sequentially remains debated (Walter et al., 2011; Walter et al., 2013). On the one hand, calcium sensors are assumed to inhibit/clamp spontaneous release at rest; on the other hand, they are thought to trigger exocytosis upon calcium activation. Besides the sensor, calcium channels and buffers, and internal calcium sources can regulate release too (Mochida et al., 2008). Channels can be either tightly or loosely coupled, and different types can be expressed (Catterall and Few, 2008). For a review on calcium-dependent mechanisms of CNS presynaptic control see Rusakov, 2006.

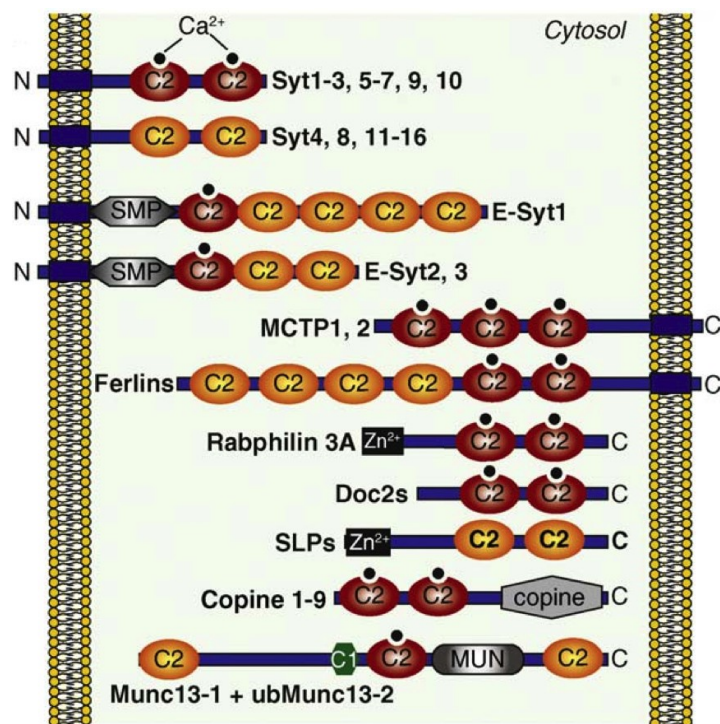


**Figure 13.** C2 domain-containing proteins in mammals (from Pang and Südhof, 2010)

### 2.1.4. Regulatory Proteins

Besides SNARE proteins, Munc18-1, syt1, and calcium-dependent mechanisms, there is a plethora of active zone proteins that can regulate synaptic release at different stages, including: Munc13, RIM-1alpha, CAPS, Complexins, NSF & SNAPs, rabphilin, Rab3, tomosyn, RIM-BP, alpha-liprin, CASK, Bassoon, Piccolo, VGLUTs, ELKS, Mint, AP2, clathrin, dynamin, or calmodulin (Chua et al., 2010). The amount of proteins expressed by SVs is for instance very high (see Figure 10). Reviewing the accumulated knowledge on regulatory proteins is beyond the scope of this work (for review see Südhof and Rizo, 2011; Cornelisse et al., 2012).

### 2.1.5. The Role of Lipids

Obviously, the lipids composing the plasma and vesicles membranes also play a role in neurotransmitter release. The classical view pictures lipids as fusion-averse that only merge after the action of certain proteins. However, this has been challenged in a study on sphingosine, which is reported to push reluctant VAMP2 to cooperate with protein complexes, and thus stimulate fusion (Darios et al., 2009, commented in Verhage and Meer, 2009). Moreover, extended synaptotagmins have been reported to mediate transfer of lipids between the endoplasmic reticulum and the plasma membrane in a calcium-regulated manner and dependent on phosphoinositides (Giordano et al., 2013). Diacylglycerol, a metabolite of this type of lipids, enhances secretion by activating various presynaptic signaling cascades that are reciprocally influenced (Wierda et al., 2007). Overall, understanding the interactions between lipid domains and protein complexes is needed for a complete theory of neurotransmitter release.

## 2.2. Types of Release and Vesicle Pools

There are two main release modes: evoked and spontaneous. The former can be further dissected into synchronous and asynchronous depending on the delay between stimulation and fusion –i.e. synchronous within few milliseconds, and asynchronous persisting for tens of milliseconds to tens of seconds (see Figure 14).

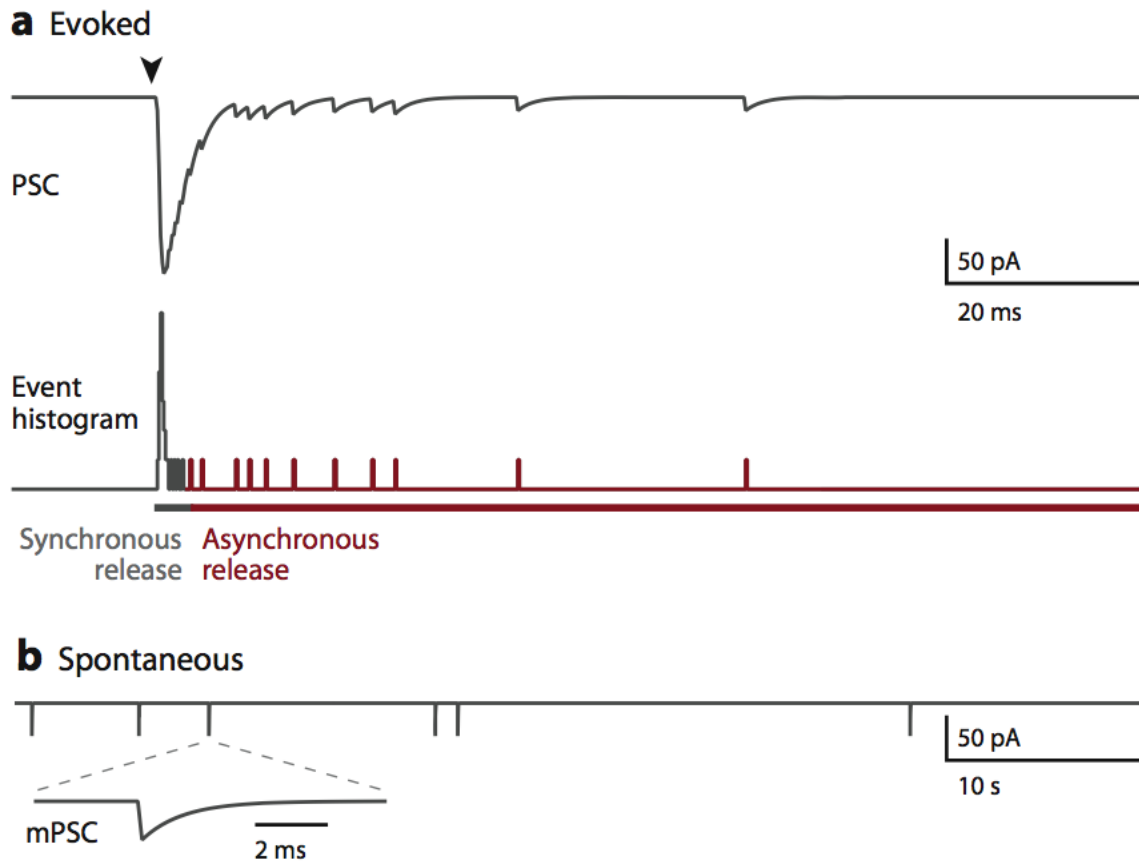


**Figure 14** Modes of synaptic release illustrated with simulated data (from Kaeser and Regehr, 2014)

Some studies attribute a specific vesicle pool to each release mode (Fredj and Burrone, 2009; Chang et al., 2010; Melom et al., 2013), while others claim a unique vesicle pool to be responsible for all release modes (Wilhelm et al., 2010; Kaeser and Regehr, 2014; Loy et al., 2014). Besides the 3 structural pools mentioned in section 1.1.1 above (Denker and Rizzoli, 2010), many molecular differences have been reported to account for release modes including VGLUT expression (Weston et al., 2011), ZnT3 expression (Lavoie et al., 2011), dependence on calcium channels (Goswami et al., 2012), dependence on calcium sensors (Walter et al., 2011; Walter et al., 2013), dependence on G-protein-coupled receptors (Vyleta and Smith, 2011), dependence on SV recycling pathways (Chung et al., 2010), or vSNARE expression (Hua et al., 2011; Raingo et al., 2012; Ramirez and Kavalali, 2012; Ramirez et al., 2012) (see Figure 15). Whether these difference translate into functional subpools is an on-going debate. Finally, inter-synaptic vesicle sharing has also been reported (Staras, 2010).

## 2. Neurotransmitter Release

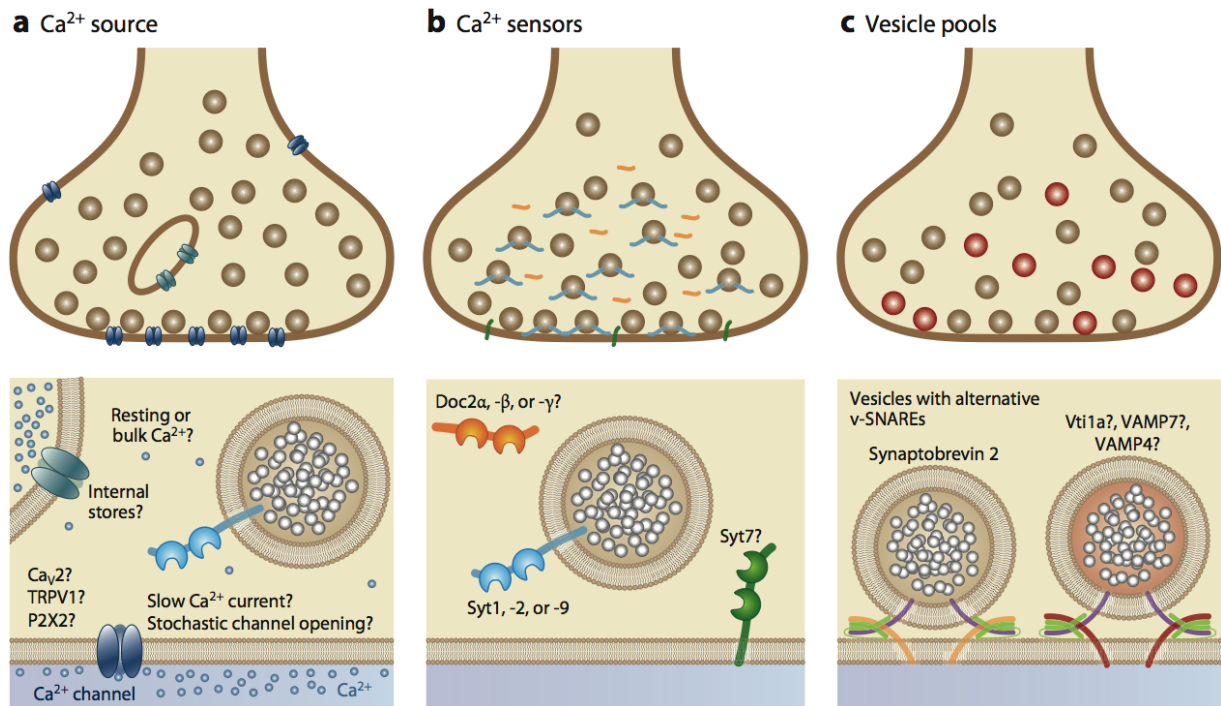


**Figure 15** Representation of certain molecular determinants proposed for different release modes (from Kaeser and Regehr, 2014)

### 3. Hippocampal Formation

The hippocampus was named by the neuroanatomist Julius Caesar Aranzi (1564) after its resemblance to a seahorse (from the Greek ιππος = horse, and καμπος = sea monster). Its elongated shape has been compared also to a banana and a ram's horn, the latter leading to the latin denomination for hippocampal subregions as "Cornu Ammonis" (CA) –in association with the ram's horns of the ancient Egyptian god Ammon. The hippocampus belongs to the limbic system and is located in the medial temporal lobe. Vladimir Bekhterev noted in 1900 the hippocampus involvement in memory after studying the brain of a patient who became amnesic after a bilateral lesion. This observation remained neglected until Scoville and Milner's study (1957) of Henry Molaison's amnesia after bilateral hippocampal removal intended to treat his epilepsy (for an update on HM's case see Annese et al., 2014). Specifically, the hippocampus is involved in the formation of new memories, and in the consolidation of previous ones, playing an important role in pattern separation and completion (Nakashiba et al., 2012). Besides its role in learning and memory, the hippocampus is also important for spatial navigation, as it became clear with the discovery of place cells in rats (O'Keefe and Dostrovsky, 1971) –place cells are neurons that fire at high rates in a particular location in the environment; or the larger hippocampal size of London taxi-drivers (Maguire et al., 2000). Another particularity of the hippocampus is its capability of generating new nerve cells into adulthood (Altman, 1963). This process, known as "adult neurogenesis", is restricted in mammals to the subgranular zone of the hippocampal dentate gyrus, and the subventricular zone –cells born in this region migrate to the olfactory bulb in rodents, but in humans there is little neurogenesis in the olfactory system (Brus et al., 2013). Furthermore, the hippocampus is one of the most studied regions of the brain due to its well-defined cellular architecture, which makes it convenient for physiological research at the synaptic and network level.

#### 3.1. Circuitry and Functions

The first functional description of hippocampal circuits was provided by Santiago Ramón y Cajal at the end of the 19th century from mere anatomical observation under a monocular microscope and the use of a several staining methods (see Figure 16). Since then, this structure has been the subject of an immense literature. With a scattered drawing of a transverse section, Ramón y Cajal depicted the structure and all the pathways of the hippocampal circuit, establishing



### 3. Hippocampal Formation

the principle of neuronal dynamic polarization: a neuron receives signals at the dendrites and soma, and transmits them unidirectionally down the axon (although exceptions exist: dendrites as output, synapses on axons). The hippocampal formation comprises the Cornus Ammonis (divided in four regions: CA1 to CA4), the dentate gyrus, the subiculum and the entorhinal cortex (EC). The perforant path fibers arise from layer II of the EC and synapse onto the granule cells of the dentate gyrus (follow arrows in Figure 16). The granule cells' mossy fibers (MFs) in turn, synapse onto CA3 pyramidal cells. Then, schaffer collaterals project from CA3 through the stratum radiatum to synapse onto CA1 pyramidal cells, which finally send their axons to the subiculum.

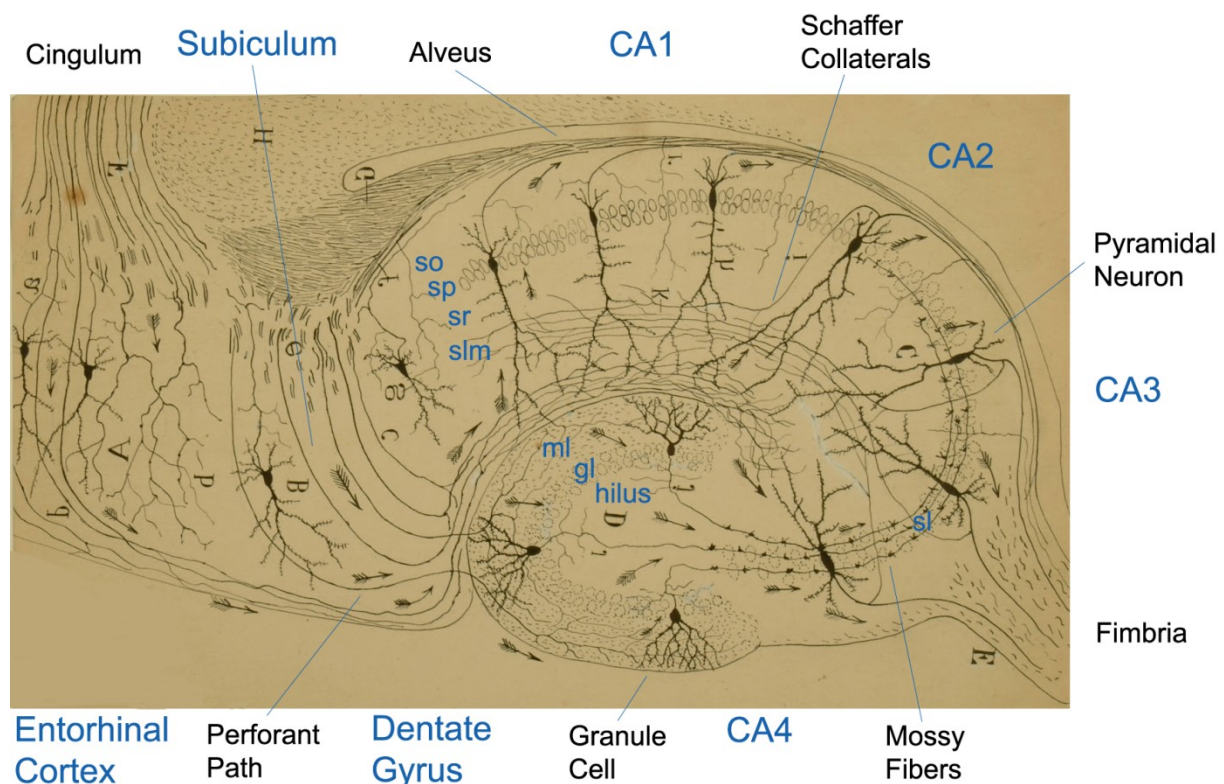


**Figure 16** Diagram of hippocampal structure and connexions (modified from Ramón y Cajal, 1911)

Recent discoveries have confirmed and completed Cajal's hippocampal circuit with the following connections: EC layer II to GCs, but also to CA3 and CA2 pyramidal cells; EC layer III to CA1 and subiculum; GCs to Mossy cells and vice versa (Scharfman, 2013); GCs to CA4 and CA2 pyramidal cells; GCs in the CA3 area (Szabadics et al., 2010); CA3-CA3 recurrent connections (Associational/Commissural or A/C) (Miles and Wong, 1986; Le Duigou et al., 2014); CA3 to GC backprojections (Scharfman, 2007); and CA2 to CA1 pyramidal cells (Kohara et al., 2013). Besides these excitatory pathways, there are numerous inhibitory interneurons (INs), estimated to be 20% of all cells in the hippocampus (Amaral et al., 1990). The INs

### 3. Hippocampal Formation

form intricate networks between each other and the excitatory cells (i.e. see feedback and feedforward inhibition in section 3.2 below and Figure 19C), which profoundly affect the physiology of the circuit (Mcbain and Kauer, 2009). For instance, GABAergic interneurons control the *in vitro* generation of oscillatory activity, like gamma oscillations, in hippocampal networks (Traub et al., 2004, but see also control of gamma oscillations by gap junctions between CA3 pyramidal cell axons).

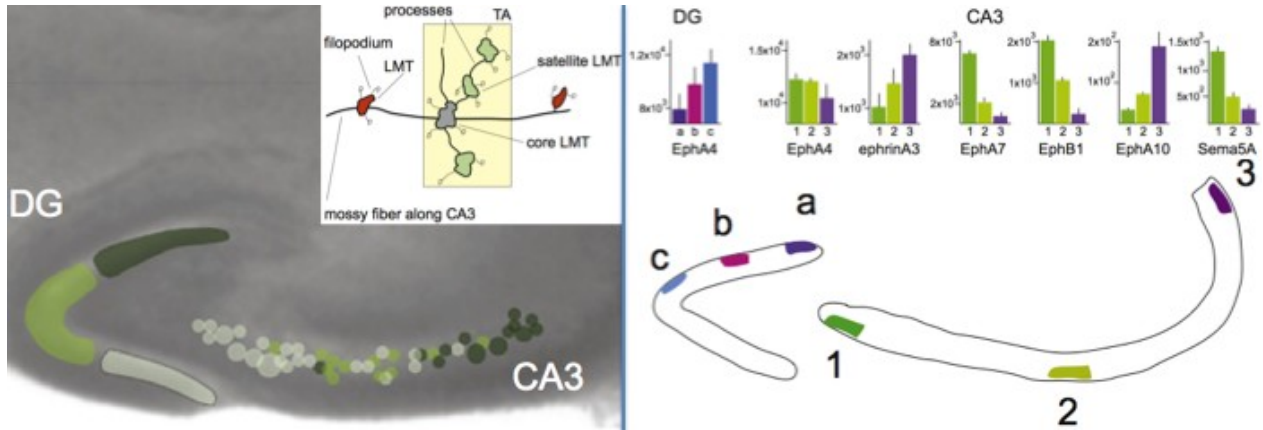


**Figure 17** Topographic clustering *in vivo* of GC somas and their Terminal Arborizations (TAs) of core and satellite Large Mossy Terminals (LMTs) (left) and graded guidance molecule expression along the juvenile DG and CA3 (modified from Galimberti et al., 2010)

The hippocampus has been divided into subregions according to genetic differences (Thompson et al., 2008). Gene expression has helped in dissecting topographical clusters of subfield-interconnections in DG-CA3 (Galimberti et al., 2010; see Figure 17), while CA1 cell-type-specific differences exist for CA3 and CA2 inputs (Sun et al., 2014). Circuit diversity has also been established along the longitudinal axis of the hippocampus: dorsal (septal) vs. ventral (temporal) (Moser and Moser, 1998; Fanselow and Dong, 2010; Poppenk et al., 2013; Zarei et al., 2013). These subregions are diversely connected to the amygdala, posterior cingulate cortex (PCC), prefrontal cortex (PFC), and thalamus (Zarei et al., 2013). For instance, dorsal hippocampus connectivity with the PCC supports episodic memory, while ventral hippocampus-amygdala connections are used in emotional processing (Ohara et al., 2013; Zarei et al., 2013). Discrepancies remain about the exact limits between the dorsal and ventral subregions (Tanti and Belzung, 2013). Parametric Anatomical Modeling suggests a heterogeneous distribution of the number of neurons and connections across the main anatomical axes due to layer morphology (Pyka et al., 2014) (see Figure 18). Finally, the composition of hippocampal circuits is constantly remodeled, as adult-born granule cells are incorporated throughout life (Deng et al., 2010; Vivar and Van Praag, 2013).



Recently, hilar mossy cells have been reported to be the first exciting new-born GCs (Chancey et al., 2014).

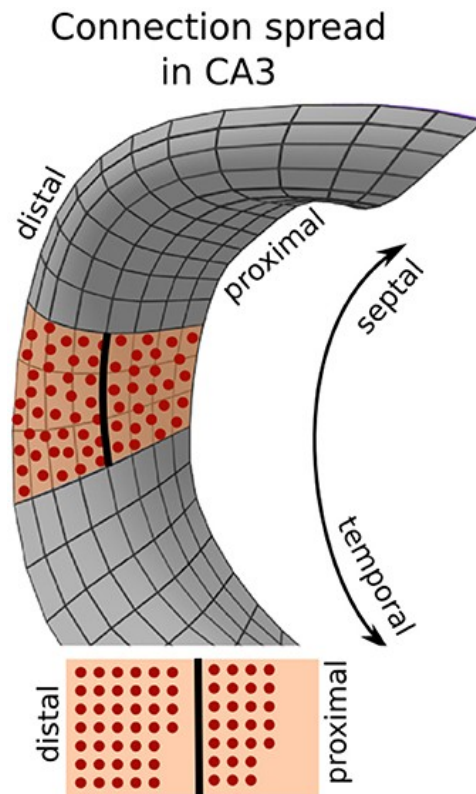
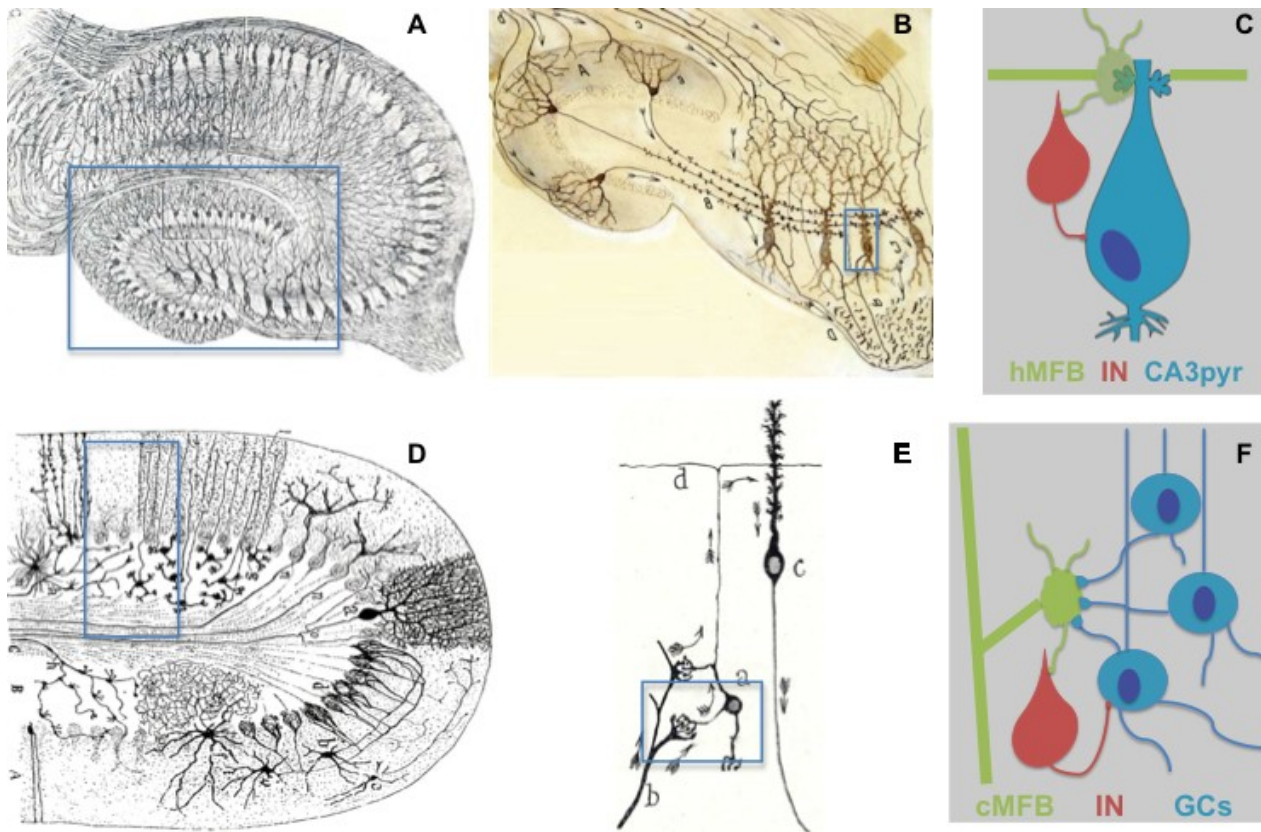


**Figure 18. Heterogeneous number of neurons and connections along the axis due to layer morphology (from Pyka et al., 2014)**

### 3.2. Mossy Fiber Synapses

Ramón y Cajal was also the first to describe GC axons, which he named “hippocampal mossy fibers” (hMFs) because the giant terminals scattered along the axons gave them the appearance of being covered in moss (Ramón y Cajal, 1911). He had previously used “mossy fibers” to refer to axons in the cerebellum (i.e. “cerebellar mossy fibers” or cMFs), which originate from pontine nuclei in the brainstem and synapse on cerebellar granule cells (see Figure 19) (for a detailed comparison between both “mossy fibers” see Delvendahl et al., 2013). Electron microscopy (EM) was used to describe hMF boutons (hMFBs) in more detail. These studies confirmed that hMFBs are complex, large terminals, tightly packed with synaptic vesicles (Blackstad and Kjaerheim, 1961; Laatsch and Cowan, 1966). In large hMFB there are 2 to 15 docked vesicles, a RRP of 80 to 400 SVs, and three types of vesicles: normal-sized SVs (33-38 nm in diameter), large clear vesicles (50-150 nm in diameter), and large dense-core vesicles (100-150 nm in diameter) (Rollenhagen and Lübke, 2006) (see Figure 20).

### 3. Hippocampal Formation



G	hMF	cMF
<b>Myelinated axon</b>	No	Yes
<b>Axon diameter (<math>\mu\text{m}</math>)</b>	$\sim 0.2$	$\sim 1$
<b>Boutons/axon</b>	Few large (10-18) and $\sim 140$ varicosities ( $\sim 1 \mu\text{m}$ diameter)	Many large at intervals of $20\text{-}80\mu\text{m}$
<b>Principal cells contacted/bouton</b>	1 CA3	50 GCs
<b>Bouton diameter (<math>\mu\text{m}</math>)</b>	2 – 8	3 – 12
<b>Bouton surface area (<math>\mu\text{m}^2</math>)</b>	32 – 106	69 – 266
<b>AZs/bouton</b>	18 – 45	190 – 440
<b>Average AZ area (<math>\mu\text{m}^2</math>)</b>	$0.21 \pm 0.11$	$0.04 \pm 0.02$
<b>Nearest distance between AZs (<math>\mu\text{m}</math>)</b>	0.40	0.46
<b>RRP (#/AZ)</b>	Large ( $\sim 40$ )	Small (1 - 2)
<b>Total number of SVs</b>	2,500 – 25,000	700 – 200,000
<b>Probability of release</b>	Low ( $<0.1$ )	High ( $\sim 0.5$ )
<b>Plasticity induced by moderate frequencies</b>	Facilitation	Moderate depression
<b><math>\tau_{\text{EPSC}}</math> (ms) at RT</b>	6.2	1.3
<b>Membrane capacitance (pF)</b>	1.4	1.8
<b>In vivo firing pattern</b>	Gamma bursts (30 - 100 Hz)	Rate coding (1 - 1,000 Hz)

**Figure 19 Hippocampal (A-C), cerebellar (D-F) mossy fibers, and table comparing these two morphologically similar but functionally distinct synapses (data from adult rats) (G) (A,B,D and E from Ramón y Cajal, 1894; Ramón y Cajal, 1911; Ramón y Cajal, 1933; G from Delvendahl et al., 2013 and Rollenhagen and Lübke, 2006)**

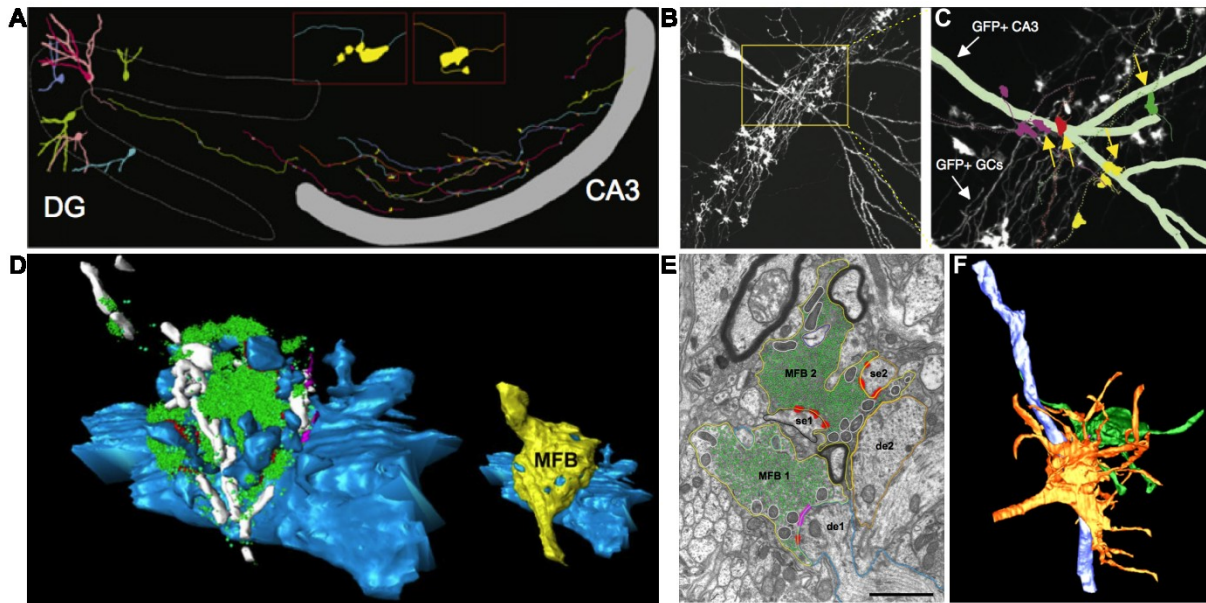


**Figure 20 MF morphology** (Panel A from Deguchi et al., 2011, B and C from Galimberti et al., 2010, D from Rollenhagen and Lübke, 2006, E from Rollenhagen et al., 2007, and F from Wilke et al., 2013)

Furthermore, the postsynaptic spines on the proximal apical dendrites of CA3 pyramidal cells showed to be equally complex. Such giant spines are called “thorny excrescences” (TEs) for their similarity to thorny excrescences of plants, which are multifarious protrusions that sprout from the main stem. Another cell type presenting TEs, not only on proximal dendrites but also on the soma, are hilar mossy cells (Scharfman, 2013). Quantification analyses estimated that in the rat 1 million granule cells (Boss et al., 1985) innervate the 300,000 CA3 pyramidal cells (Amaral et al., 1990). Each GC contacts ~14 CA3 pyramidal cells (low divergence) (Claiborne et al., 1986), each of which receives inputs from ~46 different GCs (low convergence) (Rolls, 2013; Pyka et al., 2014). Most of the GC outputs are actually via filopodial extensions from hMFBs onto CA3 interneurons –each granule cell innervates 40 to 50 CA3 interneurons (Acsády et al., 1998). On the other hand, most CA3 pyramidal cell excitatory inputs come from non-MFs: ~3,600 PP contacts from EC layer II, and ~12000 from recurrent axon collaterals of other CA3 pyramidal cells (Rolls, 2013). Nonetheless, single GCs can exert direct control of their CA3 pyramidal cell targets, as it has been shown *in vivo* (Henze et al., 2002). As mentioned in section 1, conduction velocity in unmyelinated axons is generally slow; in hMF axons it has been estimated to be around 0.25 m/s (Kress et al., 2008; Schmidt-Hieber et al., 2008). Single spikes are not sufficient for *in vivo* transmission from a GC to CA3, but instead trains of spikes are required (Henze et al., 2002). The average GC firing rate recorded *in vivo* is very low: ~0.01–0.1 Hz (Jung and McNaughton, 1993), but trains of spikes have been recorded in physiological conditions such as granule cell place

### 3. Hippocampal Formation

activity, when firing frequency can reach 10 to 50 Hz and each burst get as far as 100 to 300 Hz (Jung and McNaughton, 1993; Skaggs et al., 1996; Gundlfinger et al., 2010) (see Figure 21). On the other hand, many CA3 recurrents and/or PP inputs need to converge to make the CA3 pyramidal fire. Hence, computationalists nicknamed the MF as ‘detonator’ or ‘teacher’ synapse, and it is modelled as critical for directing information storage in the auto-associative CA3 network (Rolls, 2013). Recently, mossy fiber-evoked subthreshold responses have been reported to induce timing-dependent plasticity at hippocampal CA3 recurrent synapses (Brandalise and Gerber, 2014). In conclusion, MFs provide a sparse (0.005%) but powerful connection, while CA3 recurrents are weaker but numerous (~2%). This could fit with the concept of synaptic “distance-dependent scaling”: synapses closer to soma have larger RRP but fewer receptors at the postsynapse, and viceversa for those further from soma (De Jong et al., 2012; Lee et al., 2013) –alternatively the peculiar MF synapse might account for a convergent evolutionary mechanism. Molecular diversity between the strata where the different inputs synapse onto CA3 pyramidal cells further points into this direction –i.e. MF in stratum lucidum, A/C in stratum radiatum, and PP in stratum moleculare. The weight of MFs and CA3 recurrents is further determined by feedforward (MF-IN-CA3; see Figure 21) and feedback (CA3-IN-CA3) inhibitory circuits, respectively (Mori et al., 2004).

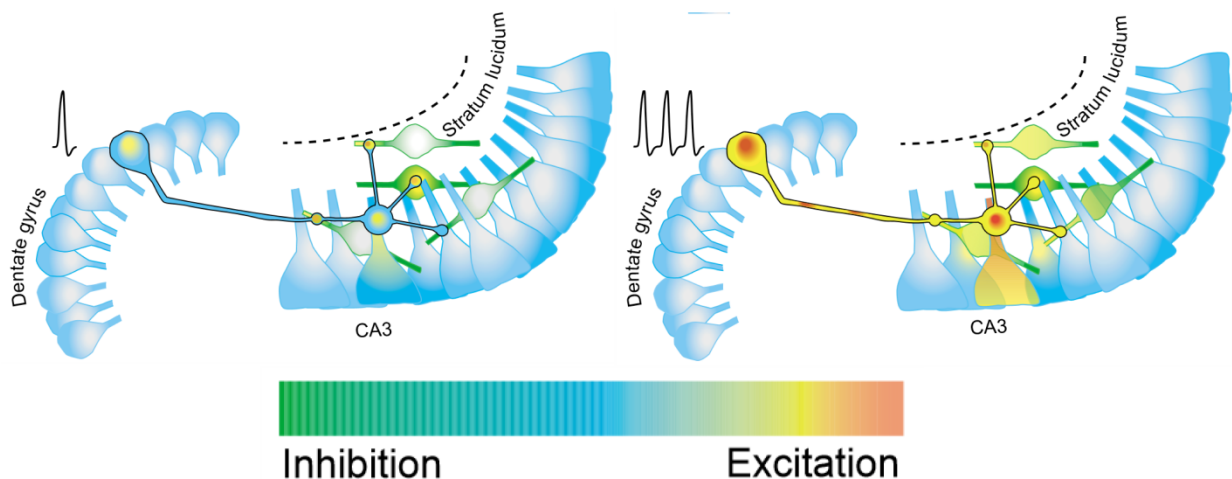


**Figure 21 GC firing: single vs. train of spikes (modified from Lawrence and McBain, 2003)**

## 4. Synaptic Plasticity

How synapses can retain long-term memories while experiencing constant molecular and structural changes is a conundrum. In 1949, Donald Hebb proposed activity-dependent synaptic plasticity to underlie learning, which is now known as the “Hebbian theory” (Hebb, 1949). Besides Hebbian types, AP-independent forms of synaptic plasticity also exist. Plastic changes are further categorized according to duration into short- and long-term forms, and according to effect into facilitating or depressing. Moreover, a given plasticity type is described by its pre- or postsynaptic nature. The overview below lists MF characteristic plasticity forms as compared to more archetypal synapses, with a special emphasis on short-term presynaptic facilitation (for general review see Pan and Zucker, 2009; Fioravante and Regehr, 2011; Kaeser and Regehr, 2014).

### 4.1. AP-dependent

Activity-dependent synaptic plasticity is the most thoroughly studied form. Initially, studies used only artificial stimulation protocols, but nowadays more physiological patterns are also applied. The hMFB is characterized by its low basal release probability, and distinctive presynaptic facilitation –i.e. Paired Pulse Facilitation (PPF), Frequency Facilitation (FF), and presynaptic Long-Term Potentiation (preLTP) (Harris and Cotman, 1986; Salin et al., 1996; Henze et al., 2000; Nicoll and Schmitz, 2005; Rollenhagen and Lübke, 2010; Clarke, 2012; Evstratova and Tóth, 2014). Postsynaptic changes also play a role in MF STP, and they are of paramount importance at other synapses.

#### 4.1.1. Short-Term Plasticity

Plasticity lasting from milliseconds to minutes is said to be “short-term” (STP). The probability of release often determines the direction of STP: normally a high-release probability synapse tends to depression, while a low-release probability synapse has more chances to facilitate upon repetitive stimulation. Besides release probability ( $Pr$ ), neurotransmission also depends on the number ( $n$ ) of primed vesicles, and the amount/quanta ( $q$ ) of neurotransmitter contained per vesicle (for the most important factors in  $Pr$ ,  $n$  and  $q$ , see Figure 22). Notice that  $q$  depends also on the amount of postsynaptic receptors that can be activated. Furthermore, the giant MF-CA3 synapse, can engage multisite release (equivalent to coincident multisynaptic release on the same dendrites), which has been recently reported to



act in tandem with multivesicular release in MF STP (Chamberland et al., 2014), and to depend on calcium coupling (Vyleta and Jonas, 2014) (see Figure 22).

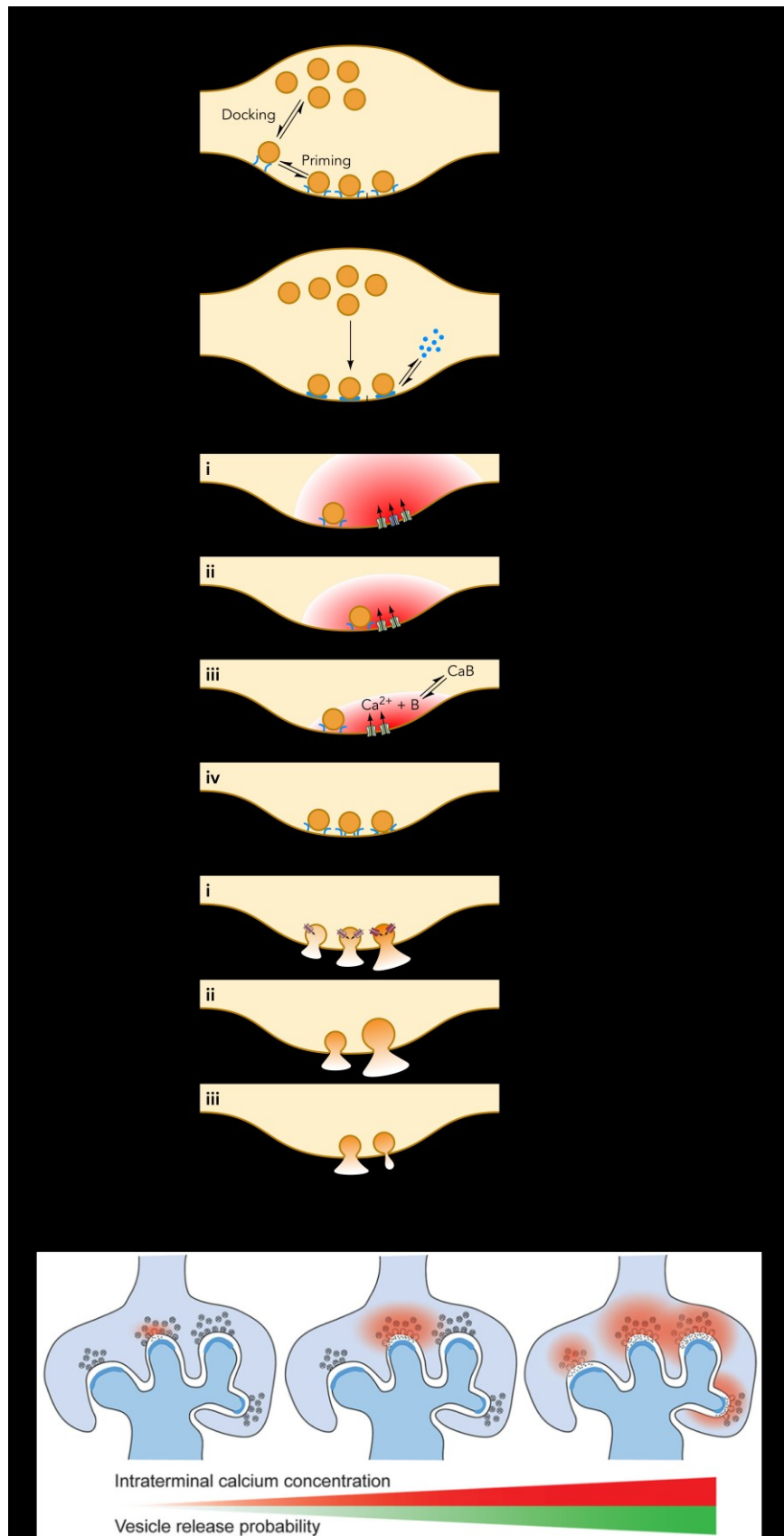


**Figure 22 Key determinants of neurotransmission and MF model (A-C from Ariel and Ryan, 2012 and D from Chamberland et al., 2014).**

The most commonly established form of STP relates to changes in the amplitude of EPSCs occurring following a pair of pulses consecutively applied within a range of few milliseconds (typically 40 to 500 ms). This is thought to rely on residual calcium (Fioravante and Regehr, 2011). At MF-CA3 synapses this results in robust facilitation (Nicoll and Schmitz, 2005). Another form of pronounced facilitation at this synapse results from increasing stimulation frequency from basal (0.1Hz) to moderate (1-3 Hz) (Salin et al., 1996; Breustedt et al., 2010), but the mechanisms for this Frequency Facilitation (FF) remain elusive. Short trains/bursts of activity also lead to facilitation at Mf-synapses. At higher frequencies, the timing and efficacy of release is crucial, but GCs seems to be evolutionary adapted to fire at higher rates (Bischofberger et al., 2002). Further STP forms have been described and characterized including: augmentation and PTP (Fioravante and Regehr, 2011), spike-timing-dependent plasticity (STDP) (Rebola et al., 2007; Lanore et al., 2009), depolarization-induced potentiation of excitation (DPE) (Carta et al., 2014a), and metaplasticity (Rebola et al., 2011). Co-release of Zinc can affect NMDA transmission at many synapses (Paoletti et al., 2009), including MF-CA3 synapses (Vogt et al., 2000; Frederickson et al., 2006; Pan et al., 2011; Vergnano et al., 2014).

Activity-dependent analog plasticity is also remarkable at MFs, where the AP can be broadened in a regulated fashion (Geiger and Jonas, 2000; Debanne et al., 2011; Carta et al., 2014a) (see Figure 23). Finally, a membrane lipid, arachidonic acid, is released after activity at postsynaptic CA3 pyramidal cells and acts as a retrograde messenger at the presynaptic mossy fiber, broadening the AP by modulating voltage-gated potassium channels, thus leading to robust facilitation of synaptic transmission (Carta et al., 2014a, commented in Welberg, 2014 and Schmitz et al., 2014).

##### 4.1.2. Long-Term Plasticity

Longer activity changes are termed as “long-term”, and include potentiation (LTP) and depression (LTD) forms. Classical LTP relies on NMDA receptor activation and subsequent increase in AMPAR responses, but at MF-CA3 a presynaptic NMDA-independent form of LTP (preLTP) also exists (Harris and Cotman, 1986). NMDA/AMPA ratio at MFs is lower (Monaghan and Cotman, 1982) and subunit expression is distinct from other brain areas (Berg et al., 2013). Besides reports under experimental conditions, plasticity has also been observed *in vivo* (Hagena and Manahan-Vaughan, 2010), and after more physiologically relevant stimulation by

natural spike patterns recorded from GCs during spatial navigation (Dobrunz and Stevens, 1999; Sachidhanandam et al., 2009).

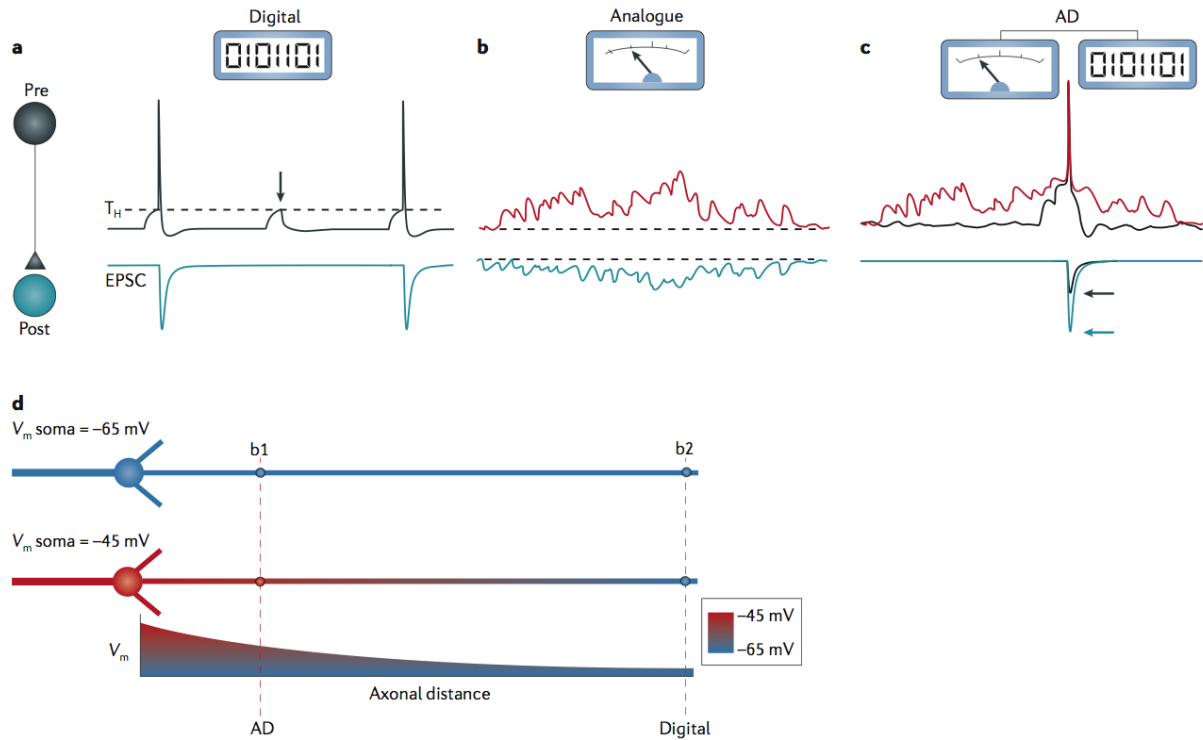


**Figure 23 Analog, digital and mixed transmission (from Debanne et al., 2013)**

### 4.2. AP-independent

Synaptic plasticity is known to result also in an action potential-independent manner. This type of plasticity plays a role for instance in homeostatic processes (Lee et al., 2013, commented in Chater and Goda, 2013). Furthermore, nicotine and caffeine-mediated release has been reported to occur at MF synapses (Sharma and Vijayaraghavan, 2003; Cheng and Yakel, 2014). Other forms of AP-independent plasticity at MF-CA3 synapses involve activation by phorbol ester (Honda et al., 2000), by insulin (Burgo et al., 2013), and by reelin (Bal et al., 2013). Subthreshold depolarization of GCs has been reported to attain MFBs (Alle and Geiger, 2006), and to affect the function of the CA3 recurrent network (Brandalise and Gerber, 2014).



## 5. Neuronal Tracing

Understanding the mechanisms that affect synaptic function –ranging from neurodevelopment and synaptogenesis, to circuit rewiring due to homeostasis, pathologies, or memory encoding- requires knowledge of the synaptic connectivity. Neuroanatomists have used a range of neuronal tracers to visualize neuronal connectivity. At the end of the 19<sup>th</sup> century, the concepts of neuron, synapse, and directionality of synaptic transmission were inferred, partly, by visualizing neuronal morphology revealed by the random staining pattern of Golgi's *reazione nera*. Rudimentary tracing methods of that time relied on physically damaging fibers by surgical, thermoelectric or chemical means (Waller, 1850). This approach was later combined with subsequent selective staining –i.e. heavy metal staining for severed myelinated axons (Marchi and Algeri, 1885; Pitman et al., 1972), and silver affinity staining for both myelinated and unmyelinated axons) (Nauta, 1952; Fink and Heimer, 1967). Pathological changes at the somas, of those cells with severed axons, helped identify the brain region of origin for the given projection. Staining techniques till this point were based on physical diffusion of dyes in fixed tissue.

In the 1970s, a new neuroanatomical era blossomed with the breakthrough of tracers that can use active physiological transport in living neurons (Kristensson and Olsson, 1971; Kristensson et al., 1971; LaVail and LaVail, 1972). Many pioneering tracing techniques came out from Krister Kristensson's laboratory (i.e. Evans blue, horseradish peroxidase, herpes simplex virus), and from Martin Schwab's laboratory (i.e. wheat-germ agglutinin and tetanus toxin C-fragment). Neuronal tracers can be further classified by two criteria: the spreading direction and their ability to cross synapses (or not). If a tracer travels from the soma through the axon to presynaptic terminals, it is referred as "anterograde". On the other hand, if a tracer is transported in the opposite direction, from presynaptic terminals back to the soma, it is referred as "retrograde". Some tracers can travel both antero- and retrogradely. According to the other criterion, we can differentiate between conventional tracers and trans-synaptic tracers. A conventional tracer is a chemical probe that allows neuronal labelling, thus elucidating which brain areas are interconnected, as well as the identity and location of the traced neurons. However, they do not cross synapses. Tracers that can jump from one cell to another are called trans-synaptic, and can be either viral or non-viral (see Table 4). A state-of-the-art tool to unravel neuronal connectivity combines neurotropic viral vectors and fluorescent proteins, which enables neuronal infection,

self-replication, and trans-synaptic spread that literally “lights up” the entire circuit (Kuypers and Ugolini, 1990; Callaway, 2008; Ekstrand et al., 2008). Today, neurotropic viral vectors also allow to monitor network activity, to manipulate the activity and/or genome of the circuit, and their infection can be restricted to a defined population by using mutant mouse lines, stem cell-derived neurons, or transfection techniques (i.e. single-cell electroporation, helper viruses).

### 5.1. Conventional Tracers

Current knowledge in systems neuroscience is based to a large extent on studies using conventional anterograde and retrograde tracers (Cowan, 1998; Luo et al., 2008; Lichtman and Denk, 2011). Over the past 40 years, these studies have described connectivity between brain areas and the identity of the projecting neurons. In spite of this, conventional tracers cannot be used to accurately elucidate neuronal connectivity because they cannot cross synapses. These tracers exploit intrinsic cellular transport to label the cell. The most widely applied conventional tracer is biotinylated dextran amine (BDA) (Glover et al., 1986; Veenman et al., 1992). Dextran-based tracers are macromolecules conjugated with fluorescent dyes (i.e. fluorescein, rhodamine, or lysine), and their transport direction depends on molecular weight and pH. For instance, BDA 10kDa is of widespread use for anterograde tracing, while BDA 3kDa is the prevailing choice for retrograde tracing (Reiner et al., 2000). Conventional tracers have been routinely complemented with techniques like electrophysiology and/or immunohistochemistry. Common tracers are listed in Table 3, but the advantages and limitations of non-trans-synaptic traces will not be directly addressed, for review see Lanciego and Wouterlood, 2011; Wouterlood et al., 2014.

Table 3 Neuronal tracers (modified from Carter and Shieh, 2009)

		Tracer	Direction (order)	Comments
<b>Physical diffusion</b>		Golgi staining	n/a	Random staining pattern
		Heavy metals	n/a	Cobalt ions can also spread by active physiological transport
		Selective silver staining	n/a	Combined with induced lesions
<b>Active physiological transport</b>	<b>Conventional tracers</b>	Biotinylated dextran amine (BDA)	Both	Widely used; direction of transport depends on molecular weight and pH; can be visualized by EM
		Cholera toxin, subunit B (CTB)	Mainly retrograde	May go anterogradely
		Diamidino yellow	Retrograde	Produces yellow fluorescence
		Dil, DiO	Both	Lipophilic dye crystals; mainly used in fixed tissue
		Fast blue	Retrograde	Stable, rapid labeling
		Fluorescent microspheres	Retrograde	Available in many different colors; nontoxic
		Fluoro-Gold	Retrograde	Widely used, rapid labeling
		Horseradish peroxidase (HRP)	Retrograde	Produces brown precipitate after reaction with hydrogen peroxide and DAB (diaminobenzidine)
		Phaseolus vulgaris-leucoagglutinin (PHA-L)	Anterograde	Plant lectin; can be visualized by EM
		Radioactive amino acids	Anterograde (poly)	Detected by autoradiography; only tracer virtually 100% anterograde
	<b>Transsynaptic</b>	Clostridial toxins	BoNTs	Normally nontoxic fragments; can be used to label genetically defined neural circuits; cloning vector; disruption of activity possible
			TTC	
		Plant lectins	BL	Often conjugated with HRP for detection; can be used to label genetically defined neural circuits; cloning vector
			WGA	
		Diffusion MRI or DTI		Non-invasively used in humans; myelinated fibers only
		Herpesviruses	HSV	Broad host range, including humans; can be used to label genetically defined neural circuits; cloning vector
			PRV	Does not infect primates; less virulent bartha strain most commonly used; can be used to label genetically defined neural circuits; cloning vector
		Rhabdoviruses	RABV	Can be used to label genetically defined neural circuits; tropism can be modified; cloning vector
			VSV	Infects neurons and glia by diffusion; can be used to label genetically defined neural circuits; tropism can be modified; cloning vector
		Other (sindbis, semliki, AAV, lenti, CAV-2, , etc.)	Both possible (mainly poly)	Direction, order, and properties vary depending on viral strain

## 5.2. Trans-Synaptic Tracers

Conventional tracers label only direct antero- and retrograde projections. However, functional networks include second-order connections, and beyond. Trans-synaptic tracers also appeared in the 1970s, allowing for the study of multisynaptic circuits. As mentioned above, they are further categorized according to whether they infect cells (viral tracers) or not (non-viral tracers). The use of viruses is advantageous because they are “genetic machines”, thus they naturally amplify labeling, and recent genetically modified viruses achieve: specificity of infection (initial cell type and/or extent), choice of direction, and cloning vector capability. On the other hand, certain species or strains of viruses spread also non-synaptically, and all viruses are more or less cytotoxic. Such cytotoxicity has implications for both the study and the experimenter. This drawback has been reduced with the introduction of less aggressively spreading strains. Nonetheless, eventual mutations should never be disregarded. Therefore, the biosafety of research facilities needs to be certified and in the case of rabies virus use, prior vaccination is mandatory for researchers. Non-viral tracers are generally safer for the experimenter (except for radioactive amino acids), but can also induce physiological changes. Moreover, many non-viral tracers can also be genetically encoded. In contrast with viruses, the signal of most of them is diluted with each synaptic step, limiting tracing to 2<sup>nd</sup> order neurons. Non-conventional tracers can be targeted with cell-type specific promoters (Huh et al., 2010).

### 5.2.1. Non-Viral Tracers

#### 5.2.1.1. *Radioactive Amino Acids*

Neurons, as any other cell, absorb amino acids to incorporate them into polypeptides, some of which are eventually transported anterogradely to synaptic terminals, secreted, and uptaken by postsynaptic cells. Radioactive amino acids like <sup>3</sup>H leucine and <sup>3</sup>H proline (“<sup>3</sup>H” is pronounced “tritiated”) were established in the second half of the 20<sup>th</sup> century as tools to visualize uptake and transport mechanisms in the nervous system by autoradiography (Droz and Leblond, 1962, 1963). The systematic use as neuronal tracers came a decade later from the hand of Anita Hendrickson and collaborators (Cowan, 1972). This tracing method is the only one virtually 100% anterograde (Hendrickson, 1982}).

## 5.2.1.2. Plant Lectins

Lectins are plant proteins with a high-affinity binding to certain sugars, such as glycoproteins on the neuronal plasma membrane. Bound lectins are subsequently internalized and transported within the cell, including to neurites. Not all lectins are trans-synaptic (i.e. Phaseolus vulgaris-leucoagglutinin, or PHA-L). Two representative cases that can cross synapses are wheat-germ agglutinin (WGA) (Schwab et al., 1978), and barley lectin (BL) (Horowitz et al., 1999). WGA weights 18kDa and it is a cysteine-rich lectin that binds to *N*-acetylglucosamine and sialic acid of carbohydrate moieties part of glycoproteins or glycolipids. Its function is to protect wheat from insects, yeast and bacteria but it poses no danger for the experimenter. However, lectins can affect synaptic physiology –i.e. lectin-dependent desensitization of AMPA/Kainate receptor (Thio et al., 1992), and lower release probability (Vyklícky et al., 1991). Initially, WGA was traced by radiolabeling, but shortly after it was conjugated with HRP (Schwab et al., 1978; Gonatas et al., 1979). Besides immunodetection against HRP, lectins can now be detected using also antibodies against a lectin (i.e. anti-WGA recognizes both WGA and BL, since both species belong to the triticeae tribe) (Horowitz et al., 1999). Recently, WGA variants fused to fluorescent proteins have been produced –i.e. WGA:GFP (Oh et al., 2009), and WGA: DsRed (Sugita and Shiba, 2005; Oh et al., 2009) (see Figure 24). Finally, WGA has been use as genetic tool (Braz et al., 2002) and it has been combined with rabies virus tracing (Wall et al., 2010)

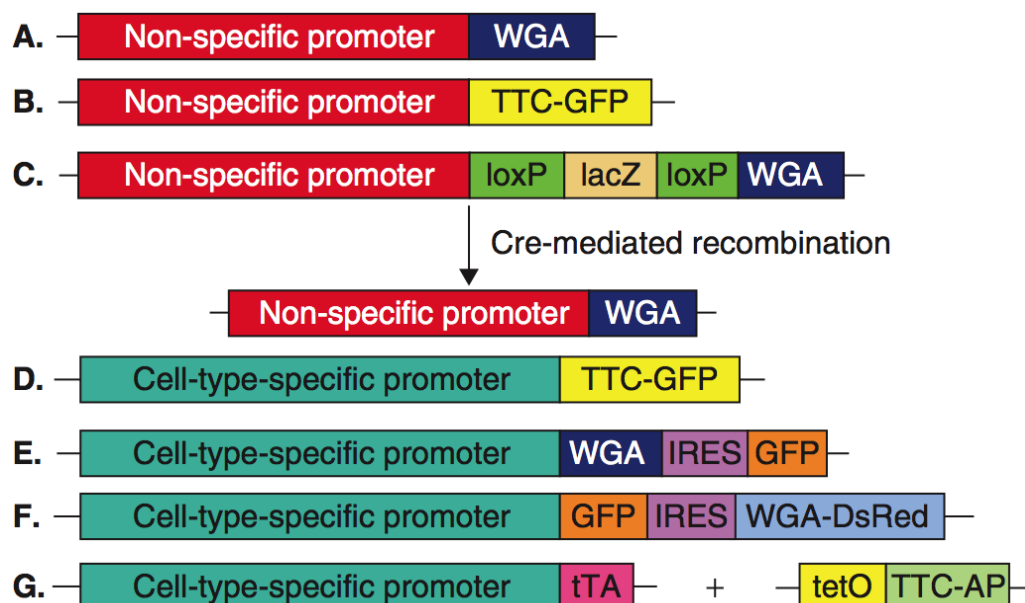


**Figure 24 WGA and TTC-based constructs for neuronal tracing (from Huh et al., 2010)**

#### 5.2.1.3. *Clostridial Toxins*

Of the bacterial toxins, those with the highest neuronal specificity are the clostridial toxins –i.e. botulinum neurotoxins (BONTs), and tetanus neurotoxin (TeNT). TeNT is the toxin most developed for tracing. This toxin is taken up by nerve terminals at the neuromuscular junction and retrogradely transported to trans-synaptic spinal cord interneurons (Habermann et al., 1973). Trans-synaptic spread was demonstrated by autoradiography in the 1970s by another tracing pioneer, Martin E. Schwab (Schwab and Thoenen, 1976). He soon found that TeNT, as WGA, could be used as a tracer conjugated with HRP (Schwab et al., 1978; Schwab and Agid, 1979). However, this approach was limited by rapid development of clinical symptoms and consequent death of the experimental animals. TeNT binds to neurons through its nontoxic C fragment (TTC) (Bizzini et al., 1977), which was thereafter used as neuronal tracer (Bizzini et al., 1980). To my knowledge, TTC was the first trans-synaptic tracer to be used as a carrier, when it was fused to *lacZ* (Coen et al., 1997). As for WGA, in the last decade TTC has been also fused to a fluorescent protein –i.e. TTC: GFP (Kissa et al., 2002; Maskos et al., 2002; Roux et al., 2005; reviewed in Huh et al., 2010). Furthermore, targeted genetical expression of tetanus toxin light chain has been used to disrupt synaptic transmission (Harms and Craig, 2005; Ehlers et al., 2007). A drawback of the TTC fragment is that, since it lacks the translocation domain, it is retained in endosomes. TTC has been fused to diptheria toxin C and T domains to obtain translocation properties (Francis et al., 2000). Longer persistence in the cytoplasm has been achieved by a nontoxic derivative of another clostridial toxin: BoNT/A, which normally cleaves SNAP25 (Pellett et al., 2011; Vazquez-Cintron et al., 2014). Besides the use as neuronal tracers, clostridial toxins are also clinically useful as immunotoxins against cancer and viral infections, and can be misused as biological weapons.

#### 5.2.1.4. *Diffusion MRI or DTI*

This method is a breakthrough for non-invasive human brain tracing. It combines magnetic resonance imaging (MRI) and computer algorithms called “tractography”. In 1990, Michael Moseley described water diffusion in white matter as anisotropic, and to be optimally fitted by a tensor (Moseley et al., 1990). Without a clear mechanistic understanding, the obvious application for tract tracing in the human brain was developed based on the assumption that the direction of the fastest diffusion should be indicative of the orientation of the fibres as first shown by Le

Bihan and collaborators (Douek et al., 1991). This method is known as diffusion MRI or DTI (for “diffusion tensor imaging”). DTI data from large fascicles and tracts are analyzed with tractography softwares to reveal the trajectories of white matter fiber bundles (Conturo et al., 1999). However, only the path is unveiled but not its direction. Another disadvantage of DTI, as compared to histology, is the current low resolution of the images and unfeasible application to unmyelinated fibers. However, both drawbacks are constantly improved by advances in MRI and computing technologies.

DTI has led to a new discipline called “connectomics”, parallelly put forward in 2005 by Patric Hagmann and Olaf Sporns (Hagmann, 2005; Sporns et al., 2005). In his Ph. D. thesis titled “From diffusion MRI to brain connectomics”, Hagmann (2005) defines the concept of “connectome” as follows:

*“Accordingly, It is clear that, like the genome, which is much more than just a juxtaposition of genes, the set of all neuronal connections in the brain is much more than the sum of their individual components. The genome is an entity it-self, as it is from the subtle gene interaction that li[f]e emerges. In a similar manner, one could consider the brain connectome, set of all neuronal connections, as one single entity, thus emphasizing the fact that the huge brain neuronal communication capacity and computational power critically relies on this subtle and incredibly complex connectivity architecture”*

Besides its revolutionary application in human brain tracing, DTI has also been used in rodents. An example of DTI tracing of the hippocampal mossy fiber can be seen in Figure 25 (Ropireddy and Ascoli, 2011).

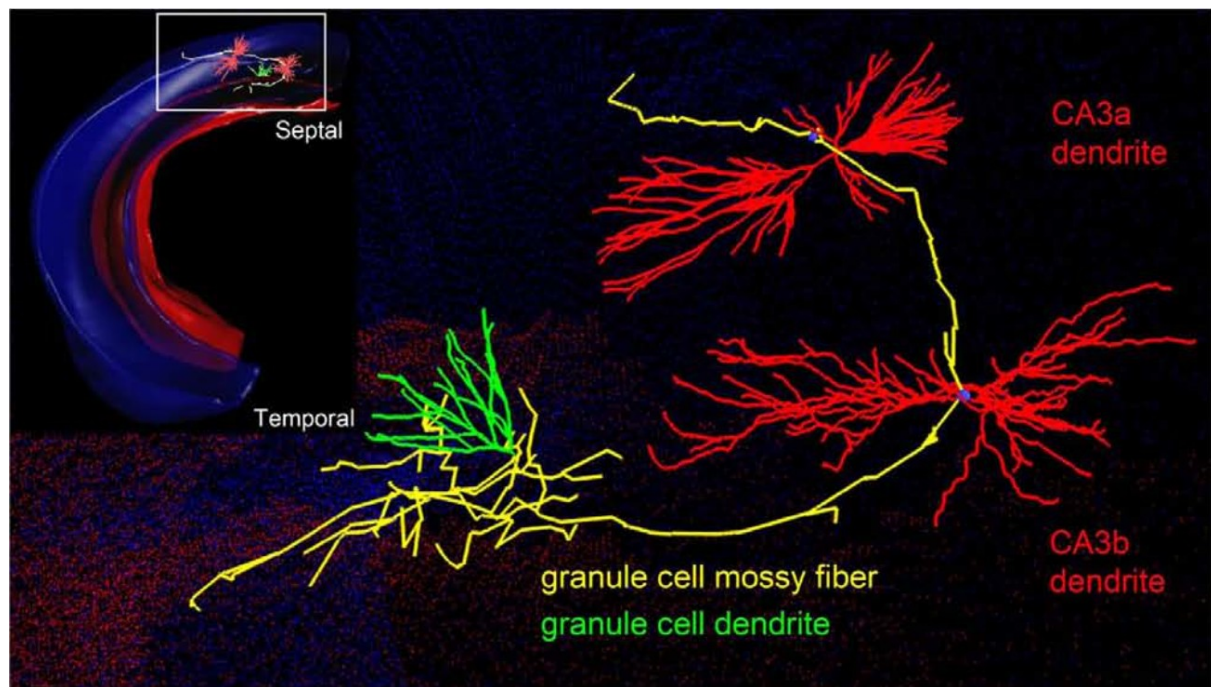


**Figure 25** DTI tracing of the hippocampal mossy fiber (adapted from Ropireddy and Ascoli, 2011).

#### 5.2.2. Viral Tracers


The application of viral infections for neuronal tracing arises from the ability of certain viruses, known as neurotropic viruses, to trans-synaptically infect neurons. Viruses are obligate parasites which are not alive, thus they are not phylogenetic. Therefore, Linnaean taxonomy to classify viruses goes from order to strain (i.e. only 3 orders are in use, so many viruses are not assigned to any order). Alternative classification also exist, like the Baltimore and LHT classifications. The former places viruses into 7 classes according to method of replication and nucleic acid characteristics (i.e. DNA or RNA, single- or double-stranded, and sense or anti-sense). The LHT classification also differentiates between DNA and RNA viruses, plus other physical and chemical characteristics (i.e. symmetry, presence of envelope, diameter of capsid, number of capsomers). The first neurotropic virus considered for tracing was a species of the Herpesviridae family: the Herpes simplex virus (Kristensson et al., 1974; Ugolini et al., 1987). The other main family used for tracing is the rhabdoviridae family (see Table 4). Herpes simplex virus type 1 (HSV1), together with pseudorabies virus (PRV), and the fixed Challenge Virus Standard (CVS) strain of rabies virus (RABV), are the main trans-synaptic viral tracers used in their naturally occurring variants with subsequent immunohistochemical detection. Decades of studies have significantly advanced our knowledge of neuroanatomic connectivity, especially for higher orders of connectivity. RABV-CVS can practically trace an unlimited number of synapses, however, all



## 5. Neuronal Tracing

viruses are more or less cytotoxic. Thus, the longer the infection time, the more synapses traced, but also the more likely the 1<sup>st</sup> order neurons would have died. Moreover, RABV-CVS and the Bartha strain of PRV spread predominantly synaptically, but other species or strains spread also non-synaptically (reviewed in Callaway, 2008; Van Den Pol et al., 2009; Ugolini, 2010). These drawbacks of natural strains have been addressed by recent genetic modifications. Additional modifications have exploited further the potential of neurotropic viruses to incorporate marker genes, control tracing direction, limit synapse crossing to mono-synaptic partners, and to exploit viruses beyond labeling (i.e. strategies to monitor or manipulate activity/genomics of connected neurons or entire circuits). This field has boomed during the last decade and many advances are still expected in the short-term. For instance, neurotropic viruses that belong to other families and are not currently used for neuronal tracing, could be developed in a few years. Besides their use in tracing, neurotropic viruses are developed for opposing ends in therapy and biowarfare.

**Table 4 Classification and properties of the most remarkable viral tracers (modified from Beuret, 2000)**

Classification criteria	Nucleic acid							
	RNA				DNA			
	Icosahedral	Icosahedral	Helical	Helical	Icosahedral	Icosahedral	Icosahedral	
	Enveloped	Enveloped	Enveloped	Enveloped	Naked	Enveloped	Enveloped	
Genome architecture	(+) ss cont.	(+) ss cont.	(-) ss cont.	(-) ss cont.	ss linear (+) or (-)	ds linear	ds linear	
Baltimore Class	IV	IV	V	V	II	I	I	
ICTV Classification	Order	Unassigned	Unassigned	Mononegavirales	Mononegavirales	Unassigned	herpesvirales	herpesvirales
	Family	togaviridae	togaviridae	rhabdoviridae	rhabdoviridae	parvoviridae	herpesviridae	herpesviridae
	Subfamily	n/a	n/a	n/a	n/a	parvovirinae	α-herpesvirus	α-herpesvirus
	Genus	alphavirus	alphavirus	lyssavirus	vesiculovirus	dependoparvovirus	simplexvirus	varicellovirus
	Species	sindbis virus	semliki forest virus	rabies virus	VSV	AAV	Herpes simplex virus	pseudorabies virus
								
Properties	Virion polymerase	(-)	(-)	(+)	(+)	(-)	(-)	(-)
	Virion diameter (nm)	60-70	60-70	70-85x130-380	70-85x130-380	18-26	150-200	150-200
	Genome size (kb) (genes)	12	12	11.9 (5)	11-12 (5)	4.7 (2)	152 (80)	143 (72)
	Cloning capacity (kb)	5	5	5	<5	<5	100	100

### 5.2.2.1. *Herpesviridae*

The herpesviridae family consists of double-stranded DNA, icosahedral, enveloped viruses. Their genome encodes approximately 80 genes in its 150 to 200 thousand base pairs. They can be used as vectors for up to 100kb.

#### a) *Herpes Simplex Virus (HSV)*

Also known as human  $\alpha$ -Herpesvirus, this was the first trans-synaptic viral tracer (Kristensson et al., 1974; Ugolini et al., 1987). Initially, natural strains of herpes simplex virus type 1 (HSV1) were used for tracing. Most strains can travel in both direction, but the McIntyre-B strain goes exclusively retrogradely, and the H129 strain predominantly spreads anterogradely (reviewed in Callaway, 2008). Later on, the fact that around half of the 80 genes encoded by HSV are not essential for its replication (Mocarski et al., 1980), was exploited to use HSV for gene transfer, and as a vector coding for antisense RNA to reduce NMDA receptor expression (reviewed in Van Den Pol et al., 2009). In the past years, a recombined HSV containing the brainbow cassette has also been produced (Card et al., 2011).

#### b) *Pseudorabies Virus (PRV)*

PRV, as HSV, is part of the  $\alpha$ -Herpesviruses subfamily, but it belongs to the varicellovirus genus instead of the simplexvirus. PRV is also known as *Herpes suis* or porcine  $\alpha$ -Herpesvirus, and it cannot infect primates. Thus, it is a safe choice for experiments in non-primate species. It should be mentioned to avoid confusion that, although it is called pseudorabies, it is NOT a rabies virus (i.e. “pseudorabies” was used due to the similarities between its infection-induced behaviors and those caused by RABV infection). Initially used natural PRV strains can also travel in different directions: the Becker strain can go in both, while the Bartha strain is preferentially retrograde (Loewy, 1998; Aston-Jones and Card, 2000). Later on, a modified PRV variant was developed to replicate conditionally in cre-expressing cells (DeFalco et al., 2001).

### 5.2.2.2. *Rhabdoviridae*

In contrast to herpesviruses, the rhabdoviruses are helical and contain single-stranded, antisense RNA. Importantly for potential modifications, both families are enveloped. The rhabdoviruses' genome is much smaller (around 12 kb) and it encodes only 5 genes. Therefore, their cloning capacity is also limited to just 5kb. One of the genes encodes the glycoprotein (G) that the new virions incorporate as

envelope after replication, which is also exploited for generation of recombinant variants.

### *a) Vesicular Stomatitis Virus (VSV)*

The vesicular stomatitis virus (VSV) is a species of the vesiculovirus genus. Wild-type VSV has been reported to be actively transported in both directions (Lundh, 1990). However, the recombinant variants generally employed spread principally by diffusion, infecting both neurons and glia (van den Pol et al., 2002). Neuroscientists have started to use VSV rather recently. What makes it an interesting virus in tracing is its capability to rapidly infect and replicate. It has been reported to infect cells within one hour (Van Den Pol et al., 2009), and to cross to 1<sup>st</sup> order neurons 30 minutes after starter-cell infection (Kretzschmar et al., 1996; Wagner and Rose, 1996). Thus, VSV can potentially be used for *in vitro* electrophysiology recordings of previously infected slices, which would overcome the risk of cutting axons when infection is previously done *in vivo*. Furthermore, the heterogenous VSV cell specificity can be modified by pseudotyping VSV with another viral envelope and replacing the native glycoprotein (VSV-G) by that of another virus, while specific initial infection can also be achieved by selectively expressing an exogenous envelope-complementary surface protein in a cell or cell population. Both approaches were combined in a recent study to obtain a monosynaptic VSV tracer that can go anterogradely if the new G comes from the lymphocytic choriomeningitis virus (LCMV-G), and retrogradely if it is from the rabies virus (RABV-G) (Beier et al., 2011). However, the same authors reported a year later that the VSV (LMCV-G) findings were due to contamination with native VSV-G, and that pure VSV (LMCV-G) infect mostly glia and just few anterograde neurons (Beier et al., 2012). They could, however, replicate *in vivo* the findings for the VSV (RABV-G) (Beier et al., 2013a, b).

### *b) Rabies Virus (RABV)*

The other main species of the rhabdoviridae family used for tracing is the rabies virus (RABV), which belongs to the lyssavirus genus and has been widely applied for retrograde labeling. A distinction should be done between the two different RABV tracing strategies applied so far. On the one hand, naturally occurring strains, such as RABV-CVS, have been used for poly-trans-synaptic tracing combined with posterior immunohistochemical detection. On the other hand, modified variants of the Street Alabama Dufferin B19 (SAD B19), commonly used in vaccines, have been developed to allow more sophisticated applications, not limited to tracing

(see Figure 26). An overview of those strains, as well as potential new variants, is provided below. Importantly for tracing application, there are viral mechanisms that have evolved to reduce CNS damage while enabling viral spread (Hemachudha et al., 2013) (see Figure 27 for RABV replication cycle). Thus, the least cytotoxic strains are the most advantageous for tracing, as damage is minimal. It should not be dismissed that, although new strains are attenuated and/or modified, they all exhibit a certain degree of cytotoxicity, which has implications for both the infected cells and the experimenter. RABV spontaneously mutates at higher rates than DNA viruses (Gomme et al., 2011). Therefore, interpretations of results need to account for cytotoxicity, the biosafety of research facilities needs to be certified, and researchers must be vaccinated before any experiment is carried out.

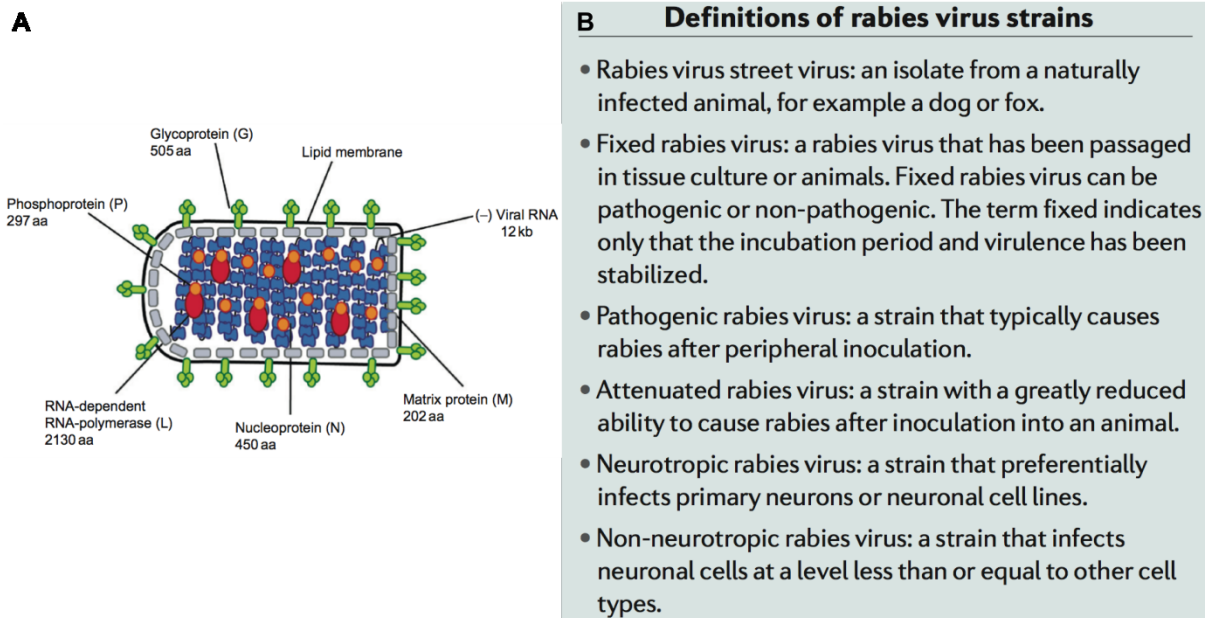


**Figure 26 Rabies virus virion structure (left) and definitions of strains (right) (from Albertini et al., 2011, and Schnell et al., 2010, respectively)**

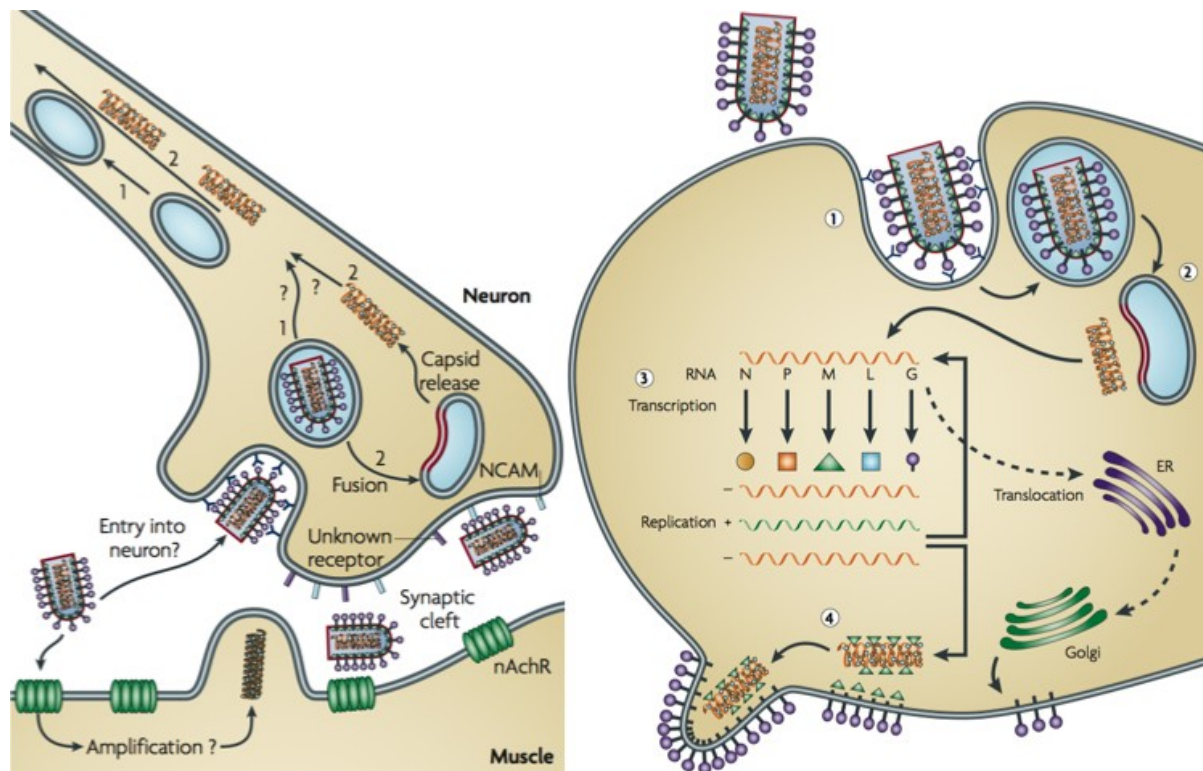


**Figure 27 RABV entry into neurons (left) and replication cycle (right) (modified from Schnell et al., 2009)**

#### *b1) Wild Type RABV (fixed variants)*

These were the first RABV strains used, both for tracing and rabies virus vaccines. Besides tracing, early neuroanatomist like Ramón y Cajal observed tissue samples from RABV-infected animals to describe the pathophysiological consequences on cellular morphology (see Ramón y Cajal, 1906).

RABV was shown to be suitable for neuronal tracing in rodents and primates (Astic et al., 1993; Ugolini, 1995; Kelly and Strick, 2000). These reports remarked the low cytotoxicity, the timely spread, and the practically restricted neuronal specificity. The seminal work carried out by in parallel by Ugolini and Kelly paved the way for the wide application of the CVS-11 strain, which was used alone or combined with conventional tracers to unveil circuits in many animal models (reviewed in Gomme et al., 2011).

#### *b2) Modified RABV (recombinant variants)*

The second generation of RABV variants were characterized for being pseudotyped and/or genetically modified. The most revolutionary modification introduced the expression of a fluorescent reporter, which is amplified by native cell expression and yields a bright visualization of traced neurons. Modified RABV variants have been used for advanced tracing, but also in vaccines for rabies and

other infectious diseases of viral and bacterial origin (Wiktor et al., 1984; Thomas and Luxon, 2013). The main variants for tracings are listed below.

### *b2.1) VSV Pseudotyped and Glycoprotein-deleted RABV*

RABV naturally spreads strictly retrogradely: it enters through presynaptic terminals and is transported to the cell body (see Figure 27). The glycoprotein encoded in the RABV gene 'G' is responsible for trans-synaptic spread (Eteessami et al., 2000). Glycoprotein-deleted RABV (RABV  $\Delta$ G) variants cannot spread trans-synaptically. A gene coding a fluorescent reporter can be inserted instead of G. Finally, by pseudotyping RABV particles with the VSV envelope, RABV can infect also anterogradely: enter the cell through the soma and subsequently label neurites (Haberl et al., 2014). Thus, this technique labels first order neurons anterograde to the site of infection but it does not trace trans-synaptically.

### *b2.2) EnvA Pseudotyped and Glycoprotein-deleted RABV*

As in the previous variant, RABV  $\Delta$ G particles were pseudotyped, in this case with the envelope from ASLV-A (for "Avian Sarcoma and Leukosis Virus A"), termed EnvA, which complemented with expression of TVA (i.e. cognate surface membrane protein for the avian virus, which is not present in mammalian cells) in a cell or a population can limit initial infection to a defined target without further trans-synaptic spread (Wickersham et al., 2007a). If the glycoprotein is not deleted, EnvA pseudotyped RABV infection is limited to the target and higher-order neurons are poly-transsynaptically traced (Nguyen et al., 2012).

### *b2.3) EnvA pseudotyped RABV $\Delta$ G and RG expression*

If EnvA pseudotyped RABV  $\Delta$ G is complemented with TVA and RABV glycoprotein (RG) expression, only the defined target cell or population is infected, but in this case the mono-trans-synaptic retrograde neurons are also traced (spread stops in the 2<sup>nd</sup>-order cells since RG is not expressed) (see Figure 28) (Wickersham et al., 2007a, b). Using this approach anterograde trans-synaptic tracing has also been reported from primary sensory neurons to CNS neurons (Zampieri et al., 2014).

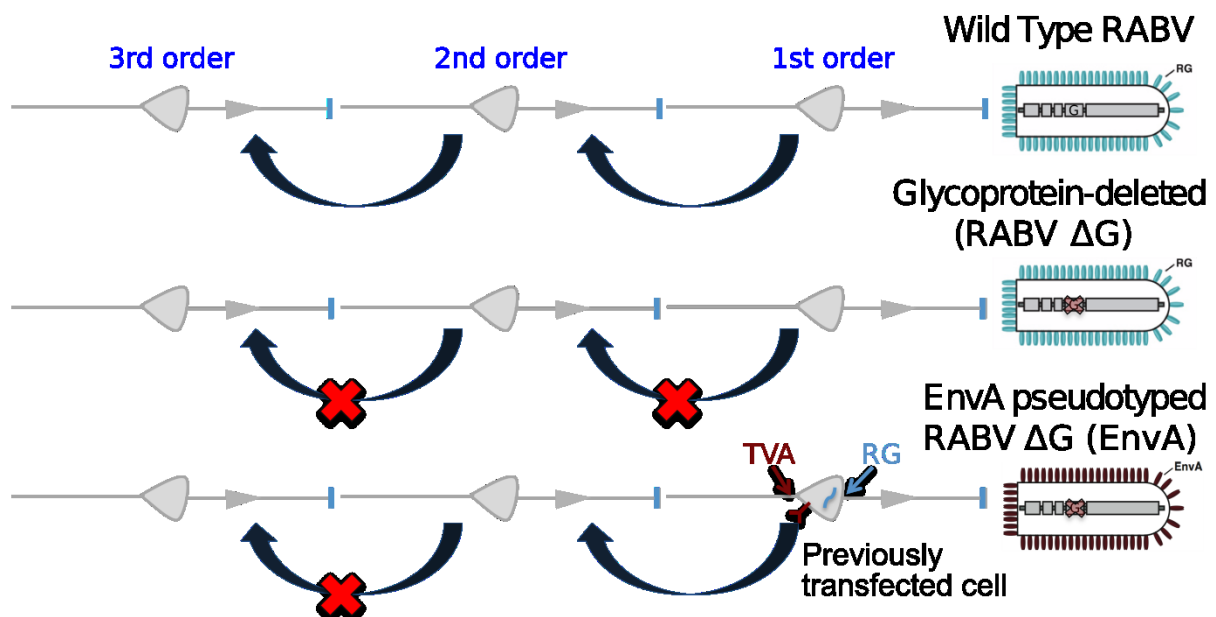


**Figure 28 WT and modified RABV tracing (modified from Ginger et al., 2013).**

It is possible to trace networks of a targeted starter cell and a cell population by using single-cell electroporation and Cre-dependent helper viruses, respectively (see also the use of stem cell-derived neurons: Garcia et al., 2013). These techniques are used to express RG and TVA in the cell or cell population of interest, permitting subsequent RABV  $\Delta G$ (EnvA) infection to be limited to the predefined target(s).

Modified RABV variants have been widely applied including:

- improved transsynaptic tracing (Miyamichi et al., 2013 reviewed in Dum and Strick, 2013).
- double recombinant viral transsynaptic tracing (Ohara, 2009; Ohara et al., 2013)
- cre-dependent tracing (Wall et al., 2010; Sun et al., 2014)
- single-cell starter and poly-transsynaptic tracing (Nguyen et al., 2012)
- single-cell starter and mono-transsynaptic tracing (Marshall et al., 2010)
- tracing of excitatory or inhibitory neurons (Liu et al., 2013)
- unveiling monosynaptic circuits such as:

1) new born GC neurons (Vivar et al., 2012; Deshpande et al., 2013; Vivar and Van Praag, 2013). This was achieved by using the Moloney murine leukemia virus (MMLV) as helper virus to express the TVA, RG, and fluorescent reporters, as this virus only spreads in dividing cells.

2) Hippocampus : CA2-EC II (Rowland et al., 2013) and Weible et al., 2010

3) Olfactory system (Choi et al., 2008; Arenkiel et al., 2011; Choi and Callaway, 2011)

4) in vivo tracing of a single cell: Marshel et al., 2010 (SCE), Rancz et al., 2011; Velez-Fort et al., 2014 (via whole-cell transfection)

### *b2.4) New RABV variants*

Furthermore, neurotropic viral vectors have been recently combined with genetically encoded calcium indicators, with molecules to control neuronal activity (i.e. rhodopsins, allosteric receptor), or with recombinases for conditional expression of specific genes (i.e. reverse tetracycline transactivator, flippase recombinase, Cre), rendering this technique extremely valuable for physiologists. For new versions see Osakada et al., 2011 (see Figure 29).

### *5.2.2.3. Other Neurotropic Viruses*

Besides the viruses covered above, which are the most widely exploited for current tracing approaches, there are several other viruses with a great potential. Among them are viruses of the following neurotropic families: parvoviridae (i.e. AAV), adenoviridae (i.e. CAV-2), retroviridae (i.e. lentivirus), togaviridae (i.e. sindbis virus and semliki forest virus), paramyxoviridae (i.e. measles and mumps), or picornaviridae (i.e. polio and coxsackie). Although all these viruses exhibit neurotropism to some extent, and can potentially act as tracers, not all of them are currently used for this purpose. This is not an exhaustive list, but advances in the short-term are more likely expected in the ones mentioned.



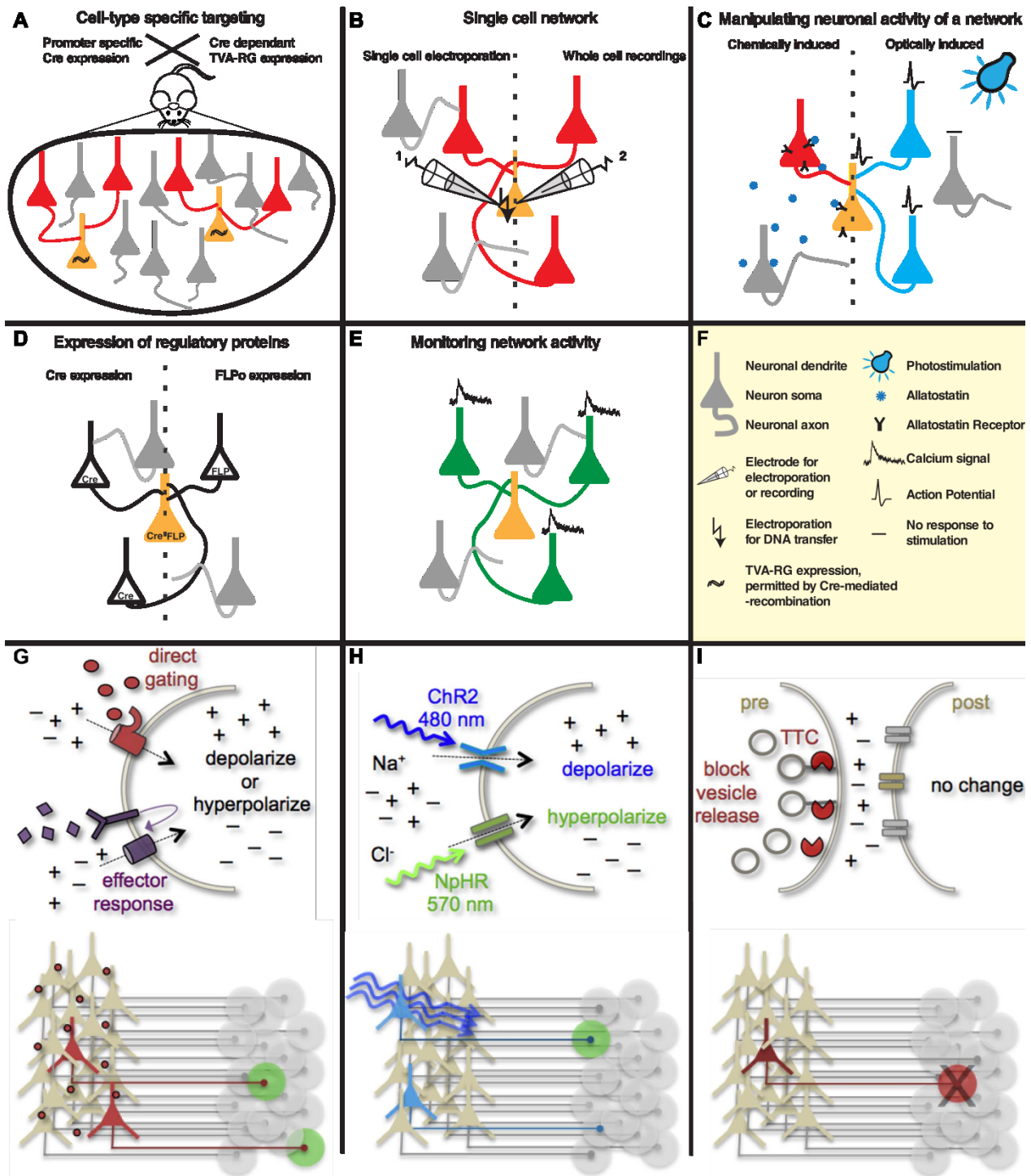


**Figure 29 Beyond labeling: trans-synaptic tracing strategies to monitor or manipulate activity/genomics of connected neurons or entire circuits. (A-F from Ginger et al., 2013 and G-I from Arenkiel, 2011)**

### 6. Scope of This Work

Since its first description, mossy fibers and the synapses they make onto CA3 neurons have been characterized by their particular morphology. Numerous physiological studies have reported MF-CA3 synapses to be distinct with a wide dynamic range of presynaptic facilitation stemming from a low initial release probability and multiple glutamate release sites. Nevertheless, the specific molecular mechanisms underlying the specific synaptic properties remain in great part elusive.

This work is composed of two main parts:

#### 1) Phenotyping hippocampal mossy fiber synapses in VAMP7 KO mice

We investigated the molecular mechanisms of presynaptic plasticity at hippocampal mossy fiber synapses by carrying out a detailed physiological characterization of a KO mouse for TI-VAMP/VAMP7.

#### 2) CA3 circuits probed with RABV-tracing and paired recordings

We developed a technique to establish paired recordings between connected dentate gyrus granule cells and CA3 pyramidal cells (GC-CA3) in mouse hippocampal organotypic slice cultures with the perspective to allow refined characterization of presynaptic parameters of MF-CA3 synapses. To identify direct presynaptic partners to a defined target CA3 pyramidal cell, we combined single-cell electroporation (SCE) and mono-trans-synaptic tracing based on a pseudotyped, recombinant rabies virus (EnvA pseudotyped RABV  $\Delta$ G). Using SCE we transfected a single CA3 pyramidal cell per slice with the plasmids encoding: RABV envelope glycoprotein (RG), a fluorescent reporter, and TVA (EnvA cognate surface receptor which has no homologue in mammalian cells). The slices were subsequently infected with EnvA pseudotyped RABV  $\Delta$ G. After 3-4 days, the RABV mono-trans-synaptic tracing revealed the presynaptic inputs of that single neuron. Then, we were able to establish paired recordings between connected GC-CA3 cells, as well as to quantify the inputs to the starter CA3 pyramidal cell.

# **Results**

# **&**

# **Discussion**

## Results & Discussion

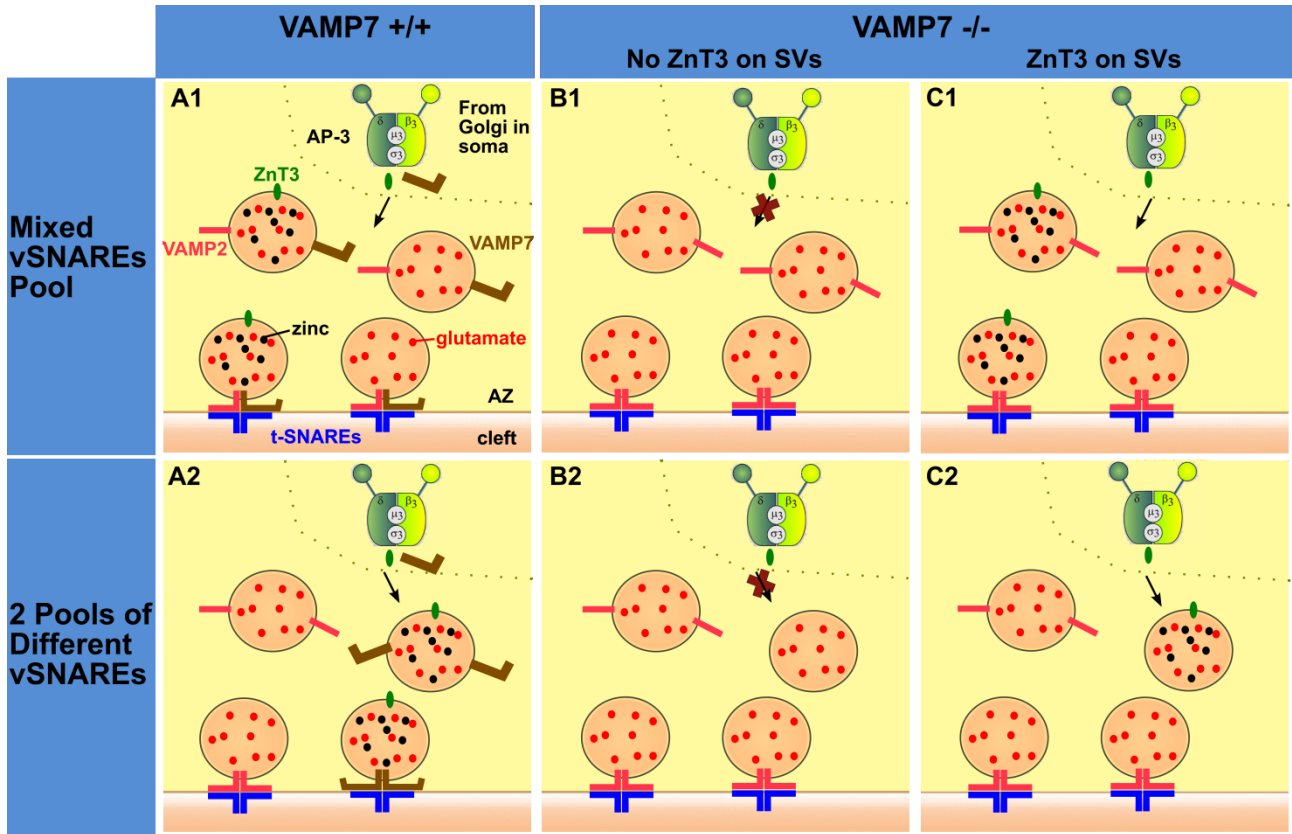
### Phenotyping Hippocampal Mossy Fiber Synapses in VAMP7 KO Mice

A current endeavour in cellular neuroscience is to better understand the molecular determinants of plasticity mechanisms. Given the rich expression of the vesicular SNARE TI-VAMP/VAMP7 in hippocampal mossy fibers, we decided to phenotype transmission at this synapse in an available knockout mouse model (Danglot et al., 2012).

Reports quantify the expression of VAMP2 in around 70 copies per synaptic vesicle (Takamori et al., 2006). The alternative vSNARE, TI-VAMP/VAMP7, is highly expressed in a subset of terminals, including hippocampal mossy fibers (MF) (Muzerelle et al., 2003), and possibly at many other synapses (Hua et al., 2011). It remains unknown how many copies are present per vesicle, and whether all vesicles in MF boutons (MFBs) express VAMP2 and/or VAMP7. Furthermore, the adaptor protein-3 (AP-3) packages VAMP7, ZnT3 and PI4KII $\alpha$ , together with other cargos, into synaptic vesicles that may form a subpool (Martinez-Arca et al., 2003; Salazar et al., 2004). It has been shown that ZnT3 is only present in a subset, around 17%, of MF SVs (Lavoie et al., 2011). Thus, two possible scenarios exist in VAMP7-expressing (WT) animals: a single pool of mixed vSNAREs (Table 1.A1), or 2 pools of different vSNAREs (Table 1.A2); a further variable, whether ZnT3 is absent or present, makes it four possible scenarios for KO (see Table 1.B1-2, and C1-2, respectively).

For the sake of simplicity, recycling pathway differences are not shown in Table 1. However, they are a potential source of pool sorting, as VAMP7-containing vesicles might be bulk endocytosed, and refilled with neurotransmitter(s) via an indirect way route that passes through endosomes, from which SV budding is AP-3-mediated (Blumstein et al., 2001; Cheung and Cousin, 2012), and spared when clathrin function is disrupted (Zlatic et al., 2013). On the other hand, VAMP2-containing SVs can be endocytosed through either short routes (i.e. kiss-and-run, or kiss-and-stay), if not fully fused with the plasma membrane, or through clathrin-dependent endocytosis if fully fused, from which SV budding is AP-2-mediated (Koo et al., 2011; Gordon and Cousin, 2013; Poudel and Bai, 2014).

**Table 1. Hypotheses VAMP7 pools and zinc release**



For instance, in calcyon KO mice, a protein that regulates the subcellular distribution of AP-3 and the targeting of AP-3 cargoes, ZnT3 and PI4KII $\alpha$  seem to be decreased at hMFs (Muthusamy et al., 2012), while a similar PI4KII $\alpha$  decrease was also observed in *mocha* mice, which lack the AP-3 $\delta$  subunit (Salazar et al., 2005). Disruption of AP-3 in *mocha* neurons resulted in loss of ZnT3 targeting, while synaptophysin, which was reduced in PC12 cells after AP-2 disruption, was not altered (Salazar et al., 2004). Moreover, in *mocha* mice evoked transmission is normal but spontaneous miniature EPSCs (mEPSCs) release frequency is increased (Scheuber et al., 2006). This might be explained by the absence of SNARE complex clamping exerted by the longin domain of VAMP7. Furthermore, asynchronous release was shown to be selectively diminished in AP-3b2 KO mice (Evstratova et al., 2014).

We first characterized basal properties like spontaneous transmission, EPSC amplitude, failures, evoked short-term plasticity—including paired-pulse ratio (PPR) and frequency facilitation (FF). Then we looked at evoked and asynchronous release triggered by short or long bursts of activity. Finally, we checked the possible implication of VAMP7 in the co-release of zinc with glutamate by monitoring NMDA EPSCs.

### **Phenotyping Hippocampal Mossy Fiber Synapses in VAMP7 KO Mice**

At the moment, we are testing a possible action-potential-independent facilitation through  $\alpha$ -7 nicotinic acetylcholine receptors ( $\alpha$ 7-nAChRs). But those experiments are not included in this work. The rest of the data is presented below in an article format, currently under preparation.

# Phenotyping hippocampal mossy fiber synapses in VAMP7 KO mice

In preparation

Bernat González i Llinares<sup>1,2,3</sup>, Lydia Danglot<sup>4,5</sup>, Matthijs Verhage<sup>3</sup>, Thierry Galli<sup>4,5</sup>  
and Christophe Mulle<sup>1,2</sup>

<sup>1</sup> Université de Bordeaux  
Institut Interdisciplinaire de Neurosciences, Bordeaux, F-33000 France

<sup>2</sup> CNRS UMR 5297, Bordeaux, F-33000 France

<sup>3</sup> Department of Functional Genomics and Clinical Genetics, Center for  
Neurogenomics and Cognitive Research, VU University Amsterdam and VU Medical  
Center, Amsterdam, The Netherlands

<sup>4</sup> Institut Jacques Monod, Unité Mixte de Recherche 7592, Centre National de la  
Recherche Scientifique, Université Paris Diderot, Sorbonne Paris Cité, Paris, France

<sup>5</sup> Institut National de la Santé et de la Recherche Médicale Equipe de Recherche  
Labelisée U950, Membrane Traffic in Neuronal and Epithelial Morphogenesis, Paris,  
France

Correspondence to:  
Christophe Mulle (christophe.mulle@u-bordeaux.fr)

**Key words:** v-SNARE, VAMP7, synaptic plasticity, hippocampus



## **Abstract**

VAMP7 is a vesicular SNARE of the longin family that localizes to axons and dendrites during development, where it has been shown to be important in neurite growth. In the adult brain, VAMP7 is enriched in a subset of nerve terminals, particularly in hippocampal mossy fibers (MFs) originating from the dentate gyrus. We analyzed the VAMP7 function in neurotransmitter release by detailed functional characterization of MF synapses onto CA3 pyramidal cells in knockout mutant mice for VAMP7. We have evaluated the role of VAMP7 in different forms of short-term synaptic plasticity and in a potential contribution of the co-release of glutamate and zinc. Albeit extensive, this analysis in mice has not revealed any significant impact of the loss of VAMP7 for basal properties of synaptic transmission, for short-term plasticity, for asynchronous release and for the ability of MF vesicles to release ionic zinc. The potential role of VAMP7 in the structural and functional organization and plasticity of the presynaptic compartment is discussed.

## Introduction

At chemical synapses, neurotransmitter release relies on synaptic vesicle (SV) exocytosis. This process is mediated, like all other intracellular membrane fusion events, by SNARE (for “soluble *N*-ethylmaleimide-sensitive factor attachment protein receptor”) proteins present at vesicles (v-SNAREs) and at the target membrane (t-SNAREs) (also called R- and Q-SNAREs respectively, according to the conserved arginine or glutamine residue) (Weber et al., 1998). SNAREs are small (14-40 kDa) membrane-bound proteins that contain the 60-70 amino-acid  $\alpha$ -helical coiled-coil domain called the SNARE motif (Jahn & Scheller, 2006). The interaction between opposed v- and t-SNAREs impels the formation of a trans-SNARE complex, or SNAREpin, in which four SNARE motifs zipper into a four-helix bundle that brings the membranes together and ultimately catalyzes their fusion (Söllner et al., 1993; Weber et al., 1998). The human genome encodes 38 SNAREs, with numerous members in each subfamily, which results in a large array of possible combinations (Gordon et al., 2010). Particular SNARE collections reside predominantly in specific subcellular compartments, where they are specialized for individual intracellular fusion reactions (Jahn & Scheller, 2006). However, there are redundancies in fusion pathways, such as a SNARE complex which functions at multiple compartments, or several SNARE complexes mediating the same membrane fusion.

v-SNAREs are classified into the following subfamilies: the “longins”, which contain the N-terminal longin domain (LD) extension of ~120 residues, and the “brevins”, which are shorter (Filippini et al., 2001). The main SV SNARE is the brevin synaptobrevin2/VAMP2 (for “vesicle-associated membrane protein” 2). Its canonical partners at the plasma membrane are syntaxin1 and SNAP-25. In the absence of VAMP2, evoked and spontaneous neurotransmission are reduced to around 1% and 10% of control respectively (Schoch et al., 2001). In normal physiological conditions, two VAMP2 molecules are sufficient for SV exocytosis (Sinha et al., 2011). A prototypic SV contains ~70 VAMP2 copies, but also lower levels of noncanonical v-SNAREs such as Vti1a, VAMP4 and VAMP7 (also called “tetanus neurotoxin-insensitive” or TI-VAMP) (Takamori et al., 2006; Wilhelm et al., 2014). The expression of these alternative v-SNAREs probably explains the residual synaptic transmission in VAMP2 KO mice. The remaining debate is whether low levels of these v-SNAREs play a role in SV exocytosis in the presence of VAMP2. The existence of SV populations expressing different v-SNAREs, or at different ratios, has been proposed to account for distinct forms of SV exocytosis (for review see Ramirez

and Kavalali, 2012). However, others claim a unique origin for SVs, independently of whether their mode of release is evoked or spontaneous (for review see Kaeser and Regehr, 2014).

VAMP7 is a longin that was first shown to associate with SNAP-23, and syntaxin3 in clostridial neurotoxin-resistant exocytotic processes at the apical plasma membrane of epithelial cells (Galli et al., 1998). VAMP7 has been reported to mediate lysosomal and granule exocytosis in several cell types (Chaîneau et al., 2009) including neurons (Burgo et al., 2012). Depending on the cell type, VAMP7 can interact with several t-SNAREs (syntaxin1, 3, 4, 6, 7, 8 and 10; SNAP-23, -25 and -29; and Vti1b), but neither with syntaxin 13, nor 16 (for review see Rossi et al., 2004). VAMP7 is the SNARE of secretory lysosomes contributing to ATP secretion from astrocytes (Verderio et al., 2012), and to zinc secretion from HeLa cells (Kukic et al., 2014). Furthermore, VAMP7 localizes to axons and dendrites during development (Coco et al., 1999), where it has been shown to be important in neurite growth in cultured neurons and *in vivo* (Alberts et al., 2003; Gupton and Gertler, 2010; Racchetti et al., 2010). In the adult brain, VAMP7 is enriched in a subset of nerve terminals, particularly in mossy fibers originating from the dentate gyrus granule cells as indicated by strong labeling in the projecting region (the stratum lucidum) in CA3 (Muzerelle et al., 2003).

The LD of VAMP7 targets it to SVs by binding to the  $\delta$ -subunit of the clathrin-coat AP-3 (AP3 $\delta$ ) (Scheuber et al., 2006). In *mocha* mice, which lack AP3 $\delta$ , SVs do not contain VAMP7 and the zinc-transporter ZnT3 –among other cargos, and the SV and RRP size have been reported to be increased (Newell-Litwa et al., 2010; Danglot and Galli, 2007). The LD also inhibits the formation of SNARE complexes (Martinez-Arca et al., 2003; Vivona et al., 2010; Schäfer et al., 2012). Thus, VAMP7 has a lower capacity than VAMP2 to assemble in SNARE complexes. Decreased membrane fusion efficiency due to the LD affects neurite outgrowth (Martinez-Arca et al., 2000; Martinez-Arca et al., 2001), as well as SV release (Hua et al., 2011; Burgo et al., 2013). VAMP7-mediated exocytosis relies on tyrosine 45 phosphorylation by c-Src kinase, which happens after treatment with insulin but not after depolarization or intracellular calcium rise (Burgo et al., 2013).

VAMP7-containing SVs remain in a pool reluctant to fuse, and which seems to engage preferentially in spontaneous neurotransmitter release in crayfish (Hua et al., 1998) and rodents (Scheuber et al., 2006; Hua et al., 2011; Ramirez et al., 2012). Furthermore, asynchronous release was shown to be selectively diminished in AP-

3b2 KO mice (Evstratova et al, 2014). Recently, Reelin has been reported to enhance such spontaneous release in an action potential-independent manner (Bal et al., 2013).

Loss of VAMP7 in mice does not cause major developmental or neurological deficits (Sato et al., 2011; Danglot et al., 2012), but it has been associated with increased anxiety-related behavior (Danglot et al., 2012). In addition, neurite outgrowth showed a moderate reduction in cultured mutant hippocampal neurons (Sato et al., 2011), albeit no overt sign of this defect was found *in vivo* (Danglot et al., 2012). Here, we set out to analyze VAMP7 function in neurotransmitter release and presynaptic forms of synaptic plasticity by characterizing synaptic transmission at hippocampal MF-CA3 synapses in VAMP7 knock-out mice.

## Materials and Methods

All experiments were performed in accordance with the European Communities Council Directive of 24 November 1986 and the European Directive 2010/63/EU on the Protection of Animals used for Scientific Purposes.

### ***Animal procedures and genetically modified mice***

Mice were housed in a temperature – and humidity- controlled animal colony on a 12h dark-light cycle with food and water available ad libitum. VAMP7 knockout (KO) mice were generated as described in Danglot et al., 2012. WT and VAMP7 KO mice were male littermates.

### ***Slice Electrophysiology***

Parasagittal hippocampal slices (320  $\mu$ m) were obtained from 18- to 25-day-old male VAMP7 KO mice and WT littermates. Slices were transferred to a recording chamber in which they were continuously superfused with an oxygenated extracellular medium (95% O<sub>2</sub> and 5% CO<sub>2</sub>) containing 125 mM NaCl, 2.5 mM KCl, 2.3 mM CaCl<sub>2</sub>, 1.3 mM MgCl<sub>2</sub>, 1.25 mM NaH<sub>2</sub>PO<sub>4</sub>, 26 mM NaHCO<sub>3</sub>, and 20 mM glucose (pH 7.4). Bicuculline (10  $\mu$ M) was present in the superfusate of all experiments. Whole-cell voltage-clamp recordings were made at room temperature (except for NMDA EPSCs and mEPSCs, which were made at ~32°C) from CA3 pyramidal cells under infrared differential interference contrast imaging with borosilicate glass capillaries, which had resistances between 4–8 M $\Omega$ . For MF-CA3 EPSCs at -70 mV, the patch electrodes were filled with a solution containing 140 mM CsCH<sub>3</sub>SO<sub>3</sub>, 2 mM MgCl<sub>2</sub>, 4 mM NaCl, 5 mM phospho-creatine, 2 mM Na<sub>2</sub>ATP, 0.2 mM EGTA, 10 mM HEPES, and 0.33 mM GTP (pH 7.3) adjusted with CsOH. For NMDA EPSCs the patch electrodes were filled with a solution containing (in mM): 120 cesium methanesulfonate, 2 MgCl<sub>2</sub>, 4 NaCl, 5 phospho-creatine, 2 Na<sub>2</sub>ATP, 20 BAPTA, 10 HEPES, 0.33 GTP (pH 7.3) adjusted with CsOH.

MF-CA3 EPSCs were evoked by minimal intensity stimulation via a glass electrode (about 1  $\mu$ m tip diameter) positioned in the hilus region of the dentate gyrus. Stimulation pipettes were filled with 1M NaCl and stimulation pulses in basal conditions were provided at 0.1 Hz (200 ms duration, 5 - 40 V and 15 - 30 mA amplitude). MF synaptic currents were identified according to the following criteria: robust low frequency facilitation, low release probability at 0.1 Hz, rapid single rise times (~1 ms), and decays free of secondary peaks that may indicate the presence of polysynaptic contamination.

The access resistance was  $< 20 \text{ M}\Omega$  and recordings were discarded if it changed by  $> 20 \%$ . No series resistance compensation was used. Recordings were made using an EPC 9.0 or EPC 10.0 amplifier, which were run with Pulse and Patch Master software (HEKA Elektronik, Lambrecht/Pfalz, Germany), respectively. Data were filtered at 3 kHz, digitized at 10 or 20 kHz, and stored on a personal computer for additional analysis.

To record NMDA EPSCs, cells were voltage-clamped at +40 mV and NMDA EPSCs isolated by blocking AMPA and kainate receptors with 20  $\mu\text{M}$  NBQX. The selective GABA<sub>B</sub> receptor antagonist CGP 55845 was also added at 3  $\mu\text{M}$  to better record responses to trains of stimuli.

To record mEPSCs, 0,5  $\mu\text{M}$  TTX was added to the extracellular medium.

Bicuculline methochloride, 2,3-dihydroxy-6-nitro-7-sulfamoyl-benzo[f]quinoxaline-2,3-dione (NBQX), D-(-)-2-amino-5-phosphonovaleric acid (D-APV), CGP 55845, and TTX were from Tocris. All other compounds were from Sigma-Aldrich.

### ***Data Analysis and Statistics***

Data were analyzed using IGOR Pro (Wavemetrics, Lake Oswego, OR). Results are expressed as mean  $\pm$  SEM, unless otherwise indicated; n indicates the number of different cells. Statistical comparisons were performed using Student's t test and statistical significance was set at 0.05. Statistical comparison between normalized data was performed using nonparametric Mann-Whitney test. EPSP amplitudes during trains of stimulation were obtained by measuring the maximal amplitude value reached during the train of EPSPs. Statistical analysis was performed with GraphPad Prism software.

### ***Immunohistochemistry***

Mice were anesthetized with pentobarbital (60 mg/kg, ip) then intracardially perfused with 4% paraformaldehyde (PFA) in PBS. Tissues were postfixed for 1 h in 4% PFA and cryoprotected in PBS-sucrose 30% (w/v) overnight. Cryotome sections (50  $\mu\text{m}$ ) were incubated in PBS-NH<sub>4</sub>Cl (20 min, room temperature) and permeabilized in PBS + 0.1% Triton, 0.2% gelatin (PBSTg). Sections were then incubated for 2 days at 4°C with the primary antibodies in PBSTg and with the secondary antibodies for 3 h. Controls without primary antibody were always negative. Specimens were observed with a 20x oil immersion objective, followed by a 1.1 digital zoom magnification. Images were acquired on a Leica SP5 confocal microscope by sequential scanning of the emission lines. Alexa 488 was detected by using the 488 nm-line of an argon

laser for excitation; Cy3 and Cy5 were respectively excited by the 543 nm-line of a green neon laser and the 650 nm-line of a helium neon laser. Typically, sections (4096 X 4096 pixels), with an interval of 0.32  $\mu$ m, were scanned three times, to optimize the signal/noise ratio. Quantifications were performed using ICY software.

The antibodies used were: against TI-VAMP/VAMP7 (described in Muzerelle et al., 2003), rabbit polyclonal anti-Munc13-1 (Synaptic Systems), mouse monoclonal anti-ZnT3 (Synaptic Systems), and rabbit polyclonal anti-VIAAT (provided by B. Gasnier, Paris).



## Results

### ***The expression of presynaptic proteins in the stratum lucidum is moderately affected in VAMP7 KO mice***

Because VAMP7 is highly expressed in the hippocampal MF track, we tested whether the loss of the presynaptic VAMP7 impacts on the expression of canonical presynaptic proteins in the stratum lucidum (sl), the region where MFs make synaptic contacts onto CA3 cells. We used immunolabeling for several presynaptic proteins, and expression intensity in VAMP7 KO mice was normalized to the average WT expression. VAMP7 staining was completely lost in KO (Figure 1A). Munc13-1 (Figure 1B) protein was used as a canonical presynaptic marker. Munc-13-1 intensity increased to  $180\% \pm 48$  ( $n=2$  for both WT and KO,  $>20$  confocal slices/animal). This increase in Munc13 intensity could be interpreted as an increase in synapse density. To answer this question, we quantified the amount of synaptic boutons by measuring the density of Munc-13 puncta in the stratum lucidum. Here again the density of Munc13 puncta was increased in the 2 KO ( $140\% \pm 12$  of the WT), suggesting an increased density of synaptic terminals. To rule out a potential general effect on excitatory and inhibitory synapses, we proceeded to the labeling of GABAergic presynaptic boutons with a VIAAT (Vesicular Inhibitory Amino Acid Transporter) staining. In contrast to Munc13 staining, VIAAT intensity (Figure 1C) remained unchanged ( $94\% \pm 5$ ,  $n=2$  animals,  $>20$  confocal slices/animal). We found that the intensity of Munc13 was stable in stratum pyramidale and stratum radiatum ( $99.5 \pm 9\%$  in stratum pyramidale, and  $87 \pm 19\%$  in stratum radiatum), indicating that the increase of synaptic density was specific to stratum lucidum where MF terminals are enriched. Because, VAMP7 targeting in presynaptic terminals is dependent on the molecular adaptor AP3, we also checked the expression of the zinc transporter ZnT3, a presynaptic vesicular molecule whose targeting is also AP3-dependent. In VAMP7 KO mice, ZnT3 intensity (Figure 1D) decreased to  $67 \pm 16\%$  ( $n=2$ ,  $>20$  confocal slices/animal), indicating that ZnT3 is still able to reach the presynaptic MF boutons in the absence of the VAMP7 vSNARE on the AP3 vesicles.

### ***Basal transmission and short-term plasticity are not impaired in VAMP7 KO mice***

We tested the potential role of VAMP7 in controlling neurotransmitter release and plasticity at MF-CA3 synapses. We recorded CA3 pyramidal cells in the whole-cell voltage clamp mode in slices from WT and VAMP7 KO mice, and we evoked MF-EPSCs by minimal stimulation of MFs with an electrode positioned in the DG (Marchal, 2004) (Figure 2A). The average amplitude of MF-EPSCs evoked at a

frequency of 0.1Hz was not significantly different between the two genotypes (WT:  $46.7 \pm 5.3$  pA,  $n=14$ ; VAMP7 KO:  $39.2 \pm 2.9$  pA,  $n=15$ ;  $P$  value = 0.2184) (Figure 2B). The rate of failure of MF-EPSCs, which is indicative of the initial release probability at MF-CA3 release sites, was similar in WT and VAMP7 KO mice ( $22.7 \pm 5.6\%$  and  $23.3 \pm 3.9\%$ , respectively,  $P$  value = 0.9306) (Figure 2C). These results indicate that the basal properties of MF-CA3 synapses are not affected by the loss of VAMP7.

We then examined whether different forms of short-term plasticity were altered in VAMP7 KO mice. Differences in the extent of paired-pulse facilitation, consisting in two stimulation separated by a short time interval (e.g 40 ms), is generally used to test for changes in release probability. Paired-pulse ratio (PPR) was slightly higher in VAMP7 KO mice, but this tendency did not reach statistical significance ( $4.7 \pm 0.7$  in VAMP7 KO vs.  $3.5 \pm 0.5$  in WT,  $P$  value = 0.2155) (Figure 2D, E). MF-CA3 synapses undergo a rather unique form of presynaptic plasticity named frequency facilitation (FF). FF corresponds to the marked facilitation of MF-CA3 synaptic transmission upon increasing the steady rate of stimulation from low (0.1 Hz) to moderate (from 0.5 to 3 Hz). FF was not significantly altered in VAMP7 KO mice (WT:  $388 \pm 19\%$ ,  $n=14$ ; VAMP7 KO:  $418 \pm 47\%$ ,  $n=15$ ; Student's unpaired  $t$  test,  $P$  value = 0.5782) (Figure 2F-H). We also tested synaptic facilitation by stimulating MFs with either five or ten stimuli at 20Hz (Figure 3). MF-EPSC facilitation, as normalized to the average amplitude of the first stimulus, was not affected for neither train stimuli number (Figure 3B and F), although the amplitude of the first EPSC in either of the trains was higher for VAMP7 KO slices ( $42.6 \pm 7.6$  pA in VAMP7 KO vs.  $30.1 \pm 5.0$  pA in WT for 5 stimuli, and  $47.2 \pm 5.7$  pA in VAMP7 KO vs.  $34.3 \pm 7.3$  pA in WT for 10 stimuli). It could be that the great variability masks eventual significant differences (Student's unpaired  $t$  test,  $P$  value = 0.2087 and 0.175 respectively) (Figure 3C and G). Finally, the charge for each train was also slightly higher in mutant mice ( $20.2 \pm 2.1$  pC in VAMP7 KO vs.  $15.6 \pm 1.6$  pC in WT for 5 stimuli, and  $36.5 \pm 5.7$  pC in VAMP 7 KO vs.  $30.6 \pm 6.3$  pC in WT for 10 stimuli), but this was not statistically significant (Student's unpaired  $t$  test,  $P$  value = 0.1062 and 0.5424 respectively) (Figure 3D and H).

### ***Spontaneous release is not altered in VAMP7 KO slices***

Immunocytochemical labeling of Munc13 indicate a possible increase of synaptic release sites in VAMP7 KO mice. Functionally this could be translated into increased spontaneous release activity. Unexpectedly, neither the frequency nor the

amplitude of mEPSCs were altered in VAMP7 KO mice (Figure 4). mEPSCs recorded in CA3 pyramidal cells arise from MF synapses as well as from A/C and perforant path glutamatergic synapses. We separated synaptic events according to their amplitude, considering that MF-CA3 EPSCs display on average higher quantal size (Henze et al., 2002). The frequency of large mEPSCs ( $>25\text{pA}$ ) was not significantly different in both genotypes ( $0.92 \pm 0.17\text{ Hz}$ ,  $n=23$  in WT vs  $1.20 \pm 0.19$ ,  $n=23$  in VAMP7 KO). It thus appeared that evoked and spontaneous EPSCs are not significantly altered in VAMP7 KO mice.

### ***Plasticity of evoked MF-EPSCs after long bursts is not altered by loss of VAMP7***

ZnT3-containing (Lavoie et al., 2011) and VAMP7-containing (Hua et al., 2011) SVs have been reported to be released more reluctantly. We thus reasoned that synaptic release events evoked after long trains of stimulation could be impaired. In order to further investigate the release of the RRP, we applied 5 s-trains at 10, 20, and 40 Hz (Figure 5). Similarly to shorter trains, when MF-EPSC amplitude was normalized to the average of the first stimuli, the extent of plasticity evoked by long trains was also unaffected (Figure 5). The amplitude of the first EPSC in either of the trains were not significantly different between the two genotypes for 10, 20 Hz and 40 Hz trains (10Hz:  $165 \pm 39\text{ pA}$  vs.  $123 \pm 66\text{ pA}$  in WT; 20Hz:  $166 \pm 25\text{ pA}$  vs.  $115 \pm 32\text{ pA}$ ; 40Hz:  $129 \pm 22\text{ pA}$  vs.  $143 \pm 65\text{ pA}$ ; Student's unpaired t test, P value = 0,5652; 0,2401, and 0,8063 respectively).

### ***Asynchronous release after short and long bursts is not altered by loss of VAMP7***

Treatment of cultures with TeNT revealed an asynchronous release component in WT but not in slices of *mocha* mice, and no asynchronous release was observed in TeNT-untreated explants by stimulation at 0.1 Hz (Scheuber et al., 2006). We thus investigated asynchronous release in VAMP7 KO mice. Asynchronous MF-EPSCs occur during several hundreds of ms following prolonged bursts of stimulation (Figure 6). We calculated for each genotype the average number of asynchronous events and median amplitude (per bins of 10ms), in the 500 ms preceding and following short bursts (i.e. trains of five and ten stimuli at 20 Hz) (Figure 6A and D). Next, we compared the frequency of events in the 100 ms post-stimulation, as a ratio of the events in the 500ms baseline (Figure 6B and E). Those frequencies did not differ in the absence of VAMP7 after either number of stimuli (5st:  $18.2 \pm 5.3\text{ Hz}$  vs.  $17.7 \pm 6.5\text{ Hz}$  in WT, P value = 0.9561; 10st:  $30.5 \pm 10.3\text{ Hz}$  vs.  $26.1 \pm 5.8\text{ Hz}$ , P value = 0.7098). We also compared the cumulative probability of the

asynchronous events (Figure 6C and F), without finding any disparity (Kolmogorov-Smirnov test, P value = 0.1798 and > 0.9999, for 5 and 10st respectively). Finally, we compared the average median amplitude of the preceding 500ms ('pre'), the 100ms post-stimulation ('10bins post'), and the 500ms post-stimulation ('post') (Figure 6G and H). The one-way ANOVA tables for these multiple comparisons are shown below (Supplementary Table 1 and 2, for 5 and 10st respectively).

We then examined whether asynchronous release following long bursts of stimulation was altered in the absence of VAMP7. Long bursts (namely trains of 5 seconds at 10, 20, and 40Hz (Figure 7) give rise to numerous and complex EPSCs that follow bursts of stimulation for up to 500ms. Thus, instead of counting the number of events, we chose to compare the charges of the first 500ms of each train, the total train charge (5s), and the subsequent 500ms of asynchronous release (Figure 7G, H, and I, respectively). The initial charge (1<sup>st</sup> 500ms) increased linearly with increasing stimulation frequency, and despite a higher charge at all frequencies in KO slices, this tendency did not reach statistical significance (Figure 7G and Supplementary Table 3). On the other hand, the total train charge and asynchronous charge attained a maximum at 20 Hz, and decreased at 40 Hz, while no significant difference was observed between genotypes (Figure 7H and I, and Supplementary Table 4 and 5, respectively). Overall our comparison did not reveal any significant differences in the ability of MF-CA3 synapses to evoke asynchronous release in the absence of VAMP7.

### ***Synaptic release of zinc in the absence of VAMP7***

The targeting of the zinc transporter ZnT3 depends on the molecular adaptor AP3 like VAMP7. This suggests that VAMP7 is expressed in zinc containing vesicles. Although the expression of ZnT3 is only moderately decreased in VAMP7 KO mice, we tested whether zinc release from MF terminals may be affected in the absence of VAMP7. To examine the dynamics of zinc release at excitatory synapses, in particular at MF-CA3 synapses, we took advantage of the high nanomolar sensitivity of the GluN2A NMDAR subunit for zinc (Vergnano et al, 2014). Despite the presence of the GluN2A subunit at MF-CA3 synapses, it has been recently shown that a single synaptic event is unable to produce zinc modulation of NMDA currents at this low release probability synapse, while modulation is apparent at higher release probability SC-CA1 synapses and at MF-CA3 synapses which were conditionally shifted to higher release probability (Vergnano et al., 2014).

We recorded from NMDA-mediated EPSCs at + 40 mV in the presence of NBQX to block AMPA and kainate receptors. To allow to detect modulation of NMDA-EPSCs by synaptically released zinc at MF-CA3 synapses, we increased release probability by conditioning with 10 stimuli at 3 Hz, then applied a train of 7 stimuli at 25 Hz (Figure 8). This protocol should enable to evaluate whether the amount of zinc being released at MF-CA3 is altered in VAMP7 KO mice, by the extent of NMDA-EPSC inhibition during the train. We found no difference in the NMDA-response to the train at 25 Hz between the two genotypes (Figure 8) indicating that zinc is released at comparable levels in WT and VAMP7 KO mice.

## Discussion

VAMP7 is a synaptic v-SNARE abundantly expressed in the hippocampal stratum lucidum, the region where MFs make synaptic contacts with CA3 pyramidal cells and interneurons. In *mocha* mice, which are deficient in functional AP-3, VAMP7 is similarly lost in hippocampal MF terminals, whereas the localization of synaptobrevin 2 is unaffected (Scheuber et al, 2006). In these mice, evoked MF-CA3 transmission is normal, but spontaneous miniature EPSCs (mEPSCs) release frequency recorded in CA3 pyramidal cells is increased (Scheuber et al., 2006). The loss of VAMP7 and the absence of SNARE complex clamping exerted by the longin domain of VAMP7 seemed most likely to explain the perturbation described in *mocha* mice. The Longin domain of VAMP7 was recently further proposed to regulate spontaneous release but not evoked release in cultured hippocampal neurons (Hua et al., 2011). This prompted us to directly examine the consequences of the loss of VAMP7 on spontaneous and evoked synaptic transmission and plasticity at MF-CA3 synapses.

Immunolabeling experiments confirmed the loss of VAMP7 in MF terminals and showed moderate increase in the labeling intensity for the presynaptic protein Munc13 which is consistent with an increase in synapse density, whereas no change in the GABAergic marker VIAAT was observed. Our detailed electrophysiological analysis has provided no evidence that functional properties of MF-CA3 synapses were affected by the loss of VAMP7. In contrast to findings in *mocha* mice, we found no significant difference in the frequency of spontaneous EPSCs in CA3 pyramidal cells, even when restricting the analysis to EPSCs of higher amplitude (>25 pA), which likely arise from MF synapses (Henze et al., 2002). The basic properties of evoked EPSCs, using a minimal stimulation protocol were not affected, indicating no overt change in the quantal parameters and release probability. In addition, the frequency and amplitude of asynchronous events, which occur in a delayed manner following short trains of stimulation were not different in the two genotypes. Interestingly, this form of synaptic release was recently shown to be selectively diminished in AP-3b2 KO mice (Evstratova et al, 2014). Overall, our data suggest that the synaptic phenotype of mice lacking AP-3 cannot be accounted by a deficient targeting of VAMP7 to MF synaptic vesicles. Disruption of AP-3 mediated endocytosis should be considered. Similar to VAMP7, ZnT3 has also been shown to be selectively present in vesicles derived through an AP-3-dependent mechanism (Kantheti et al, 1998), suggesting that the loss of VAMP7 may affect the release of a

specific pool of vesicles containing zinc (Lavoie et al, 2011). Using a recently described protocol to assess the dynamics of zinc at MF-CA3 synapses (Vergnano et al, 2014), we observed that zinc was normally released during short trains of stimulation at MF-CA3 synapses.

VAMP7-containing vesicles have been shown to preferentially replenish resting pool that contributes only minimally to evoked release but may comprise a reluctantly released pool of vesicles (Hua et al, 2011). However, the compound synaptic responses to long trains of stimulation were not impacted by the loss of VAMP7. In general, characteristic forms of short term plasticity at MF-CA3 synapses, such as paired pulse facilitation, frequency facilitation or train facilitation were not different in WT and VAMP7 KO mice.

The apparent lack of a synaptic phenotype is rather unexpected. Compensatory mechanisms may be invoked. However there is clear evidence for impairment in certain features of synaptic transmission (i.e spontaneous or asynchronous release) in mice lacking AP-3 which also lack VAMP7 at MF-CA3 synapses (Scheuber et al, 2006; Estratova et al, 2014). Compensatory mechanisms to explain the lack of an apparent phenotype in VAMP7 KO mice are not consistent with a synaptic phenotype in AP-3 deficient mice. On the other hand, we found altered expression of presynaptic proteins like Munc13-1 and ZnT3. Particularly, the lack of Munc13-2 at MFs, leaving Munc13-1 as the only isoform expressed, has been reported to result in decreased release probability, increased frequency facilitation, and remarkable reduction of asynchronous release (Breustedt et al., 2010). The paralog VAMP1, recently shown to be expressed in the subpopulation of neurons that display release in the absence of VAMP2 (Zimmermann et al., 2014) may also account for compensatory changes.

Loss of VAMP7 in mice does not cause major developmental or neurological deficits (Sato et al., 2011; Danglot et al., 2012). VAMP7 KO mice display increased anxiety (Danglot et al., 2012), and this behavior has been linked to the ventral hippocampus (Ohara et al., 2013; Zarei et al., 2013). Hence synaptic transmission at MF-CA3 synapses in the ventral hippocampus may be preferentially affected in the absence of VAMP7 although we have no evidence for a differential regional expression of VAMP7 in MFs.

Although rather extensive, our comparison study may have omitted less conventional roles for synaptic vesicle release. Of particular relevance, reelin acts



presynaptically to enhance spontaneous release without affecting properties of evoked neurotransmission in hippocampal cultured neurons, an action which requires VAMP7 and SNAP-25 but not synaptobrevin2 (Bal et al, 2014). There is yet no evidence for a reelin dependent enhancement of MF-EPSCs, and application of reelin in a slice preparation may prove uneasy. However, activation of presynaptic  $\alpha 7$  nicotinic acetylcholine receptors similarly increase MF-EPSCs in an action potential-independent manner, and this is mimicked by caffeine operating through internal calcium stores (Sharma and Vijayaraghavan, 2003). It will thus be very interesting to compare the effects of an  $\alpha 7$  nAChR agonist and/or caffeine on MF-EPSCs in WT and VAMP7 KO mice. An additional possibility for a role of VAMP7 in MF axons relates to their localization to axons and dendrites during development (Coco et al., 1999) and their potential role in neurite outgrowth (Sato et al, 2011). MF terminals show prominent forms of structural plasticity, in particular in response to one-trial learning (Ruediger et al, 2011) or following housing in an enriched environment (Galimberti et al, 2006). We could further test the possibility that the plasticity of MF filopodia which make synaptic contacts with CA3 interneurons could be affected by the loss of VAMP7.

Overall, VAMP7 a v-SNARE particularly enriched at MF-CA3 terminals does not appear to play a conventional role in synaptic transmission, and further work is needed to shed light on its presynaptic function.

## **Acknowledgements**

This work was supported by the CNRS to CM and by the University of Bordeaux and the VU University Amsterdam to BLG. We are grateful to B. Gasnier for antibodies against VIAAT.

## **Author contribution**

C.M. and M.V. designed and supervised the study. L.D. performed immunohistological analyses. B.G.L. performed all the electrophysiological recordings. C.B. helped with the electrophysiological analyses and contributed with discussion. M.V. and T.G. contributed to the discussion. B.G.L., and C.M. wrote the manuscript.

## References

- Alberts, P., R. Rudge, I. Hinners, A. Muzerelle, S. Martinez-Arca, T. Irinopoulou, V. Marthiens, S. Tooze, F. Rathjen, P. Gaspar and T. Galli (2003). Cross talk between tetanus neurotoxin-insensitive vesicle-associated membrane protein-mediated transport and L1-mediated adhesion. *Mol Biol Cell* 14(10): 4207-20.
- Bal, M., J. Leitz, Austin L. Reese, Denise M. O. Ramirez, M. Durakoglugil, J. Herz, Lisa M. Monteggia and Ege T. Kavalali (2013). Reelin Mobilizes a VAMP7-Dependent Synaptic Vesicle Pool and Selectively Augments Spontaneous Neurotransmission. *Neuron*: 1-13.
- Breustedt, J., A. Gundlfinger, F. Varoqueaux, K. Reim, N. Brose and D. Schmitz (2010). Munc13-2 Differentially Affects Hippocampal Synaptic Transmission and Plasticity. *Cerebral Cortex* 20(5): 1109-1120.
- Burgo, A., A. M. Casano, A. Kuster, S. T. Arold, G. Wang, S. Nola, A. Verraes, F. Dingli, D. Loew and T. Galli (2013). Increased activity of the Vesicular Soluble N-Ethylmaleimide-sensitive Factor Attachment Protein Receptor TI-VAMP/VAMP7 by Tyrosine Phosphorylation in the Longin Domain. *Journal of Biological Chemistry* 288(17): 11960-11972.
- Burgo, A., V. Proux-Gillardeaux, E. Sotirakis, P. Bun, A. Casano, A. Verraes, R. K. H. Liem, E. Formstecher, M. Coppey-Moisand and T. Galli (2012). A molecular network for the transport of the TI-VAMP/VAMP7 vesicles from cell center to periphery. *Developmental Cell* 23(1): 166-80.
- Chaineau, M., L. Danglot and T. Galli (2009). Multiple roles of the vesicular-SNARE TI-VAMP in post-Golgi and endosomal trafficking. *FEBS Letters* 583(23): 3817-3826.
- Coco, S., G. Raposo, S. Martinez, J. J. Fontaine, S. Takamori, A. Zahraoui, R. Jahn, M. Matteoli, D. Louvard and T. Galli (1999). Subcellular localization of tetanus neurotoxin-insensitive vesicle-associated membrane protein (VAMP)/VAMP7 in neuronal cells: evidence for a novel membrane compartment. *J Neurosci* 19(22): 9803-12.
- Danglot, L. and T. Galli (2007). What is the function of neuronal AP-3? *Biology of the Cell* 99(7): 349-361.
- Danglot, L., K. Zylbersztejn, M. Petkovic, M. Gauberti, H. Meziane, R. Combe, M.-F. Champy, M.-C. Birling, G. Pavlovic, J.-C. Bizot, F. Trovero, F. Della Ragione, V. Proux-Gillardeaux, T. Sorg, D. Vivien, M. D'esposito and T. Galli (2012). Absence of TI-VAMP/Vamp7 Leads to Increased Anxiety in Mice. *Journal of Neuroscience* 32(6): 1962-1968.
- Evstratova, A., S. Chamberland, V. Faundez and K. Tóth (2014). Vesicles derived via AP-3-dependent recycling contribute to asynchronous release and influence information transfer. *Nat Commun* 5.
- Filippini, F., V. Rossi, T. Galli, A. Budillon, M. D'Urso and M. D'esposito (2001). Longins: a new evolutionary conserved VAMP family sharing a novel SNARE domain. *Trends Biochem Sci* 26(7): 407-9.
- Galimberti, I., N. Gogolla, S. Alberi, A. F. Santos, D. Muller and P. Caroni (2006). Long-term rearrangements of hippocampal mossy fiber terminal connectivity in the adult regulated by experience. *Neuron* 50(5): 749-63.
- Galli, T., A. Zahraoui, v. v. vaidyanathan, G. Raposo, j. m. tian, m. karin, h. niemann and D. Louvard (1998). A novel tetanus neurotoxin-insensitive vesicle-associated membrane protein in SNARE complexes of the apical plasma membrane of epithelial cells. *Mol Biol Cell*.
- Gordon, D. E., L. M. Bond, D. A. Sahlender and A. A. Peden (2010). A Targeted siRNA Screen to Identify SNAREs Required for Constitutive Secretion in Mammalian Cells. *Traffic* 11(9): 1191-1204.

- Gupton, S. L. and F. B. Gertler (2010). Integrin Signaling Switches the Cytoskeletal and Exocytic Machinery that Drives Neuritogenesis. *Developmental Cell* 18(5): 725-736.
- Henze, D. A., D. B. T. McMahon, K. M. Harris and G. Barrionuevo (2002). Giant miniature EPSCs at the hippocampal mossy fiber to CA3 pyramidal cell synapse are monoquantal. *Journal of Neurophysiology* 87(1): 15-29.
- Hua, Z., S. Leal-Ortiz, Sarah M. Foss, Clarissa L. Waites, Craig C. Garner, Susan M. Voglmaier and Robert H. Edwards (2011). v-SNARE Composition Distinguishes Synaptic Vesicle Pools. *Neuron* 71(3): 474-487.
- Jahn, R. and R. H. Scheller (2006). SNAREs — engines for membrane fusion. *Nat Rev Mol Cell Biol* 7(9): 631-643.
- Kaesler, P. S. and W. G. Regehr (2014). Molecular mechanisms for synchronous, asynchronous, and spontaneous neurotransmitter release. *Annu. Rev. Physiol.* 76: 333-63.
- Kanethi, P., X. Qiao, M. E. Diaz, A. A. Peden, G. E. Meyer, S. L. Carskadon, D. Kapfhamer, D. Sufalko, M. S. Robinson, J. L. Noebels and M. Burmeister (1998). Mutation in AP-3 delta in the mocha mouse links endosomal transport to storage deficiency in platelets, melanosomes, and synaptic vesicles. *Neuron* 21(1): 111-22.
- Kukic, I., S. L. Kelleher and K. Kiselyov (2014). Zn<sup>2+</sup> efflux through lysosomal exocytosis prevents Zn<sup>2+</sup>-induced toxicity. *Journal of Cell Science* 127(14): 3094-3103.
- Lavoie, N., D. V. Jeyaraju, M. R. Peralta, L. Seress, L. Pellegrini and K. Toth (2011). Vesicular Zinc Regulates the Ca<sup>2+</sup> Sensitivity of a Subpopulation of Presynaptic Vesicles at Hippocampal Mossy Fiber Terminals. *Journal of Neuroscience* 31(50): 18251-18265.
- Marchal, C. and C. Mulle (2004). Postnatal maturation of mossy fibre excitatory transmission in mouse CA3 pyramidal cells: a potential role for kainate receptors. *The Journal of Physiology* 561(1): 27-37.
- Martinez-Arca, S., P. Alberts, A. Zahraoui, D. Louvard and T. Galli (2000). Role of tetanus neurotoxin insensitive vesicle-associated membrane protein (TI-VAMP) in vesicular transport mediating neurite outgrowth. *The Journal of Cell Biology* 149(4): 889-900.
- Martinez-Arca, S., S. Coco, G. Mainguy, U. Schenk, P. Alberts, P. Bouillé, M. Mezzina, A. Prochiantz, M. Matteoli, D. Louvard and T. Galli (2001). A common exocytotic mechanism mediates axonal and dendritic outgrowth. *J Neurosci* 21(11): 3830-8.
- Martinez-Arca, S., R. Rudge, M. Vacca, G. Raposo, J. Camonis, V. Proux-Gillardeaux, L. Daviet, E. Formstecher, A. Hamburger, F. Filippini, M. D'Esposito and T. Galli (2003). A dual mechanism controlling the localization and function of exocytic v-SNAREs. *Proc Natl Acad Sci USA* 100(15): 9011-6.
- Muzerelle, A., P. Alberts, S. Martinez-Arca, O. Jeannequin, P. Lafaye, J.-C. Mazié, T. Galli and P. Gaspar (2003). Tetanus neurotoxin-insensitive vesicle-associated membrane protein localizes to a presynaptic membrane compartment in selected terminal subsets of the rat brain. *Neuroscience* 122(1): 59-75.
- Newell-Litwa, K., S. Chintala, S. Jenkins, J.-F. Pare, L. Mcgaha, Y. Smith and V. Faundez (2010). Hermansky-Pudlak Protein Complexes, AP-3 and BLOC-1, Differentially Regulate Presynaptic Composition in the Striatum and Hippocampus. *Journal of Neuroscience* 30(3): 820-831.
- Ohara, S., S. Sato, K. Tsutsui, M. P. Witter and T. Iijima (2013). Organization of multisynaptic inputs to the dorsal and ventral dentate gyrus: retrograde trans-synaptic tracing with rabies virus vector in the rat. *PLoS One* 8(11): e78928.

- Racchetti, G., A. Lorusso, C. Schulte, D. Gavello, V. Carabelli, R. D'alessandro and J. Meldolesi (2010). Rapid neurite outgrowth in neurosecretory cells and neurons is sustained by the exocytosis of a cytoplasmic organelle, the enlargeosome. *Journal of Cell Science* 123(2): 165-170.
- Ramirez, D. M. O. and E. Kavalali (2012). The role of non-canonical SNAREs in synaptic vesicle recycling. *Cellular Logistics* 2(1): 20-27.
- Ramirez, Denise M. O., M. Khvotchev, B. Trauterman and Ege T. Kavalali (2012). Vti1a Identifies a Vesicle Pool that Preferentially Recycles at Rest and Maintains Spontaneous Neurotransmission. *Neuron* 73(1): 121-134.
- Rossi, V., D. K. Banfield, M. Vacca, L. E. P. Dietrich, C. Ungermann, M. D'Esposito, T. Galli and F. Filippini (2004). Longins and their longin domains: regulated SNAREs and multifunctional SNARE regulators. *Trends Biochem Sci* 29(12): 682-8.
- Ruediger, S., C. Vittori, E. Bednarek, C. Genoud, P. Strata, B. Sacchetti and P. Caroni (2011). Learning-related feedforward inhibitory connectivity growth required for memory precision. *Nature* 473(7348): 514-8.
- Sato, M., S. Yoshimura, R. Hirai, A. Goto, M. Kunii, N. Atik, T. Sato, K. Sato, R. Harada, J. Shimada, T. Hatabu, H. Yorifuji and A. Harada (2011). The Role of VAMP7/TI-VAMP in Cell Polarity and Lysosomal Exocytosis in vivo. *Traffic* 12(10): 1383-1393.
- Schäfer, I. B., G. G. Hesketh, N. A. Bright, S. R. Gray, P. R. Pryor, P. R. Evans, J. P. Luzio and D. J. Owen (2012). The binding of Varp to VAMP7 traps VAMP7 in a closed, fusogenically inactive conformation. *Nat Struct Mol Biol* 19(12): 1300-9.
- Scheuber, A., R. Rudge, L. Danglot, G. Raposo, T. Binz, J. C. Ponce and T. Galli (2006). Loss of AP-3 function affects spontaneous and evoked release at hippocampal mossy fiber synapses. *Proceedings of the National Academy of Sciences* 103(44): 16562.
- Schoch, S., F. Deák, A. Königstorfer, M. Mozhayeva, Y. Sara, T. C. Südhof and E. T. Kavalali (2001). SNARE function analyzed in synaptobrevin/VAMP knockout mice. *Science* 294(5544): 1117-22.
- Sharma, G. and S. Vijayaraghavan (2003). Modulation of presynaptic store calcium induces release of glutamate and postsynaptic firing. *Neuron* 38(6): 929-39.
- Sinha, R., S. Ahmed, R. Jahn and J. Klingauf (2011). Two synaptobrevin molecules are sufficient for vesicle fusion in central nervous system synapses. *Proceedings of the National Academy of Sciences* 108(34): 14318-14323.
- Söllner, T., S. W. Whiteheart, M. Brunner, H. Erdjument-Bromage, S. Geromanos, P. Tempst and J. E. Rothman (1993). SNAP receptors implicated in vesicle targeting and fusion. *Nature* 362(6418): 318-24.
- Takamori, S., M. Holt, K. Stenius, E. A. Lemke, M. Grønborg, D. Riedel, H. Urlaub, S. Schenck, B. Brügger, P. Ringler, S. A. Müller, B. Rammner, F. Gräter, J. S. Hub, B. L. De Groot, G. Mieskes, Y. Moriyama, J. Klingauf, H. Grubmüller, J. Heuser, F. Wieland and R. Jahn (2006). Molecular anatomy of a trafficking organelle. *Cell* 127(4): 831-46.
- Verderio, C., C. Cagnoli, M. Bergami, M. Francolini, U. Schenk, A. Colombo, L. Riganti, C. Frassoni, E. Zuccaro, L. Danglot, C. Wilhelm, T. Galli, M. Canossa and M. Matteoli (2012). TI-VAMP/VAMP7 is the SNARE of secretory lysosomes contributing to ATP secretion from astrocytes. *Biology of the Cell* 104(4): 213-228.
- Vergnano, Angela M., N. Rebola, Leonid P. Savtchenko, Paulo S. Pinheiro, m. casado, Brigitte L. Kieffer, Dmitri A. Rusakov, C. Mulle and p. paoletti (2014). Zinc Dynamics and Action at Excitatory Synapses. *Neuron* 82(5): 1101-1114.

- Vivona, S., C. W. Liu, P. Strop, V. Rossi, F. Filippini and A. T. Brunger (2010). The Longin SNARE VAMP7/TI-VAMP Adopts a Closed Conformation. *Journal of Biological Chemistry* 285(23): 17965-17973.
- Weber, T., B. V. Zemelman, J. A. McNew, B. Westermann, M. Gmachl, F. Parlati, T. H. Sollner and J. E. Rothman (1998). SNAREpins: minimal machinery for membrane fusion. *Cell* 92(6): 759-72.
- Wilhelm, B. G., S. Mandad, S. Truckenbrodt, K. Krohnert, C. Schafer, B. Rammner, S. J. Koo, G. A. Classen, M. Krauss, V. Haucke, H. Urlaub and S. O. Rizzoli (2014). Composition of isolated synaptic boutons reveals the amounts of vesicle trafficking proteins. *Science* 344(6187): 1023-1028.
- Zarei, M., C. F. Beckmann, M. A. Binnewijzend, M. M. Schoonheim, M. A. Oghabian, E. J. Sanz-Arigita, P. Scheltens, P. M. Matthews and F. Barkhof (2013). Functional segmentation of the hippocampus in the healthy human brain and in Alzheimer's disease. *Neuroimage* 66: 28-35.
- Zimmermann, J., T. Trimbuch and C. Rosenmund (2014). Synaptobrevin 1 mediates vesicle priming and evoked release in a subpopulation of hippocampal neurons. *J Neurophysiol* 112(6): 1559-65.

## Figures and Legends

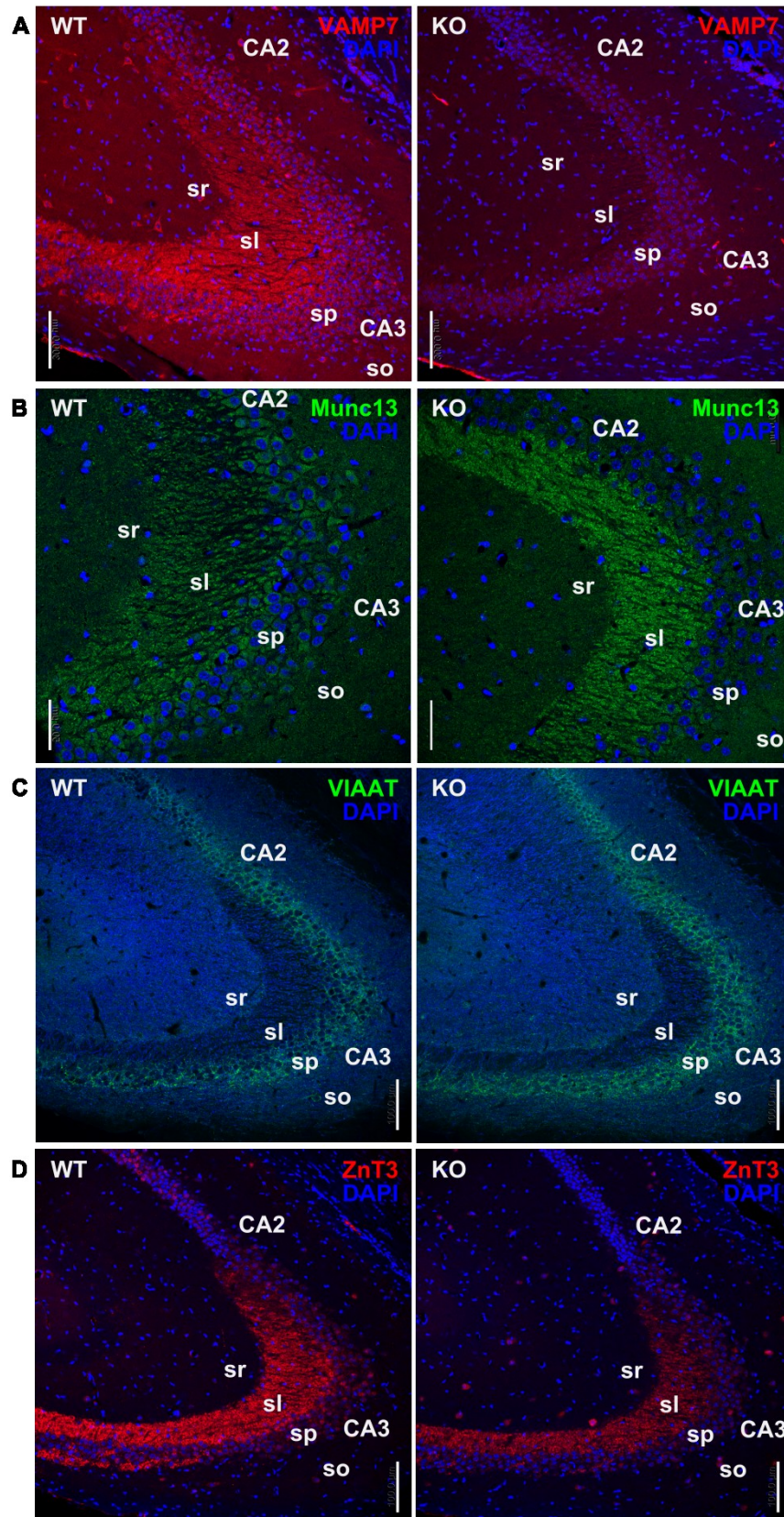


**Figure 1. Sagittal sections of WT and KO hippocampus stained with DAPI plus VAMP7, Munc13, VIAAT and ZnT3.**

A, VAMP7 intensity is totally lost in KO. Scale bar=90  $\mu$ m. B, Munc13-1 expression seems increased in KO. Scale bar=50  $\mu$ m. C, VIAAT expression is relatively constant. Scale bar=100  $\mu$ m. D, ZnT3 expression shows a decreasing tendency. Scale bar=100  $\mu$ m. CA2/CA3: Cornus Ammonis 2 and 3, sr: stratum radiatum, sl: stratum lucidum, sp: stratum pyramidale, so: stratum oriens.



## Figures and Legends

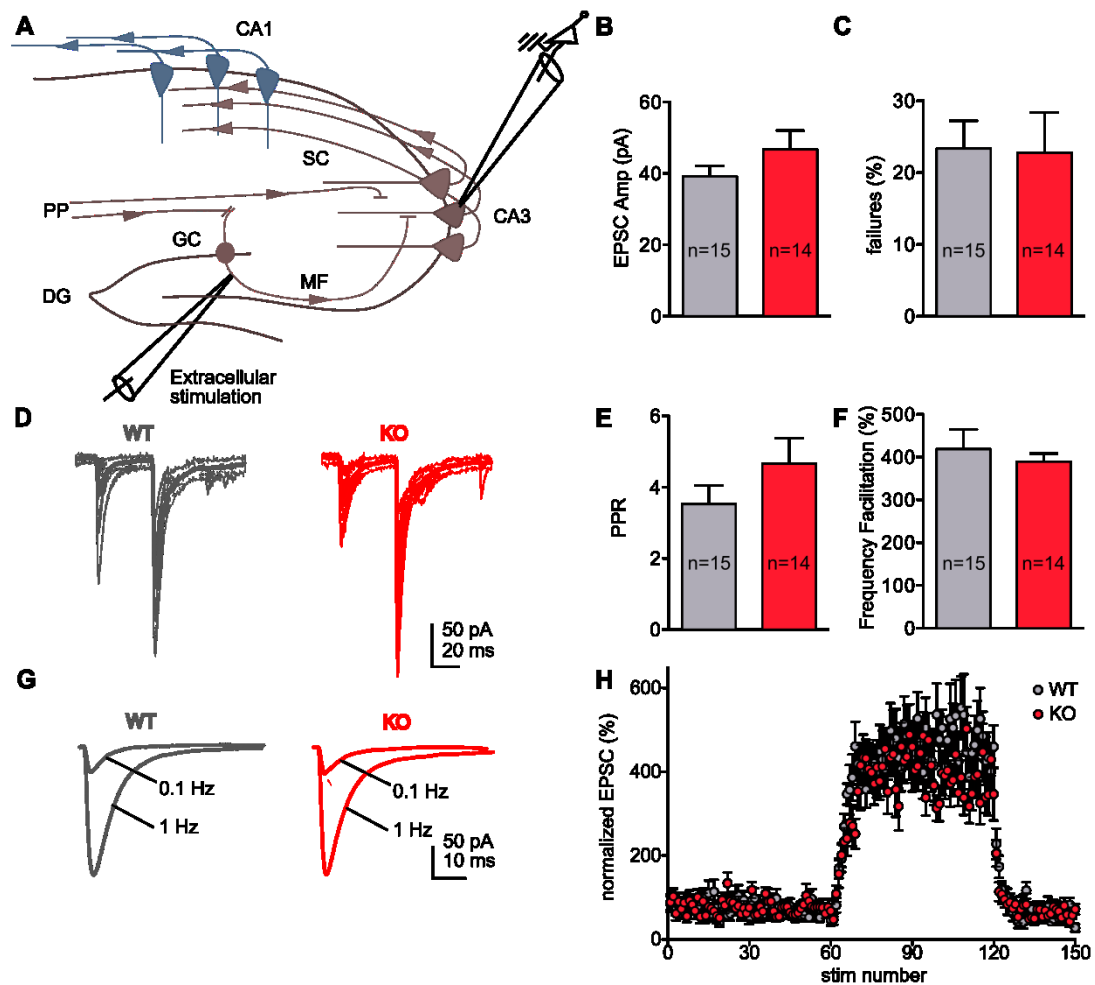


**Figure 2. Basal evoked transmission and short-term plasticity are unaltered in VAMP7 KO.**

*A*, Schematic diagram of a hippocampal slice displaying the recording (right, in a CA3 pyramidal cell) and stimulating electrodes (left, inside the dentate gyrus). *B-C*, Comparison for average basal EPSC amplitudes and percentage of failures. *D*, Sample traces evoked by two stimuli with a 40ms inter-stimulus interval and over-imposed average. *E-F*, Comparison for Paired Pulse Ratio (PPR) and Frequency Facilitation (FF). *G*, Sample average traces evoked at 0.1 and 1Hz. *H*, Time course of FF, EPSCs were normalized to the mean amplitude of the 10 min baseline at 0.1Hz (60 stimuli) preceding the stimulation increase to 1Hz (60-120<sup>th</sup> stimuli), and final 30 stimuli at 0.1 Hz. The error bars represent  $\pm$  S.E.M.

## Figures and Legends

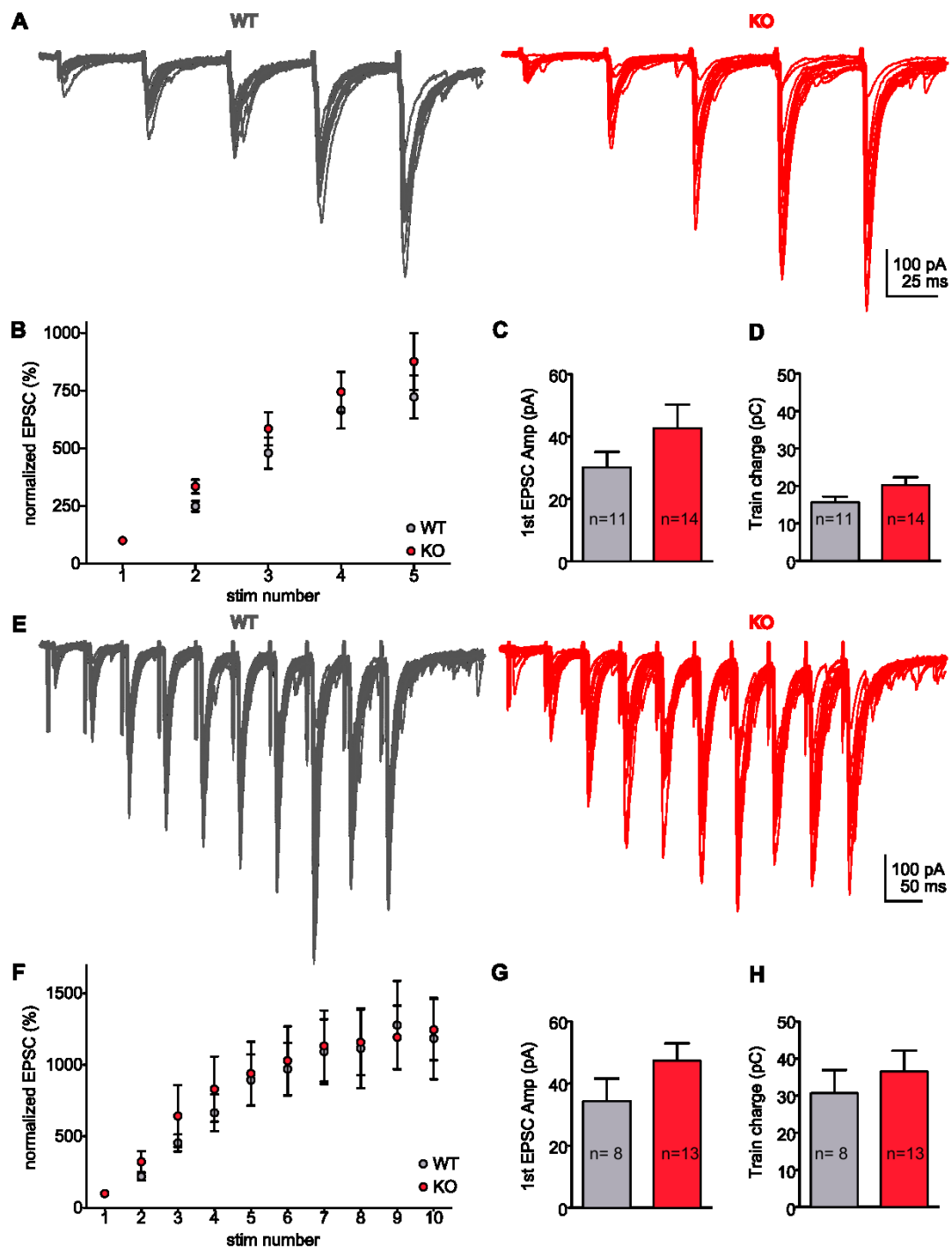


**Figure 3. Evoked plasticity by short bursts is not affected in the absence of VAMP7**

A, Sample traces evoked by 5 stimuli at 20 Hz and over-imposed average. B, EPSC facilitation as normalized to the average amplitude of the first stimulus. C-D, Comparison of the average EPSC amplitude of the first stimulus, and average train charge. E, Sample traces evoked by 10 stimuli at 20 Hz and over-imposed average. F, EPSC facilitation as normalized to the average amplitude of the first stimulus. G-H, Comparison of the average EPSC amplitude of the first stimulus, and average train charge. The error bars represent  $\pm$  S.E.M.

## Figures and Legends

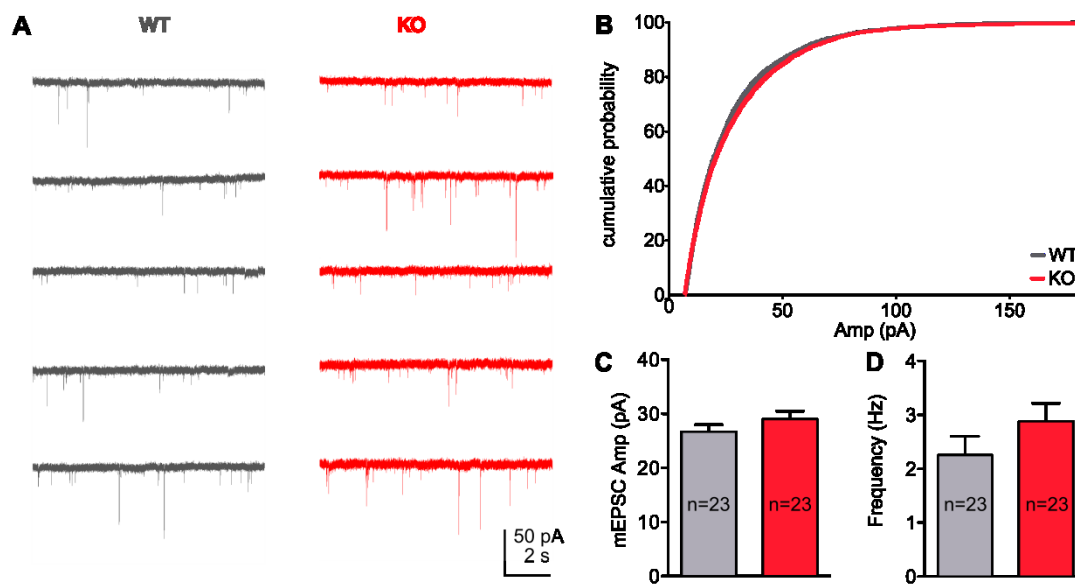


**Figure 4. Spontaneous release is unaltered in VAMP7 KO.**

A, Sample traces of mEPSCs. B, Cumulative probability plot for the first 300 events of 23 cells. C-D, Comparison of the average amplitude and frequency of mEPSCs. The error bars represent  $\pm$  S.E.M.

## Figures and Legends

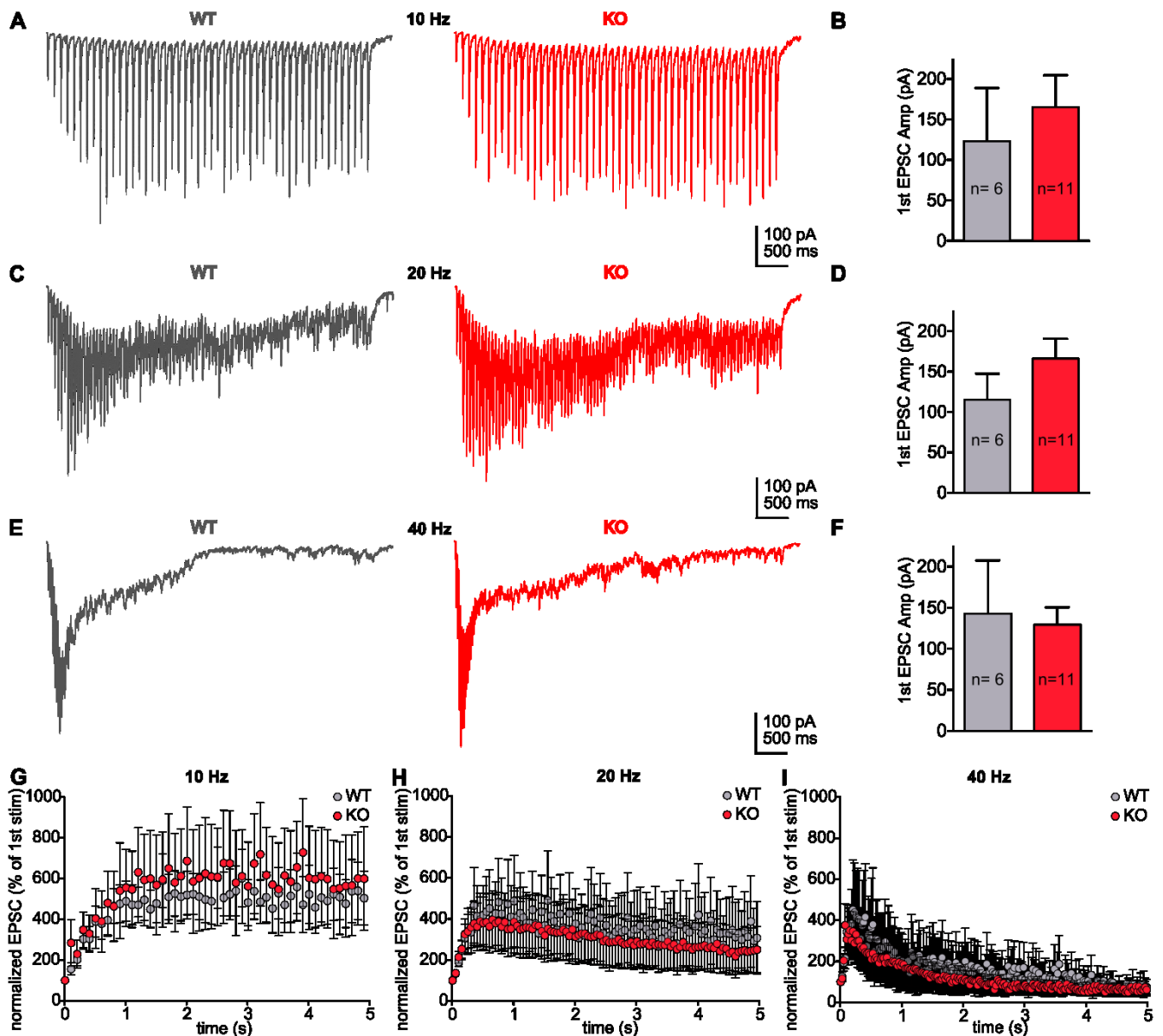


**Figure 5. Evoked plasticity by long bursts is not affected in the absence of VAMP7.**

A, Sample traces of average EPSCs evoked by 5s-trains at 10 Hz. B, Comparison of the average EPSC amplitude of the first stimulus at 10 Hz. C, Sample traces of average EPSCs evoked by 5s-trains at 20 Hz. D, Comparison of the average EPSC amplitude of the first stimulus at 20 Hz. E, Sample traces of average EPSCs evoked by 5s-trains at 40 Hz. F, Comparison of the average EPSC amplitude of the first stimulus at 40 Hz. G-I, EPSC facilitation as normalized to the average amplitude of the first stimulus for 5s-trains at 10, 20, and 40 Hz, respectively. The error bars represent  $\pm$  S.E.M.

## Figures and Legends

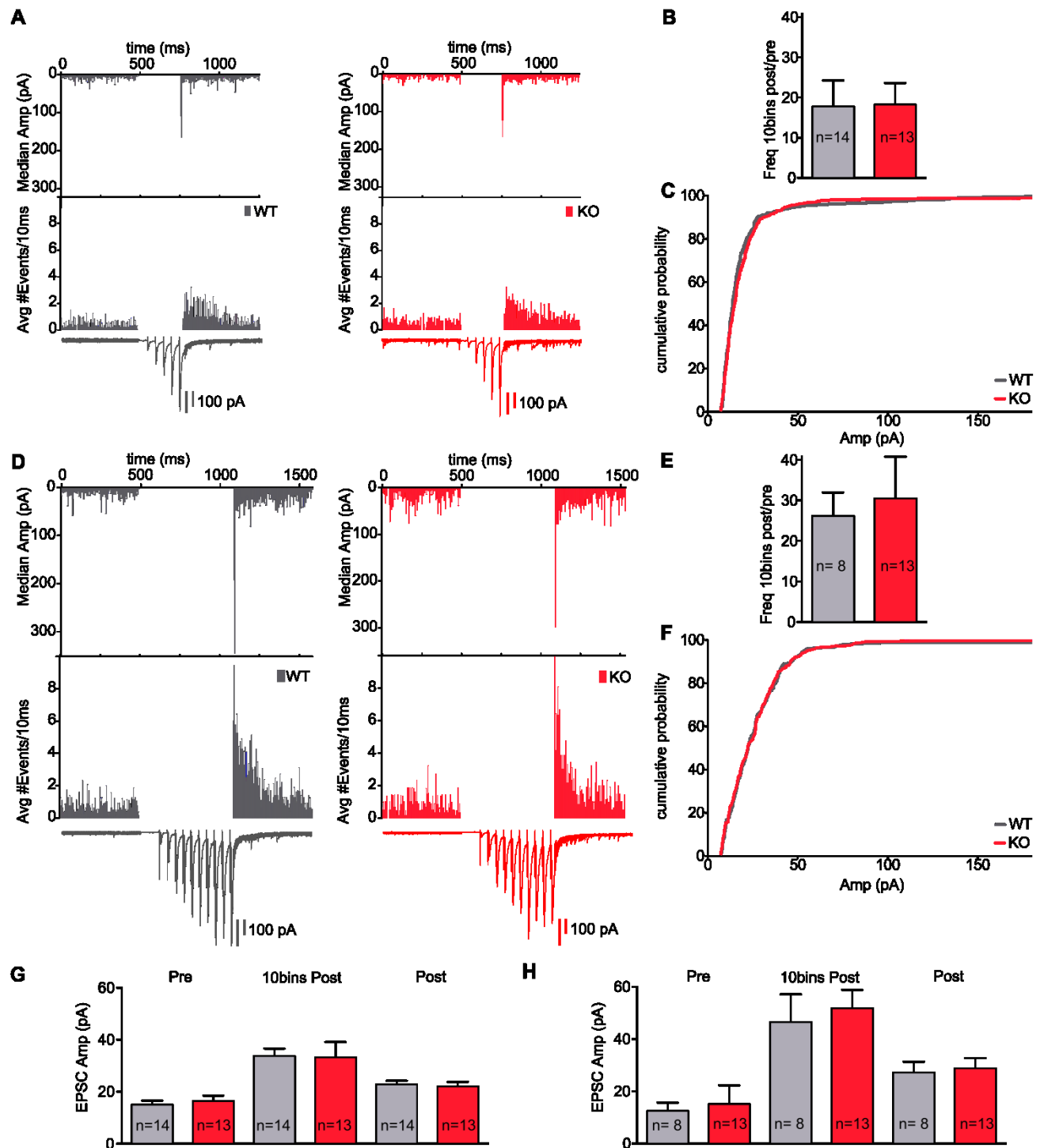


**Figure 6. Asynchronous release after short bursts is not affected in the absence of VAMP7**

A, From top to bottom, median amplitude and average number of events per 10ms bins, displayed over sample traces of average EPSCs evoked by trains of five stimuli, flanked by overlaid sample traces of baseline and asynchronous events. B, Comparison of the frequency of events in the 100ms post-stimulation as ratio of the events during the preceding 500ms. C, Cumulative probability plot for the asynchronous events. D, From top to bottom, median amplitude and average number of events per 10ms bins, displayed over sample traces of average EPSCs evoked by trains of ten stimuli, flanked by overlaid sample traces of baseline and asynchronous events. E, Comparison of the frequency of events in the 100ms post-stimulation as ratio of the events during the preceding 500ms. F, Cumulative probability plots for the asynchronous events. G,H, Comparisons of the average median amplitudes of the events in: the preceding 500ms, the 100ms post-stimulation, and 500ms post-stimulation, for trains of five and ten stimuli, respectively. The error bars represent  $\pm$  S.E.M.

# Figures and Legends

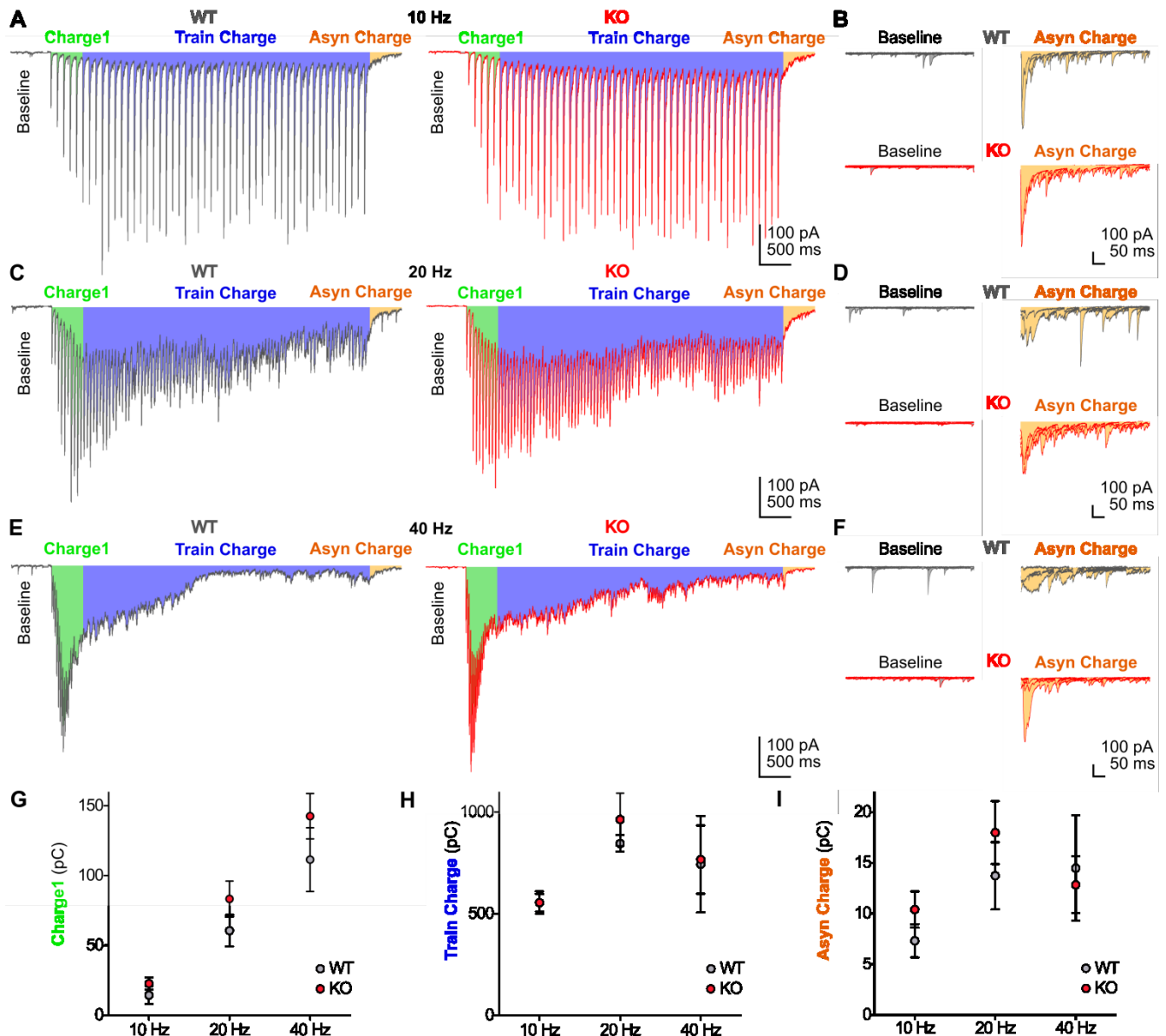


**Figure 7. Asynchronous release during and after long bursts is not different in VAMP7 KO**

A, Sample traces of average EPSCs evoked by 5s-trains at 10 Hz, including the preceding 500ms baseline, and subsequent 500ms of asynchronous release. Charges calculated are represented by the respective colored area (train charge includes both the blue and green areas). B, Overlaid sample traces of 500ms baseline and asynchronous release, with calculated area colored in grey and orange, respectively. C, Sample traces of average EPSCs evoked by 5s-trains at 20 Hz, including the preceding 500ms baseline, and subsequent 500ms of asynchronous release. Charges calculated are represented by the respective colored area (train charge includes both the blue and green areas). D, Overlaid sample traces of 500ms baseline and asynchronous release, with calculated area colored in grey and orange, respectively. E, Sample traces of average EPSCs evoked by 5s-trains at 40 Hz, including the preceding 500ms baseline, and subsequent 500ms of asynchronous release. Charges calculated are represented by the respective colored area (train charge includes both the blue and green areas). F, Overlaid sample traces of 500ms baseline and asynchronous release, with calculated area colored in grey and orange, respectively. G-I, Comparisons between genotypes of the different charges calculated for each frequency. The error bars represent  $\pm$  S.E.M.

## Figures and Legends

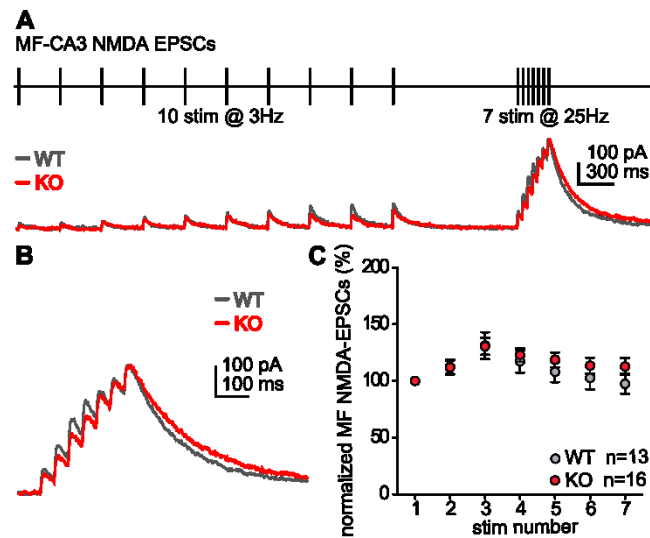


**Figure 8. Zinc is normally released in the absence of VAMP7**

A, The probability of release at mossy fiber synapses was increased by applying a conditioning stimulus (ten stimulations at 3 Hz) prior to burst stimulation (seven stimuli at 25 Hz). B, After the conditioning stimulus, burst stimulation induced similar potentiation of NMDA-EPSCs in WT and KO slices, which indicates similar zinc release in both genotypes. C, Data were normalized to the amplitude of the first NMDA-EPSC in the burst and are presented as mean  $\pm$  S.E.M.

## Supplementary Information

**Supplementary Table 1 One-way ANOVA comparing average median amplitude of events around 5stim@20Hz**

Test details	Mean WT	Mean KO	Mean Diff,	SE of diff,	n WT	n KO	t	DF	Summary
preWT vs. preKO	14.95	16.34	-1.397	4.259	14	13	0.328	77	ns
1st 10post WT vs. 1st 10post KO	33.72	33.19	0.5291	4.167	14	13	0.127	77	ns
postWT vs. postKO	22.73	21.99	0.7436	4.167	14	13	0.179	77	ns
preWT vs. 1st 10post WT	14.95	33.72	-18.77	4.015	14	13	4.676	77	****
preWT vs. postWT	14.95	22.73	-7.788	4.015	14	13	1.94	77	ns
preKO vs. 1st 10post KO	16.34	33.19	-16.85	4.402	14	13	3.827	77	**
preKO vs. postKO	16.34	21.99	-5.647	4.402	14	13	1.283	77	ns

**Supplementary Table 2 One-way ANOVA comparing average median amplitude of events around 10stim@20Hz**

Test details	Mean WT	Mean KO	Mean Diff.	SE of diff.	n WT	n KO	t	DF	Summary
preWT vs. preKO	12.5	15.06	-2.56	9.651	8	13	0.265	15	ns
1st 10post WT vs. 1st 10post KO	46.46	51.74	-5.279	9.651	8	13	0.547	15	ns
postWT vs. postKO	27.17	28.79	-1.619	9.651	8	13	0.168	15	ns
preWT vs. 1st 10post WT	12.5	46.46	-33.96	8.935	8	13	3.801	15	*
preWT vs. postWT	12.5	27.17	-14.67	8.935	8	13	1.642	15	ns
preKO vs. 1st 10post KO	15.06	51.74	-36.68	10.32	8	13	3.555	15	*
preKO vs. postKO	15.06	28.79	-13.73	10.32	8	13	1.331	15	ns

**Supplementary Table 3. Two-way ANOVA comparing the charge of the 1<sup>st</sup> 500ms of 5-second trains at 10. 20. and 40Hz.**

Test details	Mean WT	Mean KO	Mean Diff.	SE of diff.	n WT	n KO	q	DF	Summary
<b>WT</b>									
10 Hz vs. 20 Hz	14.36	60.56	-46.2	22.72	6	6	2.88	45	Ns
10 Hz vs. 40 Hz	14.36	111.4	-97.07	22.72	6	6	6.04	45	***
20 Hz vs. 40 Hz	60.56	111.4	-50.87	22.72	6	6	3.17	45	Ns
<b>KO</b>									
10 Hz vs. 20 Hz	22.67	83.28	-60.61	16.78	11	11	5.11	45	**
10 Hz vs. 40 Hz	22.67	142.5	-119.8	16.78	11	11	10.1	45	****
20 Hz vs. 40 Hz	83.28	142.5	-59.22	16.78	11	11	4.99	45	**
<b>multiple t tests</b>	<b>Mean1</b>	<b>Mean2</b>							<b>P value</b>
10Hz WT vs KO	14.357	22.674							0.280626
20Hz WT vs KO	60.555	83.282							0.259174
40Hz WT vs KO	111.43	142.5							0.279246



**Supplementary Table 4. Two-way ANOVA comparing the total charge of 5-second trains at 10, 20, and 40Hz.**

Test details	Mean WT	Mean KO	Mean Diff.	SE of diff.	n WT	n KO	q	DF	Summary
<b>WT</b>									
10 Hz vs. 20 Hz	554.1	845.4	-291.3	228.9	6	6	1.8	45	Ns
10 Hz vs. 40 Hz	554.1	743.9	-189.8	228.9	6	6	1.17	45	Ns
20 Hz vs. 40 Hz	845.4	743.9	101.5	228.9	6	6	0.63	45	Ns
<b>KO</b>									
10 Hz vs. 20 Hz	555	963.4	-408.4	169.1	11	11	3.42	45	Ns
10 Hz vs. 40 Hz	555	766.3	-211.3	169.1	11	11	1.77	45	Ns
20 Hz vs. 40 Hz	963.4	766.3	197.2	169.1	11	11	1.65	45	Ns
<b>multiple t tests</b>	<b>Mean1</b>	<b>Mean2</b>							<b>P value</b>
10Hz WT vs KO	554.1	555							0.991365
20Hz WT vs KO	845.4	963.44							0.522161
40Hz WT vs KO	743.89	766.29							0.938818

**Supplementary Table 5. Two-way ANOVA comparing the charge of the 500ms asynchronous release subsequent to 5-second trains at 10, 20, and 40Hz.**

Test details	Mean WT	Mean KO	Mean Diff.	SE of diff.	n WT	n KO	q	DF	Summary
<b>WT</b>									
10 Hz vs. 20 Hz	7.304	13.72	-6.417	5.083	6	6	1.79	45	Ns
10 Hz vs. 40 Hz	7.304	14.47	-7.166	5.083	6	6	1.99	45	Ns
20 Hz vs. 40 Hz	13.72	14.47	-0.749	5.083	6	6	0.21	45	Ns
<b>KO</b>									
10 Hz vs. 20 Hz	10.39	17.97	-7.585	3.754	11	11	2.86	45	Ns
10 Hz vs. 40 Hz	10.39	12.83	-2.439	3.754	11	11	0.92	45	Ns
<b>multiple t tests</b>	<b>Mean1</b>	<b>Mean2</b>							<b>P value</b>
10Hz WT vs KO	7.3037	10.389							0.274538
20Hz WT vs KO	13.721	17.974							0.397194
40Hz WT vs KO	14.47	12.828							0.763274
20 Hz vs. 40 Hz	17.97	12.83	5.147	3.754	11	11	1.94	45	Ns

### CA3 Circuits Probed with RABV-Tracing and Paired Recordings

It was clear since the beginning of my Ph.D. project that studying presynaptic mechanisms of synaptic plasticity at hippocampal mossy fiber synapses was technically limited by the current recording paradigm: *in vitro* CA3 whole-cell recordings probed with MF(s) extracellular stimulation. While this technique has widely increase our knowledge about the physiology of MF-CA3 synapses, a single fiber cannot be unequivocally stimulated, nor specifically targeted. Therefore, we needed to develop a technique that would allow us to establish granule cell – CA3 pyramidal cell paired recordings. This is challenging due to the low connectivity between these two populations. Acute slices make it even harder, as fibers can be cut when dissecting, with the slicing angle determining to a large extent the chances of success. Thus, we chose to use hippocampal organotypic slices and a viral tracing strategy.

To identify direct presynaptic partners to a defined target CA3 pyramidal cell, we combined single cell electroporation (SCE) and mono-trans-synaptic tracing based on a pseudotyped, recombinant rabies virus (EnvA pseudotyped RABV  $\Delta G$ ). This approach proved succesful to obtain GC-CA3 paired recordings and to quantify presynaptic inputs to the starter CA3 pyramidal cell. Nonetheless, this technique is still cumbersome for reasons that will be discussed. While certain drawbacks could be improved, others are inalienable to the technique. The latter need to be considered when evaluating the suitability of this method for a particular research question.

# CA3 Circuits Probed with RABV-Tracing and Paired Recordings

In preparation

Bernat González i Llinares<sup>1,2,3</sup>, Melanie Ginger<sup>1,2,4</sup>, Virginie Labrousse<sup>1,2,4</sup>, Mario Carta<sup>1,2</sup>, Christophe Blanchet<sup>1,2</sup>, Andreas Frick<sup>1,4</sup>, Matthijs Verhage<sup>3</sup>, Christophe Mulle<sup>1,2</sup>

<sup>1</sup> Université de Bordeaux  
Institut Interdisciplinaire de Neurosciences, Bordeaux, F-33000 France

<sup>2</sup> CNRS UMR 5297, Bordeaux, F-33000 France

<sup>3</sup> Department of Functional Genomics and Clinical Genetics, Center for Neurogenomics and Cognitive Research, VU University Amsterdam and VU Medical Center, Amsterdam, The Netherlands

<sup>4</sup> INSERM U 862, Bordeaux, F-33000 France

Correspondence to:  
Christophe Mulle (christophe.mulle@u-bordeaux.fr)

**Key words:** Hippocampus, Short-Term Plasticity, Rabies Virus Tracing, Paired Recordings

## Abstract

Presynaptic modulation is a crucial factor in the adaptive capacity of the nervous system. The coupling between incoming action potentials and synaptic vesicle exocytosis is modulated by recent activity of presynaptic neurons, and by activation of presynaptic receptors by external signals. The extent of synaptic plasticity is remarkable at the hippocampal mossy fiber synapse onto CA3 pyramidal cells. Here we develop a method to analyze such plasticity by recording pairs of synaptically connected dentate gyrus granule cells and CA3 pyramidal cells (GC-CA3) in mouse hippocampal organotypic slice cultures. To identify direct presynaptic partners to a defined target CA3 pyramidal cell, we have combined single-cell electroporation (SCE) and mono-trans-synaptic tracing based on a pseudotyped, recombinant rabies virus (EnvA pseudotyped RABV  $\Delta$ G). Using SCE we have transfected a single CA3 pyramidal cell per slice with the plasmids encoding: RABV envelope glycoprotein (RG), a fluorescent reporter, and TVA (EnvA cognate surface receptor which has no homologue in mammalian cells). The slices were subsequently infected with EnvA pseudotyped RABV  $\Delta$ G. After 3-4 days the RABV mono-trans-synaptic tracing reveals the presynaptic inputs of that single neuron. Then, we were able to establish paired recordings between GC-CA3, as well as to quantify the presynaptic partners of the starter CA3 pyramidal cell. This approach has enabled us to study the mechanisms of presynaptic plasticity in conditions of scarce connectivity between two neuronal populations. Furthermore, it allows the simultaneous study of synaptic architecture and physiology in slices from both wild type and mutant mice with altered neurotransmitter release.

## Introduction

Synaptic connectivity in the hippocampus has been extensively studied due to its well-defined cellular architecture. CA3 pyramidal cells are particularly interesting for understanding the specific properties of different excitatory and inhibitory circuits. Their connections onto CA1 pyramidal cells, known as Schaffer collateral [fiber] (SC)-CA1 synapses, are among the most researched. Plasticity at these synapses is considered to be representative of “canonical glutamatergic synapses”. The excitatory inputs from granule cell mossy fibers have also been the subject of many investigations. In contrast to SC-CA1 synapses, these synapses are known for their particular morphology, distinct synaptic transmission and forms of presynaptic plasticity. Moreover, the numerous recurrent connections (CA3-CA3), made it possible to establish in vitro paired recordings by random double patch with a reasonably high probability (MacVicar and Dudek, 1980; Miles and Wong, 1986; Debanne et al., 1995; Pavlidis and Madison, 1999; reviewed in Le Duigou et al., 2014). CA3-CA1 in vitro paired recordings have also been established by random double patch (Sayer et al., 1990; Malinow, 1991; Debanne et al., 1995; Debanne et al., 1996). On the other hand, the scarce connectivity between GCs and CA3 pyramidal cells renders randomly obtained GC-CA3 paired recordings unpromising. Nonetheless, during the last decade various strategies have achieved, albeit at low success rates, in vitro GC-CA3 paired recordings (Mori et al., 2004; Galimberti et al., 2006; Mori et al., 2007; Toni et al., 2008; Szabadics et al., 2010).

The recent advent of recombinant viral tracing opens new avenues to achieve paired recordings between populations with low inter-connectivity. This potential use was already demonstrated in the first reports of a recombinant rabies virus (RABV), which is pseudotyped with the EnvA envelope and expresses a fluorescent reporter instead of the native glycoprotein (Wickersham et al., 2007a). However, since gene gun transfection resulted in many starter cells per slice, pairs of connected cells could not be obtained in 100 % of the attempts, indicating the need to combine RABV tracing with single-cell transfection. Two techniques proved successful in this respect both in vitro and in vivo: single-cell electroporation (Marshall et al., 2010) and transfection via whole-cell (Rancz et al., 2011; Velez-Fort et al., 2014). However, these approaches have focused on the posterior anatomical study of inputs to a single neuron. Here we combine SCE and RABV tracing in mouse organotypic hippocampal slice cultures to establish GC-CA3 paired recordings.

# Materials, Methods, and Results

## *Animals and Reagents*

- Experimental animals: C57/Bl6 mice
- SCE plasmids: tdTomato\_TVA (P15) and RG (P2) (from Frick's Team, University of Bordeaux)
- EnvA pseudotyped RABV  $\Delta$ G vectors (obtained from KK Conzelmann, Ludwig-Maximilians-Universität, Munich) were amplified and pseudotyped with the hybrid surface protein EnvA by M Haberl and M Ginger (Frick's Team, University of Bordeaux), as described by Wickersham et al., 2007a, b (for design and generation of rabies virus vectors see Osakada and Callaway, 2013).

### Culture media

#### Dissection medium (500 mL)

- Add 5 mL D-glucose (Sigma G8679) and 5 mL Hepes (Gibco) to 500 mL GBSS (Sigma G9779). Filter and add 5 mL Penicillin-streptomycin. Maintain and use the solution at 4°C. Discard after 28 days.

#### Opti-mem medium

- Add 1 mL D-glucose (Sigma G8679) and 25 mL HBSS (Gibco 24020) to 50 mL opti-mem (Gibco 31985). Filter and add 25 mL Horse Serum and 2 mL Penicillin-streptomycin. Maintain at 4°C until required. Condition and warm up the medium to 37 °C using a 5% CO<sub>2</sub> incubator before use.

#### Neurobasal medium

- To 490 mL Neurobasal (Gibco 12349) add: 5 mL D-glucose (Sigma G8679), 2.5 mL of 200 mM glutamine, and 10 mL B27 (Gibco). After filtration add 5 mL Penicillin-streptomycin. Maintain 4°C. Condition and warm up the medium to 37 °C using a 5% CO<sub>2</sub> incubator before use. Fresh medium is prepared every week.

#### HEPES-based extracellular solution (for SCE)

- 145 mM NaCl, 2 mM KCl, 2 mM CaCl<sub>2</sub>, 2 mM MgCl<sub>2</sub>, 10 mM glucose, and 10 mM Hepes, adjusted to 320 mOsm per liter and titrated with NaOH to pH 7.4. This solution is prepared every day from 10x stock.

#### Standard ACSF

- 125 mM NaCl, 2.5 mM KCl, 0.8 mM NaH<sub>2</sub>PO<sub>4</sub>, 26 mM NaHCO<sub>3</sub>, 3 mM CaCl<sub>2</sub>, 2 mM MgCl<sub>2</sub>, 50  $\mu$ M phenol red and 11 mM D-glucose. This solution is prepared every day and saturated with carbogen at least 10 min before use.

#### Patch-pipette solutions for SCE and whole-cell recording

(1 ml aliquots and can be stored for 6–8 months at –20 °C)

- SCE and presynaptic cell (current clamp): 130 mM K-gluconate, 10 mM HEPES, 0.2 mM EGTA, 2 mM MgCl<sub>2</sub>, 4 mM NaCl, 5 mM phospho-creatine, 2 mM Na<sub>2</sub>ATP, and 0.33 mM GTP, adjusted to 310 mOsm per liter and titrated with KOH to pH 7.3. Biocytin (0.2–0.4%) can be added to visualize the morphology of the recorded pairs of connected neurons.
- Postsynaptic cell (voltage clamp): 140 mM CsCH<sub>3</sub>SO<sub>3</sub>, 2 mM MgCl<sub>2</sub>, 4 mM NaCl, 5 mM phospho-creatine, 2 mM Na<sub>2</sub>ATP, 0.2 mM EGTA, 10 mM HEPES, and 0.33 mM GTP (pH 7.3) adjusted with CsOH

## *Equipment*

- Dissection tools for removing the brain (scissors, forceps, spatula and Pasteur pipettes)
- Bunsen burner
- Tissue chopper (McIlwain, Brinkmann, Westbury, NY)
- Incubator

- Microfilters (World Precision Instruments, cat. no. MF3465)
- Millicell culture plate inserts (Millipore)
- Microscope for dissections (Stemi 2000-C; Zeiss)
- Filter paper (VWR, cat. no. 516-0015)
- Plastic Petri dishes (diameter 35, 60 and 145 mm)
- Upright, fixed-stage microscope configured for differential interference contrast (DIC)-infrared video microscopy (Olympus BX51 WI; Olympus)
- Temperature controller for perfusion chamber (TC-324B; Warner Instruments) to maintain the temperature at 34 °C
- Grid (no need for nylon threads, which could hindered the positioning of two recording electrodes in the region of interest, 'U'-shaped weight on top of membrane is sufficient)
- Vibration isolation table (with a pneumatic system; TMC or Newport)
- XY stage for microscope to allow the independent movement of the microscope from the slice chamber and the recording pipettes (Siskiyou)
- Culture room microscope with dual filter (CK40; Olympus) and coupled to mercury lamp (U-RFLT50; Olympus)
- Water-immersion objective:  $\times 40$  or  $\times 60$ , high numerical aperture ( $\geq 0.8$ ) with long working-distance ( $\geq 2$  mm) and specific design (cone shaped) to allow the insertion of two recording electrodes between the objective and the recording tissue
- Infrared-sensitive camera (CoolSNAP EZ; Roper Scientific)
- Imaging Software (Micromanager; see Edelstein et al., 2010)
- Software for cell quantification (Imaris 3D spot measurement; Bitplane, and Image J 2D threshold measurement macro by V. Labrousse; see Collins, 2007)
- Dual-wavelength LED system: 470/550 nm (pE-2; CoolLED)
- Multiband filter (59022; Chroma)
- Peristaltic pump (Minipuls 3; Gilson)
- Two-channels Patch Clamp amplifier (EPC 10.0 run with Patch Master; HEKA Elektronik) (or MultiClamp 700B; Molecular Devices)
- Two stable micromanipulators (MC1000e; Siskiyou)  
Critical: They should be arranged such that the pipette on one side can be removed and changed without disturbing the pipette on the other side.
- Acquisition equipment (AD/DA converter and computer with data acquisition software)
- Thick-walled borosilicate glass tubing (Harvard Apparatus, cat. no. GC150F-10; outer diameter 1.5 mm, inner diameter 0.86 mm).
- Two three-way pressure valves for maintaining pressure in the lines behind the patch pipettes
- Horizontal pipette puller (P-97; Sutter Instruments)
- Patch-pipette filler tips (20  $\mu$ L microfiller; Eppendorf)

# Procedure

## *Overview and Timing*

For Timeline and graphic diagram see Figure 1.

- A. Hippocampal organotypic slices: 90 min
- B. CA3 single-cell electroporation: 20 min/slice
- C. Retrograde viral tracing: 15 min to blot and 3-4 days to trace.
- D. GC-CA3 paired recordings: 60-150 min
- E. Quantification of inputs to starter CA3: 90-120 min

### **A. Hippocampal organotypic slices**

Interface organotypic hippocampal slices were prepared from P5–P7 C57BL6 mice as described previously (Stoppini et al., 1991), according to the guidelines of the University of Bordeaux/CNRS Animal Care and Use Committee. Three to four days after plating, Opti-mem medium was replaced with Neurobasal medium, which was changed every 2–3 days.

### **B. CA3 single-cell electroporation**

Slices at 7 DIV were taken from incubator using a petri dish with 1-2 mL HEPES-buffered solution (HBS) and placed in the recording chamber filled also with HBS. Plasmids expressing TVA-RG-GFP were electroporated in one cell per slice following Single Cell Electroporation protocol, adapted from Rathenberg et al., 2003. Micropipettes had a tip diameter of around 1µm and a resistance of 7-8 MΩ. They were pulled from GB150F capillary glass on a P-97 micropipette puller. Hippocampal organotypic slices for SCE were kept in the recording chamber filled with a HEPES-buffered solution (HBS). The whole volume of medium in the recording chamber was routinely refreshed after each electroporation. Slices were kept for a maximum of 30 minutes in the recording chamber. Slice morphology was visualized using a Olympus BX51 WI microscope. Voltage pulses were delivered using a voltage stimulator (model DS3A, DigiTimer Ltd) controlled by an EPC 10.0 amplifier (Heka elektronik) using the software Patch Master. The plasmids were diluted as follows: P2 at 50 ng/µL, P15 at 25 ng/µL in 40 µL potassium gluconate intracellular solution. Intracellular solution was centrifuged to prevent pipette clogging. 5 µl of the plasmid-containing solution were loaded into the micropipette for every electroporation. Electroporation was monitored by visualizing membrane deflection after pulse application.

### **C. Retrograde viral tracing**

1 day after SCE, transfection was revealed under culture room microscope, we proceeded with infection of transfected slices by “blotting” method: 1 µL of RABV-



$\Delta$ G-EGFP was loaded on a squared piece of membrane (MiliCell). This membrane was placed upside-down on top of the slice. The membrane was removed after 24 hours. Virus infection of organotypic slices was performed in sterile conditions and following the guidelines of Bordeaux University.

#### **D. GC-CA3 paired recordings**

We monitored viral tracing till putative presynaptic granule cell tracing was visible (typically 3-4 days after infection). Then the slice was transferred in a petri dish with 1-2 mL ACSF to the recording chamber perfused with bubbled (95% O<sub>2</sub> and 5% CO<sub>2</sub>) ACSF. The slice was visualized under a 4x objective and repositioned if necessary to an orientation that would allow for both recording electrodes to access target cells without crossing. Then, cells were visualized under a 40X objective. Fluorescence was excited with a dual-wavelength (470/550 nm) LED lighting system and emission was filtered with a multiband filter that allowed for dual DIC – fluorescence (red or green) visualization, which reduced vibrations since the filter cube was not constantly switched.

At first, while simultaneously visualizing in DIC and green fluorescence, a presynaptic granule cell was patched and kept in current clamp with a pipette filled with potassium gluconate intracellular solution. Then, by simultaneously visualizing in DIC and red fluorescence, the starter CA3 pyramidal cell was patched and kept at -70 mV in voltage clamp with a pipette filled with cesium methanesulfonate intracellular solution. The presynaptic cell was acquired at a gain of 0.2 mV/pA and APs were triggered by injecting current (800 pA during 1 ms). Excitatory postsynaptic currents (EPSCs) were recorded from the postsynaptic CA3 cell, which was acquired at a gain of 10 mV/pA. Steps of voltage (-5 mV, 50 ms) or current (-10 pA, 50 ms) were injected in order to control access resistance. Access resistance was <20 M $\Omega$  and remained stable throughout the recording. Recordings were performed at 32°C.

For post hoc analysis, traces were analyzed using Igor Pro (Wavemetrics).

#### **E. Quantification of inputs to starter CA3**

After recording, slices were fixed for 5min in 2% PFA and subsequently washed 3 times in 1X PBS. Slices were kept in 1x PBS at 4°C until mounting and further processing. Slices can be immunostained for instance with antibodies against GAD67 (Millipore) as described previously (Haberl et al., 2014).

High-resolution images of mounted slices were acquired with a confocal microscope Leica SP8 WLL2 on an upright stand DM6000 (Leica Microsystems,

Mannheim, Germany), using objectives HC Plan Apo CS2 20X multi-immersion NA 0.75 and HC Plan Apo CS2 40X oil NA 1.30. The confocal microscope was equipped of a white light laser 2 (WLL2) with freely tuneable excitation from 470 to 670 nm (1 nm steps) and a diode laser at 405 nm. The scanning was done using either a conventional scanner (10Hz to 1800 Hz) or a resonant scanner (8000Hz). The microscope was composed of 2 internal PMT, 2 internal hybrid detectors and 1external PMT for transmission. In cases where the image was too big to fit in the field of view, tiled acquisition was performed. Presynaptic partners were quantified using two different softwares: Image J and Imaris.

### ***Troubleshooting table***

<b>Problem</b>	<b>Possible reason</b>	<b>Solution</b>
Fungal contamination	Contaminated medium	Throw away any unused medium and make fresh
	Contaminated incubator	Empty the incubator and clean it thoroughly
Low SCE success rate	Pipette diameter (big or small) Pipette clogging	Optimize diameter Centrifuge IS
Multiple CA3 starters	Co-transfection of soma and process from another cell Gap junction present	Reduce pipette diameter (no solution available for gap junction presence)
No EPSCs at CA3	Silent synapse	Apply “wake up” train (see Mori et al., 2004, 2007)

## Results

Following the procedure described above it was possible to establish GC-CA3 paired recordings (see Figure 2). Besides allowing visualization of connected cells for physiological study, RABV tracing also reveals the presynaptic partners to a single CA3 pyramidal cell, which can be easily quantified by confocal imaging of the fixed slice following recording (see Figure 3).

In Table 1, basal transmission and short-term plasticity data for four GC-CA3 paired recordings are provided. Two other pairs were obtained but starter cell died without completing the protocol. Thus, we successfully patched 6 connected GC-CA3 pairs out of 31 attempts that were carried out in total. Many, more slices were processed but did not reach the final stage (i.e. starter cell died, multiple starters were present, or slice was contaminated by mushrooms). Duration of the recording ranged from less than one hour to almost two. In this project we focused on short-term plasticity, but if conditions are optimized, long-term forms could be studied also.

**Table 1. Basal transmission and short-term plasticity in four GC-CA3 paired recordings.**

	Total time recorded (min)	0.1 Hz EPSC amp (pA)	Failures (%)	FF	PP EPSC amp (pA)	PPR	5st20Hz (% of 1st)			
							2	3	4	5
<b>Pair 1</b>	114.00	20.28	56.67	195.39	11.73	334.98	148.47	175.55	392.39	502.57
<b>Pair 2</b>	49.00	20.20	80.00	155.00	18.80	175.00	178.71	142.57	53.47	171.04
<b>Pair 3</b>	99.00	24.85	80.00	176.69	19.85	147.98	252.50	1228.75	789.58	536.67
<b>Pair 4</b>	48.00	24.01	36.67	98.69	21.09	132.00	n/a	n/a	n/a	n/a
<b>Avg</b>	77.50	22.34	63.34	156.44	17.87	197.49	193.23	515.62	411.81	403.43
<b>±</b>	±	±	±	±	±	±	±	±	±	±
<b>SEM</b>	17.02	1.22	10.45	20.94	2.10	46.68	30.90	356.7	212.7	116.6

In Figure 2 sample traces from Pair 1 are shown for frequency facilitation from 0.1 to 1 Hz (Figure 2G), for paired-pulse stimulation with 40 ms interval (Figure 2H), and for trains of five stimuli at 20 Hz (Figure 2I). The images accompanying the traces illustrate how visually-guided GC-CA3 pyramidal cell paired recordings were established in RABV-traced organotypic slice cultures.

After recordings the slices were fixed and processed for confocal imaging. Confocal data were subsequently analyzed using two different softwares to quantify the inputs to the starter CA3 pyramidal cell. Images from Pair 1 are shown as example in Figure 3. One method consisted on setting a threshold detection in z-

projections using an Image J macro (Figure 3C and D). The other method relied on 3D spot measurements by Imaris software (Figure 3E and F). In Table 2, the putative inputs (GFP-expressing cells) to the starter CA3 pyramidal cell of two slices were quantified using these two different methods (slice 1 corresponds to Pair 1).

**Table 2. Quantification of two slices using two different software-based methods: Imaris 3D spot measurement and Image J 2D threshold measurement.**

	<b>DG</b>	<b>CA3</b>	<b>CA2</b>	<b>CA1</b>
<b>slice 1 IMARIS</b>	22	188	10	9
<b>slice 1 IMAGE J</b>	16	95	7	7
<b>slice 2 IMARIS</b>	22	91	6	4
<b>slice 2 IMAGE J</b>	23	61	6	10

Higher CA1 count in slice 2 with Image J (10 cells) as compared to Imaris (4 cells) reflects the putative INs that were manually removed in the latter –i.e. 3D spot measurement allows to manually select or unselect cells to be included in the quantification, while Image J is based on a threshold detection. On the other hand, lower CA3 counts in both slices with Image J are due to lower cellular discrimination in this z-projection-based method. Moreover, the signal is extremely variable, depending on the number of neighboring cells, to set a threshold adapted for the whole CA3 region. Finally, we included CA2 counts based on anatomical location – although a conclusive quantification would require specific CA2 markers, but we do not provide the number of INs traced, despite the fact that they are also traced. We are optimizing the GAD67 immunostaining to be able to include INs in future quantifications.

## Discussion

RABV-tracing combined with SCE was successfully implemented to establish visually-guided GC-CA3 pyramidal cell paired recordings in organotypic slice cultures. SCE is a powerful tool that allows time-efficient transfection of targeted cells *in vitro* (Rathenberg et al., 2003) and *in vivo* (Wang et al., 2010). We achieved successful transfection rates of up to 80 %. However, success rate was still variable, ranging from 10 to 80 %. Optimizing this step to consistently transfect at high success rate will be crucial. We showed the advantage of using single-cell electroporation as compared to the gene gun, which was used in the first report showing successful RABV-traced paired recordings (Wickersham et al., 2007a). Furthermore, SCE is more time efficient than transfection via whole-cell. However, this other technique could provide interesting information, for instance, on how cell properties prior to manipulation affect the number of traced inputs from each region, or on longitudinal changes of the intrinsic properties after SCE and RABV infection.

Viral infection by the so-called “blotting method” was straight-forward, time efficient and required a low volume of virus.

The basal amplitudes we recorded are lower than those from acute slices and extracellular stimulation. This phenomenon was reported in previous studies using GC-CA3 paired recordings (Mori et al., 2004). Multiple reasons might account for this difference including: the maturity of the slice cultures; no selection bias for fibers with higher release and pronounced plasticity typical of MF-CA3 synapses; an artifact of RABV-tracing (i.e. cytotoxicity and/or tracing bias) and/or SCE (i.e. changes in postsynaptic cell membrane potential that lead to a homeostatic reduction of release). On the other hand, the number of GC and CA3 inputs to a single CA3 pyramidal cell are within the expected range from previous anatomical studies (Amaral et al., 1990). Nonetheless, differences might be accounted by changes in slice cultures, which are known to undergo synaptogenesis after plating (Robain et al., 1994).

Compared to previous approaches to obtain GC-CA3 paired recordings, this method is advantageous because it enables the quantification of inputs to the CA3 pyramidal cell. Moreover, if biocytin is added to the intracellular solution of the presynaptic cell (and imaged in a color different than green and red), the physiology can be compared to the anatomy, revealed by confocal or even electron microscopy.

To exploit the great potential of the technique reported here further optimization will be required. As mentioned, the SCE success rate needs to be faithfully increased, which would reduce transfection time, number of slices and amount of plasmids needed. Secondly, presynaptic cell(s) could be activated by light instead of current injection (see Osakada et al., 2011 for RABV variants expressing rhodopsins). By doing so, only the postsynaptic cell would require whole-cell patch clamp, thus increasing the chances of successful paired-recordings and allowing stimulation of different presynaptic cells. However, optogenetic activation is only possible if traced inputs are sparse and far from the starter cell, otherwise multiple presynaptic cells or the neurites of the starter cell could be unintentionally activated. Therefore, CA3 circuits are particularly suitable given the scarce GC-CA3 connectivity. For instance, the GC(s) light activation can be combined with double patch of a CA3 interneuron and the starter pyramidal cell (to study feedforward inhibition: GC-CA3In-CA3Pyr); or optogenetic control of EC presynaptic cell(s) with recordings from a traced GC and the starter CA3 (to study the disynaptic circuit: EC-GC-CA3Pyr). Conversely, cell activity could be monitored by using a RABV variant expressing a genetically-encoded calcium indicator (Osakada et al., 2011). Injecting current into a single presynaptic cell would light up the starter CA3 and all other cells synapsed by the patched cell.

The possibility to record pairs other than GC-CA3 (i.e. CA3-CA3, IN-CA3, EC-CA3, etc.) provides a way to control for RABV-tracing effects. Randomly patching connected GC-CA3 pairs is extremely unlikely. However, random CA3-CA3 paired recordings can be established with reasonably high probability (see protocol by Debanne et al., 2008). We are currently working on the comparison between random and RABV-traced CA3-CA3 paired recordings –including random pairs in which the postsynaptic CA3 has also undergone SCE of the RABV complementary plasmids).

Using the reported version of the technique, important biological questions such as the nature of calcium buffers at MFs can be studied by simply patching GCs with two different EGTA concentrations (ex. 0.1 vs. 10mM), as it has been recently addressed by patching connected MFbouton-CA3 pairs (Vyleta and Jonas, 2014). Finally, the simultaneous study of synaptic architecture and physiology is possible in slices from both wild type and mutant mice with altered neurotransmitter release. Overall, this method provides great potential in the study of CA3 circuits both *in vitro* and *in vivo*.

## **Acknowledgements**

This work was supported by the CNRS to CM and by the University of Bordeaux and the VU University Amsterdam to BLG. We would like to thank K.K. Conzelmann for providing plasmid constructs and recombinant rabies virus.

## **Author contribution**

M.C., C.M. and M.V. designed and supervised the study. M.G. and V.L. processed fixed slices and acquired confocal images, V.L. quantified traced cells. B.G.L. performed all the electrophysiological recordings. C.B. helped with the electrophysiological analyses and contributed with discussion. M.V., M.C. and A.F. contributed to the discussion. B.G.L., and C.M. wrote the manuscript.

## References

- Amaral, D. G., N. Ishizuka and B. Claiborne (1990). Neurons, numbers and the hippocampal network. *Prog Brain Res* 83: 1-11.
- Collins, T. J. (2007). ImageJ for microscopy. *Biotechniques* 43(1 Suppl): 25-30.
- Debanne, D., S. Boudkkazi, E. Campanac, R. H. Cudmore, P. Giraud, L. Fronzaroli-Molinieres, E. Carlier and O. Caillard (2008). Paired-recordings from synaptically coupled cortical and hippocampal neurons in acute and cultured brain slices. *Nat Protoc* 3(10): 1559-1568.
- Debanne, D., N. C. Guérineau, B. H. Gähwiler and S. M. Thompson (1995). Physiology and pharmacology of unitary synaptic connections between pairs of cells in areas CA3 and CA1 of rat hippocampal slice cultures.
- Debanne, D., N. C. Guérineau, B. H. Gähwiler and S. M. Thompson (1996). Paired-pulse facilitation and depression at unitary synapses in rat hippocampus: quantal fluctuation affects subsequent release. *The Journal of Physiology* 491 (Pt 1): 163-76.
- Edelstein, A., N. Amodaj, K. Hoover, R. Vale and N. Stuurman (2010). Computer control of microscopes using microManager. *Curr Protoc Mol Biol* Chapter 14: Unit14 20.
- Le Duigou, C., J. Simonnet, M. T. Teleńczuk, D. Fricker and R. Miles (2014). Recurrent synapses and circuits in the CA3 region of the hippocampus: an associative network. *Front. Cell. Neurosci.* 7: 1-13.
- MacVicar, B. A. and F. E. Dudek (1980). Local synaptic circuits in rat hippocampus: interactions between pyramidal cells. *Brain Research* 184(1): 220-3.
- Malinow, R. (1991). Transmission between pairs of hippocampal slice neurons: quantal levels, oscillations, and LTP. *Science* 252(5006): 722-4.
- Marshall, J. H., T. Mori, K. J. Nielsen and E. M. Callaway (2010). Targeting Single Neuronal Networks for Gene Expression and Cell Labeling In Vivo. *Neuron* 67(4): 562-574.
- Miles, R. and R. K. Wong (1986). Excitatory synaptic interactions between CA3 neurones in the guinea-pig hippocampus. *The Journal of Physiology* 373: 397-418.
- Mori, M., M. H. Abegg, B. H. Gähwiler and U. Gerber (2004). A frequency-dependent switch from inhibition to excitation in a hippocampal unitary circuit. *Nature* 431(7007): 453-6.
- Osakada, F. and E. M. Callaway (2013). Design and generation of recombinant rabies virus vectors. *Nat Protoc* 8(8): 1583-1601.
- Osakada, F., T. Mori, Ali H. Cetin, James H. Marshall, B. Virgen and Edward M. Callaway (2011). New Rabies Virus Variants for Monitoring and Manipulating Activity and Gene Expression in Defined Neural Circuits. *Neuron* 71(4): 617-631.
- Pavlidis, P. and D. V. Madison (1999). Synaptic Transmission in Pair Recordings From CA3 Pyramidal Cells in Organotypic Culture. *Journal of Neurophysiology* 81(6): 2787-2797.
- Rancz, E. A., K. M. Franks, M. K. Schwarz, B. Pichler, A. T. Schaefer and T. W. Margrie (2011). Transfection via whole-cell recording in vivo: bridging single-cell physiology, genetics and connectomics. *Nature Neuroscience*: 1-7.
- Rathenberg, J., T. Nevian and V. Witzemann (2003). High-efficiency transfection of individual neurons using modified electrophysiology techniques. *J Neurosci Methods* 126(1): 91-8.



- Robain, O., G. Barbin, T. Billette de Villemeur, L. Jardin, T. Jahchan and Y. Ben-Ari (1994). Development of mossy fiber synapses in hippocampal slice culture. *Developmental brain research* 80(1): 244-250.
- Sayer, R. J., M. J. Friedlander and S. J. Redman (1990). The time course and amplitude of EPSPs evoked at synapses between pairs of CA3/CA1 neurons in the hippocampal slice. *J Neurosci* 10(3): 826-36.
- Stoppini, L., P. A. Buchs and D. Muller (1991). A simple method for organotypic cultures of nervous tissue. *J Neurosci Methods* 37(2): 173-82.
- Velez-Fort, M., C. V. Rousseau, C. J. Niedworok, I. R. Wickersham, E. A. Rancz, A. P. Brown, M. Strom and T. W. Margrie (2014). The stimulus selectivity and connectivity of layer six principal cells reveals cortical microcircuits underlying visual processing. *Neuron* 83(6): 1431-43.
- Vyleta, N. P. and P. Jonas (2014). Loose coupling between Ca<sup>2+</sup> channels and release sensors at a plastic hippocampal synapse. *Science* 343(6171): 665-70.
- Wang, M., O. Orwar, J. Olofsson and S. G. Weber (2010). Single-cell electroporation. *Anal Bioanal Chem* 397(8): 3235-3248.
- Wickersham, I. R., D. C. Lyon, R. J. O. Barnard, T. Mori, S. Finke, K.-K. Conzelmann, J. A. T. Young and E. M. Callaway (2007a). Monosynaptic restriction of transsynaptic tracing from single, genetically targeted neurons. *Neuron* 53(5): 639-47.
- Wickersham, I. R., S. Finke, K.-K. Conzelmann and E. M. Callaway (2007b). Retrograde neuronal tracing with a deletion-mutant rabies virus. *Nat Meth* 4(1): 47-49.

# Figures and Legends

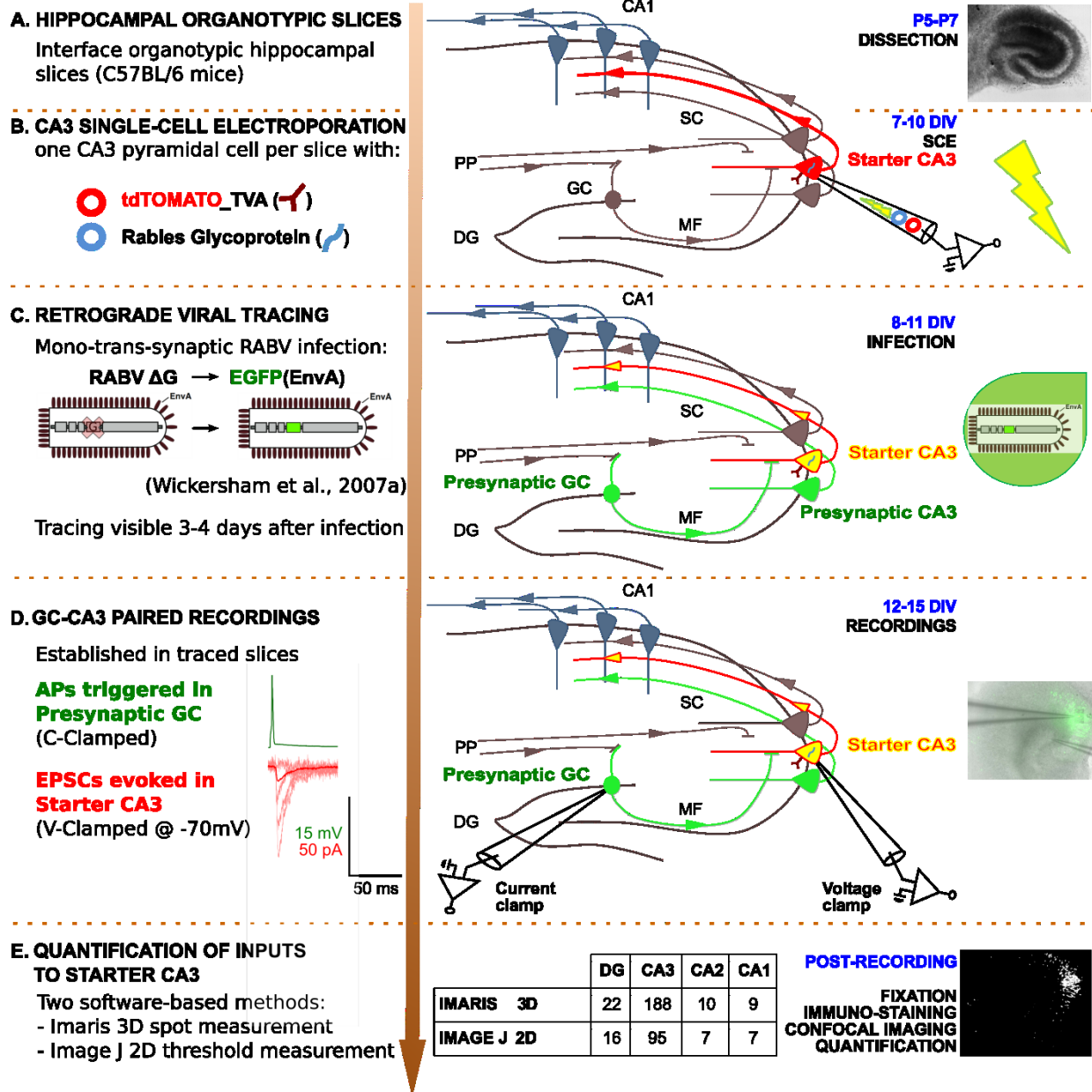


**Figure 1. Timeline of RABV-traced GC-CA3 paired recordings and quantification of inputs to starter CA3 pyramidal cell.**

From top to bottom: we used mouse hippocampal organotypic slice cultures from P5-P7 pups. At 7-10 DIV, we transfected by single-cell electroporation (SCE) a single CA3 pyramidal cell per slice with the plasmids encoding: a fluorescent reporter (tdTomato) and TVA (the EnvA cognate surface receptor, which has no homologue in mammalian cells), and the RABV envelope glycoprotein (RG). The slices were subsequently infected with EnvA pseudotyped RABV ΔG. After 3-4 days, the RABV mono-trans-synaptic tracing revealed the presynaptic inputs of that single neuron. Then, we were able to establish paired recordings between connected GC-CA3 cells, as well as to quantify the presynaptic partners of the starter CA3 pyramidal cell.

## Figures and Legends

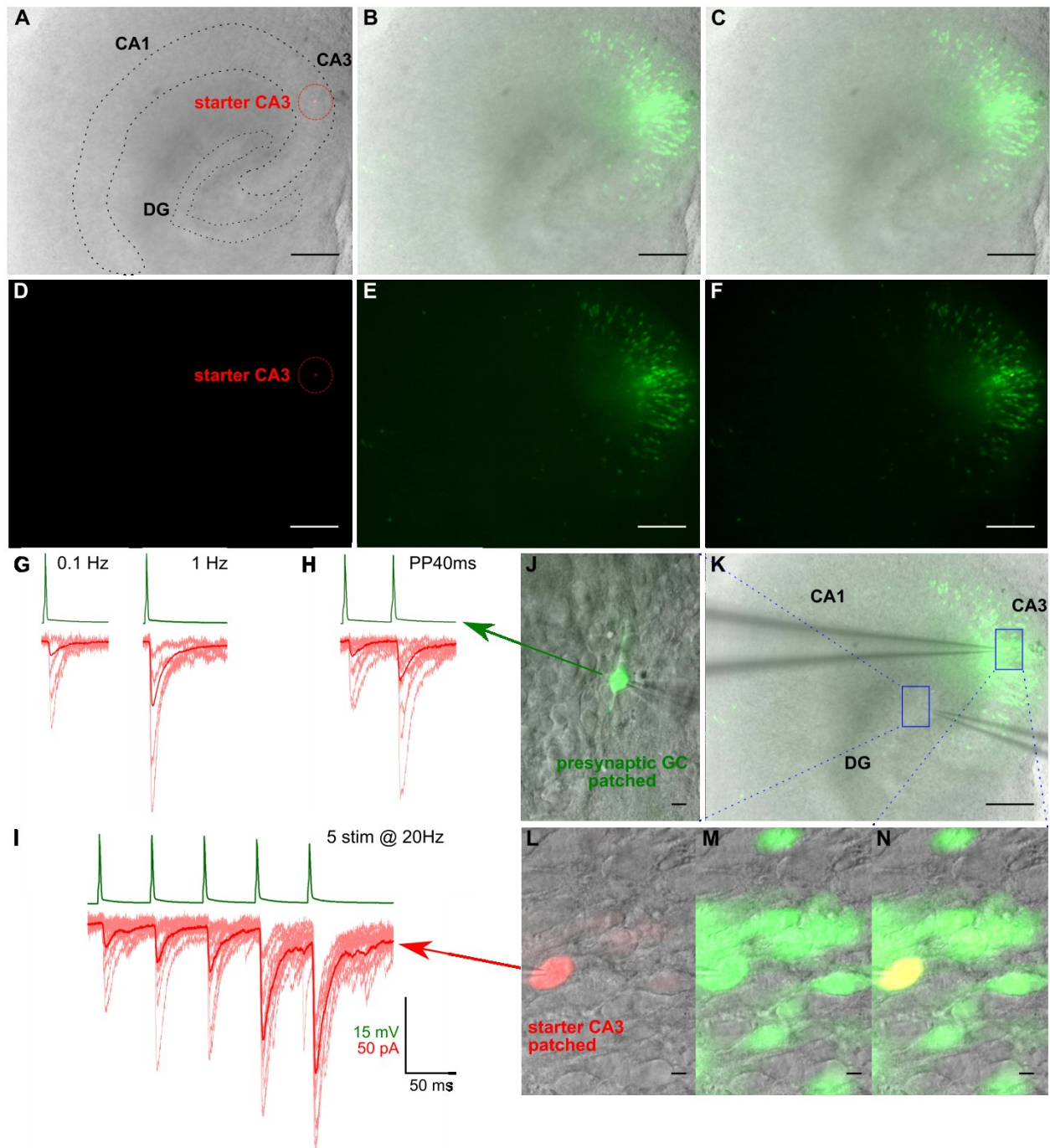


**Figure 2. Example of GC-CA3 paired recording after RABV mono-trans-synaptic retrograde tracing.**

A-F, Images of RABV-traced hippocampal organotypic slice as visualized under the epifluorescence microscope of the electrophysiology setup using a dual LED, multi-band filter and 4x objective. A, DIC/red overlay showing starter CA3 pyramidal cell (red soma inside circle). Areas delineated by dotted lines correspond to principal layers. B, DIC/green overlay showing traced presynaptic partners (green). C, DIC/red/green overlay. D, Starter CA3 pyramidal cell (red soma inside circle). E, Traced presynaptic partners (green). F, Red/green overlay. G-I, Traces of GC-CA3 paired recording. Green traces on top correspond to sample APs triggered in presynaptic GC, while red traces at the bottom are EPSCs recorded at the starter CA3 (darker red trace shows average). Scale bar applies to all traces. G, Frequency facilitation (from 0.1 to 1 Hz), H, Paired pulse facilitation (40ms inter-stimulus interval), and I, facilitation induced by a train of 5 stimuli at 20 Hz. J-N, Patch pipettes arrangement during GC-CA3 paired recording. Boxes over patched cells in K are shown at 40x magnification in J and L-N for GC and CA3, respectively. DG: dentate gyrus, and CA1/CA3: Cornu ammonis 1 and 3. For 4x images (A-F, and K) scale bar=150μm. J, Green/DIC overlay of the presynaptic GC patched (pipette from right). L-N, DIC images of the starter CA3 pyramidal cell patched in red (L), green (M), and red/green overlay (N) (pipette from left). For 40x images (J and L-N) scale bar=5μm.

## Figures and Legends

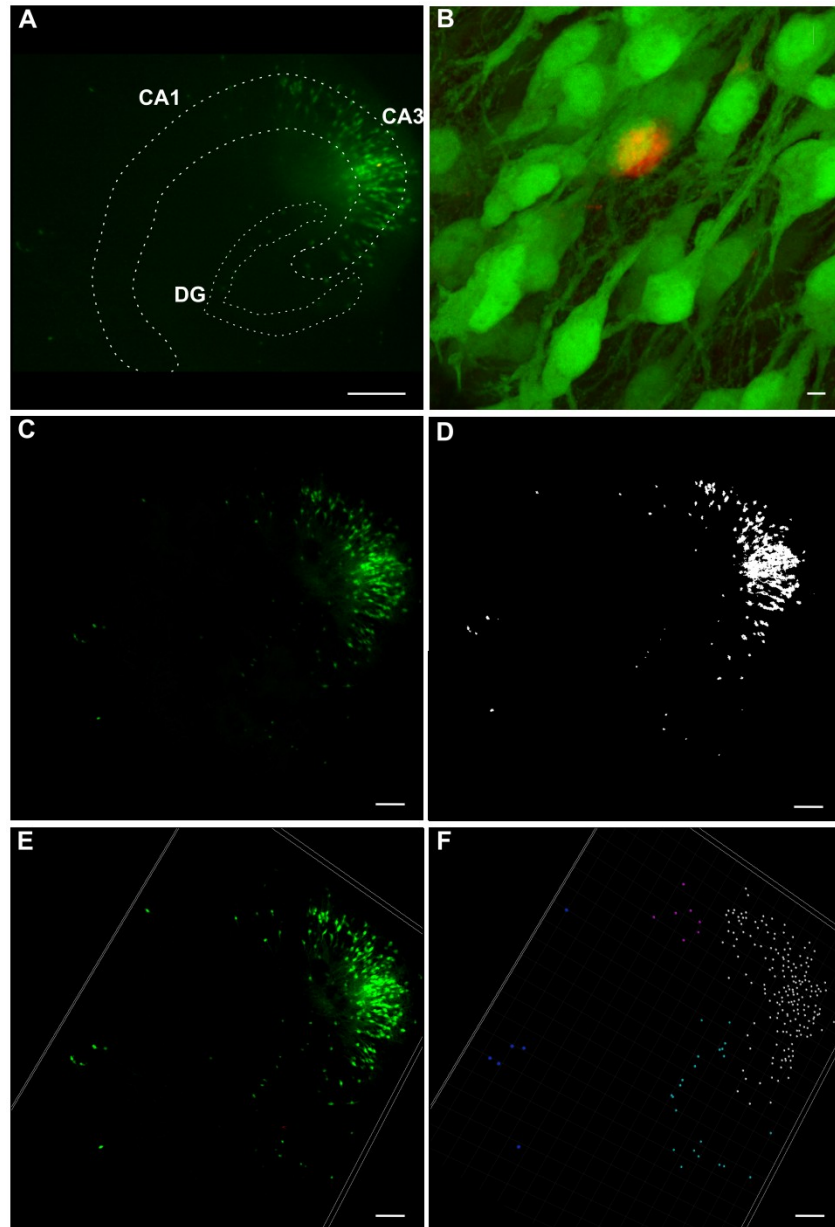


**Figure 3. Confocal images of fixed slice after GC-CA3 paired recording and comparison of two methods to quantify RABV-traced presynaptic partners.**

**A**, Example of 4x epifluorescent image of hippocampal organotypic slice as visualized under the microscope of the electrophysiology setup using a dual LED and multi-band filter, scale bar=150 $\mu$ m. **B**, Red/green overlay of confocal acquisition at 40x of the CA3 starter cell (red channel) and nearby presynaptic partners (green channel) scale bar=5 $\mu$ m. **C-D**, Example of Image J-based method to quantify cells connected to the starter cell. **C**, Z projection of confocal acquisition at 20x and **D**, counting mask. **E-F**, Example of Imaris-based method to quantify cells connected to the starter cell. **E**, 3D view of confocal acquisition at 20x and **F**, spot volume counting. For confocal images at 20x (**C-F**) scale bar=150 $\mu$ m.

**Conclusions**

**&**

**Perspectives**

## Conclusions & Perspectives

### Phenotyping Hippocampal Mossy Fiber Synapses in VAMP7 KO Mice

Hippocampal mossy fiber synapses from TI-VAMP/VAMP7 KO mice are indistinguishable from those of WT littermates. Changes in presynaptic protein expression might underlie mechanisms that compensate for the loss of VAMP7. Recent reports describe VAMP7-mediated forms of release that are action potential-independent and get activated by insulin (Burgo et al., 2013) or reelin application (Bal et al., 2013). Furthermore, nicotine and caffeine-mediated release have also been reported at MF synapses (Sharma and Vijayaraghavan, 2003; Cheng and Yakel, 2014). A recent study shows that a low dose nicotine challenge can induce increased social anxiety-like behavior, accompanied of increased MF sprouting, in rats that display high rate (HR) locomotor reactivity in a novel environment (Aydin et al., 2014). The same group had previously shown increased MF sprouting in HR rats after a behaviorally-sensitizing nicotine regimen (Bhatti et al., 2007). In a different study, MF sprouting has also been correlated with anxiety-like behavior in the light-dark box test (De Oliveira et al., 2008). Thus, we are currently testing neurotransmission after application of an  $\alpha 7$  nAChR agonist (PNU-282987) in VAMP7 KO and WT slices. As already pointed out, it might be necessary to select only ventral hippocampal slices. In the future, it would be interesting to test anxiety in VAMP7 KO mice after *in vivo*  $\alpha 7$  nAChR agonist treatment, having previously classified mice according to locomotor reactivity rate in a novel environment.

Moreover, future studies should address the possible role of VAMP7 in MF filopodial plasticity and the physiological impact of VAMP7-mediated ATP release from astrocytes (Verderio et al., 2012).

To study the role of VAMP7 in MF synapses avoiding developmental compensatory mechanisms, a conditional KO strategy should be used instead of constitutive KO mice. Various conditional KO strategies are possible but rather difficult: VAMP7 loxP mice could be developed, and GC(s) selectively targeted with a Cre-expressing vector (possibly expressing also a rhodopsin for optogenetic activation) driven by a GC-specific promoter or transfected by SCE, if a single GC is targeted and GC-CA3 paired recordings are subsequently established.

## CA3 Circuits Probed with RABV-Tracing and Paired Recordings

About this second project, more methodological, we showed that it is possible to establish visually-guided GC-CA3 paired recordings after RABV-tracing in organotypic slices. However, the technique requires optimization before using it to answer any research question, as it remains quite arduous in its current form. While certain drawbacks could be improved, other are intrinsic to this technique and should be considered when evaluating the suitability of this method for a particular research question. In order to assess possible RABV-inherent effects, we have planned to compare RABV-traced CA3-CA3 paired recordings to randomly obtained recordings –which cannot be obtained for GC-CA3 due to the scarce connectivity. We envision alternative techniques to attain this objective like: single GC transfection (including rhodopsin) and patch of CA3 cells near bouton; the previous possibly combined with bulk loading of calcium indicators (Sasaki et al., 2009), or E-SARE expression (Kawashima et al., 2013) in CA3 stratum pyramidale; or use of a different viral vector (i.e. CAV2, which allows longer cell survival) (Soudais et al., 2001; Soudais et al., 2004).

This method certainly offers plenty of perspectives. To those already mentioned –use transfection via whole-cell to provide information on how cell properties prior to manipulation affect the number of traced inputs from each region; add biocytin to the intracellular solution of the presynaptic cell to compare physiology to anatomy (by confocal or electron microscopy); study the nature of calcium buffers at MFs by simply patching GCs with two different EGTA concentrations (ex. 0.1 vs. 10mM), as it has been recently addressed by patching MFB-CA3 (Vyleta and Jonas, 2014); patch other pairs (i.e. CA3-CA3, IN-CA3, EC-CA3, etc.); study microcircuits (i.e. GC-IN-CA3 or EC-GC-CA3); use RABV variants that allow optogenetic activation or expression of genetically-encoded calcium indicators (Osakada et al., 2011)- we can add many other such as: change starter cell population (i.e. CA2 pyramidal cells); improve 3D quantification accuracy by applying clearing method; use cultures from adult animals or even human samples (see Eugène et al., 2014); or render tracing anterograde by expressing a different glycoprotein (i.e. possibly VSV-G) (see Figure 30), which would allow genetic modification of the presynaptic GC (finally allowing for conditional KO experiments, for instance in Munc18-1 LoxP mice, like those performed in the Calyx of Held in Genc et al., 2014). Anterograde tracing would be more suitable for optogenetic activation as the rhodopsin could be transfected by



SCE, assuring that the only cell activated by light would be the presynaptic starter cell. Combined with a RABV variant expressing a genetically encoded calcium indicator (Osakada et al., 2011), it would allow wireless functional monitoring and activation of the circuit. Thus, the plasticity of the circuit could be tested *in vivo* –for instance, before and after contextual fear conditioning. Overall, this method provides great potential for the study of CA3 circuits, as well as any other circuit.

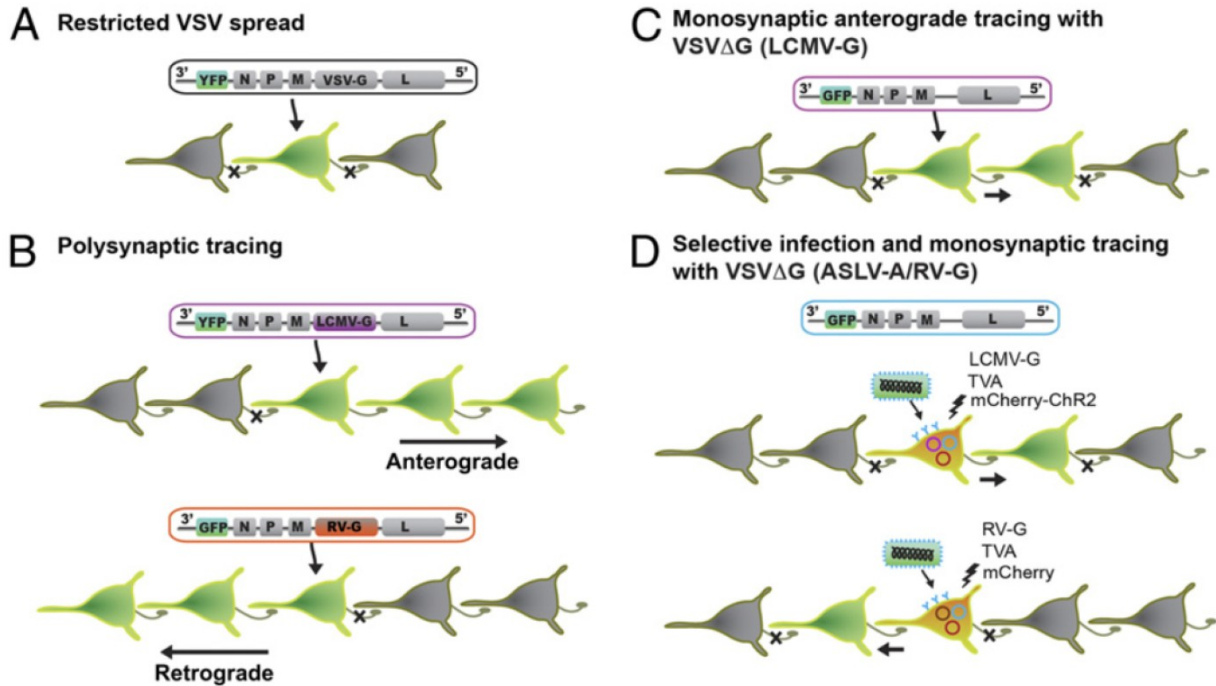


**Figure 30 Potential anterograde monosynaptic RABV-tracing by VSV-G or LCMV-G expression like D for VSV (modified from Tuncdemir and Fishell, 2011)**

Out of all the possibilities mentioned, the two projects that I would like to test using RABV-traced GC-CA3 paired recordings are:

1) Study the nature of calcium buffers at MFs by patching GCs with two different EGTA concentrations (ex. 0.1 vs. 10mM). Vyleta and Jonas (2014), have recently reported a mechanism relying on loose-coupling. Paired recordings established at the GC soma instead of the MF bouton will confirm this finding, since patching the bouton leads to dialysis that could interfere with physiological calcium buffers.

2) Mossy fiber conditional KO experiments in Munc18-1 LoxP mice like those performed in the Calyx of Held (Genc et al., 2014). Since the beginning of my thesis, under a joint-PhD supervision, the objective was to combine *in vitro* slice recordings routinely performed at Mulle's Lab in Bordeaux, with KO mice with altered neurotransmitter release from Verhage's Lab in Amsterdam. This collaboration would have confirmed findings obtained in recordings from autaptic cultures of those KO



mice, as well as dissected the role of the mutated proteins in MF-CA3 synapses. However, studying presynaptic mechanism synaptic plasticity at hippocampal mossy fiber synapses was technically limited by the current recording paradigm: *in vitro* CA3 whole-cell recordings probed with MF(s) extracellular stimulation. While this technique has widely increase our knowledge about the physiology of MF-CA3 synapses, a single fiber cannot be unequivocally stimulated, nor specifically targeted. We succeeded in our efforts to develop a technique that allows us to establish granule cell – CA3 pyramidal cell paired recordings in hippocampal organotypic slices. However, the technique still requires optimization. Furthermore, the postsynaptic cell can be genetically manipulated by SCE, but the presynaptic GCs can only be modified by RABV variants that we have not yet tested. Moreover, RABV-driven genetic modification will also affect the starter cell and other cells in the circuit (i.e. interneurons responsible for feedforward inhibition), thus making it hard to interpret eventual findings. In conclusion, we will need to develop an anterograde tracing technique to be able to study slice physiology in Munc18-1 LoxP mice.

# **Bibliography**

## Bibliography

- Acsády, L., A. Kamondi, A. Sík, T. Freund and G. Buzsáki (1998). GABAergic cells are the major postsynaptic targets of mossy fibers in the rat hippocampus. *J Neurosci* 18(9): 3386-403.
- Albertini, A. A., R. W. Ruigrok and D. Blondel (2011). Rabies virus transcription and replication. *Adv Virus Res* 79: 1-22.
- Alberts, P., R. Rudge, I. Hinners, A. Muzerelle, S. Martinez-Arca, T. Irinopoulou, V. Marthiens, S. Tooze, F. Rathjen, P. Gaspar and T. Galli (2003). Cross talk between tetanus neurotoxin-insensitive vesicle-associated membrane protein-mediated transport and L1-mediated adhesion. *Mol Biol Cell* 14(10): 4207-20.
- Alle, H. and J. R. P. Geiger (2006). Combined analog and action potential coding in hippocampal mossy fibers. *Science* 311(5765): 1290-3.
- Altevogt, B. M., K. A. Kleopa, F. R. Postma, S. S. Scherer and D. L. Paul (2002). Connexin29 is uniquely distributed within myelinating glial cells of the central and peripheral nervous systems. *J Neurosci* 22(15): 6458-70.
- Altman, J. (1963). Autoradiographic investigation of cell proliferation in the brains of rats and cats. *Anat Rec* 145: 573-91.
- Amaral, D. G., N. Ishizuka and B. Claiborne (1990). Neurons, numbers and the hippocampal network. *Prog Brain Res* 83: 1-11.
- Annese, J., N. M. Schenker-Ahmed, H. Bartsch, P. Maechler, C. Sheh, N. Thomas, J. Kayano, A. Ghatan, N. Bresler, M. P. Frosch, R. Klaming and S. Corkin (2014). Postmortem examination of patient H.M.'s brain based on histological sectioning and digital 3D reconstruction. *Nat Commun* 5: 3122.
- Aranzi, G. C. (1564). *De Humano foetu*.
- Archbold, J. K., A. E. Whitten, S. H. Hu, B. M. Collins and J. L. Martin (2014). SNARE-ing the structures of Sec1/Munc18 proteins. *Curr Opin Struct Biol* 29C: 44-51.
- Arenkiel, B. R. (2011). Genetic Approaches to Reveal the Connectivity of Adult-Born Neurons. *Front. Neurosci.* 5: 1-8.
- Arenkiel, B. R., H. Hasegawa, J. J. Yi, R. S. Larsen, M. L. Wallace, B. D. Philpot, F. Wang and M. D. Ehlers (2011). Activity-Induced Remodeling of Olfactory Bulb Microcircuits Revealed by Monosynaptic Tracing. *PLoS ONE* 6(12): e29423.
- Ariel, P. and T. A. Ryan (2012). New Insights Into Molecular Players Involved in Neurotransmitter Release. *Physiology* 27(1): 15-24.
- Astic, L., D. Saucier, P. Coulon, F. Lafay and A. Flamand (1993). The CVS strain of rabies virus as transneuronal tracer in the olfactory system of mice. *Brain Res* 619(1-2): 146-56.
- Aston-Jones, G. and J. P. Card (2000). Use of pseudorabies virus to delineate multisynaptic circuits in brain: opportunities and limitations. *J Neurosci Methods* 103(1): 51-61.
- Aydin, C., O. Oztan and C. Isgor (2014). Hippocampal Y2 receptor-mediated mossy fiber plasticity is implicated in nicotine abstinence-related social anxiety-like behavior in an outbred rat model of the novelty-seeking phenotype. *Pharmacology, Biochemistry and Behavior* 125(C): 48-54.
- Bal, M., J. Leitz, Austin L. Reese, Denise M. O. Ramirez, M. Durakoglugil, J. Herz, Lisa M. Monteggia and Ege T. Kavalali (2013). Reelin Mobilizes a VAMP7-Dependent Synaptic Vesicle Pool and Selectively Augments Spontaneous Neurotransmission. *Neuron*: 1-13.
- Bandtlow, C. E. and D. R. Zimmermann (2000). Proteoglycans in the developing brain: new conceptual insights for old proteins. *Physiol Rev* 80(4): 1267-90.

- Beier, K. T., A. B. Saunders, I. A. Oldenburg, B. L. Sabatini and C. L. Cepko (2013a). Vesicular stomatitis virus with the rabies virus glycoprotein directs retrograde transsynaptic transport among neurons in vivo. *Front. Neural Circuits* 7: 1-13.
- Beier, K. T., A. Saunders, I. A. Oldenburg, K. Miyamichi, N. Akhtar, L. Luo, S. P. J. Whelan, B. Sabatini and C. L. Cepko (2011). Anterograde or retrograde transsynaptic labeling of CNS neurons with vesicular stomatitis virus vectors. *Proceedings of the National Academy of Sciences* 108(37): 15414-15419.
- Beier, K. T., A. Saunders, I. A. Oldenburg, K. Miyamichi, N. Akhtar, L. Luo, S. P. J. Whelan, B. Sabatini and C. L. Cepko (2012). Anterograde or retrograde transsynaptic labeling of CNS neurons with vesicular stomatitis virus vectors\_Correction. *Proceedings of the National Academy of Sciences* 109(23): 9219-9219.
- Beier, K. T., B. G. Borghuis, R. N. El-Danaf, A. D. Huberman, J. B. Demb and C. L. Cepko (2013b). Transsynaptic Tracing with Vesicular Stomatitis Virus Reveals Novel Retinal Circuitry. *Journal of Neuroscience* 33(1): 35-51.
- Bekhterev, V. M. I. (1900). *Les voies de conduction du cerveau et de la moelle*, Storck.
- Bennett, M. V. (2000). Seeing is relieving: electrical synapses between visualized neurons. *Nature neuroscience* 3: 7-8.
- Benson, D. L., L. M. Schnapp, L. Shapiro and G. W. Huntley (2000). Making memories stick: cell-adhesion molecules in synaptic plasticity. *Trends Cell Biol* 10(11): 473-82.
- Berg, L. K., M. Larsson, C. Morland and V. Gundersen (2013). Pre- and postsynaptic localization of NMDA receptor subunits at hippocampal mossy fibre synapses. *Neuroscience* 230(C): 139-150.
- Bernardinelli, Y., D. Muller and I. Nikonenko (2014). Astrocyte-synapse structural plasticity. *Neural plasticity* 2014.
- Beuret, C. (2000). Virology: Classification of Viruses. [www.nlv.ch/Virologytutorials/Classification.htm](http://www.nlv.ch/Virologytutorials/Classification.htm).
- Bhatti, A. S., P. Hall, Z. Ma, R. Tao and C. Isgor (2007). Hippocampus modulates the behaviorally-sensitizing effects of nicotine in a rat model of novelty-seeking: Potential role for mossy fibers. *Hippocampus* 17(10): 922-933.
- Bischofberger, J. and P. Jonas (2002). TwoB or not twoB: differential transmission at glutamatergic mossy fiber-interneuron synapses in the hippocampus. *Trends in Neurosciences* 25(12): 600-3.
- Bischofberger, J., J. R. P. Geiger and P. Jonas (2002). Timing and efficacy of Ca<sup>2+</sup> channel activation in hippocampal mossy fiber boutons. *J Neurosci* 22(24): 10593-602.
- Bizzini, B., K. Stoeckel and M. Schwab (1977). An antigenic polypeptide fragment isolated from tetanus toxin: chemical characterization, binding to gangliosides and retrograde axonal transport in various neuron systems. *J Neurochem* 28(3): 529-42.
- Bizzini, B., P. Grob, M. A. Glicksman and K. Akert (1980). Use of the B-IIb tetanus toxin derived fragment as a specific neuropharmacological transport agent. *Brain Research* 193(1): 221-7.
- Blackstad, T. W. and A. Kjaerheim (1961). Special axo-dendritic synapses in the hippocampal cortex: electron and light microscopic studies on the layer of mossy fibers. *J Comp Neurol* 117: 133-59.
- Blausen (2014) Blausen Gallery. Wikiversity Journal of Medicine DOI: 10.15347/wjm/2014.010 ISSN: 20018762

- Blumstein, J., V. Faundez, F. Nakatsu, T. Saito, H. Ohno and R. B. Kelly (2001). The neuronal form of adaptor protein-3 is required for synaptic vesicle formation from endosomes. *J Neurosci* 21(20): 8034-42.
- Boss, B. D., G. M. Peterson and W. M. Cowan (1985). On the number of neurons in the dentate gyrus of the rat. *Brain Res* 338(1): 144-50.
- Brandalise, F. and U. Gerber (2014). Mossy fiber-evoked subthreshold responses induce timing-dependent plasticity at hippocampal CA3 recurrent synapses. *Proc Natl Acad Sci USA*.
- Braz, J. M., B. Rico and A. I. Basbaum (2002). Transneuronal tracing of diverse CNS circuits by Cre-mediated induction of wheat germ agglutinin in transgenic mice. *Proc Natl Acad Sci U S A* 99(23): 15148-53.
- Breustedt, J., A. Gundlfinger, F. Varoqueaux, K. Reim, N. Brose and D. Schmitz (2010). Munc13-2 Differentially Affects Hippocampal Synaptic Transmission and Plasticity. *Cerebral Cortex* 20(5): 1109-1120.
- Brose, N. (2014). All Roads Lead to Neuroscience: The 2013 Nobel Prize in Physiology or Medicine. *Neuron* 81(4): 723-727.
- Brus, M., M. Keller and F. Lévy (2013). Temporal features of adult neurogenesis: differences and similarities across mammalian species. *Front. Neurosci.* 7: 1-9.
- Bruzzone, R., S. G. Hormuzdi, M. T. Barbe, A. Herb and H. Monyer (2003). Pannexins, a family of gap junction proteins expressed in brain. *Proc Natl Acad Sci U S A* 100(23): 13644-9.
- Burgo, A., A. M. Casano, A. Kuster, S. T. Arold, G. Wang, S. Nola, A. Verraes, F. Dingli, D. Loew and T. Galli (2013). Increased activity of the Vesicular Soluble N-Ethylmaleimide-sensitive Factor Attachment Protein Receptor TI-VAMP/VAMP7 by Tyrosine Phosphorylation in the Longin Domain. *Journal of Biological Chemistry* 288(17): 11960-11972.
- Burgo, A., V. Proux-Gillardeaux, E. Sotirakis, P. Bun, A. Casano, A. Verraes, R. K. H. Liem, E. Formstecher, M. Coppey-Moisand and T. Galli (2012). A molecular network for the transport of the TI-VAMP/VAMP7 vesicles from cell center to periphery. *Developmental Cell* 23(1): 166-80.
- Burkhardt, P., C. M. Stegmann, B. Cooper, T. H. Kloepper, C. Imig, F. Varoqueaux, M. C. Wahl and D. Fasshauer (2011). Primordial neurosecretory apparatus identified in the choanoflagellate *Monosiga brevicollis*. *Proceedings of the National Academy of Sciences* 108(37): 15264-15269.
- Burkhardt, P., D. A. Hattendorf, W. I. Weis and D. Fasshauer (2008). Munc18a controls SNARE assembly through its interaction with the syntaxin N-peptide. *The EMBO Journal* 27(7): 923-933.
- Callaway, E. M. (2008). Transneuronal circuit tracing with neurotropic viruses. *Curr Opin Neurobiol* 18(6): 617-23.
- Card, J. P., O. Kobiler, J. McCambridge, S. Ebdlahad, Z. Shan, M. K. Raizada, A. F. Sved and L. W. Enquist (2011). Microdissection of neural networks by conditional reporter expression from a Brainbow herpesvirus. *Proc Natl Acad Sci U S A* 108(8): 3377-82.
- Carta, M., F. Lanore, N. Rebola, Z. Szabo, Silvia V. Da Silva, J. Lourenço, A. Verraes, A. Nadler, C. Schultz, C. Blanchet and C. Mulle (2014a). Membrane Lipids Tune Synaptic Transmission by Direct Modulation of Presynaptic Potassium Channels. *Neuron*: 1-13.
- Carta, M., S. Fièvre, A. Gorlewicz and C. Mulle (2014b). "Kainate receptors in the hippocampus." *European Journal of Neuroscience* 39(11): 1835-1844.
- Carter, M. and J. Shieh (2009). *Guide to research techniques in neuroscience*, Academic Press.

- Catterall, W. A. and A. P. Few (2008). Calcium channel regulation and presynaptic plasticity. *Neuron* 59(6): 882-901.
- Chaineau, M., L. Danglot and T. Galli (2009). Multiple roles of the vesicular-SNARE TI-VAMP in post-Golgi and endosomal trafficking. *FEBS Letters* 583(23): 3817-3826.
- Chamberland, S., A. Evstratova and K. Tóth (2014). Interplay between Synchronization of Multivesicular Release and Recruitment of Additional Release Sites Support Short-Term Facilitation at Hippocampal Mossy Fiber to CA3 Pyramidal Cells Synapses. *J Neurosci* 34(33): 11032-47.
- Chancey, J. H., D. J. Poulsen, J. I. Wadiche and L. Overstreet-Wadiche (2014). Hilar mossy cells provide the first glutamatergic synapses to adult-born dentate granule cells. *J Neurosci* 34(6): 2349-54.
- Chang, C. Y., X. Jiang, K. L. Moulder and S. Mennerick (2010). Rapid activation of dormant presynaptic terminals by phorbol esters. *The Journal of Neuroscience* 30(30): 10048-10060.
- Chater, Thomas E. and Y. Goda (2013). CA3 Mossy Fiber Connections: Giant Synapses that Gain Control. *Neuron* 77(1): 4-6.
- Cheng, Q. and J. L. Yakel (2014). Presynaptic 7 Nicotinic Acetylcholine Receptors Enhance Hippocampal Mossy Fiber Glutamatergic Transmission via PKA Activation. *Journal of Neuroscience* 34(1): 124-133.
- Cheung, G. and M. A. Cousin (2012). Adaptor Protein Complexes 1 and 3 Are Essential for Generation of Synaptic Vesicles from Activity-Dependent Bulk Endosomes. *Journal of Neuroscience* 32(17): 6014-6023.
- Choi, D., S. Law, G. Raisman and D. Li (2008). Olfactory ensheathing cells in the nasal mucosa of the rat and human. *Br J Neurosurg* 22(2): 301-2.
- Choi, J. and E. M. Callaway (2011). Monosynaptic inputs to ErbB4-expressing inhibitory neurons in mouse primary somatosensory cortex. *J Comp Neurol* 519(17): 3402-14.
- Chua, J. J. E., S. Kindler, J. Boyken and R. Jahn (2010). The architecture of an excitatory synapse. *Journal of Cell Science* 123(6): 819-823.
- Chung, C., B. Barylko, J. Leitz, X. Liu and E. T. Kavalali (2010). Acute Dynamin Inhibition Dissects Synaptic Vesicle Recycling Pathways That Drive Spontaneous and Evoked Neurotransmission. *Journal of Neuroscience* 30(4): 1363-1376.
- Claiborne, B. J., D. G. Amaral and W. M. Cowan (1986). A light and electron microscopic analysis of the mossy fibers of the rat dentate gyrus. *J Comp Neurol* 246(4): 435-58.
- Coco, S., G. Raposo, S. Martinez, J. J. Fontaine, S. Takamori, A. Zahraoui, R. Jahn, M. Matteoli, D. Louvard and T. Galli (1999). Subcellular localization of tetanus neurotoxin-insensitive vesicle-associated membrane protein (VAMP)/VAMP7 in neuronal cells: evidence for a novel membrane compartment. *J Neurosci* 19(22): 9803-12.
- Coen, L., R. Osta, M. Maury and P. Brulet (1997). Construction of hybrid proteins that migrate retrogradely and transynaptically into the central nervous system. *Proc Natl Acad Sci U S A* 94(17): 9400-5.
- Collins, M. O., H. Husi, L. Yu, J. M. Brandon, C. N. Anderson, W. P. Blackstock, J. S. Choudhary and S. G. Grant (2006). Molecular characterization and comparison of the components and multiprotein complexes in the postsynaptic proteome. *J Neurochem* 97 Suppl 1: 16-23.
- Condorelli, D. F., R. Parenti, F. Spinella, A. Trovato Salinaro, N. Belluardo, V. Cardile and F. Cicirata (1998). Cloning of a new gap junction gene (Cx36) highly expressed in mammalian brain neurons. *Eur J Neurosci* 10(3): 1202-8.

- Conturo, T. E., N. F. Lori, T. S. Cull, E. Akbudak, A. Z. Snyder, J. S. Shimony, R. C. McKinstry, H. Burton and M. E. Raichle (1999). Tracking neuronal fiber pathways in the living human brain. *Proc Natl Acad Sci U S A* 96(18): 10422-7.
- Cornelisse, L. N., E. Tsivtsivadze, M. Meijer, T. M. H. Dijkstra, T. Heskes and M. Verhage (2012). Molecular Machines in the Synapse: Overlapping Protein Sets Control Distinct Steps in Neurosecretion. *PLoS Comput Biol* 8(4): e1002450.
- Cowan, W. M. (1998). The emergence of modern neuroanatomy and developmental neurobiology. *Neuron* 20(3): 413-26.
- Cowan, W. M., D. I. Gottlieb, A. E. Hendrickson, J. L. Price and T. A. Woolsey (1972). "The autoradiographic demonstration of axonal connections in the central nervous system." *Brain Res* 37(1): 21-51.
- Dacks, J. B. (2007). Evolution of the SNARE protein superfamily. *SNARE Proteins*.
- Danglot, L. and T. Galli (2007). What is the function of neuronal AP-3? *Biology of the Cell* 99(7): 349-361.
- Danglot, L., K. Zylbersztejn, M. Petkovic, M. Gauberti, H. Meziane, R. Combe, M.-F. Champy, M.-C. Birling, G. Pavlovic, J.-C. Bizot, F. Trovero, F. Della Ragione, V. Proux-Gillardeaux, T. Sorg, D. Vivien, M. D'esposito and T. Galli (2012). Absence of TI-VAMP/Vamp7 Leads to Increased Anxiety in Mice. *Journal of Neuroscience* 32(6): 1962-1968.
- Darios, F., C. Wasser, A. Shakirzyanova, A. Giniatullin, K. Goodman, J. L. Munoz-Bravo, J. Raingo, J. Jorgacevski, M. Kreft, R. Zorec, J. M. Rosa, L. Gandia, L. M. Gutierrez, T. Binz, R. Giniatullin, E. T. Kavalali and B. Davletov (2009). Sphingosine facilitates SNARE complex assembly and activates synaptic vesicle exocytosis. *Neuron* 62(5): 683-94.
- De Jong, A. P. H., S. K. Schmitz, R. F. G. Toonen and M. Verhage (2012). Dendritic position is a major determinant of presynaptic strength. *The Journal of Cell Biology*: 1-14.
- De Oliveira, D. L., A. Fischer, R. S. Jorge, M. C. Da Silva, M. Leite, C. A. Gonçalves, J. A. Quillfeldt, D. O. Souza, T. M. E Souza and S. Wofchuk (2008). Effects of early-life LiCl-Pilocarpine-induced status epilepticus on memory and anxiety in adult rats are associated with mossy fiber sprouting and elevated CSF S100B protein. *Epilepsia* 49(5): 842-852.
- Debanne, D., A. Bialowas and S. Rama (2013). What are the mechanisms for analogue and digital signalling in the brain? *Nat Rev Neurosci* 14(1): 63-69.
- Debanne, D., E. Campanac, A. Bialowas, E. Carlier and G. Alcaraz (2011). Axon physiology. *Physiol Rev* 91(2): 555-602.
- DeFalco, J., M. Tomishima, H. Liu, C. Zhao, X. Cai, J. D. Marth, L. Enquist and J. M. Friedman (2001). Virus-assisted mapping of neural inputs to a feeding center in the hypothalamus. *Science* 291(5513): 2608-13.
- Deguchi, Y., F. Donato, I. Galimberti, E. Cabuy and P. Caroni (2011). "Temporally matched subpopulations of selectively interconnected principal neurons in the hippocampus." *Nature Neuroscience*: 1-11.
- Delvendahl, I., A. Weyhersmüller, A. Ritzau-Jost and S. Hallermann (2013). Hippocampal and cerebellar mossy fibre boutons - same name, different function. *The Journal of Physiology*.
- Deng, W., J. B. Aimone and F. H. Gage (2010). New neurons and new memories: how does adult hippocampal neurogenesis affect learning and memory? *Nat Rev Neurosci* 11(5): 339-350.
- Denker, A. and S. Rizzoli (2010). Synaptic vesicle pools: an update. *Front.Syna.Neurosci.*: 1-12.
- Deshpande, A., M. Bergami, A. Ghanem, K.-K. Conzelmann, A. Lepier, M. Gotz and B. Berninger (2013). Retrograde monosynaptic tracing reveals the temporal

- evolution of inputs onto new neurons in the adult dentate gyrus and olfactory bulb. *Proceedings of the National Academy of Sciences* 110(12): E1152-E1161.
- D'Esposito, M., A. Ciccodicola, F. Gianfrancesco, T. Esposito, L. Flagiello, R. Mazzarella, D. Schlessinger and M. D'Urso (1996). A synaptobrevin-like gene in the Xq28 pseudoautosomal region undergoes X inactivation. *Nat Genet* 13(2): 227-9.
- Dityatev, A., M. Schachner and P. Sonderegger (2010). The dual role of the extracellular matrix in synaptic plasticity and homeostasis. *Nat Rev Neurosci* 11(11): 735-46.
- Dobrunz, L. E. and C. F. Stevens (1999). Response of hippocampal synapses to natural stimulation patterns. *Neuron* 22(1): 157-66.
- Dosemeci, A., A. J. Makusky, E. Jankowska-Stephens, X. Yang, D. J. Slotta and S. P. Markey (2007). Composition of the synaptic PSD-95 complex. *Mol Cell Proteomics* 6(10): 1749-60.
- Douek, P., R. Turner, J. Pekar, N. Patronas and D. Le Bihan (1991). MR color mapping of myelin fiber orientation. *J Comput Assist Tomogr* 15(6): 923-9.
- Drachman, D. A. (2005). Do we have brain to spare?. *Neurology*, 64(12), 2004-2005.
- Dresbach, T., B. Qualmann, M. M. Kessels, C. C. Garner and E. D. Gundelfinger (2001). The presynaptic cytomatrix of brain synapses. *Cell Mol Life Sci* 58(1): 94-116.
- Droz, B. and C. P. Leblond (1962). "Migration of proteins along the axons of the sciatic nerve." *Science* 137(3535): 1047-1048.
- Droz, B. and C. P. Leblond (1963). "Axonal Migration of Proteins in the Central Nervous System and Peripheral Nerves as Shown by Radioautography." *J Comp Neurol* 121: 325-346.
- Dum, R. P. and P. L. Strick (2013). Transneuronal tracing with neurotropic viruses reveals network macroarchitecture. *Curr Opin Neurobiol* 23(2): 245-249.
- Ehlers, M. D., M. Heine, L. Groc, M. C. Lee and D. Choquet (2007). Diffusional trapping of GluR1 AMPA receptors by input-specific synaptic activity. *Neuron* 54(3): 447-60.
- Ekstrand, M. I., L. W. Enquist and L. E. Pomeranz (2008). The alpha-herpesviruses: molecular pathfinders in nervous system circuits. *Trends Mol Med* 14(3): 134-40.
- Emes, R. D., A. J. Pocklington, C. N. Anderson, A. Bayes, M. O. Collins, C. A. Vickers, M. D. Croning, B. R. Malik, J. S. Choudhary, J. D. Armstrong and S. G. Grant (2008). Evolutionary expansion and anatomical specialization of synapse proteome complexity. *Nat Neurosci* 11(7): 799-806.
- Etessami, R., K. K. Conzelmann, B. Fadai-Ghotbi, B. Natelson, H. Tsiang and P. E. Ceccaldi (2000). Spread and pathogenic characteristics of a G-deficient rabies virus recombinant: an in vitro and in vivo study. *J Gen Virol* 81(Pt 9): 2147-53.
- Evstratova, A., S. Chamberland, V. Faundez and K. Tóth (2014). Vesicles derived via AP-3-dependent recycling contribute to asynchronous release and influence information transfer. *Nat Commun* 5.
- Faissner, A., M. Pyka, M. Geissler, T. Sobik, R. Frischknecht, E. D. Gundelfinger and C. Seidenbecher (2010). Contributions of astrocytes to synapse formation and maturation - Potential functions of the perisynaptic extracellular matrix. *Brain Res Rev* 63(1-2): 26-38.
- Fanselow, M. S. and H.-W. Dong (2010). Are the Dorsal and Ventral Hippocampus Functionally Distinct Structures? *Neuron* 65(1): 7-19.
- Fasshauer, D., W. Antonin, V. Subramaniam and R. Jahn (2002). SNARE assembly and disassembly exhibit a pronounced hysteresis. *Nat Struct Biol* 9(2): 144-51.



- Filiou, M. D., B. Bisle, S. Reckow, L. Teplytska, G. Maccarrone and C. W. Turck (2010). Profiling of mouse synaptosome proteome and phosphoproteome by IEF. *Electrophoresis* 31(8): 1294-301.
- Filippini, F., V. Rossi, T. Galli, A. Budillon, M. D'Urso and M. D'esposito (2001). Longins: a new evolutionary conserved VAMP family sharing a novel SNARE domain. *Trends Biochem Sci* 26(7): 407-9.
- Fink, R. P. and L. Heimer (1967). Two methods for selective silver impregnation of degenerating axons and their synaptic endings in the central nervous system. *Brain Res* 4(4): 369-74.
- Fioravante, D. and W. G. Regehr (2011). Short-term forms of presynaptic plasticity. *Curr Opin Neurobiol* 21(2): 269-274.
- Francis, J. W., R. H. Brown, D. Figueiredo, M. P. Remington, O. Castillo, M. A. Schwarzschild, P. S. Fishman, J. R. Murphy and J. C. vanderSpek (2000). Enhancement of diphtheria toxin potency by replacement of the receptor binding domain with tetanus toxin C-fragment: a potential vector for delivering heterologous proteins to neurons. *Journal of neurochemistry* 74(6): 2528-36.
- Fredj, N. B. and J. Burrone (2009). A resting pool of vesicles is responsible for spontaneous vesicle fusion at the synapse. *Nature Neuroscience* 12(6): 751-758.
- Galimberti, I., E. Bednarek, F. Donato and P. Caroni (2010). EphA4 Signaling in Juveniles Establishes Topographic Specificity of Structural Plasticity in the Hippocampus. *Neuron* 65(5): 627-642.
- Galli, T., A. Zahraoui, v. v. vaidyanathan, G. Raposo, j. m. tian, m. karin, h. niemann and D. Louvard (1998). A novel tetanus neurotoxin-insensitive vesicle-associated membrane protein in SNARE complexes of the apical plasma membrane of epithelial cells. *Mol Biol Cell*.
- Garcia, E. P., E. Gatti, M. Butler, J. Burton and P. De Camilli (1994). A rat brain Sec1 homologue related to Rop and UNC18 interacts with syntaxin. *Proc Natl Acad Sci U S A* 91(6): 2003-7.
- Garcia, I., C. Kim and B. R. Arenkiel (2013). *Current Protocols in Stem Cell Biology*. 1-25.
- Garcia, I., L. Huang, K. Ung and B. R. Arenkiel (2012). Tracing synaptic connectivity onto embryonic stem cell-derived neurons. *Stem Cells* 30(10): 2140-51.
- Garner, C. C., S. Kindler and E. D. Gundelfinger (2000). Molecular determinants of presynaptic active zones. *Curr Opin Neurobiol* 10(3): 321-7.
- Genc, O., O. Kochubey, R. F. Toonen, M. Verhage and R. Schneggenburger (2014). Munc18-1 is a dynamically regulated PKC target during short-term enhancement of transmitter release. *Elife* 3: e01715.
- Gerber, S. H., J.-C. Rah, S.-W. Min, X. Liu, H. De Wit, I. Dulubova, A. C. Meyer, J. Rizo, M. Arancillo, R. E. Hammer, M. Verhage, C. Rosenmund and T. C. Sudhof (2008). Conformational Switch of Syntaxin-1 Controls Synaptic Vesicle Fusion. *Science* 321(5895): 1507-1510.
- Ginger, M., M. Haberl, K.-K. Conzelmann, M. K. Schwarz and A. Frick (2013). Revealing the secrets of neuronal circuits with recombinant rabies virus technology. *Front. Neural Circuits* 7: 1-15.
- Giordano, F., Y. Saheki, O. Idevall-Hagren, S. F. Colombo, M. Pirruccello, I. Milosevic, Elena O. Gracheva, Sviatoslav N. Bagriantsev, N. Borgese and P. De Camilli (2013). PI(4,5)P2-Dependent and Ca<sup>2+</sup>-Regulated ER-PM Interactions Mediated by the Extended Synaptotagmins. *Cell* 153(7): 1494-1509.

- Glover, J. C., G. Petursdottir and J. K. Jansen (1986). Fluorescent dextran-amines used as axonal tracers in the nervous system of the chicken embryo. *J Neurosci Methods* 18(3): 243-54.
- Gomme, E. A., C. N. Wanjalla, C. Wirblich and M. J. Schnell (2011). Rabies virus as a research tool and viral vaccine vector. *Adv Virus Res* 79: 139-64.
- Gonatas, N. K., C. Harper, T. Mizutani and J. O. Gonatas (1979). Superior sensitivity of conjugates of horseradish peroxidase with wheat germ agglutinin for studies of retrograde axonal transport. *J Histochem Cytochem* 27(3): 728-34.
- Gordon, D. E., L. M. Bond, D. A. Sahlender and A. A. Peden (2010). A Targeted siRNA Screen to Identify SNAREs Required for Constitutive Secretion in Mammalian Cells. *Traffic* 11(9): 1191-1204.
- Goswami, S. P., I. Bucurenciu and P. Jonas (2012). Miniature IPSCs in Hippocampal Granule Cells Are Triggered by Voltage-Gated Ca<sup>2+</sup> Channels via Microdomain Coupling. *Journal of Neuroscience* 32(41): 14294-14304.
- Goyal, R. K. and A. Chaudhury (2013). Structure activity relationship of synaptic and junctional neurotransmission. *Auton Neurosci* 176(1-2): 11-31.
- Grimpe, B. and J. Silver (2002). The extracellular matrix in axon regeneration. *Prog Brain Res* 137: 333-49.
- Gundlfinger, A., J. Breustedt, D. Sullivan and D. Schmitz (2010). Natural Spike Trains Trigger Short- and Long-Lasting Dynamics at Hippocampal Mossy Fiber Synapses in Rodents. *PLoS ONE* 5(4): e9961.
- Gupton, S. L. and F. B. Gertler (2010). Integrin Signaling Switches the Cytoskeletal and Exocytic Machinery that Drives Neuritogenesis. *Developmental Cell* 18(5): 725-736.
- Haberl, M. G., S. Viana Da Silva, J. M. Guest, M. Ginger, A. Ghanem, C. Mulle, M. Oberlaender, K.-K. Conzelmann and A. Frick (2014). An anterograde rabies virus vector for high-resolution large-scale reconstruction of 3D neuron morphology. *Brain Struct Funct*: 1-11.
- Habermann, E., W. Dimpfel and K. O. Raker (1973). Interaction of labelled tetanus toxin with substructures of rat spinal cord in vivo. *Naunyn Schmiedeberg's Arch Pharmacol* 276(3-4): 361-73.
- Hagena, H. and D. Manahan-Vaughan (2010). Frequency Facilitation at Mossy Fiber-CA3 Synapses of Freely Behaving Rats Contributes to the Induction of Persistent LTD via an Adenosine-A1 Receptor-Regulated Mechanism. *Cerebral Cortex* 20(5): 1121.
- Hagmann, P. (2005). From diffusion MRI to brain connectomics.
- Harms, K. J. and A. M. Craig (2005). Synapse composition and organization following chronic activity blockade in cultured hippocampal neurons. *J Comp Neurol* 490(1): 72-84.
- Harris, E. W. and C. W. Cotman (1986). "Long-term potentiation of guinea pig mossy fiber responses is not blocked by N-methyl D-aspartate antagonists." *Neurosci Lett* 70(1): 132-137.
- Harris, K. M. and R. J. Weinberg (2012). Ultrastructure of synapses in the mammalian brain. *Cold Spring Harbor perspectives in biology* 4(5).
- Harris, R. M. and H. A. Hofmann (2014). Neurogenomics of behavioral plasticity. *Adv Exp Med Biol* 781: 149-68.
- Hebb, D. O. (1949). *The organization of behavior: Aneuropsychological theory*, Wiley.
- Heimer-McGinn, V., A. C. H. Murphy, J. C. Kim, S. M. Dymecki and P. W. Young (2013). Decreased dendritic spine density as a consequence of tetanus toxin light chain expression in single neurons in vivo. *Neuroscience letters* 555: 36-41.

- Hemachudha, T., G. Ugolini, S. Wacharapluesadee, W. Sungkarat, S. Shuangshoti and J. Laothamatas (2013). Human rabies: neuropathogenesis, diagnosis, and management. *Lancet Neurol* 12(5): 498-513.
- Hendrickson, A. (1982). "The orthograde axoplasmic transport autoradiographic tracing technique and its implications for additional neuroanatomical analysis of the striate cortex." *Cytochemical Methods in Neuroanatomy*, Alan R. Liss, New York: 1-16.
- Hendry, S. H., H. D. Schwark, E. G. Jones and J. Yan (1987). Numbers and proportions of GABA-immunoreactive neurons in different areas of monkey cerebral cortex. *J Neurosci* 7(5): 1503-19.
- Henze, D. A., D. B. T. McMahon, K. M. Harris and G. Barrionuevo (2002). Giant miniature EPSCs at the hippocampal mossy fiber to CA3 pyramidal cell synapse are monoquantal. *Journal of Neurophysiology* 87(1): 15-29.
- Hirokawa, N., K. Sobue, K. Kanda, A. Harada and H. Yorifuji (1989). The cytoskeletal architecture of the presynaptic terminal and molecular structure of synapsin 1. *J Cell Biol* 108(1): 111-26.
- Hnasko, T. S. and R. H. Edwards (2012). Neurotransmitter corelease: mechanism and physiological role. *Annu Rev Physiol* 74: 225-43.
- Honda, I., H. Kamiya and H. Yawo (2000). Re-evaluation of phorbol ester-induced potentiation of transmitter release from mossy fibre terminals of the mouse hippocampus. *The Journal of Physiology* 529 Pt 3: 763-76.
- Horowitz, L. F., J. P. Montmayeur, Y. Echelard and L. B. Buck (1999). A genetic approach to trace neural circuits. *Proc Natl Acad Sci U S A* 96(6): 3194-9.
- Hua, S.-Y., D. A. Raciborska, W. S. Trimble and M. P. Charlton (1998). "Different VAMP/synaptobrevin complexes for spontaneous and evoked transmitter release at the crayfish neuromuscular junction." *J Neurophysiol*.
- Hua, Z., S. Leal-Ortiz, Sarah M. Foss, Clarissa L. Waites, Craig C. Garner, Susan M. Voglmaier and Robert H. Edwards (2011). v-SNARE Composition Distinguishes Synaptic Vesicle Pools. *Neuron* 71(3): 474-487.
- Huh, Y., M. S. Oh, P. Leblanc and K.-S. Kim (2010). Gene transfer in the nervous system and implications for transsynaptic neuronal tracing. *Expert Opin Biol Ther* 10(5): 763-72.
- Jahn, R. and D. Fasshauer (2012). Molecular machines governing exocytosis of synaptic vesicles. *Nature* 490(7419): 201-207.
- Jahn, R. and R. H. Scheller (2006). SNAREs — engines for membrane fusion. *Nat Rev Mol Cell Biol* 7(9): 631-643.
- Jung, M. W. and B. L. McNaughton (1993). Spatial selectivity of unit activity in the hippocampal granular layer. *Hippocampus* 3(2): 165-82.
- Kaesler, P. S. and W. G. Regehr (2014). Molecular mechanisms for synchronous, asynchronous, and spontaneous neurotransmitter release. *Annu. Rev. Physiol*. 76: 333-63.
- Kasai, H., N. Takahashi and H. Tokumaru (2012). Distinct Initial SNARE Configurations Underlying the Diversity of Exocytosis. *Physiol Rev* 92(4): 1915-1964.
- Kawashima, T., K. Kitamura, K. Suzuki, M. Nonaka, S. Kamijo, S. Takemoto-Kimura, M. Kano, H. Okuno, K. Ohki and H. Bito (2013). Functional labeling of neurons and their projections using the synthetic activity&ndash;dependent promoter E-SARE. *Nat Meth*: 1-11.
- Kelly, R. M. and P. L. Strick (2000). Rabies as a transneuronal tracer of circuits in the central nervous system. *J Neurosci Methods* 103(1): 63-71.
- Kohara, K., M. Pignatelli, A. J. Rivest, H.-Y. Jung, T. Kitamura, J. Suh, D. Frank, K. Kajikawa, N. Mise, Y. Obata, I. R. Wickersham and S. Tonegawa (2013). Cell

- type-specific genetic and optogenetic tools reveal hippocampal CA2 circuits. *Nature Neuroscience*: 1-15.
- Kress, G. J., M. J. Dowling, J. P. Meeks and S. Mennerick (2008). High threshold, proximal initiation, and slow conduction velocity of action potentials in dentate granule neuron mossy fibers. *J Neurophysiol* 100(1): 281-91.
- Kretzschmar, E., R. Peluso, M. J. Schnell, M. A. Whitt and J. K. Rose (1996). "Normal replication of vesicular stomatitis virus without C proteins." *Virology* 216(2): 309-316.
- Kristensson, K. and Y. Olsson (1971). Uptake of exogenous proteins in mouse olfactory cells. *Acta Neuropathol* 19(2): 145-54.
- Kristensson, K., B. Ghetti and H. M. Wisniewski (1974). Study on the propagation of Herpes simplex virus (type 2) into the brain after intraocular injection. *Brain Res* 69(2): 189-201.
- Kristensson, K., Y. Olsson and J. Sjostrand (1971). Axonal uptake and retrograde transport of exogenous proteins in the hypoglossal nerve. *Brain Res* 32(2): 399-406.
- Kuypers, H. G. and G. Ugoletti (1990). Viruses as transneuronal tracers. *Trends in Neurosciences* 13(2): 71-5.
- Kwok, J. C., G. Dick, D. Wang and J. W. Fawcett (2011). Extracellular matrix and perineuronal nets in CNS repair. *Dev Neurobiol* 71(11): 1073-89.
- Laatsch, R. H. and W. M. Cowan (1966). Electron microscopic studies of the dentate gyrus of the rat. I. Normal structure with special reference to synaptic organization. *J Comp Neurol* 128(3): 359-95.
- Lanciego, J. L. and F. G. Wouterlood (2011). A half century of experimental neuroanatomical tracing. *Journal of Chemical Neuroanatomy* 42(3): 157-183.
- Lanore, F., N. Rebola and M. Carta (2009). Spike-Timing-Dependent Plasticity Induces Presynaptic Changes at Immature Hippocampal Mossy Fiber Synapses. *Journal of Neuroscience* 29(26): 8299-8301.
- LaVail, J. H. and M. M. LaVail (1972). Retrograde axonal transport in the central nervous system. *Science* 176(4042): 1416-7.
- Lavoie, N., D. V. Jeyaraju, M. R. Peralta, L. Seress, L. Pellegrini and K. Toth (2011). Vesicular Zinc Regulates the Ca<sup>2+</sup> Sensitivity of a Subpopulation of Presynaptic Vesicles at Hippocampal Mossy Fiber Terminals. *Journal of Neuroscience* 31(50): 18251-18265.
- Lawrence, J. J. and C. J. McBain (2003). Interneuron diversity series: containing the detonation-feedforward inhibition in the CA3 hippocampus. *Trends in Neurosciences* 26(11): 631-640.
- Le Duigou, C., J. Simonnet, M. T. Teleńczuk, D. Fricker and R. Miles (2014). Recurrent synapses and circuits in the CA3 region of the hippocampus: an associative network. *Front. Cell. Neurosci.* 7: 1-13.
- Lee, Kea J., Bridget N. Queenan, Aaron M. Rozeboom, R. Bellmore, Seung T. Lim, S. Vicini and Daniel T. S. Pak (2013). Mossy Fiber-CA3 Synapses Mediate Homeostatic Plasticity in Mature Hippocampal Neurons. *Neuron* 77(1): 99-114.
- Lichtman, J. W. and W. Denk (2011). The big and the small: challenges of imaging the brain's circuits. *Science* 334(6056): 618-23.
- Liu, Y.-J., Markus U. Ehrenguber, M. Negwer, H.-J. Shao, Ali H. Cetin and David C. Lyon (2013). Tracing Inputs to Inhibitory or Excitatory Neurons of Mouse and Cat Visual Cortex with a Targeted Rabies Virus. *Current Biology* 23(18): 1746-1755.
- Loewy, A. D. (1998). Viruses as transneuronal tracers for defining neural circuits. *Neurosci Biobehav Rev* 22(6): 679-84.

- Loy, K., O. Welzel, J. Kornhuber and T. W. Groemer (2014). Common strength and localization of spontaneous and evoked synaptic vesicle release sites. *Mol Brain* 7(1): 1-6.
- Lundh, B. (1990). Spread of vesicular stomatitis virus along the visual pathways after retinal infection in the mouse. *Acta Neuropathol* 79(4): 395-401.
- Luo, L., E. M. Callaway and K. Svoboda (2008). Genetic dissection of neural circuits. *Neuron* 57(5): 634-60.
- Maguire, E. A., D. G. Gadian, I. S. Johnsrude, C. D. Good, J. Ashburner, R. S. Frackowiak and C. D. Frith (2000). Navigation-related structural change in the hippocampi of taxi drivers. *Proc Natl Acad Sci U S A* 97(8): 4398-403.
- Marchi, V. and G. Algeri (1885). Sulle degenerazioni discendenti consecutive a lesioni sperimentale in diverse zone della corteccia cerebrale. *Riv. Sper. Freniatr. Med. Leg. Alienazioni Ment* 11: 492-494.
- Marshall, J. H., T. Mori, K. J. Nielsen and E. M. Callaway (2010). Targeting Single Neuronal Networks for Gene Expression and Cell Labeling In Vivo. *Neuron* 67(4): 562-574.
- Martinez-Arca, S., P. Alberts, A. Zahraoui, D. Louvard and T. Galli (2000). Role of tetanus neurotoxin insensitive vesicle-associated membrane protein (TI-VAMP) in vesicular transport mediating neurite outgrowth. *The Journal of Cell Biology* 149(4): 889-900.
- Martinez-Arca, S., R. Rudge, M. Vacca, G. Raposo, J. Camonis, V. Proux-Gillardeaux, L. Daviet, E. Formstecher, A. Hamburger, F. Filippini, M. D'Esposito and T. Galli (2003). A dual mechanism controlling the localization and function of exocytic v-SNAREs. *Proc Natl Acad Sci USA* 100(15): 9011-6.
- Martinez-Arca, S., S. Coco, G. Mainguy, U. Schenk, P. Alberts, P. Bouillé, M. Mezzina, A. Prochiantz, M. Matteoli, D. Louvard and T. Galli (2001). A common exocytotic mechanism mediates axonal and dendritic outgrowth. *J Neurosci* 21(11): 3830-8.
- Mcbain, C. J. and J. A. Kauer (2009). Presynaptic plasticity: targeted control of inhibitory networks. *Curr Opin Neurobiol* 19(3): 254-262.
- Melom, J. E., Y. Akbergenova, J. P. Gavornik and J. T. Littleton (2013). Spontaneous and Evoked Release Are Independently Regulated at Individual Active Zones. *Journal of Neuroscience* 33(44): 17253-17263.
- Meredith, J. E., Jr., B. Fazeli and M. A. Schwartz (1993). The extracellular matrix as a cell survival factor. *Mol Biol Cell* 4(9): 953-61.
- Miles, R. and R. K. Wong (1986). Excitatory synaptic interactions between CA3 neurones in the guinea-pig hippocampus. *The Journal of Physiology* 373: 397-418.
- Miyamichi, K., Y. Shlomai-Fuchs, M. Shu, Brandon C. Weissbourd, L. Luo and A. Mizrahi (2013). Dissecting Local Circuits: Parvalbumin Interneurons Underlie Broad Feedback Control of Olfactory Bulb Output. *Neuron* 80(5): 1232-1245.
- Mocarski, E. S., L. E. Post and B. Roizman (1980). Molecular engineering of the herpes simplex virus genome: insertion of a second L-S junction into the genome causes additional genome inversions. *Cell* 22(1 Pt 1): 243-55.
- Mochida, S., A. P. Few, T. Scheuer and W. A. Catterall (2008). Regulation of presynaptic Ca<sub>v</sub>2.1 channels by Ca<sup>2+</sup> sensor proteins mediates short-term synaptic plasticity. *Neuron* 57(2): 210-6.
- Monaghan, D. T., V. R. Holets, D. W. Toy and C. W. Cotman (1983). Anatomical distributions of four pharmacologically distinct 3H-L-glutamate binding sites. *Nature* 306(5939): 176-9.

- Mori, M., M. H. Abegg, B. H. Gähwiler and U. Gerber (2004). A frequency-dependent switch from inhibition to excitation in a hippocampal unitary circuit. *Nature* 431(7007): 453-6.
- Mori, M., Gähwiler, B. H., & Gerber, U. (2007). Recruitment of an inhibitory hippocampal network after bursting in a single granule cell. *Proceedings of the National Academy of Sciences*, 104(18), 7640-7645.
- Moseley, M. E., J. Kucharczyk, J. Mintorovitch, Y. Cohen, J. Kurhanewicz, N. Derugin, H. Asgari and D. Norman (1990). Diffusion-weighted MR imaging of acute stroke: correlation with T2-weighted and magnetic susceptibility-enhanced MR imaging in cats. *AJNR Am J Neuroradiol* 11(3): 423-9.
- Moser, M. B. and E. I. Moser (1998). Functional differentiation in the hippocampus. *Hippocampus* 8(6): 608-19.
- Mouton, P. R., Price, D. L., & Walker, L. C. (1997). Empirical assessment of synapse numbers in primate neocortex. *Journal of neuroscience methods*, 75(2), 119-126.
- Muthusamy, N., V. Faundez and C. Bergson (2012). Calcyon, a mammalian specific NEEP21 family member, interacts with adaptor protein complex 3 (AP-3) and regulates targeting of AP-3 cargoes. *Journal of neurochemistry* 123(1): 60-72.
- Muzerelle, A., P. Alberts, S. Martinez-Arca, O. Jeannequin, P. Lafaye, J.-C. Mazié, T. Galli and P. Gaspar (2003). Tetanus neurotoxin-insensitive vesicle-associated membrane protein localizes to a presynaptic membrane compartment in selected terminal subsets of the rat brain. *Neuroscience* 122(1): 59-75.
- Nadim, F. and D. Bucher (2014). Neuromodulation of neurons and synapses. *Curr Opin Neurobiol* 29C: 48-56.
- Nakashiba, T., Jesse D. Cushman, Kenneth A. Pelkey, S. Renaudineau, Derek L. Buhl, Thomas J. Mchugh, Vanessa R. Barrera, R. Chittajallu, Keisuke S. Iwamoto, Chris J. Mcbain, Michael S. Fanselow and S. Tonegawa (2012). Young Dentate Granule Cells Mediate Pattern Separation, whereas Old Granule Cells Facilitate Pattern Completion. *Cell* 149(1): 188-201.
- Nauta, W. J. (1952). Selective silver impregnation of degenerating axons in the central nervous system. *Stain Technol* 27(3): 175-9.
- Newell-Litwa, K., S. Chintala, S. Jenkins, J.-F. Pare, L. McGaha, Y. Smith and V. Faundez (2010). Hermansky-Pudlak Protein Complexes, AP-3 and BLOC-1, Differentially Regulate Presynaptic Composition in the Striatum and Hippocampus. *Journal of Neuroscience* 30(3): 820-831.
- Nguyen, T. D., C. Wirblich, E. Aizenman, M. J. Schnell, P. L. Strick and K. Kandler (2012). Targeted single-neuron infection with rabies virus for transneuronal multisynaptic tracing. *J Neurosci Methods* 209(2): 367-370.
- Nicholls, D. G. (1989). Release of glutamate, aspartate, and gamma-aminobutyric acid from isolated nerve terminals. *J Neurochem* 52(2): 331-41.
- Nicoll, R. A. and D. Schmitz (2005). Synaptic plasticity at hippocampal mossy fibre synapses. *Nat Rev Neurosci* 6(11): 863-876.
- Oh, M. S., S. J. Hong, Y. Huh and K.-S. Kim (2009). Expression of transgenes in midbrain dopamine neurons using the tyrosine hydroxylase promoter. *Gene Ther* 16(3): 437-440.
- Ohara, S., Inoue, Ken-Ichi, Yamada, Masahiro, Yamawaki, Takuma, Koganezawa, Noriko, Tsutsui, Ken-Ichiro, Witter, Menno P, Iijima, Toshio (2009). Dual transneuronal tracing in the rat entorhinal-hippocampal circuit by intracerebral injection of recombinant rabies virus vectors. *Front. Neuroanat.* 3: 1-11.
- Ohara, S., S. Sato, K. Tsutsui, M. P. Witter and T. Iijima (2013). Organization of multisynaptic inputs to the dorsal and ventral dentate gyrus: retrograde trans-synaptic tracing with rabies virus vector in the rat. *PLoS One* 8(11): e78928.

- O'Keefe, J. and J. Dostrovsky (1971). The hippocampus as a spatial map. Preliminary evidence from unit activity in the freely-moving rat. *Brain Res* 34(1): 171-5.
- O'Rourke, N. A., N. C. Weiler, K. D. Micheva and S. J. Smith (2012). Deep molecular diversity of mammalian synapses: why it matters and how to measure it. *Nat Rev Neurosci*: 1-15.
- Osakada, F., T. Mori, Ali H. Cetin, James H. Marshel, B. Virgen and Edward M. Callaway (2011). New Rabies Virus Variants for Monitoring and Manipulating Activity and Gene Expression in Defined Neural Circuits. *Neuron* 71(4): 617-631.
- Pan, B. and R. S. Zucker (2009). A General Model of Synaptic Transmission and Short-Term Plasticity. *Neuron* 62(4): 539-554.
- Pang, Z. P. and T. C. Südhof (2010). Cell biology of Ca<sup>2+</sup>-triggered exocytosis. *Current Opinion in Cell Biology* 22(4): 496-505.
- Paoletti, P., A. M. Vergnano, B. Barbour and M. Casado (2009). Zinc at glutamatergic synapses. *NSC* 158(1): 126-136.
- Pellett, S., W. H. Tepp, L. H. Stanker, P. A. Band, E. A. Johnson and K. Ichtchenko (2011). Neuronal targeting, internalization, and biological activity of a recombinant atoxic derivative of botulinum neurotoxin A. *Biochem Biophys Res Commun* 405(4): 673-7.
- Peng, J., M. J. Kim, D. Cheng, D. M. Duong, S. P. Gygi and M. Sheng (2004). Semiquantitative proteomic analysis of rat forebrain postsynaptic density fractions by mass spectrometry. *J Biol Chem* 279(20): 21003-11.
- Pereda, A. E. (2014). Electrical synapses and their functional interactions with chemical synapses. *Nature Publishing Group* 15(4): 250-263.
- Peters, A., S. L. Palay and H. d. Webster (1991). The fine structure of the nervous system: neurons and their supporting cells, Oxford University Press New York.
- Pieribone, V. A., O. Shupliakov, L. Brodin, S. Hilfiker-Rothenfluh, A. J. Czernik and P. Greengard (1995). Distinct pools of synaptic vesicles in neurotransmitter release. *Nature* 375(6531): 493-7.
- Pitman, R. M., C. D. Tweedle and M. J. Cohen (1972). Branching of central neurons: intracellular cobalt injection for light and electron microscopy. *Science* 176(4033): 412-4.
- Pollock, J. D., D. Y. Wu and J. S. Satterlee (2014). Molecular neuroanatomy: a generation of progress. *Trends Neurosci* 37(2): 106-23.
- Popoff, M. R. and B. Poulain (2010). "Bacterial toxins and the nervous system: Neurotoxins and multipotential toxins interacting with neuronal cells." *Toxins* 2(4): 683-737.
- Poppenk, J., H. R. Evensmoen, M. Moscovitch and L. Nadel (2013). Long-axis specialization of the human hippocampus. *Trends Cogn Sci* 17(5): 230-40.
- Prashad, R. c. and M. p. Charlton (2014). "SNARE Zippering and Synaptic Strength." *PLoS ONE*.
- Purves, D., G. J. Augustine, D. Fitzpatrick, W. C. Hall, A.-S. LaMantia, J. O. McNamara and L. E. White (2001). *Neuroscience*. Sunderland, MA: Sinauer Associates 3.
- Pyka, M., S. Klatt and S. Cheng (2014). Parametric Anatomical Modeling: a method for modeling the anatomical layout of neurons and their projections. *Front. Neuroanat.* 8: 1-18.
- Ramakrishnan, N. A., M. J. Drescher and D. G. Drescher (2012). The SNARE complex in neuronal and sensory cells. *Molecular and Cellular Neuroscience* 50(1): 58-69.

- Ramirez, D. M. O. and E. Kavalali (2012). The role of non-canonical SNAREs in synaptic vesicle recycling. *Cellular Logistics* 2(1): 20-27.
- Ramón y Cajal, S. (1894). The Croonian Lecture: La fine structure des centres nerveux.
- Ramón y Cajal, S. (1906). Structure et connexions des neurones. *REV ESP PATOL* 35(4): 433-452.
- Ramón y Cajal, S. (1911). *Histologie du Système Nerveux de l'Homme et des Vertébrés*. Tome II.
- Ramón y Cajal, S. (1933). Neuronismo o reticularismo? *Archivos des Neurobiologia* 13.
- Rancz, E. A., K. M. Franks, M. K. Schwarz, B. Pichler, A. T. Schaefer and T. W. Margrie (2011). Transfection via whole-cell recording in vivo: bridging single-cell physiology, genetics and connectomics. *Nature Neuroscience*: 1-7.
- Rathenberg, J., T. Nevian and V. Witzemann (2003). High-efficiency transfection of individual neurons using modified electrophysiology techniques. *J Neurosci Methods* 126(1): 91-8.
- Rebola, N., M. Carta, F. Lanore, C. Blanchet and C. Mulle (2011). NMDA receptor-dependent metaplasticity at hippocampal mossy fiber synapses. *Nature Neuroscience*: 1-3.
- Rebola, N., S. Sachidhanandam, D. Perrais, R. A. Cunha and C. Mulle (2007). Short-term plasticity of kainate receptor-mediated EPSCs induced by NMDA receptors at hippocampal mossy fiber synapses. *J Neurosci* 27(15): 3987-93.
- Reiner, A., C. L. Veenman, L. Medina, Y. Jiao, N. Del Mar and M. G. Honig (2000). Pathway tracing using biotinylated dextran amines. *J Neurosci Methods* 103(1): 23-37.
- Roberts, E. (1986). What do GABA neurons really do? They make possible variability generation in relation to demand. *Exp Neurol* 93(2): 279-90.
- Roberts, E. and S. Frankel (1950). gamma-Aminobutyric acid in brain: its formation from glutamic acid. *J Biol Chem* 187(1): 55-63.
- Rollenhagen, A. and J. H. R. Lübke (2006). The morphology of excitatory central synapses: from structure to function. *Cell Tissue Res* 326(2): 221-237.
- Rollenhagen, A., K. Satzler, E. P. Rodriguez, P. Jonas, M. Frotscher and J. H. R. Lübke (2007). Structural Determinants of Transmission at Large Hippocampal Mossy Fiber Synapses. *Journal of Neuroscience* 27(39): 10434-10444.
- Rolls, E. T. (2013). A quantitative theory of the functions of the hippocampal CA3 network in memory. *Front. Cell. Neurosci.* 7: 1-24.
- Ropireddy, D. and G. A. Ascoli (2011). Potential Synaptic Connectivity of Different Neurons onto Pyramidal Cells in a 3D Reconstruction of the Rat Hippocampus. *Front. Neuroinform.* 5: 1-13.
- Rossi, V., D. K. Banfield, M. Vacca, L. E. P. Dietrich, C. Ungermann, M. D'Esposito, T. Galli and F. Filippini (2004). Longins and their longin domains: regulated SNAREs and multifunctional SNARE regulators. *Trends Biochem Sci* 29(12): 682-8.
- Rowland, D. C., A. P. Weible, I. R. Wickersham, H. Wu, M. Mayford, M. P. Witter and C. G. Kentros (2013). Transgenically Targeted Rabies Virus Demonstrates a Major Monosynaptic Projection from Hippocampal Area CA2 to Medial Entorhinal Layer II Neurons. *Journal of Neuroscience* 33(37): 14889-14898.
- Rusakov, D. A. (2006). Ca<sup>2+</sup>-dependent mechanisms of presynaptic control at central synapses. *Neuroscientist* 12(4): 317-26.
- Sachidhanandam, S., C. Blanchet, Y. Jeantet, Y. H. Cho and C. Mulle (2009). Kainate receptors act as conditional amplifiers of spike transmission at hippocampal mossy fiber synapses. *J Neurosci* 29(15): 5000-8.



- Sakaba, T., A. Stein, R. Jahn and E. Neher (2005). Distinct Kinetic Changes in Neurotransmitter Release After SNARE Protein Cleavage. *Science* 309(5733): 491-494.
- Salazar, G., B. Craige, B. H. Wainer, J. Guo, P. De Camilli and V. Faundez (2005). Phosphatidylinositol-4-kinase type II alpha is a component of adaptor protein-3-derived vesicles. *Mol Biol Cell* 16(8): 3692-704.
- Salazar, G., R. Love, E. Werner, M. M. Doucette, S. Cheng, A. Levey and V. Faundez (2004). The zinc transporter ZnT3 interacts with AP-3 and it is preferentially targeted to a distinct synaptic vesicle subpopulation. *Mol Biol Cell* 15(2): 575-87.
- Salin, P. A., M. Scanziani, R. C. Malenka and R. A. Nicoll (1996). Distinct short-term plasticity at two excitatory synapses in the hippocampus. *Proc Natl Acad Sci USA* 93(23): 13304-9.
- Sasaki, T., G. Minamisawa, N. Takahashi, N. Matsuki and Y. Ikegaya (2009). Reverse Optical Trawling for Synaptic Connections In Situ. *Journal of Neurophysiology* 102(1): 636-643.
- Sato, M., S. Yoshimura, R. Hirai, A. Goto, M. Kunii, N. Atik, T. Sato, K. Sato, R. Harada, J. Shimada, T. Hatabu, H. Yorifuji and A. Harada (2011). The Role of VAMP7/TI-VAMP in Cell Polarity and Lysosomal Exocytosis in vivo. *Traffic* 12(10): 1383-1393.
- Scharfman, H. E. (2007). The CA3 "backprojection" to the dentate gyrus. *Prog Brain Res* 163: 627-37.
- Scharfman, H. E. (2013). Hilar mossy cells of the dentate gyrus: a historical perspective. 1-17.
- Scheuber, A., R. Rudge, L. Danglot, G. Raposo, T. Binz, J. C. Poncer and T. Galli (2006). Loss of AP-3 function affects spontaneous and evoked release at hippocampal mossy fiber synapses. *Proceedings of the National Academy of Sciences* 103(44): 16562.
- Schmidt-Hieber, C., P. Jonas and J. Bischofberger (2008). Action potential initiation and propagation in hippocampal mossy fibre axons. *The Journal of Physiology* 586(7): 1849-1857.
- Schmitz, D., J. Breustedt and A. Gundlfinger (2014). Retrograde Signaling Causes Excitement. *Neuron* 81(4): 717-719.
- Schnell, M. J., J. P. Mcgettigan, C. Wirblich and A. Papaneri (2009). The cell biology of rabies virus: using stealth to reach the brain. *Nat Rev Micro*: 1-11.
- Schoch, S., F. Deák, A. Königstorfer, M. Mozhayeva, Y. Sara, T. C. Südhof and E. T. Kavalali (2001). SNARE function analyzed in synaptobrevin/VAMP knockout mice. *Science* 294(5544): 1117-22.
- Schrimpf, S. P., V. Meskenaite, E. Brunner, D. Rutishauser, P. Walther, J. Eng, R. Aebersold and P. Sonderegger (2005). Proteomic analysis of synaptosomes using isotope-coded affinity tags and mass spectrometry. *Proteomics* 5(10): 2531-41.
- Schwab, M. E. and H. Thoenen (1976). Electron microscopic evidence for a transsynaptic migration of tetanus toxin in spinal cord motoneurons: an autoradiographic and morphometric study. *Brain Res* 105(2): 213-27.
- Schwab, M. E. and I. Agid (1979). Labelled wheat germ agglutinin and tetanus toxin as highly sensitive retrograde tracers in the CNS: the afferent fiber connections of the rat nucleus caudatus. *Int J Neurol* 13(1-4): 117-26.
- Schwab, M. E., F. Javoy-Agid and Y. Agid (1978). Labeled wheat germ agglutinin (WGA) as a new, highly sensitive retrograde tracer in the rat brain hippocampal system. *Brain Res* 152(1): 145-50.

- Schwenk, J., D. Baehrens, A. Haupt, W. Bildl, S. Boudkkazi, J. Roeper, B. Fakler and U. Schulte (2014). Regional diversity and developmental dynamics of the AMPA-receptor proteome in the mammalian brain. *Neuron* 84(1): 41-54.
- Scoville, W.B. & Milner, B. (1957). Loss of recent memory after bilateral hippocampal lesions. *Journal of Neurology, Neurosurgery & Psychiatry*, 20, 11–21.
- Sharma, G. and S. Vijayaraghavan (2003). Modulation of presynaptic store calcium induces release of glutamate and postsynaptic firing. *Neuron* 38(6): 929-39.
- Sinha, R., S. Ahmed, R. Jahn and J. Klingauf (2011). Two synaptobrevin molecules are sufficient for vesicle fusion in central nervous system synapses. *Proceedings of the National Academy of Sciences* 108(34): 14318-14323.
- Skaggs, W. E., B. L. McNaughton, M. A. Wilson and C. A. Barnes (1996). Theta phase precession in hippocampal neuronal populations and the compression of temporal sequences. *Hippocampus* 6(2): 149-72.
- Soleman, S., M. A. Filippov, A. Dityatev and J. W. Fawcett (2013). Targeting the neural extracellular matrix in neurological disorders. *Neuroscience* 253: 194-213.
- Söllner, T., S. W. Whiteheart, M. Brunner, H. Erdjument-Bromage, S. Geromanos, P. Tempst and J. E. Rothman (1993). SNAP receptors implicated in vesicle targeting and fusion. *Nature* 362(6418): 318-24.
- Soudais, C., N. Skander and E. J. Kremer (2004). Long-term in vivo transduction of neurons throughout the rat CNS using novel helper-dependent CAV-2 vectors. *The FASEB journal* 18(2): 391-393.
- Soudais, C., S. Boutin and E. J. Kremer (2001). Characterization of cis-acting sequences involved in canine adenovirus packaging. *Molecular Therapy* 3(4): 631-640.
- Sporns, O., G. Tononi and R. Kotter (2005). The human connectome: A structural description of the human brain. *PLoS Comput Biol* 1(4): e42.
- Staras, K. (2010). Sharing vesicles between central presynaptic terminals: implications for synaptic function. *Front.Syna.Neurosci.*: 1-6.
- Südhof, T. and J. Rizo (2011). Synaptic Vesicle Exocytosis. *Cold Spring Harbor perspectives in biology*.
- Südhof, T. C. (2012). The Presynaptic Active Zone. *Neuron* 75(1): 11-25.
- Sugita, M. and Y. Shiba (2005). Genetic tracing shows segregation of taste neuronal circuitries for bitter and sweet. *Science* 309(5735): 781-5.
- Sun, Y., A. Q. Nguyen, J. P. Nguyen, L. Le, D. Saur, J. Choi, Edward M. Callaway and X. Xu (2014). Cell-Type-Specific Circuit Connectivity of Hippocampal CA1 Revealed through Cre-Dependent Rabies Tracing. *CellReports* 7(1): 269-280.
- Sykova, E. and C. Nicholson (2008). Diffusion in brain extracellular space. *Physiol Rev* 88(4): 1277-340.
- Szabadics, J., C. Varga, J. Brunner, K. Chen and I. Soltesz (2010). Granule Cells in the CA3 Area. *Journal of Neuroscience* 30(24): 8296-8307.
- Takamori, S., M. Holt, K. Stenius, E. A. Lemke, M. Grønborg, D. Riedel, H. Urlaub, S. Schenck, B. Brügger, P. Ringler, S. A. Müller, B. Rammner, F. Gräter, J. S. Hub, B. L. De Groot, G. Mieskes, Y. Moriyama, J. Klingauf, H. Grubmüller, J. Heuser, F. Wieland and R. Jahn (2006). Molecular anatomy of a trafficking organelle. *Cell* 127(4): 831-46.
- Tanti, A. and C. Belzung (2013). Neurogenesis along the septo-temporal axis of the hippocampus: are depression and the action of antidepressants region-specific? *Neuroscience* 252: 234-52.
- Thio, L. L., G. D. Clark, D. B. Clifford and C. F. Zorumski (1992). Wheat germ agglutinin enhances EPSCs in cultured postnatal rat hippocampal neurons by

- blocking ionotropic quisqualate receptor desensitization. *Journal of Neurophysiology* 68(6): 1930-8.
- Thomas, S. and B. A. Luxon (2013). Vaccines based on structure-based design provide protection against infectious diseases. *Expert Rev Vaccines* 12(11): 1301-11.
- Thompson, C. L., S. D. Pathak, A. Jeromin, L. L. Ng, C. R. Macpherson, M. T. Mortrud, A. Cusick, Z. L. Riley, S. M. Sunkin, A. Bernard, R. B. Puchalski, F. H. Gage, A. R. Jones, V. B. Bajic, M. J. Hawrylycz and E. S. Lein (2008). Genomic Anatomy of the Hippocampus. *Neuron* 60(6): 1010-1021.
- Toonen, R. F. G. and M. Verhage (2003). Vesicle trafficking: pleasure and pain from SM genes. *Trends Cell Biol* 13(4): 177-86.
- Traub, R. D., A. Bibbig, F. E. LeBeau, E. H. Buhl and M. A. Whittington (2004). Cellular mechanisms of neuronal population oscillations in the hippocampus in vitro. *Annu Rev Neurosci* 27: 247-78.
- Trudeau, L. E. and R. Gutierrez (2007). On cotransmission & neurotransmitter phenotype plasticity. *Mol Interv* 7(3): 138-46.
- Tuncdemir, S. N. and G. Fishell (2011). "Neural circuits look forward." *Proceedings of the National Academy of Sciences* 108(39): 16137-16138.
- Ugolini, G. (1995). Specificity of rabies virus as a transneuronal tracer of motor networks: transfer from hypoglossal motoneurons to connected second-order and higher order central nervous system cell groups. *J Comp Neurol* 356(3): 457-80.
- Ugolini, G. (2010). Advances in viral transneuronal tracing. *J Neurosci Methods* 194(1): 2-20.
- Ugolini, G., H. G. Kuypers and A. Simmons (1987). Retrograde transneuronal transfer of herpes simplex virus type 1 (HSV 1) from motoneurons. *Brain Res* 422(2): 242-56.
- Van Den Pol, A. N., K. Ozduman, G. Wollmann, W. S. C. Ho, I. Simon, Y. Yao, J. K. Rose and P. Ghosh (2009). Viral strategies for studying the brain, including a replication-restricted self-amplifying delta-G vesicular stomatitis virus that rapidly expresses transgenes in brain and can generate a multicolor golgi-like expression. *J. Comp. Neurol.* 516(6): 456-481.
- van den Pol, A. N., K. P. Dalton and J. K. Rose (2002). Relative neurotropism of a recombinant rhabdovirus expressing a green fluorescent envelope glycoprotein. *Journal of virology* 76(3): 1309-1327.
- Vazquez-Cintrón, E. J., M. Vakulenko, P. A. Band, L. H. Stanker, E. A. Johnson and K. Ichtchenko (2014). Atoxic derivative of botulinum neurotoxin A as a prototype molecular vehicle for targeted delivery to the neuronal cytoplasm. *PLoS One* 9(1): e85517.
- Veenman, C. L., A. Reiner and M. G. Honig (1992). Biotinylated dextran amine as an anterograde tracer for single- and double-labeling studies. *J Neurosci Methods* 41(3): 239-54.
- Velez-Fort, M., C. V. Rousseau, C. J. Niedworok, I. R. Wickersham, E. A. Rancz, A. P. Brown, M. Strom and T. W. Margrie (2014). The stimulus selectivity and connectivity of layer six principal cells reveals cortical microcircuits underlying visual processing. *Neuron* 83(6): 1431-43.
- Verderio, C., C. Cagnoli, M. Bergami, M. Francolini, U. Schenk, A. Colombo, L. Riganti, C. Frassoni, E. Zuccaro, L. Danglot, C. Wilhelm, T. Galli, M. Canossa and M. Matteoli (2012). TI-VAMP/VAMP7 is the SNARE of secretory lysosomes contributing to ATP secretion from astrocytes. *Biology of the Cell* 104(4): 213-228.

- Verhage, M. and G. v. Meer (2009). Synaptobrevin, Sphingolipids, and Secretion: Lube 'n' Go at the Synapse. *Neuron* 62(5): 603-605.
- Verhage, M., A. S. Maia, J. J. Plomp, A. B. Brussaard, J. H. Heeroma, H. Vermeer, R. F. Toonen, R. E. Hammer, T. K. van den Berg, M. Missler, H. J. Geuze and T. C. Sudhof (2000). Synaptic assembly of the brain in the absence of neurotransmitter secretion. *Science* 287(5454): 864-9.
- Vivar, C. and H. Van Praag (2013). Functional circuits of new neurons in the dentate gyrus. *Front. Neural Circuits* 7: 1-13.
- Vivar, C., M. C. Potter, J. Choi, J.-Y. Lee, T. P. Stringer, E. M. Callaway, F. H. Gage, H. Suh and H. Van Praag (2012). Monosynaptic inputs to new neurons in the dentate gyrus. *Nat Comms* 3: 1107.
- Vivona, S., C. W. Liu, P. Strop, V. Rossi, F. Filippini and A. T. Brunger (2010). The Longin SNARE VAMP7/TI-VAMP Adopts a Closed Conformation. *Journal of Biological Chemistry* 285(23): 17965-17973.
- Vos, M., E. Lauwers and P. Verstreken (2010). Synaptic mitochondria in synaptic transmission and organization of vesicle pools in health and disease. *Front.Syna.Neurosci.* 2: 139.
- Vyklicky, L., D. K. Patneau and M. L. Mayer (1991). Modulation of excitatory synaptic transmission by drugs that reduce desensitization at AMPA/kainate receptors. *Neuron* 7(6): 971-84.
- Vyleta, N. P. and P. Jonas (2014). Loose coupling between Ca<sup>2+</sup> channels and release sensors at a plastic hippocampal synapse. *Science* 343(6171): 665-70.
- Vyleta, N. P. and S. M. Smith (2011). Spontaneous Glutamate Release Is Independent of Calcium Influx and Tonically Activated by the Calcium-Sensing Receptor. *Journal of Neuroscience* 31(12): 4593-4606.
- Wagner, R. and J. Rose (1996). "Rhabdoviridae: the viruses and their replication." *Fields virology* 1.
- Wall, N. R., I. R. Wickersham, A. Cetin, M. De La Parra and E. M. Callaway (2010). Monosynaptic circuit tracing in vivo through Cre-dependent targeting and complementation of modified rabies virus. *Proceedings of the National Academy of Sciences* 107(50): 21848-21853.
- Waller, A. (1850). Experiments on the section of the glossopharyngeal and hypoglossal nerves of the frog, and observations of the alterations produced thereby in the structure of their primitive fibres. *Philosophical Transactions of the Royal Society of London* 140: 423-429.
- Walter, A. M., A. J. Groffen, J. B. Sørensen and M. Verhage (2011). Multiple Ca<sup>2+</sup> sensors in secretion: teammates, competitors or autocrats? *Trends in Neurosciences* 34(9): 487-497.
- Walter, A. M., P. S. Pinheiro, M. Verhage and J. B. Sørensen (2013). A Sequential Vesicle Pool Model with a Single Release Sensor and a Ca<sup>2+</sup>-Dependent Priming Catalyst Effectively Explains Ca<sup>2+</sup>-Dependent Properties of Neurosecretion. *PLoS Comput Biol* 9(12): e1003362.
- Wang, M., O. Orwar, J. Olofsson and S. G. Weber (2010). Single-cell electroporation. *Anal Bioanal Chem* 397(8): 3235-3248.
- Weber, J. P., K. Reim and J. B. Sørensen (2010). Opposing functions of two sub-domains of the SNARE-complex in neurotransmission. *The EMBO Journal* 29(15): 2477-2490.
- Weible, A. P., L. Schwarcz, I. R. Wickersham, L. Deblander, H. Wu, E. M. Callaway, H. S. Seung and C. G. Kentros (2010). Transgenic Targeting of Recombinant Rabies Virus Reveals Monosynaptic Connectivity of Specific Neurons. *Journal of Neuroscience* 30(49): 16509-16513.

- Welberg, L. (2014). Synaptic transmission: Membrane lipids channel a message. *Nature Publishing Group* 15(3): 135-135.
- Weston, Matthew C., Ralf B. Nehring, Sonja M. Wojcik and C. Rosenmund (2011). Interplay between VGLUT Isoforms and Endophilin A1 Regulates Neurotransmitter Release and Short-Term Plasticity. *Neuron* 69(6): 1147-1159.
- Wickersham, I. R., D. C. Lyon, R. J. O. Barnard, T. Mori, S. Finke, K.-K. Conzelmann, J. A. T. Young and E. M. Callaway (2007a). Monosynaptic restriction of transsynaptic tracing from single, genetically targeted neurons. *Neuron* 53(5): 639-47.
- Wickersham, I. R., S. Finke, K.-K. Conzelmann and E. M. Callaway (2007b). Retrograde neuronal tracing with a deletion-mutant rabies virus. *Nat Meth* 4(1): 47-49.
- Wierda, K. D. B., R. F. G. Toonen, H. de Wit, A. B. Brussaard and M. Verhage (2007). Interdependence of PKC-dependent and PKC-independent pathways for presynaptic plasticity. *Neuron* 54(2): 275-90.
- Wiktor, T. J., R. I. Macfarlan, K. J. Reagan, B. Dietzschold, P. J. Curtis, W. H. Wunner, M. P. Kieny, R. Lathe, J. P. Lecocq, M. Mackett and et al. (1984). Protection from rabies by a vaccinia virus recombinant containing the rabies virus glycoprotein gene. *Proc Natl Acad Sci U S A* 81(22): 7194-8.
- Wilhelm, B. G., T. W. Groemer and S. O. Rizzoli (2010). The same synaptic vesicles drive active and spontaneous release. *Nature Publishing Group* 13(12): 1454-1456.
- Wilke, S. A., J. K. Antonios, E. A. Bushong, A. Badkoobehi, E. Malek, M. Hwang, M. Terada, M. H. Ellisman and A. Ghosh (2013). "Deconstructing Complexity: Serial Block-Face Electron Microscopic Analysis of the Hippocampal Mossy Fiber Synapse." *Journal of Neuroscience* 33(2): 507-522.
- Williams, Megan E., Scott A. Wilke, A. Daggett, E. Davis, S. Otto, D. Ravi, B. Ripley, Eric A. Bushong, Mark H. Ellisman, G. Klein and A. Ghosh (2011). Cadherin-9 Regulates Synapse-Specific Differentiation in the Developing Hippocampus. *Neuron* 71(4): 640-655.
- Wouterlood, F. G., B. Bloem, H. D. Mansvelder, A. Luchicchi and K. Deisseroth (2014). A fourth generation of neuroanatomical tracing techniques: Exploiting the offspring of genetic engineering. *J Neurosci Methods* 235: 331-348.
- Zampieri, N., Thomas M. Jessell and Andrew J. Murray (2014). Mapping Sensory Circuits by Anterograde Transsynaptic Transfer of Recombinant Rabies Virus. *Neuron* 81(4): 766-778.
- Zarei, M., C. F. Beckmann, M. A. Binnewijzend, M. M. Schoonheim, M. A. Oghabian, E. J. Sanz-Arigita, P. Scheltens, P. M. Matthews and F. Barkhof (2013). Functional segmentation of the hippocampus in the healthy human brain and in Alzheimer's disease. *Neuroimage* 66: 28-35.
- Zhai, R. G. and H. J. Bellen (2004). The architecture of the active zone in the presynaptic nerve terminal. *Physiology (Bethesda)* 19: 262-70.
- Ziff, E. B. (1997). Enlightening the postsynaptic density. *Neuron* 19(6): 1163-74.
- Zimmermann, J., T. Trimbuch and C. Rosenmund (2014). Synaptobrevin 1 mediates vesicle priming and evoked release in a subpopulation of hippocampal neurons. *J Neurophysiol* 112(6): 1559-65.
- Zlatic, S. A., E. J. Grossniklaus, P. V. Ryder, G. Salazar, A. L. Mattheyses, A. A. Peden and V. Faundez (2013). Chemical-genetic disruption of clathrin function spares adaptor complex 3-dependent endosome vesicle biogenesis. *Mol Biol Cell* 24(15): 2378-88.

# **Annex**

## Annex: Rabies Virus Pathophysiology and Epidemics

Rabies is one of the oldest diseases known to humans (WHO FAQs on rabies, 2013). Rabies results from infection by any lyssavirus, (see Figure 1 for a list of the species in this genus), causing encephalitis of differing severity depending on the mammal infected –it is almost universally fatal for foxes and humans (Willoughby, 2012). A recent report challenges RABV intractability, as communities living in a lyssavirus-endemic region like the Peruvian Amazon, seem to be resistant to rabies after suffering vampire bat depredation (Gilbert et al., 2012).

This virus is named after 'rabere', 'rage' in Latin, which in turn roots from the Sanskrit word 'rabhas' meaning 'to do violence'. This parasite turns its host aggressive, which increases rabies transfer through biting. The word 'virus' is also derived from Latin for 'poison', which was used by Cardanus, a Roman writer, to describe the saliva of rabid dogs (Baer, 1975). Aristoteles described rabid dogs as suffering of the madness, 'lyssa/lytta' in Greek, which is now used to denominate the taxonomic genus (Baer, 1975). Strangely, Greeks did not associate human RABV with canine rabies and called it instead hydrophobia, as a distinctive behavioral change in the human host after rabies infection is the apparent fear to water –i.e. in fact a dysfunctional breathing/swallowing caused by viral neuronal apoptosis in the brain areas controlling these physiological mechanisms, which is responsible, together with increased saliva production, for the characteristic mouth foaming of rabid animals. In the 1980s, a study radio-tracking rabid foxes reported disorientation and increased locomotion as further changes in conduct (Andral et al., 1982). These parasite-induced phenotypic traits lead to greater viral propagation: a rabid fox running disorientated gets outside its territory; when it encounters another fox (or any other animal), the aggressive rabid fox bites the stranger; unable to properly swallow, the rabid fox mouth is full of saliva containing millions of RABV virion particles, which gain access through the bite wound into the new host. Nonetheless, the exact mechanisms underlying RABV synaptic crossing, and RABV-induced disorientation and aggressiveness, are still under scrutiny. For a review on RABV and the host cell interactions see Schnell et al., 2010. Altering the host's acts to reach other targets is a refined strategy common to many parasites (see special issue edited by Adamo and Webster, 2013). Furthermore, symbiotic bacteria, which account for 90% of the cells in our body, seem to also be able to modify the host's behavior (Cryan and Dinan, 2012; Moloney et al., 2014). Interestingly, the gut microbiome composition

has been recently shown to be influenced by host genetics (Goodrich et al., 2014). Bacteria are not the only microorganisms beneficial for the host, other parasites – including viruses- can also increase host survival (Grosman et al., 2008; Bondy-Denomy and Davidson, 2014; Canestrari et al., 2014). The interaction between microorganisms and the vertebrate nervous system is a fascinating topic that deserves a thorough study, which promises to help us unveiling the genomic, proteomic and neurophysiological mechanisms underlying behavior, and even gaining insight for biology of disease (i.e. see example for cancer by Pennacchio et al., 2014).

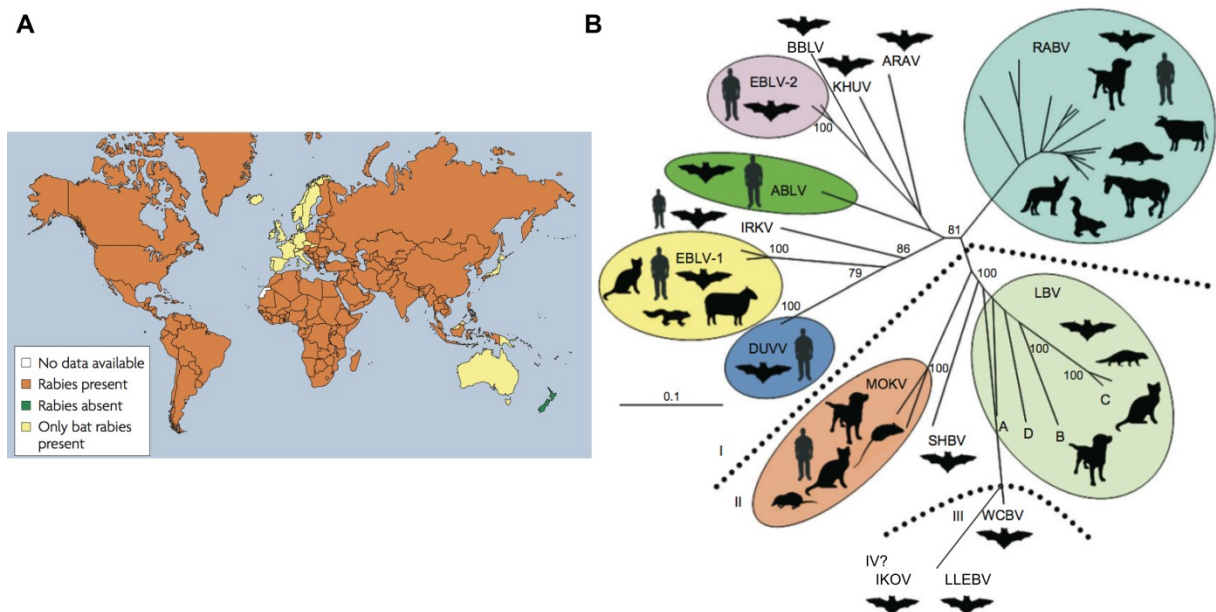


**Figure 1** Bat geographical (left) and host phylogenetic (right) *Lyssavirus* species distribution (left panel from Schnell et al., 2010, right panel adapted from Banyard et al., 2011, 2014)

RABV is wide-spread and can infect all warm-blooded animals, dogs being the most common vector to infect humans (Hemachudha et al., 2013) (see Figure 1b). Rodents, however, are rarely infected (Tintinalli et al., 2010). Birds and *Didelphis virginiana*, a mammalian species with low body temperature, are resistant but not immune to RABV (Shannon et al., 1988; McRuer and Jones, 2009), while *Cynictis penicillata* are mammals that can asymptotically carry it for years (Taylor, 1993). RABV is adapted to infect also poikilothermic vertebrates like fish, snakes, turtles, and lizards, although these animals do not develop the disease (Baer, 1975). The other 15 species known of the *Lyssavirus* genus are more specific in their hosts and geographical area —i.e. bats are known to be vectors for all species except the Mokola and Ikoma viruses, which infects terrestrial mammals, like shrews or domestic cats, in sub-Saharan Africa (WHO Technical Report Series No. 982, 2013), while RABV is the only species present in the Americas, but bats are also the main



vector, being responsible for 95% of human RABV in this continent (Banyard et al., 2014) (see Figure 1b). Nonetheless, evolutionary analyses suggest that lyssaviruses originated in bats, and it is expected that more species will be discovered (Banyard et al., 2014). Antarctica and New Zealand are the only places on earth considered lyssavirus-free (Schnell et al., 2010) (see Figure 1a). Current lyssaviruses are estimated to have evolved within the past 1500 years, and to have spread helped by European colonialism (Nadin-Davis and Real, 2011). Officially, around 70,000 humans, mainly rural children bitten by dogs in Asia and Africa, die every year due to this lethal zoonotic disease, and this number is probably an underestimation (WHO Fact Sheet N°99, 2014). Furthermore, rabies cases are increasing in China, former Soviet republics, and Central and South America (Willoughby, 2012).

A remarkable case of translational research, it was not a doctor but an organic chemist who developed a successful preventive measure against this disease. In 1881, the French chemist, Louis Pasteur and his colleague Emile Roux started to research a cure for RABV, paving the way for the fields of microbiology and immunology (Smith, 2012). Their work yielded two years later a vaccine from the spinal cord of infected rabbits, which they tested in dogs. In 1885, Joseph Meister was the first person to be saved by this vaccination after being bitten by a rabid dog (Pasteur, 1885). Vaccines prevent rabies from infecting the CNS by activating an immune response, however, no treatment exists to cure rabies after symptoms develop (Takayama, 2008). Human RABV can lead to either a furious or a paralytic pathology, with the former patients having a shorter survival due to greater amount of RABV and lower immune response in the CNS (Hemachudha et al., 2013). There are few reports of people to have recovered, but most had bat RABV variants (pointing towards differences in spread between dog and bat variants?). Some did so spontaneously, while others had followed treatment, particularly the “Milwaukee protocol” (i.e. ketamine plus midazolam) (Hemachudha et al., 2013). The current epidemic is neglected, despite the possibility of vaccinating domestic dogs inexpensively (Knobel et al., 2005). The Global Alliance for Rabies Control has established the anniversary of Pasteur's death, 28th September, as “World Rabies Day” to help raise awareness and provide preventive advice.

## References

- Adamo, S. A. and J. P. Webster (2013). Special Issue: Neural parasitology: how parasites manipulate host behaviour. *The Journal of experimental biology* 216(1): 1-160.
- Andral, L., M. Artois, M. Aubert and J. Blancou (1982). Radio-pistage de renards enrages. *Comparative Immunology, Microbiology and Infectious Diseases* 5(1): 285-291.
- Baer, G. M. (1975). Pathogenesis to the central nervous system. The natural history of rabies 1: 181-198.
- Banyard, A. C., J. S. Evans, T. R. Luo and A. R. Fooks (2014). Lyssaviruses and bats: emergence and zoonotic threat. *Viruses* 6(8): 2974-90.
- Banyard, A. C., D. Hayman, N. Johnson, L. McElhinney and A. R. Fooks (2011). Bats and lyssaviruses. *Adv Virus Res* 79: 239-89.
- Bondy-Denomy, J. and A. R. Davidson (2014). When a virus is not a parasite: the beneficial effects of prophages on bacterial fitness. *Journal of Microbiology* 52(3): 235-242.
- Canestrari, D., D. Bolopo, T. C. Turlings, G. Röder, J. M. Marcos and V. Baglione (2014). From parasitism to mutualism: unexpected interactions between a cuckoo and its host. *Science* 343(6177): 1350-1352.
- Cryan, J. F. and T. G. Dinan (2012). Mind-altering microorganisms: the impact of the gut microbiota on brain and behaviour. *Nat Rev Neurosci* 13(10): 701-12.
- Gilbert, A. T., B. W. Petersen, S. Recuenco, M. Niezgoda, J. Gomez, V. A. Laguna-Torres and C. Rupprecht (2012). Evidence of rabies virus exposure among humans in the Peruvian Amazon. *Am J Trop Med Hyg* 87(2): 206-15.
- Goodrich, Julia K., Jillian L. Waters, Angela C. Poole, Jessica L. Sutter, O. Koren, R. Blekhman, M. Beaumont, W. Van Treuren, R. Knight, Jordana T. Bell, Timothy D. Spector, Andrew G. Clark and Ruth E. Ley (2014). Human Genetics Shape the Gut Microbiome. *Cell* 159(4): 789-799.
- Grosman, A. H., A. Janssen, E. F. De Brito, E. G. Cordeiro, F. Colares, J. O. Fonseca, E. R. Lima, A. Pallini and M. W. Sabelis (2008). Parasitoid increases survival of its pupae by inducing hosts to fight predators. *PLoS One* 3(6): e2276.
- Hemachudha, T., G. Ugolini, S. Wacharapluesadee, W. Sungkarat, S. Shuangshoti and J. Laothamatas (2013). Human rabies: neuropathogenesis, diagnosis, and management. *The Lancet Neurology* 12(5): 498-513.
- Knobel, D. L., S. Cleaveland, P. G. Coleman, E. M. Fevre, M. I. Meltzer, M. E. Miranda, A. Shaw, J. Zinsstag and F. X. Meslin (2005). Re-evaluating the burden of rabies in Africa and Asia. *Bull World Health Organ* 83(5): 360-8.
- McRuer, D. L. and K. D. Jones (2009). Behavioral and Nutritional Aspects of the Virginian Opossum (*Didelphis virginiana*). *Veterinary Clinics of North America: Exotic Animal Practice* 12(2): 217-236.
- Moloney, R. D., L. Desbonnet, G. Clarke, T. G. Dinan and J. F. Cryan (2014). The microbiome: stress, health and disease. *Mamm Genome* 25(1-2): 49-74.
- Nadin-Davis, S. A. and L. A. Real (2011). Molecular phylogenetics of the lyssaviruses--insights from a coalescent approach. *Adv Virus Res* 79: 203-38.
- Pasteur, L. (1881). Note sur la maladie nouvelle provoquee par la salive d'un enfant mort de la rage. *Comptes Rendus* 92: 159-165.
- Pasteur, L. (1885). Methode pour prevenir la rage apres morsure.
- Pennacchio, F., A. Masi and A. Pompella (2014). Glutathione levels modulation as a strategy in host-parasite interactions - insights for biology of cancer. *Frontiers in pharmacology* 5.

- Schnell, M. J., J. P. McGettigan, C. Wirblich and A. Papaneri (2010). The cell biology of rabies virus: using stealth to reach the brain. *Nat Rev Micro*: 1-11.
- Shannon, L. M., J. L. Poulton, R. W. Emmons, J. D. Woodie and M. E. Fowler (1988). Serological survey for rabies antibodies in raptors from California. *J Wildl Dis* 24(2): 264-7.
- Smith, K. A. (2012). Louis pasteur, the father of immunology? *Front Immunol* 3: 68.
- Takayama, N. (2008). Rabies: a preventable but incurable disease. *J Infect Chemother* 14(1): 8-14.
- Taylor, P. (1993). A systematic and population genetic approach to the rabies problem in the yellow mongoose (*Cynictis penicillata*).
- Tintinalli, J., J. Stapczynski, O. Ma, D. Cline and R. Cydulka (2010). *Tintinalli, A's Emergency Medicine: A Comprehensive Study Guide, Seventh Edition*, McGraw-Hill.
- WHO Fact Sheet No. 99 (Updated September 2014) Rabies. [www.paho.org/common/display.asp?Lang=E&RecID=10209](http://www.paho.org/common/display.asp?Lang=E&RecID=10209)
- WHO FAQs on Rabies (2013) Frequently Asked Questions on Rabies. [www.who.int/rabies/resources/SEA\\_CD\\_278\\_FAQs\\_Rabies.pdf?ua=1](http://www.who.int/rabies/resources/SEA_CD_278_FAQs_Rabies.pdf?ua=1)
- WHO Technical Report Series No. 982 (2013) WHO Expert Consultation on Rabies. [www.who.int/neglected\\_diseases/support\\_to\\_rabies\\_elimination\\_2013/en](http://www.who.int/neglected_diseases/support_to_rabies_elimination_2013/en)
- Willoughby, R. E., Jr. (2012). Resistance to rabies. *Am J Trop Med Hyg* 87(2): 205.